László T. Kóczy
Claudiu R. Pozna
Janusz Kacprzyk   *Editors*

Issues and Challenges of Intelligent Systems and Computational Intelligence

Springer

Studies in Computational Intelligence

Volume 530

Series editor

Janusz Kacprzyk, Polish Academy of Sciences, Warsaw, Poland
e-mail: kacprzyk@ibspan.waw.pl

About this Series

The series "Studies in Computational Intelligence" (SCI) publishes new developments and advances in the various areas of computational intelligence—quickly and with a high quality. The intent is to cover the theory, applications, and design methods of computational intelligence, as embedded in the fields of engineering, computer science, physics and life sciences, as well as the methodologies behind them. The series contains monographs, lecture notes and edited volumes in computational intelligence spanning the areas of neural networks, connectionist systems, genetic algorithms, evolutionary computation, artificial intelligence, cellular automata, self-organizing systems, soft computing, fuzzy systems, and hybrid intelligent systems. Of particular value to both the contributors and the readership are the short publication timeframe and the world-wide distribution, which enable both wide and rapid dissemination of research output.

László T. Kóczy · Claudiu R. Pozna
Janusz Kacprzyk
Editors

Issues and Challenges of Intelligent Systems and Computational Intelligence

Springer

Editors
László T. Kóczy
Department of Automation
Széchenyi István University
Győr
Hungary

Janusz Kacprzyk
Systems Research Institute
Polish Academy of Sciences
Warsaw
Poland

Claudiu R. Pozna
Department of Information Technology
Széchenyi István University
Győr
Hungary

Printed on acid-free paper

Preface

The broadly perceived area of intelligent systems has been for quite a long time an object of intensive research in various areas of science and technology, exemplified by computer science, logic, mathematics, data analysis, knowledge engineering, IT/ICT, mechatronics, automation, and robotics, just to name a few more technology-oriented fields.

Novel avenues of research have appeared, and new opportunities of real-world applications have followed an intensive development of computational intelligence and soft computing that have enjoyed a rapid growth of popularity in recent decades.

As it is always the case in such a period of a rapid growth, the flow of new tools and techniques clearly implies new challenges, both conceptual, algorithmic, and implementation. This is also the case of our area. The scientific community through its involvement and hard work tries to promote the area and new tools and techniques. One of the necessary, and effective and efficient ways for reaching such goals is to prepare comprehensive exposures to the area and its main applications through the editing of volumes containing contributions of prominent and active researchers and scholars. This has been the case with this volume, too.

In such initiatives, a group of people who are committed to reach the above-mentioned goal to promote new directions in an area usually meets at some important scientific gathering and, after fruitful discussions triggered by conference contributions, questions from the audience, etc., the idea of such a volume is born. This was the case with this volume too. Its idea has appeared as a result of very interesting presentations and vivid discussions at the Fifth Győr Symposium and First Hungarian-Polish Joint Conference on Computational Intelligence held in Győr, Hungary, in September, 2012. Then, due to a high interest of the scientific community and its willingness to contribute to this important volume, the editors have been able to gather a very good collection of relevant and original papers by prominent representatives of many areas, relevant both to the theory and practice of intelligent systems, artificial intelligence, computational intelligence, soft computing, and the like. The contributions have been divided into seven parts presenting first more fundamental and theoretical contributions, and then applications in relevant areas.

Part I is devoted to conceptual and analytic foundations of the theory of fuzzy systems, and contains two papers.

V. A. Niskanen ("Prospects for Truth Valuation in Fuzzy Extended Logic") is concerned with an important problem of truth valuation in fuzzy logic, and its related alternative ways to many-valued resolution at the meta-level. His analysis is based on Zadeh's fuzzy extended logic (FLe), and is performed on the meta--level from the standpoint of philosophy of science.

D. Coufal ("Coherence and Convexity of Euclidean Radial Implicative Fuzzy Systems") discusses the case of rule-based fuzzy systems, and concentrates on one of their important classes, implicative fuzzy systems. His main concern is to obtain a class of necessary conditions for coherence of radial implicative fuzzy systems, all that in an implicit form. The minimization of a certain function is employed.

We continue with the analysis of various aspects of fuzzy sets theory and fuzzy logic in Part II in which emphasis is more on applications.

P. Nowak and M. Romaniuk ("Catastrophe Bond Pricing with Fuzzy Volatility Parameters") consider an important problem related to natural disasters and catastrophes, which may imply huge losses to the individuals, communities, regions, nations, and even the world as a whole. The authors deal with the problem of catastrophe bonds that are issued to transfer the catastrophic risk to financial markets. More specifically, they are concerned with the catastrophe bond pricing using a combination of stochastic analysis and fuzzy sets theory. Notably, the volatility of the interest rate and market price of risk are represented as fuzzy numbers, and the Monte Carlo simulation approach is used.

A. Bukovics and L. T. Kóczy ("Evaluating Condition of Buildings by Applying Fuzzy Signatures and R-fuzzy Operations") show a novel method for qualifying and ranking residential buildings based on various priority aspects and for making an optimum allocation of the material resources available for the renewal of the buildings. Their model is based on many detailed technical-static expert reports available to a stock of residential buildings in Budapest and stored in a database. First, using fuzzy logic, a model for calculating a so-called status characteristic value between 0 and 1 on the basis of the structures and status of the buildings is developed using a fuzzy singleton signature model. Then, a hierarchy is devised related to the stock of buildings to be employed for supporting decision making on intervention on the buildings concerned. Specifically, membership values characterizing the status of the load-bearing structures are defined on the basis of the deterioration of the structures, and a new method is here developed that takes into account other parameters of the structures, and the impact exerted on the quality of the structure, too. The method is based on the use of "real fuzzy values" (R-fuzzy sets), an extension of the concept of classic fuzzy sets that allows also the inversion of fuzzy set connectives under certain circumstances.

F. Lilik and L. T. Kóczy ("The Determination of the Bitrate on Twisted Pairs by Mamdani Inference Method") are concerned with the problem of how to predict the available maximal data transfer rate on dedicated telecommunication connections. The authors first provide a critical review of some tools and techniques, which are most often used for this purpose. Then, they present a method

based on the use of a Mamdani-type fuzzy reasoning system. A comprehensive computational analysis of prediction results obtained for the evaluation of the twisted-pair-based local loops of the telecommunication access networks by using various methods is provided and a comparison with those obtained by using that Mamdani-type fuzzy reasoning system is shown.

B. Kalmár, A. Kalmár, K. Balázs, and L. T. Kóczy ("Construction Site Layout and Building Material Distribution Planning Using Hybrid Algorithms") discuss some novel method for solving the layout problem for construction site and distribution planning of building materials. The layout problem considered is dealt with by applying costs on the moving of construction materials across the site, and the goal is to develop an algorithm which is specialized in solving problems of distributing building materials, exemplified by bricks, on a site by placing their pallets at optimal spots, for each unit built from a given material to be within an optimal reach. The authors describe first a solution of this problem for the engineering practice and interpret the slow but accurate method of the so-called Hungarian Algorithm, and then propose a memetic algorithm which is faster but yields almost as accurate a solution. Conclusions are drawn about the usability of this method.

Part III discusses various aspects of artificial neural networks which are widely used for systems modeling, classification, control, etc.

V. Kurková ("Accuracy of Surrogate Solutions of Integral Equations by Feedforward Networks") is devoted to a study of an important problem of using feed-forward neural networks for surrogate modeling of functional relationships. Potential applications areas range from chemistry with surrogate models of empirical functions assigning to compositions of chemicals measures of quality of catalysers produced by reactions of these chemicals, biology with surrogate models of empirical functions classifying structures of the RNA, economics with surrogate models of functions assigning credit ratings to companies, etc. The author considers from a theoretical point of view surrogate solutions of the Fredholm integral equations, which play an important role in many areas, by using feed-forward neural networks. The author proves the convergence of surrogate solutions computable by those neural networks with increasing numbers of computational units to theoretically optimal solutions, and provides upper bounds on the rates of convergence. It is shown that the results hold for a variety of computational units, notably the perceptron and Gaussian radial units.

P. Šarčević ("Vehicle Classification Using Neural Networks with a Single Magnetic Detector") discusses principles of operation, advantages, and disadvantages for different vehicle detection technologies that are meant to provide speed monitoring, traffic counting, presence detection, headway measurement, vehicle classification, and weigh-in-motion data. The author proposes the idea of a new detection and classification method for a single magnetic sensor-based system. An important feature of the new detection algorithm and the neural network classifier are an easy implementation in a microcontroller-based system. An analysis of results for various benchmark problems is given.

Part IV contains contributions covering two important areas of intelligent data analysis which are crucial for broadly perceived intelligent systems, knowledge engineering, etc., that is, classification and clustering, and image processing.

P. Kulczycki, M. Charytanowicz, P. A. Kowalski, and Sz. Łukasik ("Exemplary Applications of the Complete Gradient Clustering Algorithm in Bioinformatics, Management and Engineering") discuss various aspects related to the applications and prospects of the complete gradient clustering algorithm, a classic clustering procedure developed by Fukunaga and Hostetler. The authors present its ready-to-be-used version by providing a full set of procedures for defining all functions and values of the parameters. Moreover, they analyze how a possible change in those values influences the number of clusters and the proportion between their numbers in dense and sparse areas of data elements. The authors show some possible uses of these properties on some practical problems in the areas of bioinformatics, more specifically the categorization of grains for seed production, management, more specifically the design of a marketing support strategy for a mobile phone operator, and engineering, more specifically the synthesis of a fuzzy controller.

A. T. Duong, H. T. Phan, N. D. Le, and S. T. Tran ("A Hierarchical Approach for Handwritten Digit Recognition Using Sparse Autoencoder") are concerned with handwritten digit recognition, a very important problem that is very relevant for many practical applications, yet difficult, and which still presents a considerable challenge from a theoretical and implementation point of view. Approaches based on higher level features learning algorithms are here promising and popular giving usually better results than just using raw intensity values with classification algorithms. On the other hand, these approaches do not take the advantage of specific characteristics of data. Therefore, the authors propose a new method to learn higher level features from specific characteristics of data using a sparse autoencoder. The main idea of the approach proposed is to divide the handwritten digits into subsets corresponding to specific characteristics. The experimental results obtained show that the proposed method yields lower error rates and time complexity than the original approach of a sparse autoencoder. Moreover, the results obtained indicate that the more correlated are characteristics defined, the better higher level features can be learned.

A. Tormási and L. T. Kóczy ("Fuzzy Single-Stroke Character Recognizer with Various Rectangle Fuzzy Grids") extend theoretical and implementation results on their original FUBAR character recognition method with various fuzzy grid parameters. The accuracy and efficiency of the handwritten single-stroke character recognition algorithm with different sized rectangle (i.e., $N \times M$) fuzzy grids are investigated. The results obtained are then compared to other modified FUBAR algorithms and known commercial and academic recognition methods. Possible applications and further extensions are also discussed.

Part V contains papers on various kinds of problems, solutions, and applications on the use of various paradigms, tools, and techniques from the broadly perceived areas of artificial and computational intelligence in robotics.

   J. Kuti, P. Galambos, and P. Baranyi ("Delay and Stiffness Dependent Polytopic LPV Modeling of Impedance Controlled Robot Interaction") operate within an important area of impedance/admittance control algorithms which are considered as key technologies in human–robot interaction and other fields of advanced robotics where complex physical interaction plays a crucial role. The authors employ a tensor product (TP) model transformation-based method to derive the delay and stiffness-dependent polytopic LPV representation of the impedance-controlled physical interaction. The applied transformation method is feasible with a bounded delay that is a nonlinear function of the environmental stiffness. Therefore, the ideal transformation space is nonrectangular which makes it to be improper for the tensor product model transformation. A novel method of a dimensionless parameterization is proposed to define a rectangular grid upon which the tensor product transformation can be applied. The resulted model form is shown to be appropriate for the modern multiobjective LMI-based control design techniques for impedance-controlled robot interaction.

   K. Bolla, Zs. Cs. Johanyák, T. Kovács, and G. Fazekas ("Local Center of Gravity-based Gathering Algorithm for Fat Robots") are concerned with groups of the so-called fat (disc-like) mobile robots without global navigation, communication or memory, specifically their gathering the essence of which is the assembly of the scattered robots on the smallest possible area. They present a new and effective and efficient algorithm for solving this task assuming an obstacle-free plan, limited visibility, and synchronous operation. The key idea of the algorithm is that in the case of each robot after detecting the visible neighboring robots, the algorithm sets a target of the next step based on the center of gravity of the encountered visible robots. Positive experience and promising results of simulation for difficult problems are presented which equal or surpass those obtained by previously published algorithms in all of the cases.

   A. Ballagi, L. T. Kóczy, and C. Pozna ("Intelligent Robot Cooperation with Fuzzy Communication") deal with an extremely relevant problem of the design of a decision-making engine of a robot which works in a collaborative team. The challenges in this task are not only due to the complexity of the environment uncertainty, dynamics and imprecision, but also due to the necessity of coordination of the team of robots that has to be included in the design phase. The robots must be aware of other robots' actions in order to cooperate and to successfully achieve their common goal. In addition, decisions must be made in real-time and under limited computational resources. The authors propose some novel algorithms for action selection in ambiguous tasks where the communication opportunities among the robots are very limited. Some promising simulation results are presented.

   T. T. Cocias, S. M. Grigorescu, and F. Moldoveanu ("Indoor Pose Estimation using 3D Scene Landmarks for Service Robotics") present a new markerless approach for estimating the pose of a robot using only 3D visual information. In contrast to many methods commonly used to solve this problem, the authors' approach makes use of the 3D features to only determine a relative position between the imaged scene (for instance, landmarks present on site) and the robot.

Such a landmark is determined using a stored 3D map of the environment. The recognition of the landmark is performed using a 3D Object Retrieval (3DOR) search engine. The new pose estimation technique proposed by the authors yields reliable and accurate pose information which can be further used for complex scene understanding and/or navigation. In numerical analyses, the performance of the proposed approach is compared with those in a traditional marker-based position estimation library.

The topic of Part VI, Data Manipulation, covers many problems, topics, paradigms, and tools and techniques of data analysis, data mining, and knowledge discovery, which are crucial point of departure of virtually all methods of analysis and synthesis which, for obvious reasons, rely on the availability of tools and techniques for both retrieving proper data and making use of them.

J. Kacprzyk, S. Zadrożny, and M. Dziedzic ("A Novel View of Bipolarity in Linguistic Data Summaries") are concerned with an important problem of data summarization, that is, the derivation of a simple representation of the very essence of a large set of data. The authors assume that there is a large numerical database, which is too large for human comprehension, and—since for the human being the only fully natural way of articulation and communication is natural language—that huge numeric data set should best be summarized by a so-called linguistic summary being a short sentence(s) capturing the very essence related to relations between some important variables. The point of departure is, first, a fuzzy logic-based approach to linguistic summarization originated by Yager, and then developed by Kacprzyk and Zadrożny, and in particular its protoform-based perspective. The second point of departure is the concept of a bipolar query in the sense that the querying criteria may be mandatory and optional, i.e., those which must be satisfied and those which should be satisfied if possible, as initiated by Zadrożny, and then developed by Zadrożny, Kacprzyk, and De Tré. In this paper, the authors combine these two concepts and present a novel concept of a bipolar linguistic summary. A theoretical analysis and some numerical results show that this concept can be useful for capturing the very essence of users' intentions and is computationally viable.

M. Krawczak and G. Szkatuła ("On Reduction of Data Series Dimension") introduce a new procedure for the reduction of dimensionality of multidimensional data (time) series. The procedure proposed consists of multiple steps with each step giving a new data series representation as well as a dimension reduction. The approach is based on the concept of a data series aggregated envelope, and principal components, called here essential attributes, are generated by a multilayer neural network. The essential attributes are generated by outputs of hidden layer neurons. Next, all differences of the essential attributes are treated as new attributes. The real values of the new attributes are nominalized in order to obtain a nominal representation of data series. The approach proposed leads to a nominal representation of the original data series and considerably reduces its dimension. The proposed approach is tested numerically on some problems of classification and clustering of time series, and the results obtained are promising.

P. Kulczycki and P. A. Kowalski ("Bayesian Classification of Interval-Type Information") deal with the problem of Bayesian classification of imprecise multidimensional information of interval type by means of patterns defined through precise data, that is, deterministic or sharp. The authors apply tools and techniques of the statistical kernel estimators which helps avoid the pattern shape for the resulting algorithm, and also eliminate elements of pattern sets which have insignificant or negative influence on the correctness of classification. The idea of the procedure proposed is based on the sensitivity method used in the domain of artificial neural networks. As a result of this procedure, the number of correct classifications and—above all—the calculation speed increase significantly. Moreover, a further increase of the quality of classification is obtained by using an algorithm for the correction of classifier parameter values.

P. Kulczycki and Sz. Łukasik ("Reduction of Dimension and Size of Data Set by Parallel Fast Simulated Annealing") propose a universal method of dimension and sample size reduction designed for exploratory data analysis procedures. The dimension is reduced by applying a linear transformation with the requirement that it has the least possible influence on the respective locations of sample elements. For this purpose an original version of the heuristic parallel fast simulated annealing method is used. As an additional element of the algorithm proposed, those elements which change the location significantly as a result of the transformation may be eliminated or assigned smaller weights in further analyses. This reduces the sample size and improves the quality of the method applied for knowledge extraction. Experimental results confirm the usefulness and efficiency of the procedure for a wide variety of problems in the class considered such as clustering, classification, identification of outliers, etc.

Part VII, Control, covers some selected problems in the area of modeling and control. Basically, the two contributions are concerned with applications in a more specific and lower scale, technologically oriented problem, and those dealing with larger systems in which control problems occur and should be effectively and efficiently solved, and in which both technological and economic, social, environmental aspects are relevant.

W. Radziszewska, Z. Nahorski, M. Parol, and P. Pałka ("Intelligent Computations in an Agent-Based Prosumer-Type Electric Microgrid Control System") deal with some issues related to microgrids which have emerged as a modern and promising concept resulting from a growing number of small prosumers, progress in the construction of renewable energy sources and the opening of energy markets. To increase the efficiency of electricity consumption, production, and trading, energy managing systems (EMSs) are developed. The authors present a project of a complex EMS that will combine load scheduling, power balancing, and smart trading methods to optimize electric energy costs of running a simulated research and education center. More specifically, they present the concept of a distributed agent-based power balancing system that is meant to control the power flow in a microgrid by a decentralized and distributed decision making. The program optimizes the operating (exploitation) cost of the devices in the microgrid by internally balancing, as much as possible, the produced and

consumed power and by trading the remaining energy excesses or deficits on the external market. Agents associated with the devices cooperate using communication protocols. Their aim is to use the energy from renewable energy sources whenever it is only available, and at the same time to limit the use of energy from sources that are more expensive and less environment friendly.

J. Sziray ("Test Generation for Short-Circuit Faults in Digital Circuits") considers an important problem of how to effectively and efficiently generate tests for detecting faults in digital circuits. In the first part, the author presents a test calculation principle, called a composite justification. The considered fault model includes stuck-at-0/1 logic faults. Both single and multiple faults are taken into account. The author considers the combinational logic only. Computations are performed at the gate level. The calculation principle is comparatively simple and is based only on successive line-value justification which makes possible the development of an efficient computer program. Then, the author discusses another fault class, namely, short-circuit or bridging faults which is implied by an erroneous galvanic connection between two circuit lines. A new algorithm is presented for generating tests and the composite justification is extended to handle this type of faults too.

The volume is, therefore, a unique position in the literature both with respect to the width of coverage of tools and techniques, and to the variety of problems that could be solved by the tools and techniques presented and also many other ones known from the literature. We are sure that the academic, research, and industrial community involved in the theoretical analyses, design, and applications of broadly perceived intelligent systems will greatly benefit from this special and unique collection of papers by leading specialists.

We wish to extend our gratitude to all the authors of the papers, and also to other people present at the aforementioned scientific gatherings, the Fifth Győr Symposium and First Hungarian-Polish Joint Conference on Computational Intelligence held in Győr, Hungary, in September, 2012, who have actively participated at discussions during that event which have significantly helped both to shape this volume and inspire the participants and contributors. We wish to acknowledge partial support of contributions and the conferences mentioned by the Hungarian National Scientific Research Fund Grants OTKA K75711, K105529, and K108405, and also by the EU grant TÁMOP 4.2.2/B-10/1-2010-0010. Special thanks go to Alex Tormási for his valuable help in the organization of the conference and editing this book. Our thanks are due to Dr. Thomas Ditzinger and Dr. Leontina Di Cecco for their vision and confidence in this project, and then an extensive support, and to Mr. Holger Schaepe for his help in the implementation of this large and difficult editorial project.

Győr and Warsaw   The Editors
August 2013

Contents

Part I
Fuzzy Systems: Theory

Prospects for Truth Valuation in Fuzzy Extended Logic

Vesa A. Niskanen

Abstract Lotfi Zadeh's fuzzy extended logic is applied to approximate linguistic reasoning. The prevailing fuzzy reasoning methods still seem to have some bivalent commitments in truth valuation and thus an alternative many-valued resolution is presented at meta-level.

Keywords Fuzzy extended logic · Truth valuation

1 Introduction

Fuzzy systems, and Soft Computing in general, can apply imprecise entities fluently in theory formation and model construction, and thus they are widely used in such areas as control, decision making, pattern recognition and robotics.

Fuzzy systems also apply linguistic many-valued reasoning, but in this respect we still have some bivalent commitments in our inference methods. Central problems pivot on the linguistic values of variables, truth valuation, quantification and even in fuzzy modal logic. Below we consider these problems, and in particular we examine the role of the truth values in approximate reasoning. Our ideas and suggestions stem from Lotfi Zadeh's fuzzy extended logic (FLe) [1]. Only meta-level examinations are performed from the standpoint of philosophy of science and thus concrete specifications are left for the further studies.

Chapter 2 provides the basic principles of the FLe. Chapter 3 applies the FLe to truth valuation in approximate linguistic reasoning. Chapter 4 concludes our examination.

V. A. Niskanen (✉)

Department of Economics and Management, University of Helsinki, Helsinki, Finland
e-mail: Vesa.a.niskanen@helsinki.fi
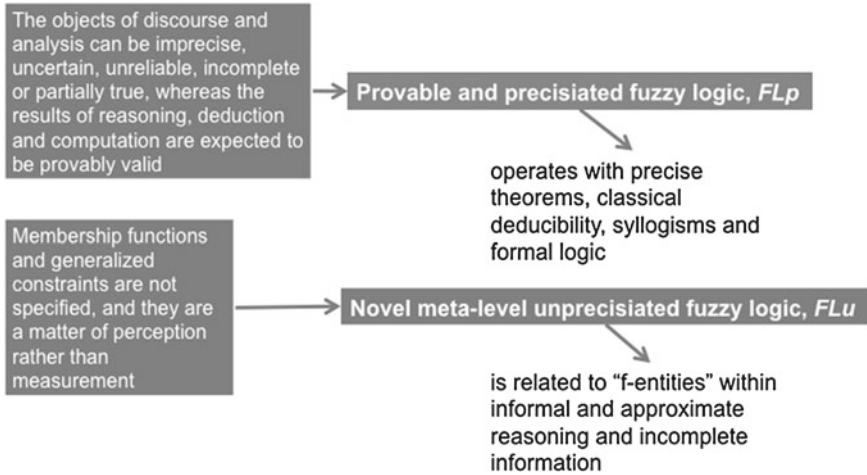
Fig. 1 Principal constituents of Zadeh's fuzzy extended logic

2 Natural Language, Approximate Reasoning and Fuzzy Extended Logic

Since the original fuzzy systems still seem to have certain bivalent commitments, Lotfi Zadeh has recently established the principles of the fuzzy extended logic, FLe, that is a combination of "traditional" provable and "precisiated" fuzzy logic, FLp, as well as a novel meta-level "unprecisiated" fuzzy logic, Flu [1]. He states that in the FLp the objects of discourse and analysis may be imprecise, uncertain, unreliable, incomplete or partially true, whereas the results of reasoning, deduction and computation are expected to be provably valid. In the Flu, in turn, the membership functions and generalized constraints are not specified, and they are a matter of perception rather than measurement.

In addition, in the FLp we use precise theorems, classical deducibility and formal logic, whereas the FLu operates with informal and approximate reasoning (Fig. 1). In practice the FLe stems from Zadeh's previous theories on information granulation, precisiated language and computing with words, as well as on the theory of perceptions [1–7].

Zadeh's ideas mean that we can apply both traditional bivalent-based and novel approximate validity, definitions, axioms, theories and explanations, inter alia. The central concept in Zadeh's f-validity is the notion of truth.

In addition to model construction, we can also apply the foregoing truth evaluation principle to theory formation, hypothesis verification and scientific explanation, inter alia [8–16]. These examinations, in turn, are based on semantical validity of reasoning, and within the FLe this means that, instead of traditional p-validity, we use approximate reasoning and other approximate entities, the f-entities. These f-entities are approximate counterparts of the corresponding traditional constructions (Fig. 2).
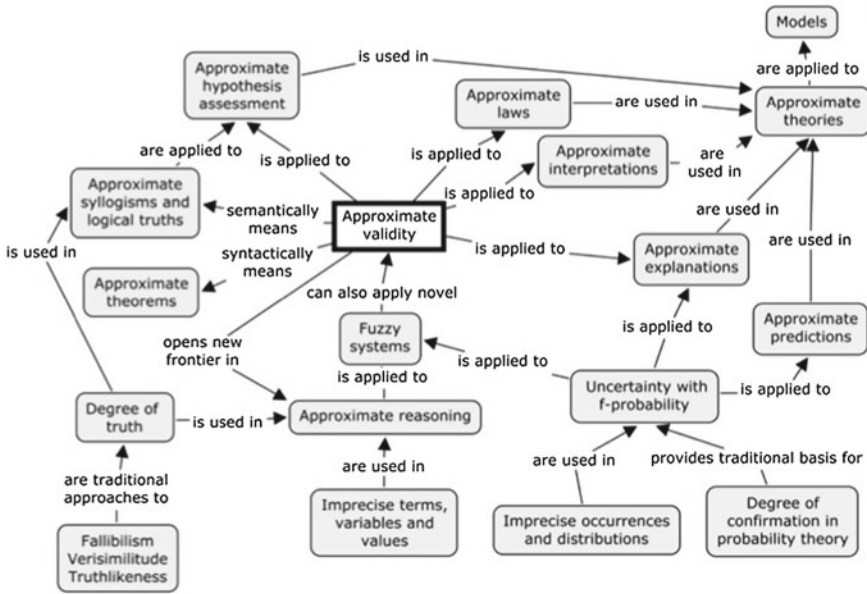
Fig. 2 A generalized version of fuzzy extended logic

The well-known fuzzified modus ponens syllogism, for example, also corresponds with Zadeh's FLe approach.

According to the FLe, our formal language should correspond well with natural language. Hence, given a problem or a description of a phenomenon in the real world, we first formulate it with natural language, and then we transform these expressions into our FLe formal language. Our formal language and their mathematical counterparts as fuzzy sets and relations, in turn, may be used in our system construction in a computer environment. This procedure is analogous to operationalization in statistics and mathematical modeling because in these contexts the original, often linguistic and imprecise, terms and hypotheses are replaced with their quantitative and numerically measurable counterparts.

A formal FLe language usually contains such linguistic variables whose values are specified by using primitive terms, linguistic modifiers (hedges), negations, connectives, quantifiers and qualifiers [2, 5, 7]. For example, if our variable is *age of persons*, we may use such values as *young*, *very young*, *not old*, *young or very young* and *some persons are old.* Hence, in a more formal manner we may state that

Age(person x) = more or less young.

In many fuzzy applications the formulations of linguistics values are more or less implicitly based on the Osgood scales (the semantic differential technique) [17, 18], and these are widely used in the human sciences. In brief, on the Osgood scales we first specify two primitive terms that are usually antonymous. Then, we use modifiers

(adverbs) for specifying the other expressions. Consider that the expressions *P* and *Q* are antonymous terms, we may thus use such linguistic scales as [17, 18]

P – more or less P – neither P nor Q (neutral value) – more or less Q – Q

We may also use such additional values as *very P* and *very Q* (usually five or seven values are sufficient). For example, given the linguistic variable *age*, the antonymous terms *P* and *Q* may be *young* and *old*, respectively.

Due to its applicability in the empirical human sciences, we adopt Osgood's approach below when we consider language formulation in the FLe.

3 Problems in Truth Valuation

3.1 Correspondence Theory of Truth

When we examine truth, in the philosophy of science we may draw a distinction between the definition (or nature) and the criteria for truth [19–22]. In the former case the mainstream approach seems to be the correspondence theory of truth in which case we assume that truth is a relation between a given language and the real world and the meanings of linguistic expressions as well as the connection between a given language and the real world are based on human conventions. In addition, the truth of a statement is determined by the real world and thus its truth is independent of our stipulations. All these examinations belong to semantics.

As regards the criteria for truth, the problem arises because truth is not a manifest property of statements, and thus it is possible that a sentence is true although we do not recognize its truth. For example, how can we assess or justify whether other persons are telling us the truth? Hence, this problem area belongs to epistemology.

In traditional logic we may actually consider various types of truths, and these are depicted in Fig. 3 [19, 22].

We focus below on the definition on truth, and in this context Alfred Tarski's approach seems to prevail [19, 20, 22]. His ideas stem from the ancient Liar's paradox in which case we have to consider the truth value of the sentence

This sentence is false.

Since this sentence may be both true and false, our paradox arises.

From Tarski's standpoint we encounter this problem because this sentence is semantically closed, and his resolution is that we should use semantically open sentences instead. In practice he draws a distinction between the object and metalanguages. The sentences submitted for truth-value assessments belong to the object language, but their truth values belong to the metalanguage. Hence, we apply the principle *truth in language L*. Tarski assumes that this provides a precise description on the connection between (natural) language and the real world. In other words, this is his definition on *truth*. In a formal manner this means that
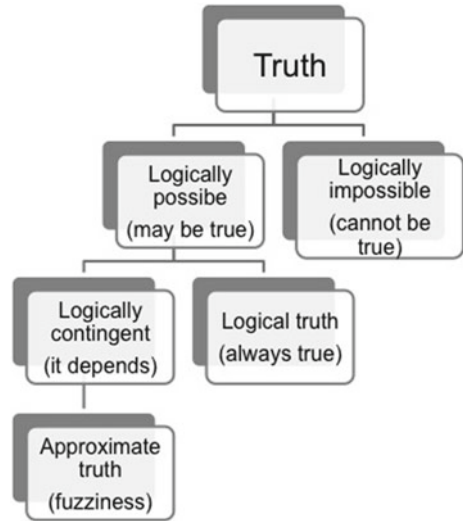
expression *x is P* is true, iff x is P.

Tarski's well-known example is

the sentence *The snow is white* is true, iff the snow is white in the real world.

In the traditional formal languages we apply this principle in the model theory in which case we examine truth in a given model.

Even though Tarski's approach has also encountered criticism [20], we will maintain it below. However, in the FLe certain modifications must be carried out, and this subject matter will be considered next.

3.2 Correspondence Theory and Fuzzy Extended Logic

Unlike in Tarski's original approach, in the FLe we apply many-valued logic, and this type of reasoning is more challenging in truth valuation. At the core of this problem area is the fact that in the FLe we may draw a distinction between antonyms and negations of terms, and this is not always possible in the bivalent logic [17, 18]. For example, the antonym of *young* is *old*, whereas the negation of *young* is *not young*, but in the bivalent case *old* may be identical with *not young*.

Hence, in the bivalent logics we often have to assume that the meaning of the expression *not P* is identical with the antonym of *P*, but in the FLe we may regard these as being distinct concepts. In the latter case *not young* includes middle-aged and old beings or objects and thus it is not identical with *old*. This idea also holds with the truth values, and thus *not true* is distinct from *false* and *not false* is distinct from *true*. In other words, *not true* means anything else but *true*, and *not false* means

Fig. 4 The scopes of the principal truth values in the fuzzy extended logic
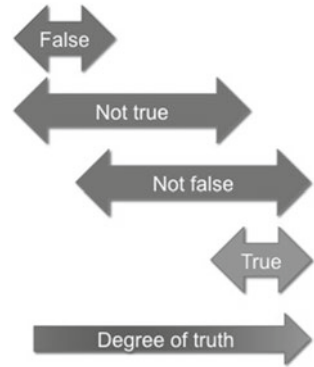
anything else but *false* (Fig. 4). It also follows that *not false* includes *true* and *not true* includes *false*, but not vice versa.

Bearing in mind our many-valued approach, we have to modify Tarski's principle for our purposes. According to Lotfi Zadeh (discussion with him in autumn 2012), we could now apply the principle

The truth-value of a term *P* is the degree of the P with reality.

Hence, in truth valuation we may apply in the FLe language the metarules

1. *x is P* is true, iff x is P
2. *x is P* is false, iff x is the antonym of P
3. *x is P* is not true, iff x is not P
4. *x is P* is not false, iff x is not the antonym of P

For example,

1. *John is young* is true, iff John is young
2. *John is young* is false, iff John is old
3. *John is young* is not true, iff John is not young
4. *John is young* is not false, iff John is not old

If we are unable to find an appropriate antonym for the expression *P*, we may use its negation.

If we assess the truth values of the modified expressions, Zadeh's version of Tarski's definition is still applicable. The author has applied fuzzy similarity relation in this context [17, 18, 23] and thus we evaluate truth according to the degrees of similarity between the given expressions and their true counterparts. True expressions have maximal and false expressions minimal degrees of similarity, respectively. In other words, we consider the similarity between the terms *P* and *Q* in the form

x is *P*, provided that x is *Q*

Fig. 5 A fuzzy-set representation of for the terms *young*, *old* and *not young*
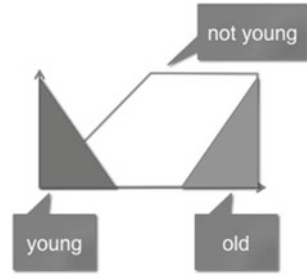
Fig. 6 Tentative fuzzy sets (numbers) for truth values when using the Osgood scale
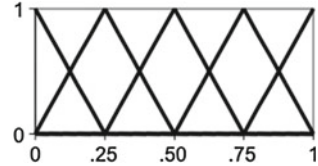
in which Q is the true counterpart of P. The higher the degree of similarity between P and Q, the closer the truth value of P is to truth. Hence, with true expressions it holds that $P = Q$.

We may apply this idea even to hypothesis verification, theory formation and scientific explanations [11–13]. For example, some Newton's physical theories are almost true because they are quite close to the corresponding (supposedly true) Einstein's theories.

For the modified expressions, we may now establish, for example,

1. *John is more or less young* is fairly true, provided that John is young.
2. *John is middle-aged* is neither true nor false ("half-true"), provided that John is young.
3. *John is more or less old* is fairly false, provided that John is young.
4. *John is old* is false, provided that John is young.
5. *John is more or less old* is neither true nor false, provided that John is more or less young.

By virtue of fuzzy similarity relation, we may operate with the foregoing linguistic values in a computer environment. If we assume that the values of the linguistic variables are appropriate fuzzy sets, we may carry out corresponding logical and mathematical operations fluently. It seems that fuzzy numbers play an essential role in this context, and then the linguistic values locate horizontally on the reference axis [24–27]. Figure 5 provides an example of this approach when the fuzzy set for the negation, not P, is the complement of P.

Within the truth values we may assume that they are fuzzy numbers from approximately zero (= false) to approximately unity (= true). Figure 6 depicts five values based on the Osgood scale, *false*, *fairly false*, *neither true nor false*, *fairly true* and *true*. Figure 7 depicts the role of negation in this context.

Fig. 7 A fuzzy-set represen-
tation of for the term *not true*
by using the complement of
the set true
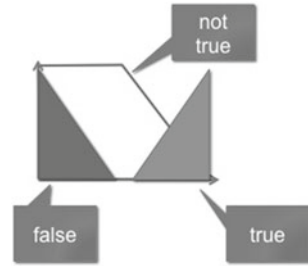
In the compound expressions with such connectives as *and* and *or*, we may first specify the truth values of their components, and then we may apply standard truth valuation [24]. This method thus corresponds to the idea on truth-functionality. For example, given the expression

John is young is fairly true *and John is heavy* is false,

the truth of *John is young and John is heavy* is min(fairly true, false) = false. In practice the extension principle [24] may be applied in this context.

At a more general level, we may apply these ideas to various problem-settings in theory formation and model construction. For example, we may use the following antonymous variable values as primitive terms in our Osgood scales

- Valid … invalid (inference)
- Confirmed … disconfirmed (hypothesis verification)
- Significant … insignificant (statistical decision making)
- Likely … unlikely (probability)
- Possible … impossible (modal logic)
- Necessary … unnecessary (modal logic)
- Informative … uninformative (semantic information)

We may also apply our framework to such approximate syllogisms as fuzzy modus ponens and modus tollens [12].

We will meet more challenges with the quantifiers. Quantifiers are such indefinite pronouns that allow us to operate with precise or imprecise "second-level" numerical concepts. In traditional predicate calculus we only use two of these "second-level functions", viz. *all* and *at least one*, and these are referred to as universal and existential quantifier, respectively [21].

In the FLe we could use *all* and *none* as the antonymous primitive quantifiers, and other tentative pronouns could be *most*, *many* and *some* [17]. Hence, we may now use the Osgood scale

none – some – many – most – all

In this context the existential quantifier would be identical with *not none*. The author has also suggested that the approximate quantifiers may denote approximate proportions in which case the foregoing pure linguistic expressions would have such numerical counterparts as approximately 0, 25, 50, 75 and 100 %, respectively.

In truth valuation we may now apply the foregoing metarules to our quantifier rules. Hence, we may establish that

All x are P is true, iff all x are P.

In other words, it holds that *x is P* is true for all individuals, *x,* in a given context or model. We may also state this that approximately 100 % of the cases, *x*, are P. For example,

All Swedes are tall is true, iff all Swedes are tall.

It follows that

1. *Most Swedes are tall* is true, iff most Swedes are tall.
2. *Many Swedes are tall* is true, iff many Swedes are tall.
3. *Some Swedes are tall* is true, iff some Swedes are tall.
4. *None Swedes are tall* is true, iff none Swedes are tall.

However, semantic and logical problems arise when we should evaluate other truth values. It still makes sense to establish that, for example,

1. *All Swedes are tall* is false, iff none Swedes are tall.
2. *All Swedes are tall* is fairly false, iff some Swedes are tall.
3. *All Swedes are tall* is fairly true, iff most Swedes are tall.

This is due to the fact that only the quantifiers varied. But the situation becomes even more complicated if the predicates can also vary, i.e., how can we assess such truth values as

1. *All Swedes are tall*, provided that all Swedes are short.
2. *All Swedes are tall*, provided that all Swedes are more or less tall.
3. *Most Swedes are tall*, provided that some Swedes are more or less tall.
4. *Some Swedes are short*, provided that many Swedes are more or less tall.

Hence, certain basic problems should be resolved in an appropriate manner when the FLe languages and their semantics are formulated. In practice we have to operate at two levels, with the predicates and the quantifiers.

We may attempt to provide one resolution. Consider the foregoing item 3, and we also use approximate percentages for the sake on conceivability. Since some (about 25 %) Swedes are more or less tall, it means that most (about 75 %) Swedes are not more or less tall. This, in turn, means that most (about 75 %) Swedes are taller or shorter than more or less tall. Hence, *most Swedes are tall* is not fairly true (i.e., true or neither true nor false or fairly false or false). This method is usable if we can transform given quantified expressions into another forms.

Another challenge is how these intuitive-based operations for quantifiers may be performed with fuzzy sets in a computer environment. The extension principle seems usable to some extent, but a truly good resolution, that provides an isomorphism between the linguistic and fuzzy-set world, is still unavailable.

4 Conclusions

We considered truth valuation within the fuzzy extended logic at meta-level from the standpoint of philosophy of science. The prevailing fuzzy systems still have some bivalent commitments, and we attempted to provide certain many-valued resolutions for them. Thanks for our enhanced truth valuation method for approximate reasoning, we may examine better such subject matters as scientific reasoning, theory formation, model construction, hypothesis verification and scientific explanation.

However, we still encounter many logico-methodological problems and meet various challenges when we attempt to specify our ideas at a more concrete level. Examples of these are quantification, probability modeling, approximate theories and approximate scientific explanations, and thus further studies are expected. By resolving these problems, we may provide a firm logical basis for our future applications as well as use more intelligible methods in the conduct of inquiry in general.

References

1. Zadeh, L.: Toward extended fuzzy logic - a first step. Fuzzy Sets Syst. **160**, 3175–3181 (2009)
2. Zadeh, L.: From computing with numbers to computing with words - from manipulation of measurements to manipulation of perceptions. IEEE Trans. Circuits Syst. **45**, 105–119 (1999)
3. Zadeh, L.: From search engines to question answering systems? the problems of world knowledge, relevance, deduction and precisiation. In: Sanchez, E. (ed.) Fuzzy Logic and the Semantic Web. Elsevier, Amsterdam (2006)
4. Zadeh, L.: Fuzzy Logic and Approximate Reasoning. Synthese **30**, 407–428 (1975)
5. Zadeh, L.: Fuzzy logic = computing with words. IEEE Trans. Fuzzy Syst. **2**, 103–111 (1996)
6. Zadeh, L.: Toward a perception-based theory of probabilistic reasoning with imprecise probabilities. J. Stat. Planning Infer. **105**(2), 233–264 (2002)
7. Zadeh, L.: Toward a theory of fuzzy information granulation and Its centrality in human reasoning and Fuzzy logic. Fuzzy Sets Syst. **90**(2), 111–127 (1997)
8. Fetzer, J.: Philosophy of Science. Paragon House, New York (1993)
9. Hempel, C.: Philosophy of Natural Science. Prentice Hall, Englewood Cliffs (1966)
10. Nagel, E.: The Structure of Science. Routledge & Kegan Paul, London (1961)
11. Niskanen, V.A.: A Meta-level approach to approximate probability. In R. Setchi et al. (Eds.): Lecture Notes in Artificial Intelligence, Vol. 6279, pp. 116–123, Springer, Heidelberg (2010)
12. Niskanen, V.A.: Application of approximate reasoning to hypothesis verification. J. Intell. Fuzzy Syst. **21**(5), 331–339 (2010)
13. Niskanen, V.A.: Application of Zadeh's impossibility principle to approximate explanation. Proceedings of the IFSA '09 Conference, 352–360, Lisbon (2009)
14. Popper, K.: The Logic of Scientific Discovery. Hutchinson, London (1959)
15. Rescher, N.: Scientific Explanation. The Free Press, New York (1970)
16. Von Wright, G.H.: Explanation and Understanding. Cornell University Press, Cornell (1971)
17. Niskanen, V.A.: Metric truth as a basis for fuzzy linguistic reasoning. Fuzzy Sets Syst. **57**(1), 1–25 (1993)
18. Niskanen, V.A.: Soft computing methods in human sciences, studies in fuzziness and soft computing, vol. 134. Springer Verlag, Berlin (2004)

19. Gadamer, H.-G.: Truth and Method. Sheed & Ward, London (1975)
20. Haack, S.: Philosophy of Logics. Cambridge University Press, Cambridge (1978)
21. Kleene, S.: Mathematical Logic. Wiley, New York (1976)
22. Niiniluoto, I.: Truthlikeness. Reidel, Dordrecht (1987)
23. Niskanen, V.A.: Fuzzy systems and scientific method - meta-level reflections and prospects. In R. Seising (Ed.) Fuzzy Set Theory - Philosophy, Logics, and Criticism, Springer, pp. 51–82 (2009)
24. Bandemer, H., Näther. Kluwer, W.: Fuzzy Data Analysis (1992)
25. Dubois, D., Prade, H.: Fuzzy sets in approximate reasoning, Part 1: inference with possibility distributions. Fuzzy Sets Syst. **40**, 143–202 (1991)
26. Approaches, Logical: Dubois, D., et al.: Fuzzy sets in approximate reasoning, Part 2. Fuzzy Sets Syst. **40**, 203–244 (1991)
27. Grzegorzewski, P., et al. (Eds.).: Soft Methods in Probability, Statistics and Data Analysis. Physica Verlag, Heidelberg (2002)

Coherence and Convexity of Euclidean Radial Implicative Fuzzy Systems

David Coufal

Abstract The chapter discuss a necessary condition for coherence of radial implicative fuzzy systems. We present the general condition in an implicit form. The condition is based on the value of the minima of a certain function. We show that this function is convex. Further an explicit solution for Euclidean systems is provided.

Keywords Fuzzy systems · Coherence · Convexity

1 Introduction

The property of *coherence* of a fuzzy system deals with the consistency of knowledge stored in the rule base the system. For *implicative fuzzy systems* this consistency means that for *any input* there always exists at least one output which is in degree 1 compatible with the given input. The notion of coherence point out the dynamical character of consistency. That is, the rule base is consistent for any input, not only for some special subset. The degree 1 compatibility is considered over the fuzzy relation representing the rule base of the system. If there is no such output, then the rule base is controversial and its rules should be revised. For example, if the system is used as a controller, then under incoherence it could happen that we end with the empty set of relevant actions. Thus the study of coherence represents a serious issue in the area of fuzzy computing [1].

To decide whether a given system is coherent on the basis of the values of its parameters is generally a difficult task. The introduction of *radial fuzzy systems*, which are the systems which employ radial fuzzy sets, allows to tackle the coherence question effectively for the class of combined systems called *radial implicative*

D. Coufal (✉)
Institute of Computer Science AS CR, Pod Vodárenskou věží 2,
182 07 Prague 8, Czech Republic
e-mail: david.coufal@cs.cas.cz

fuzzy systems [2]. The formulation of conditions of coherence in the form of a sufficient condition was presented in [3]. If this condition is satisfied, then the system is coherent, i.e., safe in the above sense of the risk of obtaining the empty output.

In this chapter we ask for how to detect incoherent systems, i.e., we ask for a necessary condition on coherence for radial implicative fuzzy systems. As a main result we state this condition explicitly for systems based on the Euclidean norm. However, in the implicit way the condition is valid for other norms as well and due to the convexity the condition can be stated also explicitly with the help of numerical optimization algorithms.

2 Radial Implicative Fuzzy Systems

The class of radial implicative fuzzy systems (radial I-FSs in short) was introduced in [2]. Let us give a brief review of the class. In radial I-FSs, IF-THEN rules are considered in MISO (multiple-input single-output) configuration. Let a rule base consist of $m \in \mathcal{N}$ IF-THEN rules. The j-th rule, $j = 1, \ldots, m$, writes as

$$A_{j1}(x_1) \star \cdots \star A_{jn}(x_n) \rightarrow B_j(y). \tag{1}$$

In the formula, A_{ji}, $i = 1, \ldots, n$, represent one-dimensional fuzzy sets specified on corresponding dimensions of n-dimensional input space $X \subseteq \mathcal{R}^n$. B_j denotes a one-dimensional fuzzy set specified on a one-dimesional output space $Y \subseteq \mathcal{R}$. The $\star$ symbol denotes a fuzzy conjunction representing AND connective and $\rightarrow$ corresponding residuated implication [4, 5] for THEN connective.

The product and minimum t-norms are typically used as fuzzy conjunctions. Corresponding residuated implications are obtained by the operation of residuation [4, 5]: $x \rightarrow_\star y = \sup\{z \in [0, 1] \,|\, z \star x \leq y\}$. The formula implies that $x \rightarrow_\star y = 1$, whenever $x \leq y$. For product or minimum, we obtain the so-called Goguen ($x \rightarrow_P y = 1$ for $x \leq y$; $x \rightarrow_P y = y/x$ for $x > y$) or Gödel implication ($x \rightarrow_M y = 1$ for $x \leq y$; $x \rightarrow_M y = y$ for $x > y$), respectively.

Individual IF-THEN rule (1) represents a fuzzy relation $R_j(x, y)$ on $\mathcal{R}^{n+1}$ space. In the short notation the rule writes as $R_j(x, y) = A_j(x) \rightarrow B_j(y)$, where $A_j(x)$ is the antecedent of the rule and $B_j(y)$ its consequent. The antecedent then read as $A_j(x) = A_{j1}(x_1) \star \cdots \star A_{jn}(x_n)$.

Individual rules are in implicative systems combined into the whole rule base by a fuzzy conjunction. The most common choice for this operation is the minimum t-norm. If the system consists of $m \in \mathcal{N}$ rules, then the whole rule base $RB(x, y)$ forms again a fuzzy relation on $\mathcal{R}^{n+1}$ space, which is specified as

$$RB(x, y) = \bigwedge_{j=1}^{m} R_j(x, y) = \min_j\{A_j(x) \rightarrow B_j(y)\}. \tag{2}$$

In radial systems, A_{ji} and B_j sets are represented by radial membership functions. Radial functions are well known from the theory of radial basis neural networks [6]. A radial function $f : \mathcal{R}^n \to \mathcal{R}$ is determined by its central point $\boldsymbol{a} \in \mathcal{R}^n$ and by a non-increasing shape function $act : \mathcal{R} \to [0, 1]$ which satisfies $act(0) = 1$ and $\lim_{z \to 0} act(z) = 0$. Finally, the application of a norm on the difference between the function's argument and its central point constitutes the final formula for a radial function as $f(x) = act(|x - a|)$ or $f(\boldsymbol{x}) = act(||\boldsymbol{x} - \boldsymbol{a}||)$ in the one-dimensional or the multi-dimensional case, respectively. In the context of radial systems, the class of scaled ℓ_p norms is relevant for parameter $p \in [1, \infty)$ (we do not consider here the limit case $p = \infty$). The norms of this class are defined for $\boldsymbol{u} \in \mathcal{R}^n$ and a vector of scaling parameters $\boldsymbol{b} = (b_1, \ldots, b_n)$, $b_i > 0$ as

$$||\boldsymbol{u}||_{\boldsymbol{b}} = \left[\sum_{i=1}^{n} (|u_i|/b_i)^p \right]^{1/p}. \tag{3}$$

The employment of radial functions for representation of membership functions in radial fuzzy systems is performed by the following specification of one-dimensional fuzzy sets

$$A_{ji}(x) = act(|x - a_{ji}|/b_{ji}), \quad B_j(y) = act(\max\{0, |y - c_j| - s_j\}/d_j) \tag{4}$$

where $a_{ji}, c_j \in \mathcal{R}$ are central points, $b_{ji}, d_j > 0$ are scaling parameters and $s_j > 0$ is a kernel's width controlling parameter. We see that the antecedent fuzzy sets are strictly radial. The formula for consequent fuzzy set is enhanced by s parameter which yields its generally trapezoid-like shape. Remark that $B_j(y)$ falls into the introduced framework of general radial functions as we can consider have $act(\max\{0, z - s_j\}/d_j)$ as another shape function.

The most prominent example of radial fuzzy sets are Gaussian fuzzy sets

$$A_{ji}(x) = \exp\left[-\frac{(x - a_{ji})^2}{b_{ji}^2} \right], \quad B_j(y) = \exp\left[-\frac{\max\{0, |y - c_j| - s_j\}^2}{d_j^2} \right]. \tag{5}$$

In Fig. 1 there are presented examples of these sets graphically.

In radial systems the combination of individual fuzzy sets by a t-norm retains the shape. That is, the following equality called *the radial property* holds

$$act\left(\frac{|x_i - a_{ji}|}{b_{j1}} \right) \star \ldots \star act\left(\frac{|x_n - a_{jn}|}{b_{jn}} \right) = act(||\boldsymbol{x} - \boldsymbol{a}_j||_{\boldsymbol{b}_j}). \tag{6}$$

In the formula on the right hand side, there is a multi-dimensional radial fuzzy set representing the antecedent of the rule $A_j(\boldsymbol{x})$. For Gaussian fuzzy sets the radial property is exhibited when the product t-norm is used and the corresponding norm is the scaled Euclidean norm ($p = 2$). Generally, shapes (act functions) cannot be
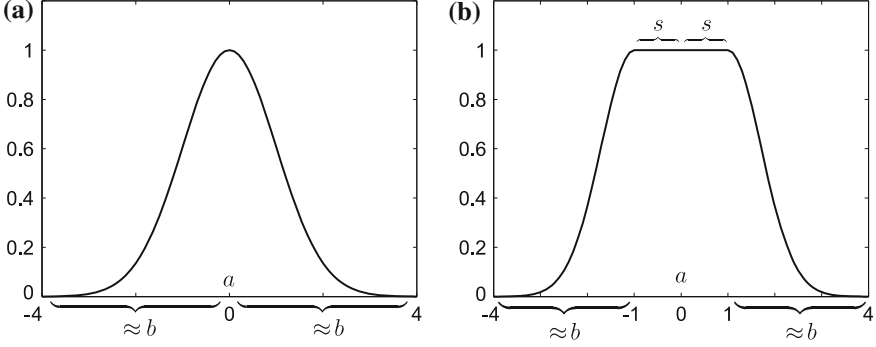
Fig. 1 An example of Gaussian radial fuzzy sets; (**a**) antecedent fuzzy set; (**b**) consequent trapezoid-like fuzzy set

combined freely with t-norms $\star$ when the validity of the radial property is required. In [7] there is proved the theorem stating the conditions on the t-norm $\star$ and the shape function act such that the radial property holds.

3 Computational Model

Computational model of radial I-FSs is based on the radial property and the basic property of residuated implications: $x \to y = 1$ iff $x \leq y$ [5].

Consider an input $\boldsymbol{x}^* \in \mathcal{R}^n$ to the system. In degree 1 compatible outputs from the j-th rule are those ys for which $A_j(\boldsymbol{x}^*) \to B_j(y) = 1$ holds. This is equivalent to the validity of inequality $A_j(\boldsymbol{x}^*) \leq B_j(y)$, and these ys are in degree 1 compatible with the fuzzy relation $R_j(\boldsymbol{x}^*, y) = A_j(\boldsymbol{x}^*) \to B_j(y)$. Due to the radial property it can be shown that the set $I_j(\boldsymbol{x}^*)$ of ys satisfiying $A_j(\boldsymbol{x}^*) \leq B_j(y)$ can be stated explicitly as

$$I_j(\boldsymbol{x}^*) = [c_j - d_j||\boldsymbol{x}^* - \boldsymbol{a}_j||_{\boldsymbol{b}_j} - s_j, \ c_j + d_j||\boldsymbol{x}^* - \boldsymbol{a}_j||_{\boldsymbol{b}_j} + s_j]. \qquad (7)$$

That is, we obtain the set of ys of interest as the closed interval with limit points specified on the basis of input $\boldsymbol{x}^*$ and parameters of the j-th rule.

Concerning the output from the whole system on the basis of formula (2), we obtain the set of compatible ys evaluating the whole rule base to degree 1 as the intersection of individual intervals $I_j(\boldsymbol{x}^*)$. Denoting the left and the right limit points of $I_j(\boldsymbol{x}^*)$ as $L(I_j(\boldsymbol{x}^*))$ and $R(I_j(\boldsymbol{x}^*))$, respectively, we have

$$I(\boldsymbol{x}^*) = \bigcap_{j=1}^{m} I_j(\boldsymbol{x}^*) = [\max_j\{L(I_j(\boldsymbol{x}^*))\}, \min_j\{R(I_j(\boldsymbol{x}^*))\}], \qquad (8)$$

under the condition $\max_j\{L(I_j(\boldsymbol{x}^*))\} \leq \min_j\{R(I_j(\boldsymbol{x}^*))\}$, otherwise $I(\boldsymbol{x}^*) = \emptyset$.

The formula (8) determines the set of in degree 1 compatible outputs of a radial implicative fuzzy system for a given input x^*. We see that the output set is again a closed interval. Practically, only one point $y^* \in I(x^*)$ is released as the output of the system. Typically, the middle point of the interval is selected.

Coherence of the systems means that for any $x^* \in \mathcal{R}^n$ we have $I(x^*) \neq \emptyset$. Note that if for some x^* it happens that there exists a pair of rules j, k such that $L(I_j(x^*)) > R(I_k(x^*))$, then $I_j(x^*) \cap I_k(x^*) = \emptyset$ and therefore $I(x^*) = \emptyset$ and the system is incoherent.

4 A Necessary Condition on Coherence of Euclidean Systems

In this section we state the necessary condition on coherence of Euclidean systems, i.e., for systems using $p = 2$ in the specification of the scaled ℓ_p norm (3). The norm occurs in the antecedents' representation formula under the validity of the radial property (6).

We start by the lemma which enables explicit computations in the main theorem. To start define for pairs of rules $j, k \in \{1, \ldots, m\}$ and corresponding scaled ℓ_p norms the following entities

$$
\begin{aligned}
J_{jk}(x) &= d_j ||x - a_j||_{b_j} + d_k ||x - a_k||_{b_k}, \\
J_{jk}^{(p)}(x) &= d_j^p ||x - a_j||_{b_j}^p + d_k^p ||x - a_k||_{b_k}^p, \\
x_{jk}^{*(p)} &= \operatorname{argmin}_x \{J_{jk}^{(p)}(x)\}.
\end{aligned}
\tag{9}
$$

The value of p is not restricted here, i.e., $p \in [1, \infty)$. However, for both norms composing J_{jk} and $J_{jk}^{(p)}$, the value of p is the same as the norms are related to the rules of the same fuzzy system.

Lemma 1. *For any* $p \in [1, \infty)$,

$$
\min_x \{J_{jk}(x)\} \leq 2[\min_x \{J_{jk}^{(p)}(x)\}]^{1/p} = 2[J_{jk}^{(p)}(x_{jk}^{*(p)})]^{1/p}.
\tag{10}
$$

If $p = 2$, then $x_{jk}^{*(2)} = (x_{jk1}^{*(2)}, \ldots, x_{jki}^{*(2)}, \ldots, x_{jkn}^{*(2)})$ *and*

$$
x_{jki}^{*(2)} = \frac{d_j^2 b_{ki}^2 a_{ji} + d_k^2 b_{ji}^2 a_{ki}}{d_j^2 b_{ki}^2 + d_k^2 b_{ji}^2}.
\tag{11}
$$

Proof. The first assertion is the corollary of the following inequality for $u, v \in \mathcal{R}$.

$$
\begin{aligned}
|u + v|^p &\leq (|u| + |v|)^p \leq 2^p \max\{|u|^p, |v|^p\} \leq 2^p (|u|^p + |v|^p), \\
|u + v| &\leq 2(|u|^p + |v|^p)^{1/p}.
\end{aligned}
\tag{12}
$$

Denoting $u(x) = d_j||x - a_j||_{b_j}$, $v(x) = d_k||x - a_k||_{b_k}$ and taking into account that both $u(x)$, $v(x) \geq 0$ we have $J_{jk}(x) = |u(x) + v(x)|$ and $J_{jk}^{(p)}(x) = |u(x)|^p + |v(x)|^p$. Applying (12) we immediately get $J_{jk}(x) \leq 2[J_{jk}^{(p)}(x)]^{1/p}$. Since the p-th root is an increasing function the application of minimum (norms are continuous) writes as $\min_x\{J_{jk}(x)\} \leq 2[\min_x\{J_{jk}^{(p)}(x)\}]^{1/p}$.

For the Euclidean norm the localization of the point of minima is based on the standard procedure of computation of partial derivatives and setting them to zero. For $p = 2$ we have

$$J_{jk}^{(2)}(x) = d_j^2 \sum_i \frac{(x_i - a_{ji})^2}{b_{ji}^2} + d_k^2 \sum_i \frac{(x_i - a_{ki})^2}{b_{ki}^2}.$$

Computing partial derivatives $\partial J_{jk}^{(2)}(x)/\partial x_i$ and setting them to zero we obtain

$$\frac{2d_j^2(x_i - a_{ji})}{b_{ji}^2} + \frac{2d_k^2(x_i - a_{ki})}{b_{ki}^2} = 0,$$

$$d_j^2 b_{ki}^2(x_i - a_{ji}) + d_k^2 b_{ji}^2(x_i - a_{ki}) = 0,$$

$$x_i(d_j^2 b_{ki}^2 + d_k^2 b_{ji}^2) - (d_j^2 b_{ki}^2 a_{ji} + d_k^2 b_{ji}^2 a_{ki}) = 0,$$

$$\frac{d_j^2 b_{ki}^2 a_{ji} + d_k^2 b_{ji}^2 a_{ki}}{d_j^2 b_{ki}^2 + d_k^2 b_{ji}^2} = x_i.$$

Using notation $x_{jki}^{*(2)}$ instead of plain x_i we get the second assertion of the lemma. $\square$

Theorem 1. *Let a radial I-FS use the Euclidean scaled norm in the specification of its rules. If the system is coherent, then the following set of inequalities holds for $j, k \in \{1, \ldots, m\}$*

$$|c_j - c_k| - (s_j + s_k) \leq 2\left[d_j^2||x_{jk}^{*(2)} - a_j||_{b_j}^2 + d_k^2||x_{jk}^{*(2)} - a_k||_{b_k}^2\right]^{1/2} \quad (13)$$

where $x_{jk}^{*(2)} = (x_{jk1}^{*(2)}, \ldots, x_{jkn}^{*(2)})$ is given by (11).

Proof. We prove the inverse implication, i.e., "if some of the above inequalities is violated, then the system is incoherent".

Suppose that for some pair of rules j, k the corresponding inequality (13) is violated, i.e.,

$$|c_j - c_k| - (s_j + s_k) > 2\left[d_j^2||x_{jk}^{*(2)} - a_j||_{b_j}^2 + d_k^2||x_{jk}^{*(2)} - a_k||_{b_k}^2\right]^{1/2}.$$

Employing notation (9) and Lemma 1 this writes as

$$|c_j - c_k| - (s_j + s_k) > 2[J_{jk}^{(2)}(x_{jk}^{*(2)})]^{1/2} \geq \min_x\{J_{jk}(x)\},$$
$$|c_j - c_k| - (s_j + s_k) > d_j||x^* - a_j||_{b_j} + d_k||x^* - a_k||_{b_k},$$

where x^* is the point at which the minimum of $J_{jk}(x)$ over $\mathcal{R}^n$ is reached.

Let $c_j - c_k \geq 0$, otherwise switch the labeling of rules. The above then writes

$$c_j - c_k - (s_j + s_k) > d_j||x^* - a_j||_{b_j} + d_k||x^* - a_k||_{b_k},$$
$$c_j - d_j||x^* - a_j||_{b_j} - s_j > c_k + d_k||x^* - a_k||_{b_k} + s_k,$$
$$L(I_j(x^*)) > R(I_k(x^*));$$

and therefore $I_j(x^*) \cap I_k(x^*) = \emptyset$, i.e., there exists an input x^* for which the system is incoherent. □

5 Convexity

By inspection of Lemma 1 and Theorem 1 we see that the core object the necessary condition is based on is the value of the minima of $J_{jk}(x)$ function. In the Euclidean systems we are able to state the upper bound on this minimum by stating the explict value of minima of $J_{jk}^{(2)}(x)$ which is reached at the point specified by formula (11).

Concerning the very value of minima of J_{jk} over $\mathcal{R}^n$, we can found it numerically by for example the Levenberg-Marquardt algorithm [8]. It helps significantly to know that J_{jk} is convex and therefore any local minimum is also the global minimum [9].

Lemma 2. *For any* $p \in [1, \infty)$ *the function* J_{jk} *of* (9) *is convex, i.e., for any* $x_1, x_2 \in \mathcal{R}^n, \alpha \in [0, 1], \beta = 1 - \alpha$ *we have* $J_{jk}(\alpha x_1 + \beta x_2) \leq J_{jk}(\alpha x_1) + J_{jk}(\beta x_2)$.

Proof. J_{jk} is specified as the sum of two different scaled norms. The value of p is the same but the scaling parameters b_j, b_k generally differ. However, for each of the scaled norms the basic norm's properties hold (a scaled ℓ_p norm is the norm in the standard sense) and we have

$$J_{jk}(\alpha x_1 + \beta x_2) = ||\alpha x_1 + \beta x_2 - a_j||_{b_j} + ||\alpha x_1 + \beta x_2 - a_k||_{b_k}$$
$$= ||\alpha(x_1 - a_j) + \beta(x_2 - a_j)||_{b_j} + ||\alpha(x_1 - a_k) + \beta(x_2 - a_k)||_{b_k}$$
$$\leq \alpha||(x_1 - a_j)||_{b_j} + \beta||(x_2 - a_j)||_{b_j} +$$
$$+ \alpha||(x_1 - a_k)||_{b_k} + \beta||(x_2 - a_k)||_{b_k}$$
$$\leq \alpha J_{jk}(x_1) + \beta J_{jk}(x_2). \qquad \square$$

Due to the convexity of J_{jk} it is reasonable to use some procedure of numerical optimization to search for approximation of $J_{jk}^* = \min_x\{J_{jk}(x)\}$. For any pair of rules $j, k \in \{1, \ldots, m\}$ denote by J_{jk}^{*n} the value of minima found by numerical

optimization and by $\boldsymbol{x}_j^{*n}$ the point where J_{jk}^{*n} is reached. Then the following lemma applies.

Lemma 3. *If the radial I-FS is coherent, then* $|c_j - c_k| - (s_j + s_k) \leq J_{jk}^{n*}$ *holds for any pair of rules* $j, k \in \{1, \ldots, m\}$.

Proof. The proof follows the proof of Theorem 1 with the $\min_{\boldsymbol{x}}\{J_{jk}(\boldsymbol{x})\}$ replaced by J_{jk}^{*n} and $\boldsymbol{x}^*$ by $\boldsymbol{x}^{n*}$. $\qquad \square$

6 Conclusions

In the paper we have stated an explicit necessary condition for an Euclidean radial implicative system to be coherent. In fact, in implicit form the condition can be extended for non-Euclidean systems, i.e., for other $p \in [1, \infty)$ than $p = 2$. In this case it reads as

$$|c_j - c_k| - (s_j + s_k) \leq J_{jk}^* = \min_{\boldsymbol{x}}\{J_{jk}(\boldsymbol{x})\}. \tag{14}$$

However, here we do not have an explicit formula for computing the value of minima of $J_{jk}(\boldsymbol{x})$ over $\mathcal{R}^n$ or at least its reasonable upper bound as in the Euclidean case. On the other hand, due to the convexity of J_{jk} we can rely on numerical optimization procedures and replace J_{jk}^* by its numerical approximation.

In the future research we aim at the further inspection of convexity of J_{jk} function in order to get more insight whether or not we are able to state the value of J_{jk}^* in some explicit form.

References

1. Dubois, D., Prade, H., Ughetto, L.: Checking the coherence and redundancy of fuzzy knowledge bases. IEEE Trans. Fuzzy Syst. **5**(3), 398–417 (1997)
2. Coufal D.: Radial implicative fuzzy systems. In: Proceedings of IEEE International Conference on Fuzzy Systems (FUZZ-IEEE 2005), pp. 963–968, Reno, Nevada, USA (2005)
3. Coufal D.: Coherence of radial implicative fuzzy Systems In: Proceedings of IEEE International Conference on Fuzzy Systems (FUZZ-IEEE), pp. 903–970, Vancouver, Canada (2006)
4. Klir, G.J., Yuan, B.: Fuzzy sets and Fuzzy logic. Theory and Applications. Prentice Hall, India (1995)
5. Hájek, P.: Metamathematics of Fuzzy Logic. Kluwer Academic Publishers, Dordrecht (1998)
6. Haykin, S.O.: Neural Networks and Learning Machines. Prentice Hall, NJ (2008)

7. Coufal D.: Representation of continuous archimedean radial fuzzy systems. In: Proceedings of International Fuzzy Systems Association World Congress (IFSA), pp. 1174–1179, Beijing, China (2005)
8. Press W.H. et al.: Numerical Recipes 3rd Edition: The Art of Scientific Computing. Cambridge University Press, NY (2007)
9. Boyd, S., Vandenberghe, L.: Convex Optimization. Cambridge University Press, NY (2004)

Part II
Fuzzy Systems: Application

Catastrophe Bond Pricing with Fuzzy Volatility Parameters

Piotr Nowak and Maciej Romaniuk

Abstract The number of natural catastrophes and losses caused by them increase in time. The damages caused by natural disasters are difficult to handle for insurers. Therefore catastrophe bonds were introduced to transfer the catastrophic risk to financial markets. In this paper we continue our research concerning catastrophe bond pricing. In our approach we use stochastic analysis and fuzzy sets theory in order to obtain catastrophe bond pricing formulas. To model the short interest rate we use the one- and two-factor Vasicek model. We take into account different sources of uncertainty, not only the stochastic one. In particular, we treat the volatility of the interest rate and market price of risk as fuzzy numbers. We use Monte Carlo simulations for data describing natural catastrophic events in the United States to illustrate the obtained results.

Keywords Catastrophe bonds · Financial mathematics · Fuzzy sets theory · Monte Carlo simulations · Vasicek model

1 Introduction

The frequency of natural catastrophes and size of economic losses caused by them rose over time and this tendency is expected to continue. Such catastrophes often hit densely populated areas and result in damages of high value. Well known examples are Hurricane Andrew (1992) with losses estimated at $30 billion or the 1997 Oder

P. Nowak (✉) · M. Romaniuk
Systems Research Institute Polish Academy of Sciences,
ul. Newelska 6, 01-447 Warszawa, Poland
e-mail: pnowak@ibspan.waw.pl

M. Romaniuk
The John Paul II Catholic University of Lublin, Lublin, Poland
e-mail: mroman@ibspan.waw.pl

Flood, which affected Poland, Germany and the Czech Republic, causing material damages estimated at \$4.5 billion.

The classical insurance model deals with high-frequency, low-severity losses (for example automobile collisions), where an insurer can assume that the law of large numbers is fulfilled. And applying this assumption it is possible to calculate the insurance premium and estimate the probability of the insurer bankruptcy. For insurers low-frequency, high-severity losses caused by natural disasters are difficult to handle. High value catastrophic damages can lead directly to their bankruptcy. Therefore new financial and insurance mechanisms are needed. One of them are catastrophe bonds (commonly called cat bonds). Cat bonds are financial instruments, which enable to transfer the natural catastrophe risk to financial markets. The payoff received by the cat bond holder is connected with the occurrence of some natural catastrophe in a specified region at a fixed time interval. Such an event is called the triggering point. The catastrophe bond payoff structure depends also on an underlying asset (e.g. LIBOR).

This paper is continuation of earlier research concerning catastrophe bond pricing. In our approach stochastic analysis and fuzzy sets theory are employed to obtain cat bond pricing formula. We consider stochastic processes with continuous time and finite time horizon. We apply Brownian motion to model the risk-free spot interest rate r and compound Poisson process to describe natural catastrophe losses. We use the one- and two-factor Vasicek model for description of the interest rate behavior. The two-factor Vasicek model (introduced by Hull and White) is a generalization of its one-factor counterpart. It contains an additional stochastic process describing deviation of the current view on the long-term level of r from its average view. We also consider two complex forms of catastrophe bond payoff functions: a stepwise one and a piecewise linear one. We assume the absence of arbitrage on the financial market and neutral attitude of investors to catastrophe risk.

Fuzzy arithmetic applied in the paper enables us to take into account different sources of uncertainty, not only the stochastic one. In order to obtain the catastrophe bond valuation formula in case of lack of precise data we apply fuzzy volatility parameters of the spot interest rate. Additionally, we treat the market price of risk as a fuzzy number. Price obtained by us has the form of fuzzy number. For a given α (e.g. $\alpha = 0.95$ or $\alpha = 0.99$) its α-level set can be interpreted by a financial analyst as the interval of the cat bond prices and can be used for investment decision-making. Similar approach was applied to option pricing in [12] and [19].

The paper is organized as follows. In Sect. 2 features of catastrophe bonds are presented. Section 3 contains basic notations and definitions concerning catastrophe bonds pricing model and valuation formulas. Section 4 is devoted to catastrophe bond pricing with fuzzy volatility and market price of risk parameters. Valuation formulas are preceded by preliminaries on fuzzy and interval arithmetic. In Sect. 5 Monte Carlo simulations are conducted to illustrate the mentioned theoretical results. Finally, Sect. 6 contains conclusions.

2 Features of Catastrophe Bonds

The insurance industry faces overwhelming risks caused by natural catastrophes, e.g. losses from mentioned earlier Hurricane Andrew hit USD 30 billion in 1992, the losses from Hurricane Katrina in 2005 are estimated at USD 40–60 billion (see [9]). Additionally, after Hurricane Andrew more than 60 insurance companies became insolvent.

Apart from problems with coverage of losses by insurance enterprises, there are known issues with dependencies among sources of risks, threats of potentially unlimited losses, problems with adverse selection, moral hazard and reinsurance pricing cycles. Therefore applying alternative financial or insurance instruments instead of classical insurance mechanisms may be profitable. The problem is to "package" natural disasters risk and appropriate losses into classical forms of tradable financial assets, like bonds or options. The most popular catastrophe-linked security is the catastrophe bond, known also as *cat bond* or *Act-of-God* bond (see, e.g. [3, 5, 11]). Cat bonds were introduced in 1992, and become wider known in April 1997, when USAA, an insurer from Texas, initiated two new classes of cat bonds: A-1 and A-2 (see [10]).

There is one important difference between cat bonds and "classical" (i.e. strictly financial) bonds—the premiums from cat bond are always connected with an additional random variable, i.e. occurrence of some natural catastrophe in specified region and fixed time interval. Such an event is called *triggering point* (see [5]). For example, the A-1 USAA bond was connected with hurricane on the east coast of USA between July 15, 1997 and December 31, 1997. If there had been a hurricane in mentioned above region with more than $1 billion loses against USAA, the coupon of the bond would have been lost. As we can see from this example, the triggering point changes the structure of payments for the cat bond.

The cat bonds may depend on various kinds of triggering points—e.g. may be connected with the issuer's actual losses (e.g. losses from a flood), losses modelled by special software based on real parameters of a catastrophe, the insurance industry index, real parameters of a catastrophe (e.g. earthquake magnitude, windspeeds in case of windstorms) or the hybrid index related to modelled losses.

As in case of standard bonds, the structure of payments for cat bonds depends also on some primary underlying asset. In case of A-1 USAA bond, the payment equalled LIBOR (London Interbank Offered Rate) plus 282 basis points.

The main aim of cat bonds is to transfer *risk* from insurance markets or governmental budgets to financial markets. Apart from transferring capital, a liquid catastrophe derivatives market allows insurance and reinsurance companies to adjust their exposure to natural catastrophic risk dynamically through hedging with those contracts at lower transaction costs. If the triggering point is connected with industry loss indices or parametric triggers, the moral hazard exposure of bond investors is greatly reduced or eliminated. Cat bonds are often rated by an agency such as Standard and Poor's, Moody's, or Fitch Ratings.
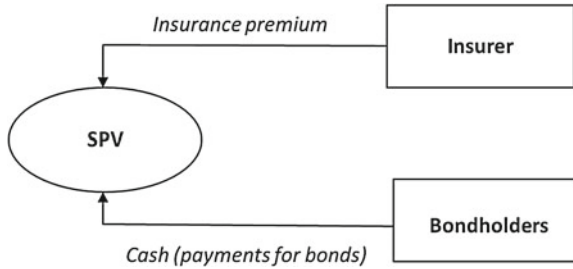
Fig. 1 Cash flows during issuing of cat bonds
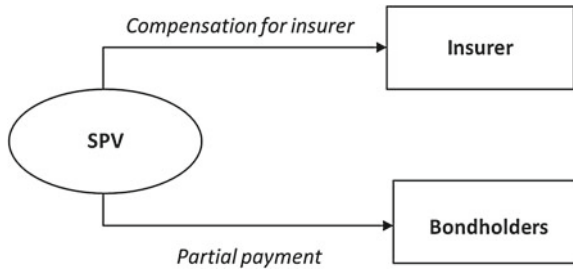
Fig. 2 Cash flows if the triggering point occurs

Fig. 3 Cash flows if the triggering point does not occur

The cash flows for catastrophe bond are managed by special tailor-made fund, called a special-purpose vehicle (SPV) (see [18]). The hedger (e.g. insurer) pays an insurance premium in exchange for coverage in case if catastrophic event occurs. The investors purchase an insurance-linked security for cash. The mentioned premium and cash flows are directed to SPV (see Fig. 1), which issues the catastrophe bonds. Usually, SPV purchases safe securities in order to satisfy future possible demands. Investors hold the issued assets whose coupons and/or principal depend on occurrence of the triggering point. If the pre-specified event occurs during the fixed period, the SPV compensates the insurer and the cash flows for investors are changed, i.e. there is full or partial forgiveness of the repayment of principal and/or interest (see Fig. 2). If the triggering point does not occur, the investors usually receive the full payment (see Fig. 3).

3 Catastrophe Bond Pricing in Crisp Case

3.1 Definitions and Notations

In this section we introduce pricing formulas for catastrophe bonds in crisp case. We begin with notations and basic definitions concerning catastrophe bonds and their pricing. We define stochastic processes with continuous time to describe the dynamics of the spot interest rate and the cumulative catastrophe losses. Time horizon has the form $[0, T']$, where $T' > 0$. The date of maturity of catastrophe bonds T is not later than T', i.e. $T \leq T'$. We consider two probability measures: P and Q and by E^P and E^Q we denote the expectations with respect to them. Stochastic processes and random variables are defined with respect to the probability P.

Let $W_t = \left(W_t^1, W_t^2, \ldots, W_t^n \right)_{t \in [0, T']}$ be n-dimensional standard Brownian motion and let $(N_t)_{t \in [0, T']}$ be Poisson process with intensity κ. The Brownian motion (for $n = 1$ and $n = 2$) will be used for description of the risk-free interest rate.

Let $(U_i)_{i=1}^{\infty}$ be random variables of the same distribution and finite second moment. We treat U_i as the value of losses during ith catastrophic event.

We define compound Poisson process by formula

$$\tilde{N}_t = \sum_{i=1}^{N_t} U_i, t \in \left[0, T' \right].$$

It will be used to model the cumulative catastrophic losses till moment t.

Filtration $(F_t)_{t \in [0, T']}$ is generated by the Brownian motion and the Poisson process. Moreover, we assume that F_0 is generated by sets of P-probability zero and that $(W_t)_{t \in [0, T']}$, $(N_t)_{t \in [0, T']}$ and $(U_i)_{i=1}^{\infty}$ are independent. Then probability space with filtration $\left(\Omega, F, (F_t)_{t \in [0, T']}, P \right)$ satisfies the standard assumptions, i.e. σ-field F is P-complete, filtration $(F_t)_{t \in [0, T']}$ is right continuous and F_0 contains all sets of P-probability zero.

Let $(B_t)_{t \in [0, T']}$ be the banking account process of the form

$$B_t = \exp \left(\int_0^t r_u du \right), t \in \left[0, T' \right],$$

where r is the risk-free interest rate.

We denote by symbol $B(t, T)$ the price at the moment t of zero-coupon bond with the maturity date $T \leq T'$ and with the face value equal to 1.

In our model we assume that investors have neutral attitude to catastrophe risk and that interest rate changes are replicable by other financial instruments. Moreover, we assume that there is no arbitrage opportunity on the market.

Definition 1. *The family $\{B(t, T), t \leq T \leq T'\}$ is called arbitrage-free family of zero-coupon bond prices with respect to r, if the following conditions hold.*

1. $B(T, T) = 1$ for each $T \in [0, T']$.
2. There exists a probability measure Q, equivalent to P, such that for each $T \in [0, T']$, the process of the discounted price of the zero-coupon bond

$$B(t, T)/B_t, t \in [0, T],$$

   is a martingale with respect to Q.

Let $\bar{\lambda}_t = (\bar{\lambda}_{1t}, \bar{\lambda}_{2t}, \ldots, \bar{\lambda}_{nt})$ be the n-dimensional market price of risk process. In our pricing model we assume that $\bar{\lambda}_{1t} = \lambda_1, \bar{\lambda}_{2t} = \lambda_2, \ldots, \bar{\lambda}_{nt} = \lambda_n$ are constant. Radon-Nikodym derivative of the following form defines probability measure Q equivalent to P:

$$\frac{dQ}{dP} = \exp\left(-\int_0^T \bar{\lambda}_t dW_t - \frac{1}{2}\int_0^T \|\bar{\lambda}_t\|^2 dt\right), \, P - a.s. \tag{1}$$

where $\|.\|$ is the Euclidean norm in R^n. For Q the family $B(t, T)$, $t \le T \le T'$, is arbitrage-free family of zero-coupon bond prices with respect to r.

We consider two types of catastrophe bonds with different payoff structures.

Let $0 < K_1 < ... < K_n$, $n \ge 1$, be levels of catastrophic losses. Let $\tau_i : \Omega \to [0, T']$, $1 \le i \le n$ be sequence of stopping times of the form

$$\tau_i(\omega) = \inf_{t \in [0, T']}\left\{\tilde{N}(t)(\omega) > K_i\right\} \wedge T', \, 1 \le i \le n.$$

Let $w_1, w_2, \ldots, w_n \ge 0$ and $\sum_{i=1}^n w_i \le 1$. Let $\Phi = \sum_{i=1}^n w_i \Phi_i$, where Φ_i are cumulative distribution functions of τ_i. We will use function Φ in pricing formulas.

Definition 2. By the symbol $IB_s(T, Fv)$ we denote catastrophe bond with the face value Fv, the date of maturity and payoff T and the payoff function of the form

$$\nu_{IB_s(T, Fv)} = Fv\left(1 - \sum_{i=1}^n w_i I_{\tau_i \le T}\right).$$

From the above definition it follows that the catastrophe bond payoff function is a stepwise function of cumulative losses $\tilde{N}_T$. If the catastrophe does not occur in the period $[0, T]$ (i.e. if $\tau_1 > T$), the bondholder is paid the face value Fv. If $\tau_n \le T$, the bondholder receives the face value minus the sum of write-down coefficients in percentage $Fv(1 - \sum_{i=1}^n w_i)$. Finally, if $\tau_{k-1} \le T < \tau_k$, $1 < k \le n$, the bondholder is paid $Fv(1 - \sum_{i=1}^{k-1} w_i)$.

To define the second type of catastrophe bond we introduce an additional constant $0 \le K_0 < K_1$.

Definition 3. By the symbol $IB_p(T, Fv)$ we denote catastrophe bond with the face value Fv, the date of maturity and payoff T and the payoff function of the form

$$\nu_{IB_p(T,Fv)} = Fv \left(1 - \sum_{j=0}^{n-1} \frac{\tilde{N}_T \wedge K_{j+1} - \tilde{N}_T \wedge K_j}{K_{j+1} - K_j} w_{j+1} \right).$$

For this type of catastrophe bond the payoff function is a piecewise linear function of $\tilde{N}_T$. Analogously to previous case, if the catastrophe does not occur ($\tilde{N}_T < K_0$), the bondholder receives the payoff equal to its face value Fv. If $\tilde{N}_T \geq K_n$, the payoff equals $Fv \left(1 - \sum_{i=1}^{n} w_i \right)$. If $K_j \leq \tilde{N}_T \leq K_{j+1}$ for $j = 0, 1, \ldots, n$, the bondholder is paid

$$Fv \left(1 - \sum_{0 \leq i < j} w_{i+1} - \frac{\tilde{N}_T \wedge K_{j+1} - \tilde{N}_T \wedge K_j}{K_{j+1} - K_j} w_{j+1} \right)$$

and when $\tilde{N}_T$ increases in the interval $[K_j, K_{j+1}]$ the payoff decreases linearly from $Fv \left(1 - \sum_{0 \leq i < j} w_{i+1} \right)$ to $Fv \left(1 - \sum_{0 \leq i \leq j} w_{i+1} \right)$.

We consider two risk-free interest rate models. The first one is the one-factor Vasicek model. The interest rate r satisfies the following stochastic equation

$$dr_t = a(b - r_t) dt + \sigma dW_t \tag{2}$$

for positive constants a, b and σ. The process r_t is mean-reverting. If we assume infinite time horizon,

$$\lim_{T \to \infty} E(r_T | F_t) = b;$$

and

$$\lim_{T \to \infty} D^2(r_T | F_t) = \frac{\sigma^2}{2a}.$$

The parameter b is called the long-term level of the interest rate.

The second model of the interest rate is the two-factor Vasicek model, which was introduced by Hull and White. The interest rate process r is Gaussian and it satisfies the following stochastic equations

$$dr_t = (a_r b_r + \varepsilon_t - a_r r_t) dt + \sigma_r dW_t^1;$$
$$d\varepsilon_t = -a_\varepsilon \varepsilon_t dt + \sigma_\varepsilon \rho dW_t^1 + \sigma_\varepsilon \sqrt{1 - \rho^2} dW_t^2.$$

All the parameters (except the correlation coefficient ρ) in the above equations are positive. The process $(\varepsilon_t)_{t \in [0,T']}$ represents the deviation of the current view on the long-term level of the interest rate $(r_t)_{t \in [0,T']}$. The parameter $\rho \in [-1, 1]$ is the correlation coefficient between changes in the interest rate and changes in the process ε.

3.2 Pricing Formulas

We present catastrophe bonds pricing formulas. Their form depend on the model of
the risk-free interest rate and the cat bond payoff structure. The following theorem
concerns the case of the one-factor Vasicek interest rate model.

Theorem 1. *Assume that IB_s (0) and IB_p (0) are prices of bonds IB_s (T, Fv) and
IB_p (T, Fv) at moment* 0. *Then*

$$IB_s (0) = Fve^{-T \cdot R(T,r_0)} \{1 - \Phi (T)\} \tag{3}$$

and

$$IB_p (0) = e^{-T \cdot R(T,r_0)} E^P \nu_{IB_p(T,Fv)}, \tag{4}$$

where

$$R (\theta, r) = R_\infty - \frac{1}{a\theta} \left\{ (R_\infty - r) \left(1 - e^{-a\theta} \right) - \frac{\sigma^2}{4a^2} \left(1 - e^{-a\theta} \right)^2 \right\}$$

and

$$R_\infty = b - \frac{\lambda\sigma}{a} - \frac{\sigma^2}{2a^2}.$$

For proofs of (3) and (4) we refer the reader to [13] and [14].

    The following theorem, proved in [15], contains analogous catastrophe bond pric-
ing formulas in case of the two-factor Vasicek interest rate model.

Theorem 2. *Assume that IB_s (0) and IB_p (0) are prices of bonds IB_s (T, Fv) and
IB_p (T, Fv) at moment* 0 *for the interest rate described by the two-factor Vasicek
model. Then*

$$IB_s (0) = Fv \exp (-a (T) - b_1 (T) r_0 - b_2 (T) \varepsilon_0) \{1 - \Phi (T)\} \tag{5}$$

and

$$IB_p (0) = \exp (-a (T) - b_1 (T) r_0 - b_2 (T) \varepsilon_0) E^P \nu_{IB_p(T,Fv)}, \tag{6}$$

where $\hat{\varphi} = a_r b_r - \lambda_1 \sigma_r$,

$$a (\tau) = \frac{\hat{\varphi}}{a_r} (\tau - b_1 (\tau)) - \frac{1}{a_r^2} \left(\frac{1}{2}\sigma_r^2 - \frac{\rho\sigma_r\sigma_\varepsilon}{a_r - a_\varepsilon} + \frac{\sigma_\varepsilon^2}{2 (a_r - a_\varepsilon)^2} \right)$$

$$\cdot (\tau - b_1 (\tau) - a_r b_1^2 (\tau) /2) - \frac{\sigma_\varepsilon^2}{4a_\varepsilon^3 (a_r - a_\varepsilon)} \left(2\tau a_\varepsilon - 3 + 4e^{-a_\varepsilon\tau} - e^{-2a_\varepsilon\tau} \right)$$

$$- \frac{\rho\sigma_r\sigma_\varepsilon}{a_r a_\varepsilon (a_r - a_\varepsilon)} \left(\tau - b_1 (\tau) - \frac{1 - e^{-a_\varepsilon\tau}}{a_\varepsilon} + \frac{1 - e^{-(a_r+a_\varepsilon)\tau}}{a_r + a_\varepsilon} \right),$$

$$b_1(\tau) = \frac{1}{a_r}\left(1 - e^{-a_r\tau}\right) \quad and$$

$$b_2(\tau) = \frac{1}{a_r(a_r - a_\varepsilon)}e^{-a_r\tau} - \frac{1}{a_\varepsilon(a_r - a_\varepsilon)}e^{-a_\varepsilon\tau} + \frac{1}{a_r a_\varepsilon}.$$

To obtain the above valuation formulas we applied the martingale method. As the equivalent martingale measure we used probability Q, described by formula (1). All assumptions concerning financial market, mentioned in the previous subsection, were used in the proof.

4 Catastrophe Bond Pricing in Fuzzy Case

4.1 Fuzzy and Interval Arithmetic

Now we recall some basic facts concerning fuzzy and interval arithmetic.

Let $\tilde{A}$ be a fuzzy subset of the set of real numbers R. We denote by $\mu_{\tilde{A}}$ its membership function $\mu_{\tilde{A}} : R \rightarrow [0, 1]$, and by $\tilde{A}_\alpha = \{x : \mu_{\tilde{A}}(x) \geq \alpha\}$ the α-level set of $\tilde{A}$, where $\tilde{A}_0$ is the closure of the set $\{x : \mu_{\tilde{A}}(x) > 0\}$.

Let $\tilde{a}$ be a fuzzy number (in particular let $\mu_{\tilde{a}}$ be upper semicontinuous). Then the α-level set $\tilde{a}_\alpha$ is a closed interval, which can be denoted by $\tilde{a}_\alpha = [\tilde{a}_\alpha^L, \tilde{a}_\alpha^U]$.

We recall the arithmetic of fuzzy numbers. Let $\odot$ be a binary operator $\oplus$, $\ominus$, $\otimes$ or $\oslash$ between fuzzy numbers $\tilde{a}$ and $\tilde{b}$, where the binary operators correspond to $\circ$: $+$, $-$, $\times$ or $/$, according to the extension principle. Let $\odot_{int}$ be a binary operator $\oplus_{int}$, $\ominus_{int}$, $\otimes_{int}$ or $\oslash_{int}$ between two closed intervals $[a, b]$ and $[c, d]$.

Then $[a, b] \odot_{int} [c, d] = \{z \in R : z = x \circ y, x \in [a, b], y \in [c, d]\}$, where $\circ$ is usual operation $+$, $-$, $\times$ and $/$, if the interval $[c, d]$ does not contain zero in the last case. Therefore, if $\tilde{a}$, $\tilde{b}$ are fuzzy numbers, then $\tilde{a} \odot \tilde{b}$ is also a fuzzy number and it is defined via its α-level sets by

$$(\tilde{a} \oplus \tilde{b})_\alpha = \tilde{a}_\alpha \oplus_{int} \tilde{b}_\alpha = \left[\tilde{a}_\alpha^L + \tilde{b}_\alpha^L, \tilde{a}_\alpha^U + \tilde{b}_\alpha^U\right],$$

$$(\tilde{a} \ominus \tilde{b})_\alpha = \tilde{a}_\alpha \ominus_{int} \tilde{b}_\alpha = \left[\tilde{a}_\alpha^L - \tilde{b}_\alpha^U, \tilde{a}_\alpha^U - \tilde{b}_\alpha^L\right],$$

$$(\tilde{a} \otimes \tilde{b})_\alpha = \tilde{a}_\alpha \otimes_{int} \tilde{b}_\alpha$$
$$= \left[\min\left\{\tilde{a}_\alpha^L\tilde{b}_\alpha^L, \tilde{a}_\alpha^L\tilde{b}_\alpha^U, \tilde{a}_\alpha^U\tilde{b}_\alpha^L, \tilde{a}_\alpha^U\tilde{b}_\alpha^U\right\}, \max\{\tilde{a}_\alpha^L\tilde{b}_\alpha^L, \tilde{a}_\alpha^L\tilde{b}_\alpha^U, \tilde{a}_\alpha^U\tilde{b}_\alpha^L, \tilde{a}_\alpha^U\tilde{b}_\alpha^U\}\right],$$

$$(\tilde{a} \oslash \tilde{b})_\alpha = \tilde{a}_\alpha \oslash_{int} \tilde{b}_\alpha$$
$$= \left[\min\left\{\tilde{a}_\alpha^L/\tilde{b}_\alpha^L, \tilde{a}_\alpha^L/\tilde{b}_\alpha^U, \tilde{a}_\alpha^U/\tilde{b}_\alpha^L, \tilde{a}_\alpha^U/\tilde{b}_\alpha^U\right\}, \max\{\tilde{a}_\alpha^L/\tilde{b}_\alpha^L, \tilde{a}_\alpha^L/\tilde{b}_\alpha^U, \tilde{a}_\alpha^U/\tilde{b}_\alpha^L, \tilde{a}_\alpha^U/\tilde{b}_\alpha^U\}\right],$$

if α-level set $\tilde{b}_\alpha$ does not contain zero for all $\alpha \in [0, 1]$ in the case of $\oslash$.

A triangular fuzzy number $\tilde{a} = (a_1, a_2, a_3)$ is a fuzzy number with the membership function of the form

$$\mu_{\tilde{a}}(x) = \begin{cases} \frac{x-a_1}{a_2-a_1} & \text{if } a_1 \leq x \leq a_2 \\ \frac{x-a_3}{a_2-a_3} & \text{if } a_2 \leq x \leq a_3 \\ 0 & \text{otherwise.} \end{cases}$$

4.2 Pricing Formulas

Some parameters of the financial market are not precisely known. In particular, the market price of risk and volatility parameters of the risk-free interest rate are uncertain and in many situations this uncertainty does not have stochastic character. They are determined by the market which fluctuates from time to time. Therefore it is unreasonable to choose fixed values of parameters, obtained from historical data, for later use in pricing model, since they can fluctuate in future (see e.g. [19]).

To estimate values of the mentioned parameters we can use knowledge of experts and regard the market price of risk and the volatility parameters as fuzzy numbers. We can ask an expert for a forecast of a parameter. In the best case the expert will provide three numbers: the smallest possible value, the greatest possible value and the most likely value of the parameter. Then we can transfer this opinion into a triangular fuzzy number (p_1, p_2, p_3), where p_1 is the minimum estimate, p_3 is the maximum estimate and p_2 is the estimate having the greatest possibility of complying. If it is possible to receive opinions of N experts (where $N > 1$) we can transfer them into triangular fuzzy numbers $\left(p_1^{(i)}, p_2^{(i)}, p_3^{(i)}\right)_{i=1}^{N}$, compute the average triangular fuzzy number

$$\left(\frac{\sum_{i=1}^{N} p_1^{(i)}}{N}, \frac{\sum_{i=1}^{N} p_2^{(i)}}{N}, \frac{\sum_{i=1}^{N} p_3^{(i)}}{N}\right)$$

and use it for estimation of the parameter. Such an estimation method was proposed in [1] and [6] for financial applications.

In what follows we assume more generally that the mentioned above parameters are fuzzy numbers, which are not necessarily triangular. In particular, we introduce fuzzy numbers $\tilde{\sigma}$, $\tilde{\sigma}_r$, $\tilde{\sigma}_\varepsilon$, $\tilde{\lambda}$ and $\tilde{\lambda}_1$ in place of their real counterparts σ, σ_r, σ_ε, λ and λ_1. We assume that $\tilde{\sigma}$, $\tilde{\sigma}_r$ and $\tilde{\sigma}_\varepsilon$ are non-negative fuzzy numbers, i.e. their membership functions are equal to 0 for all negative arguments.

Let $\mathcal{F}(R)$ be the set of all fuzzy numbers. In the further part of this section we will use the following proposition, proved in [19].

Proposition 1. *Let $f : R \to R$ be a function such that for each $r \in R$ $\{x : f(x) = r\}$ is a compact set. Then f induces a fuzzy-valued function $\tilde{f} : \mathcal{F}(R) \to \mathcal{F}(R)$ via the extension principle and for each $\tilde{\Lambda} \in \mathcal{F}(R)$ the α-level set of $\tilde{f}(\tilde{\Lambda})$ has the form $\tilde{f}(\tilde{\Lambda})_\alpha = \{f(x) : x \in \tilde{\Lambda}_\alpha\}$.*

Let $\tilde{IB}_s(0)$ and $\tilde{IB}_p(0)$ be prices of bonds $IB_s(T, Fv)$ and $IB_p(T, Fv)$ at moment 0 for fuzzy volatility and market price of risk parameters. In the following theorem we present catastrophe bonds pricing formulas for the one-factor Vasicek interest rate model.

Theorem 3. *Assume that $\tilde{IB}_s(0)$ and $\tilde{IB}_p(0)$ are prices of bonds $IB_s(T, Fv)$ and $IB_p(T, Fv)$ at moment 0 for fuzzy volatility and market price of risk. Then*

$$\tilde{IB}_s(0) = Fv \otimes e^{-T \otimes \tilde{R}(T)} \otimes \{1 - \Phi(T)\}, \tag{7}$$

and

$$\tilde{IB}_p(0) = e^{-T \otimes \tilde{R}(T)} \otimes E^P \nu_{IB_p(T,Fv)}, \tag{8}$$

where

$$\tilde{R}(T) = \tilde{R}_\infty \ominus \left\{ \left(\tilde{R}_\infty \ominus r_0 \right) \otimes \frac{(1 - e^{-aT})}{aT} \ominus \tilde{\sigma} \otimes \tilde{\sigma} \otimes \frac{(1 - e^{-aT})^2}{4a^3 T} \right\},$$

$$\tilde{R}_\infty = b \ominus \tilde{\lambda} \otimes \tilde{\sigma} \oslash a \ominus \tilde{\sigma} \otimes \tilde{\sigma} \oslash \left(2a^2 \right).$$

Moreover, for $\alpha \in [0, 1]$,

$$\left(\tilde{IB}_s(0) \right)_\alpha = \left[Fv \{1 - \Phi(T)\} e^{-T \left(\tilde{R}(T) \right)_\alpha^U}, \quad Fv \{1 - \Phi(T)\} e^{-T \left(\tilde{R}(T) \right)_\alpha^L} \right], \tag{9}$$

$$\left(\tilde{IB}_p(0) \right)_\alpha = \left[E^P \nu_{IB_p(T,Fv)} e^{-T \left(\tilde{R}(T) \right)_\alpha^U}, \quad E^P \nu_{IB_p(T,Fv)} e^{-T \left(\tilde{R}(T) \right)_\alpha^L} \right], \tag{10}$$

where

$$\left(\tilde{R}(T) \right)_\alpha^L = \left(\tilde{R}_\infty \right)_\alpha^L - \left(\left(\tilde{R}_\infty \right)_\alpha^U - r_0 \right) \frac{(1 - e^{-aT})}{aT} + \frac{\left(\tilde{\sigma}_\alpha^L \right)^2 (1 - e^{-aT})^2}{4a^3 T}, \tag{11}$$

$$\left(\tilde{R}(T) \right)_\alpha^U = \left(\tilde{R}_\infty \right)_\alpha^U - \left(\left(\tilde{R}_\infty \right)_\alpha^L - r_0 \right) \frac{(1 - e^{-aT})}{aT} + \frac{\left(\tilde{\sigma}_\alpha^U \right)^2 (1 - e^{-aT})^2}{4a^3 T}, \tag{12}$$

$$\left(\tilde{R}_\infty \right)_\alpha^L = b - \frac{\left(\tilde{\lambda}_\alpha \otimes_{int} \tilde{\sigma}_\alpha \right)^U}{a} - \frac{\left(\tilde{\sigma}_\alpha^U \right)^2}{2a^2}, \tag{13}$$

$$\left(\tilde{R}_\infty \right)_\alpha^U = b - \frac{\left(\tilde{\lambda}_\alpha \otimes_{int} \tilde{\sigma}_\alpha \right)^L}{a} - \frac{\left(\tilde{\sigma}_\alpha^L \right)^2}{2a^2}. \tag{14}$$

Proof. Replacing crisp parameters by their fuzzy counterparts and arithmetic operators $+, -, .$ by $\oplus, \ominus, \otimes$ in (3) and (4), we obtain formulas (7) and (8). Let $\alpha \in [0, 1]$. For a given fuzzy number $\tilde{A}$ we denote by $\tilde{A}_\alpha^L$ and $\tilde{A}_\alpha^U$ the lower and upper bound of its α-level set. Clearly,

$$\left(\tilde{\lambda} \otimes \tilde{\sigma}\right)_\alpha = \left[\left(\tilde{\lambda}_\alpha \otimes_{int} \tilde{\sigma}_\alpha\right)^L, \left(\tilde{\lambda}_\alpha \otimes_{int} \tilde{\sigma}_\alpha\right)^U \right].$$

Since $\tilde{\sigma}$ is non-negative,

$$(\tilde{\sigma} \otimes \tilde{\sigma})_\alpha = \left[\left(\tilde{\sigma}_\alpha^L\right)^2, \left(\tilde{\sigma}_\alpha^U\right)^2 \right]$$

and (13) and (14) hold. Since $\frac{(1-e^{-aT})}{aT} > 0$ and $\frac{(1-e^{-aT})^2}{4a^3T} > 0$, (11) and (12) are satisfied. Function $\exp(-x)$ satisfies the assumptions of Proposition 1 and is decreasing. Therefore

$$\left(e^{-T \otimes \tilde{R}(T)}\right)_\alpha = \left[e^{-T\left(\tilde{R}(T)\right)_\alpha^U}, e^{-T\left(\tilde{R}(T)\right)_\alpha^L} \right]$$

and finally, we obtain (9) and (10).   □

The following theorem provides catastrophe bonds pricing formulas for the two-factor Vasicek interest rate.

Theorem 4. *Assume that $\tilde{IB}_s(0)$ and $\tilde{IB}_p(0)$ are prices of bonds $IB_s(T, Fv)$ and $IB_p(T, Fv)$ at moment 0 for the interest rate described by the two-factor Vasicek model and fuzzy volatility parameters. Then*

$$\tilde{IB}_s(0) = Fv \otimes e^{\tilde{\gamma}(T, r_0, \varepsilon_0)} \otimes \{1 - \Phi(T)\}, \tag{15}$$

$$\tilde{IB}_p(0) = e^{\tilde{\gamma}(T, r_0, \varepsilon_0)} \otimes E^P \nu_{IB_p(T, Fv)}, \tag{16}$$

where
$$\tilde{\gamma}(T, r_0, \varepsilon_0) = -1 \otimes \tilde{a}(T) \ominus (b_1(T) r_0 + b_2(T) \varepsilon_0),$$

functions $b_1(T)$ and $b_2(T)$ are defined in Theorem 2,

$$a(T) = \tilde{\varphi} \otimes \frac{T - b_1(T)}{a_r} \ominus \left(\frac{1}{2} \otimes \tilde{\sigma}_1 \ominus \frac{\rho}{a_r - a_\varepsilon} \otimes \tilde{\sigma}_2 \oplus \frac{1}{2(a_r - a_\varepsilon)^2} \otimes \tilde{\sigma}_3 \right)$$

$$\otimes \frac{T - b_1(T) - a_r b_1^2(T)/2}{a_r^2} \ominus \tilde{\sigma}_3 \otimes \frac{2Ta_\varepsilon - 3 + 4e^{-a_\varepsilon T} - e^{-2a_\varepsilon T}}{4a_\varepsilon^3(a_r - a_\varepsilon)}$$

$$\ominus \tilde{\sigma}_3 \otimes \frac{\rho \left(T - b_1(T) - \frac{1-e^{-a_\varepsilon T}}{a_\varepsilon} + \frac{1-e^{-(a_r+a_\varepsilon)T}}{a_r+a_\varepsilon} \right)}{a_r a_\varepsilon (a_r - a_\varepsilon)},$$

$$\tilde{\varphi} = a_r b_r \ominus \tilde{\lambda}_1 \otimes \tilde{\sigma}_r, \quad \tilde{\sigma}_1 = \tilde{\sigma}_r \otimes \tilde{\sigma}_r, \quad \tilde{\sigma}_2 = \tilde{\sigma}_r \otimes \tilde{\sigma}_\varepsilon, \quad \tilde{\sigma}_3 = \tilde{\sigma}_\varepsilon \otimes \tilde{\sigma}_\varepsilon.$$

Moreover, for $\alpha \in [0, 1]$, the following equalities hold

$$\left(e^{\tilde{\gamma}(T,r_0,\varepsilon_0)} \right)^L_\alpha = e^{\tilde{\gamma}(T,r_0,\varepsilon_0)^L_\alpha}, \tag{17}$$

$$\left(e^{\tilde{\gamma}(T,r_0,\varepsilon_0)} \right)^U_\alpha = e^{\tilde{\gamma}(T,r_0,\varepsilon_0)^U_\alpha}. \tag{18}$$

Proof. We replace crisp parameters by their fuzzy counterparts and arithmetic operators $+, -, .$ by $\oplus, \ominus, \otimes$ in (5) and (6). We obtain formulas (15) and (16). Let $\alpha \in [0, 1]$. Function $\exp(x)$ satisfies the assumptions of Proposition 1 and is increasing. Therefore

$$\left(e^{\tilde{\gamma}(T,r_0,\varepsilon_0)} \right)_\alpha = \left[e^{\tilde{\gamma}(T,r_0,\varepsilon_0)^L_\alpha}, e^{\tilde{\gamma}(T,r_0,\varepsilon_0)^U_\alpha} \right],$$

i.e., (17) and (18) hold. $\square$

The forms of the lower and upper bounds of α-level sets of $\tilde{\gamma}(T, r_0, \varepsilon_0)$ can be analytically expressed as functions of lower and upper bounds of the model parameters. Since the appropriate formulas are complex and they depend on signs of several real number-valued expressions, they are ommited in Theorem 4. However, it is possible to compute them, replacing $\oplus, \ominus, \otimes$ or $\oslash$ in the above formulas by their interval counterparts $\oplus_{int}, \ominus_{int}, \otimes_{int}$ or $\oslash_{int}$.

Let $\tilde{IB}(0) = \tilde{IB}_s(0)$ or $\tilde{IB}_p(0)$. The equality

$$\mu_{\tilde{IB}(0)}(c) = \sup_{0 \le \alpha \le 1} \alpha I_{\left(\tilde{IB}(0) \right)_\alpha}(c)$$

describes the membership function of $\tilde{IB}(0)$. For a given α (e.g. $\alpha = 0.9$) the α-level set of $\tilde{IB}(0)$ can be interpreted by a financial analyst as the interval of the cat bond prices. Then the financial analyst can choose any value from this interval as the catastrophe bond price with an acceptable membership degree. Such an interval can be a very useful tool for investment decision-making.

5 Simulations

In order to price the catastrophe bonds and to analyse the features of pricing formulas presented in Sect. 4.2, the Monte Carlo simulations are conducted. As previously noted, the appropriate formulas are complicated, therefore we use simulations to

Table 1 Parameters of the model

	Parameters
Vasicek model (crisp)	$a_r = 0.0506$, $a_\varepsilon = 0.01$, $b_r = 0.06917$, $b_\varepsilon = 0.02$, $r_0 = 0.07$, $\varepsilon_0 = 0.01$, $\rho = 0.1$
Vasicek model (fuzzy)	$\sigma_r = (0.009, 0.011)$, $\sigma_\varepsilon = (0.004, 0.006)$
Intensity of HPP	$\kappa_{HPP} = 31.7143$
Lognormal distribution	$\mu_{LN} = 17.3570$, $\sigma_{LN} = 1.7643$
Triggering points	$K_1 = Q_{HPP-LN}(0.55)$, $K_2 = Q_{HPP-LN}(0.75)$, $K_3 = Q_{HPP-LN}(0.95)$
Values of losses coefficients	$w_1 = 0.25$, $w_2 = 0.25$, $w_3 = 0.25$

illustrate the possibility of applying numerical computation to obtain straightforward results. Because some of the parameters in our model are fuzzy numbers, then we set $\alpha = 0.9$ and apply relevant α-level sets for the volatility parameters of the spot interest rate and the market price of the risk. Therefore appropriate interval of the cat bond prices may be found via simulations and used by a financial analyst to make investment decisions.

We analyse the price of a catastrophe bond when the interest rate is described by the two-factor Vasicek model (see Theorem 4). The parameters of model of interest rates are similar to the values which may characterize the financial markets (see [16] for similar sets of parameters in case of U.S. Treasure bills).

We assume that the generated losses are of a catastrophic nature, i.e. they are rare, but with a high value of each loss. Therefore the quantity of losses is modelled by HPP (homogeneous Poisson process) and the value of each loss is given by a random variable with a relatively high expected value and variance (i.e. high risk with high variability). We assume that the value of the loss is modelled by lognormal distribution which is commonly used in simulations of risk events in insurance. The intensity of HPP and parameters of the applied distribution were fitted in [2] for data describing natural catastrophic events in the United States provided by the ISO's (Insurance Service Office Inc.) Property Claim Services (PCS). Other types of complex probabilistic distributions (e.g. Weibull, gamma, Burr, generalized Pareto – see [2, 7, 8, 17]) or simulations based on historical records (see [4]) are also possible.

We assume that the face value of the bond in each experiment is set to 1 (one monetary unit assumption) and the trading horizon of the catastrophe bond is set on 1 year. In the analysis we apply the stepwise payoff function (see (15)). For the market price of risk we set the interval close to zero, i.e. (0, 0.001). In each experiment we generate $N = 1000000$ simulations.

The overall parameters of the model may be found in Table 1.

The triggering points for the payment function are connected with surpassing the limits given by quantiles of the cumulative value of losses for the HPP process
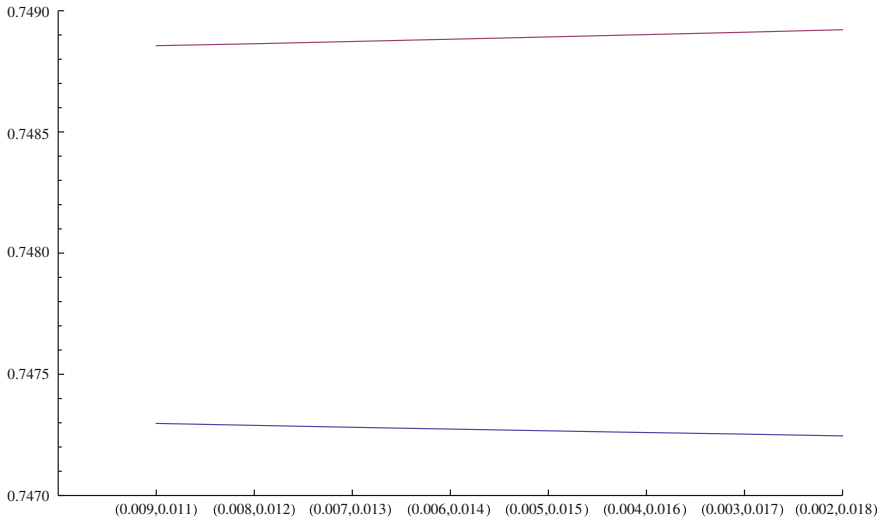
Fig. 4 Price of the bond as the function of σ_r

(number of losses) and lognormal distribution (value of each loss). Such xth quantile is denoted further by $Q_{HPP-LN}(x)$. The parameters of HPP and lognormal distribution for these quantiles are also described in [2] (i.e. they are the same as those for the simulated process of catastrophic events). Also the values of losses coefficients for the bond's holder are set.

In such case the price of the catastrophe bond is given by (0.747297, 0.748856).

Then we analyse the cat bond price if the intervals for value of σ_r are getting wider. Other parameters are the same as in Table 1. As we could see the limits of intervals seem to be linear functions of values of σ_r (see Fig. 4).

Next we analyse the price if the intervals for σ_ε are getting wider and other parameters are the same as in Table 1. As we could see the appropriate intervals seem to be not-linear functions of values of σ_ε (see Fig. 5).

We also analyse the situation similar to the one considered on Fig. 4 (i.e. with changeable σ_r) but with higher value of correlation coefficient $\rho = 0.9$ (see Fig. 6). In such case there is more strict dependency between changes in the interest rate and changes in the process ε. The appropriate values of cat bond prices for cases with $\rho = 0.1$ and $\rho = 0.9$ may be found in Table 2.

6 Conclusions

The frequency of natural catastrophes and size of economic losses caused by these events are sources of serious problems for insurers. Classical insurance models assume that the law of large numbers is fulfilled which is contrary to the situa-
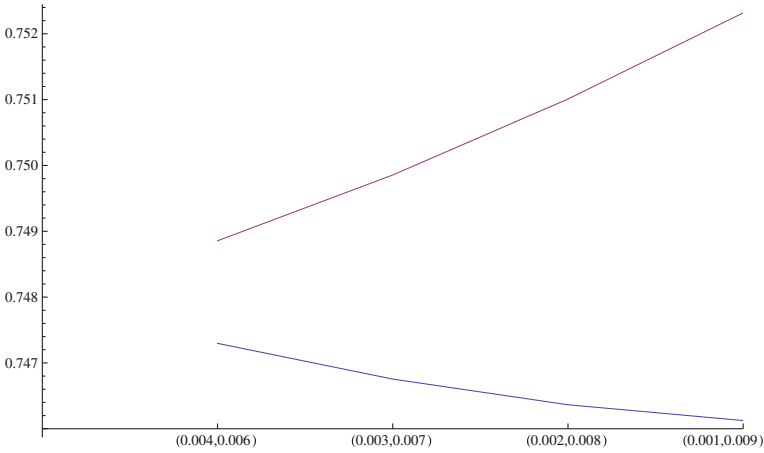
Fig. 5 Price of the bond as the function of σ_ε
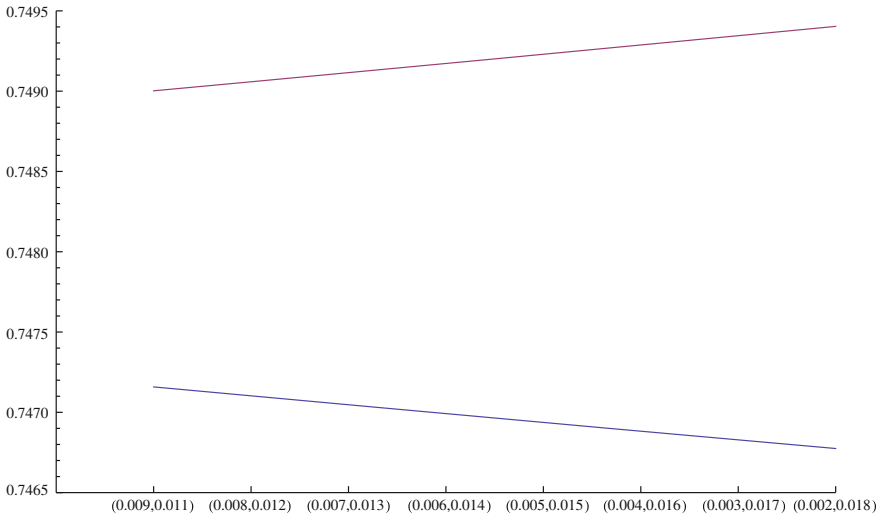
Fig. 6 Price of the bond as the function of σ_r for $\rho = 0.9$

tion for catastrophic events. Therefore new financial and insurance mechanisms are necessary. Catastrophe bonds which transfer the natural catastrophe risk to financial markets are example of such instrument.

In our paper we apply stochastic analysis and fuzzy sets theory to obtain cat bond pricing formula. We consider stochastic processes with continuous time and finite time horizon. We apply the one- and two-factor Vasicek model for description of the interest rate behavior and compound Poisson process to describe natural catastrophe losses.

Table 2 Comparing cat bond prices for various σ_r and ρ

	(0.009, 0.011)	(0.008, 0.012)	(0.007, 0.013)	(0.006, 0.014)
$\rho = 0.1$	(0.747297, 0.748856)	(0.747289, 0.748864)	(0.747281, 0.748873)	(0.747274, 0.748882)
$\rho = 0.9$	(0.747158, 0.749002)	(0.747103, 0.749058)	(0.747047, 0.749115)	(0.746992, 0.749173)
	(0.005, 0.015)	(0.004, 0.016)	(0.003, 0.017)	(0.002, 0.018)
$\rho = 0.1$	(0.747267, 0.748892)	(0.74726, 0.748902)	(0.747253, 0.748911)	(0.747246, 0.748922)
$\rho = 0.9$	(0.746937, 0.74923)	(0.746882, 0.749288)	(0.746829, 0.749345)	(0.746775, 0.749403)

Fuzzy arithmetic applied in the paper enables us to take into account different sources of uncertainty, not only the stochastic one. In order to obtain the catastrophe bond valuation formula in case of lack of precise data we apply fuzzy volatility parameters of the spot interest rate and treat the market price of risk as a fuzzy number.

Apart from obtaining theoretical formulas, we also conduct numerical simulations in order to analyse the behaviour of calculated prices.

References

1. Buckley, J.J., Eslami, E.: Pricing stock options using fuzzy sets. Iran. J. Fuzzy Syst. **4**(2), 1–14 (2007)
2. Chernobai, A., Burnecki, K., Rachev, S., Trueck, S., Weron, R.: Modeling catastrophe claims with left-truncated severity distributions. HSC, Research Reports, HSC/05/01 (2005)
3. Ermolieva, T., Romaniuk, M., Fischer, G., Makowski, M.: Integrated model-based decision support for management of weather-related agricultural losses. In: Hryniewicz, O., Studziński, J., Romaniuk, M. (eds.), Enviromental informatics and systems research. Vol. 1: Plenary and session papers—EnviroInfo 2007, Shaker Verlag, IBS PAN (2007)
4. Ermolieva, T., Ermoliev, Y.: Catastrophic risk management: flood and seismic risks case studies. In: Wallace, S.W., Ziemba, W.T. (eds.) Applications of Stochastic Programming. MPS-SIAM Series on Optimization, Philadelphia (2005)
5. George, J.B.: Alternative reinsurance: using catastrophe bonds and insurance derivatives as a mechanism for increasing capacity in the insurance markets. CPCU J. **52**(1), 50–54 (1999)
6. Gil-Lafuente, A.M.: Fuzzy Logic in Financial Analysis. Springer, Berlin (2005)
7. Hewitt, Ch. C., Lefkowitz, B.: Methods for fitting distributions to insurance loss data. In: Proceedings of the Casualty Actuarial Society Casualty Actuarial Society, vol. LXVI, pp. 139–160. Arlington, Virginia (1979)
8. Hogg, R.V., Klugman, S.A.: On the estimation of long-tailed skewed distributions with actuarial applications. J. Econom. **23**, 91–102 (1983)
9. Muermann, A.: Market price of insurance risk implied by catastrophe derivatives. N. Am. Actuarial J. **12**(3), 221–227 (2008)
10. Niedzielski J.: USAA places catastrophe bonds, National Underwriter, Jun 16 (1997)
11. Nowak, P., Romaniuk, M.: On pricing formula and numerical analysis of catastrophe bond with some payment function. In: Wilimowska, Z., Borzemski, L., Grzech, A., Swiatek, J. (eds.) Information Systems Architecture and Technology. The Use of IT Models for Organization Management, Wrocław (2012)
12. Nowak, P., Romaniuk, M.: Computing option price for Levy process with fuzzy parameters. Eur. J. Oper. Res. **201**(1), 206–210 (2010)

13. Nowak, P., Romaniuk, M.: Analiza wlasnosci portfela zlozonego z instrumentow finansowych i ubezpieczeniowych. In: STUDIA I MATERIALY POLSKIEGO STOWARZYSZENIA ZARZADZANIA WIEDZA, vol. 31, 65–76 (2010)
14. Nowak, P., Romaniuk, M.: Pricing and simulation of catastrophe bonds. Insurance: Mathematics and Economics, 52(1), 18–28 (2013)
15. Nowak, P., Romaniuk, M.: Catastrophe bond pricing for the one- and two-factor Vasicek interest rate model. Research Report, RB/3/2012, SRI PAS, Warszawa (2012)
16. Nowman, K.B.: Gaussian estimation of single-factor continuous time models of the term structure of interest rates. J. Finance **52**(4), 1695–1706 (1997)
17. Papush, D.E., Patrik, G.S., Podgaits, F.: Approximations of the aggregate loss distribution. Casualty Actuarial Society Forum Casualty Actuarial Society. Arlington, Virginia 2001 (Winter), 175–186 (2001)
18. Vaugirard, V.E.: Pricing catastrophe bonds by an arbitrage approach. Q. Rev. Econ. Finance **43**, 119–132 (2003)
19. Wu, H-Ch.: Pricing European options based on the fuzzy pattern of Black-Scholes formula. Comput. Oper. Res. **31**, 1069–1081 (2004)

Evaluating Condition of Buildings by Applying Fuzzy Signatures and R-Fuzzy Operations

Ádám Bukovics and László T. Kóczy

Abstract It is an significant task to qualify and rank residential buildings based on various priority aspects and to make optimum allocation of the material resources available for the renewal of the buildings. To this end a model based on fuzzy logic was prepared. To construct and to test this model many detailed technical-static expert reports were available all related to a stock of residential buildings in Budapest. Based on this report a database was created. With the help of this database a model was prepared, calculating a so-called status characteristic value between 0 and 1 on the basis of the structures and status of the buildings. For this calculation a fuzzy singleton signature model was prepared. Based on this a hierarchy can be set up related to the stock of buildings, which is suitable for supporting the decision-making on intervention. The model was examined by using the created database. Membership values characterising the status of the load-bearing structures—were defined on the basis of the deterioration of the structures. In this chapter a new method for the determination of the membership values is described, which in addition to the deteriorations of the structures takes into account other parameters of the structures, and the impact exerted on the quality of the structure, too. The method is suitable for the determination of the membership values of all primary and secondary structures.

Á. Bukovics (✉)
Department of Structural and Geotechnical Engineering, Széchenyi István University, Győr, Hungary
e-mail: bukovics@sze.hu

L. T. Kóczy
Department of Automation, Széchenyi István University, Győr, Hungary
e-mail: koczy@sze.hu

L. T. Kóczy
Department of Telecommunications and Media Informatics, BME, Budapest, Hungary
e-mail: koczy@tmit.bme.hu

As an example the membership values of the foundation structures of the buildings in the database were defined and the results were analysed. The method was elaborated by the use of "real fuzzy values" (R-fuzzy sets), an extension of the concept of classic fuzzy sets, the former being suitable for simultaneously taking into account various aspects.

1 Introduction

It is important from the point of view of national economic interest to keep records of and process the characteristics and status of the existing stock of buildings. During the past period in our research we have dealt with this problem.

In the course of our research work a great many detailed technical and static expert reports on residential buildings in Budapest built at the end of the nineteenth and at the beginning of the twentieth centuries had been available. A considerable part of the current stock of buildings in Budapest was built in a rather short time period all buildings having similar structural arrangement and status. Because of this the examination and diagnosis of the structures of these buildings enable us to draw general conclusions on similar constructions in other parts of Budapest, too [1, 2]. Having processed the data included in the expert opinions a database was created, suitable for making structural and diagnostic analysis of the buildings.

We propose that it is practical to express the status of the buildings by a relatively objective number, refer to as "status characteristics", whose knowledge enables ranking buildings based on various priority aspects. To achieve the foregoing goals the use of a fuzzy signature based model would practical.

2 Set Up of the Basic Structure of Fuzzy Signature

A model, based on fuzzy singleton signatures was used to determine the condition of buildings. Fuzzy logic, as the extension of the two-valued logic, is suitable for characterizing certain structures of a building, and the conditions thereof.

For modelling purposes, initially the basic structure of fuzzy singleton signature, featuring the problem was set up on the basis of the data available from the prepared data base.

Fuzzy member values, which can be used in the system, were determined for the individual data elements. It is a requirement towards the fuzzy singletons, situated on the leaves of the structure, to have their values within the interval of [0,1].

When using the qualifying and ranking method, based on the fuzzy singleton signature, the examined main load bearing structures are collectively named as "primary" structures. These are as follows: *foundation structures, wall structures, floor*

structures, side corridor structures, step structures, roof structures. "Secondary" structures are those other (not main load-bearing) structures, which play an important role in the protection of the main load bearing structures. These are as follows: *roof covering, surface formation, tin structures, insulation against soil moisture and ground water.*

As the basic structure a four-level fuzzy signature was applied, since in the course of the examination of the stock of buildings this depth was considered necessary to achieve appropriate accuracy in defining the condition [3].

The whole set-up of the fuzzy singleton signature in the format of tree-structure are demonstrated in Fig. 1.

When computing, a partial group of variables together defines a trait at a higher level. Thereby additional information can be stored with the help of the structure.

3 Definition of Relevance Weight and Aggregation Operations

In the application of fuzzy singleton signatures the sub-groups of variables together determine a component on a higher level. Therefore the components within the sub-trees of the structure may relate to the roots of the sub-trees in a way unlike the components of other sub-trees relate to their respective roots. Hence dissimilar aggregation operators should be assigned to each peak of the fuzzy singleton signature structure [4].

The aggregation operators play an important role in the comparison of two signatures, since it might be necessary to modify the structures, and the values appearing on the leaves of the modified structure largely depend on this operator. The relevance weight, connected to each peak of the signature, shows the relevance of the peak, related to the root of the sub-tree [5].

The relevance weights and the aggregation operators were defined based on professional and observation experience, and on the basis of the relevance of the structure related to the whole building.

For the aggregation The Weighted Relevance Aggregation Operator (WRAO) was used of the fuzzy singleton signature [7].

$$@(\mu_1, \mu_2, \ldots, \mu_n; \varphi_1, \varphi_2, \ldots, \varphi_n) = \left(\frac{1}{n} \sum_{l=1}^{n} (\varphi_l \cdot \mu_l)^p \right)^{\frac{1}{p}} \qquad (1)$$

Notations used in the formula: @: WRAO function, μ: value of successor 1, φ: relevance weight of successor l, n: number of successors of the junction to be aggregated, p: aggregation factor ($p \in R$, $p \neq 0$). Value of the aggregation factor (p) is 1 within the applied WRAO function.

The aggregation operators to be used were defined by using the relevance weights and the values on the root of the structure.
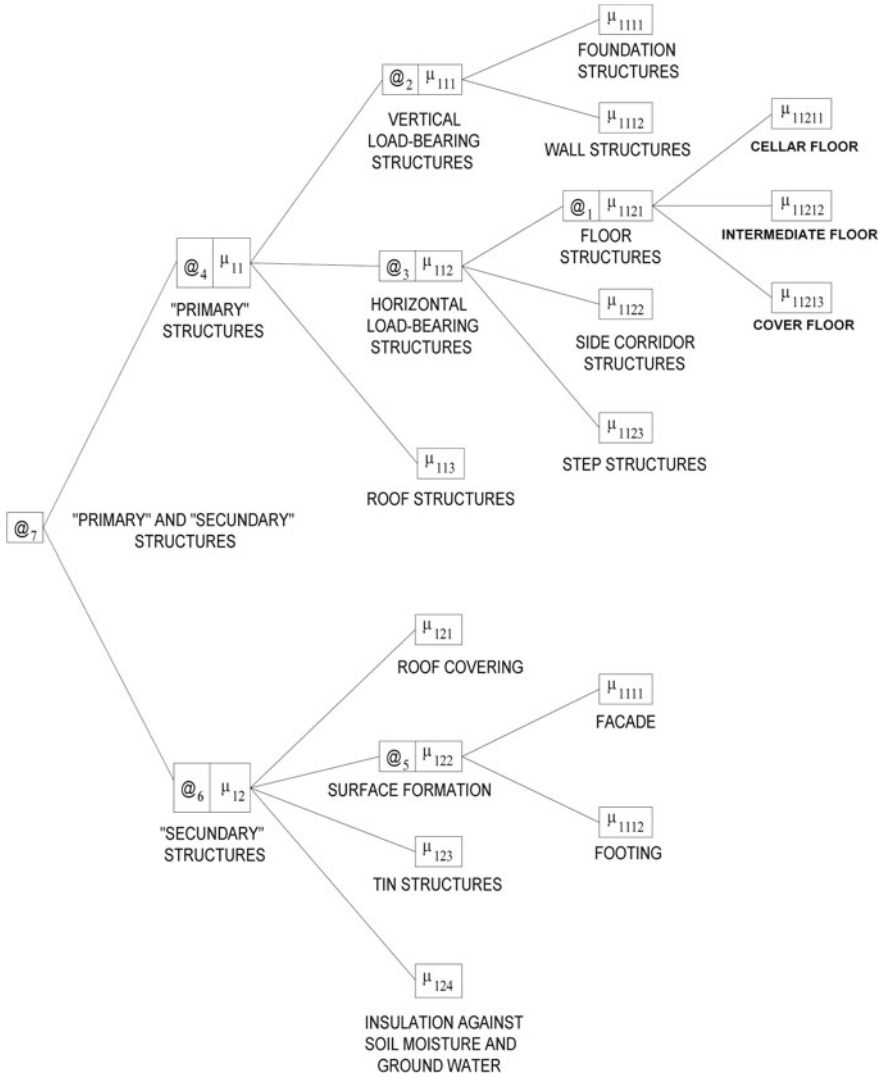
Fig. 1 Set up of fuzzy singleton signature structure in the format of tree structure

For example the aggregation operator, related to the floor structure, is given for the following value where m is the extent of the cellar built, n is the number of the storeys of the building.

$$@_1 = \frac{0{,}35 \cdot m \cdot \mu_{11211} + 0{,}45 \cdot (n-1) \cdot \mu_{11212} + 0{,}20 \cdot \mu_{11213}}{0{,}2 + 0{,}45 \cdot (n-1) + 0{,}35 \cdot m} \tag{2}$$

4 Software

The software, prepared on the basis of the fuzzy singleton signature, serves the aim of defining the condition of multi-storey buildings of similar condition and age, and the ranking thereof.

The input data related to the building are constant on the one part (formation of the building, applied structures, applied materials etc.), on the other part they alter in terms of time (condition of the structure, appearance and extent of cracks, extent of the corrosion, etc.). The aim of ranking is to define the current status of the buildings, as well as to define their future and the utilisation thereof (suggested for demolition, suggested for renewal, renewal is necessary, but not immediately).

For each member of the examined stock of buildings a value can be computed which refer to the quality of the residential building. Values fall in the interval of [0,1]. Based on this ranking a more mature decision can be made as to what can be done on the building.

5 Application of the Model in the Database Under Review

The database was studied with the fuzzy singleton signature based software. With its help useful information can be obtained on the condition of various structures and their relationship to one another. The values of the aggregate status descriptor μ_1, related to the condition of the buildings, were computed with the help of the software. The results, achieved with the computation completed in the case of the normal tuning method, are demonstrated on Fig. 2.
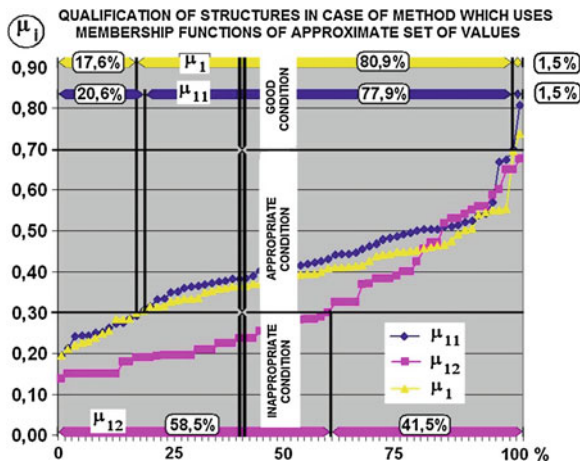
Fig. 2 Qualification of structures

From the proportions obtained it can be established that a considerable part of the examined stock of buildings is in need of renewal, partly due to the omission of former conservation and the renewal works.

6 Recursive Evaluation of the Model Related to Specific Building

Herebelow are introduced in case of a specific residential building how the values of summarised, aggregate status descriptors, characterising the status of the structures are produced at various levels of the tree structure. Systems and materials of building structures, as well as the most important characteristics of the building are described. Values of the status descriptors were expressed by figures on the basis of static expert reports related to the building, the values are included in Fig. 4. The values of status descriptors are described also by applying normal and fine tuning method.

The examined building is two-storey residential building (Fig. 3). The year of construction is 1903, having cellar underneath, with pitched and semi-pitched roof. Residential building of solid brick main wall structural system, with strip foundation. The material of the floor above the cellar and the intermediate floor is solid, and that of the top floor is timber.

The values of aggregate status descriptors, representing the status and the overall status of the structures of the examined building are shown in Fig. 4. Values obtained by applying the normal tuning method are indicated with A in the upper index, whilst at values obtained by fine tuning method there is B in the upper index.

Fig. 3 Front view of the examined building
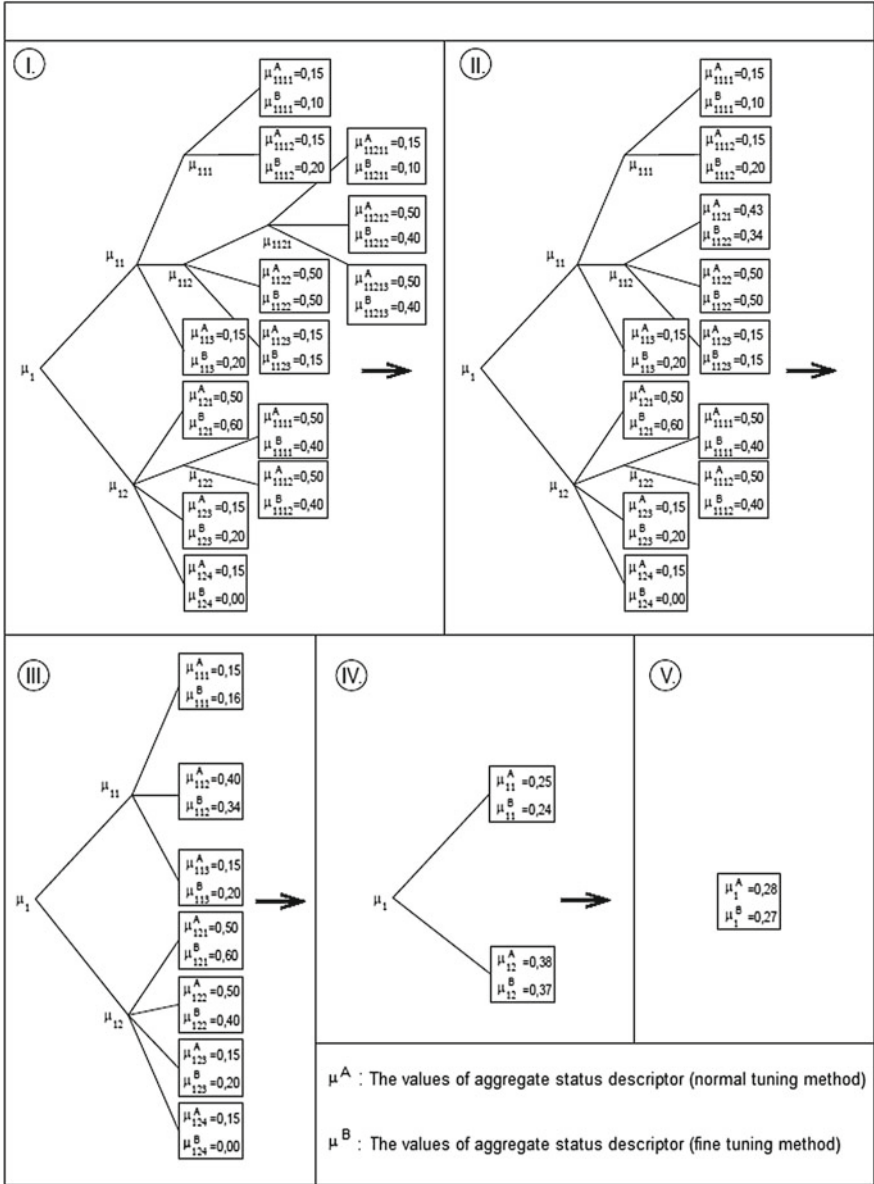
Fig. 4 Recursive evaluation of the model related to the examined building

7 Modelling the Condition of Load Bearing Structures by Real Fuzzy Sets

7.1 Creating a Model to Define Membership Values

Our further aim is to work out a method for defining the membership values, which characterise the condition of the examined load-bearing structures, which, in addition to the detected deterioration of the structures directly or indirectly, takes into account other parameters of the structure, and the respective effect, exerted on the quality of the structure.

In order to define the membership values of the investigated characteristics, as a first step a decision has to be made as to how many factors influencing the status of the structure shall be taken into consideration. The values of these factors describe the intensity and the extent of the investigated effect exerted on the condition of the examined structure of a building. Factors affecting the status of the structure in a positive direction will be called *status improving factors* and will be denoted by μ_i (i = 1, ..., n, n is the number of status improving factors taken into account). Those factors affecting the status of the structure in a negative sense will be called *status deterioration factors* and will be denoted by α_i (i = 1, ..., m, m is the number of status deterioration factors taken into account). Since each factor is supposed to affect the status in each case, the investigation must be restricted to strictly monotonously behaving fuzzy operators. The above defined fuzzy disjunction, which can be interpreted in the case of the strictly monotonously behaving fuzzy operators, is suitable for taking into account all the factors. The factor, which includes the effect of all status improving factors, is called the resultant of status improving factors and is denoted with μ_P. The factor that includes the effects of all status deterioration factors, is called the resultant of status deterioration factors and is denoted with α_N. The resultant of the status improving and status deterioration factors was defined with the help of the fuzzy disjunction (1).

Since fuzzy disjunction satisfies the associative property, a one step calculation can be made in case of any number of factors affecting the membership values.

In case of arbitrary n positive, and m negative factors effecting the membership value, using the fuzzy disjunction, the expression of factors μ_P and α_N are given as follows:

$$\mu_P = \mu_{\bigcup\limits_{i=1}^{n} A_i} = \sum_{i=1}^{n} \mu_i - \sum_{\substack{i \neq j \\ i=1}}^{n} \mu_i \cdot \mu_j \pm \cdots \pm (-1)^{n-1} \cdot \prod_{i=1}^{n} \mu_i = 1 - \prod_{i=1}^{n} (1 - \mu_i) \quad (3)$$

$$\alpha_N = \alpha_{\bigcup\limits_{i=1}^{m} A_i} = \sum_{i=1}^{m} \alpha_i - \sum_{\substack{i \neq j \\ i=1}}^{m} \alpha_i \cdot \alpha_j \pm \cdots \pm (-1)^{m-1} \cdot \prod_{i=1}^{m} \alpha_i = 1 - \prod_{i=1}^{m} (1 - \alpha_i) \quad (4)$$
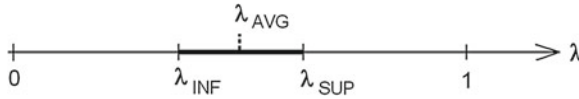
Fig. 5 Fuzzy interval value

The above so called sieve formulas could be transformed into closed format, using De Morgan's form [6]. This is the general format of the resultant of status improving and status deterioration factors.

In the next we propose two extreme values that describe the quality of the structure of a building in two different ways. These two together define a fuzzy interval value (Fig. 5). The two extreme values of the interval are determined by the membership values calculated on the basis of what we call "optimistic" and "pessimistic" estimation.

The "optimistic" estimation (λ_{SUP}) can be obtained by using the fuzzy inverse disjunction and it means the upper limit of the membership value of the examined structure (characterising its general status). The "pessimistic" estimation (λ_{INF}) is obtained by using the fuzzy conjunction (2) and it means the bottom limit of the membership value of the examined structure. The "optimistic" and "pessimistic" estimations are given by the following formulas:

$$\lambda_{SUP} = \frac{\mu_P \cdot (1 - \alpha_N)}{1 - \mu_P \cdot \alpha_N} \tag{5}$$

$$\lambda_{INF} = \mu_P \cdot (1 - \alpha_N) \tag{6}$$

Membership values, obtained as a result of the two estimations, were compared with the results of expert evaluation, and it was found that this latter one was well approximated by the average of the two values ($\lambda_{INF}, \lambda_{SUP}$). Thus we propose this interval for describing the estimated status of the examined structure of a building (λ_{AVG}). The estimated status is thus:

$$\lambda_{AVG} = \frac{\lambda_{INF} + \lambda_{SUP}}{2} \tag{7}$$

This value λ_{AVG} will be considered in the future as the overall membership value associated with the condition of of the examined structure and we state that these overall values can be applied when using the fuzzy singleton signature-based status determining and ranking model.

7.2 Testing a Model on a Load Bearing Structure

Examining a specific stock of buildings with the use of the created model, the membership values of foundation structures were defined, and it was investigated how

Fig. 6 Schematic definition
of the membership value of
the strip foundation
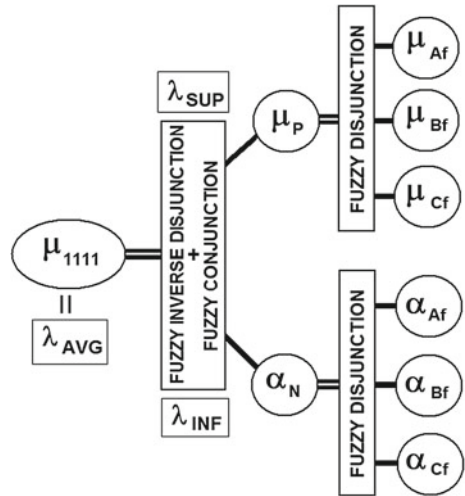
the method based on imaginary fuzzy values could be applied from the aspect of the
qualification and ranking of the load bearing structures of residential buildings. The
schematic definition of the membership value of the strip foundation model can be
seen in Fig. 6.

The membership value, featuring the foundation structure, is influenced by
Sect. 7.2.1.

7.2.1 The Factor Depending on the Material of Strip Foundation (μ_{Af})

Its value was selected in relation to the material of strip foundation of the examined
buildings.

For example, in the case of strip foundations made of stone $\mu_{Af} = 0.65$, in case
of strip foundations made of concrete, which is more reliable and less sensitive,
$\mu_{Af} = 0.90$.

7.2.2 The Factor Depending on the Conformance of the Width of Strip Foundation (Positive Direction) (μ_{Bf})

In order to determine the conformance of the width of the strip foundation, the ratio
of the width of the actual strip foundation (w_f) and the idealized, estimated width of
the strip foundation (w_{fi}) was examined. To the end of defining the width of the
idealized strip foundation it is necessary to approximately determine the loads exerted
on the strip foundation, as well as to know the characteristics of the soil under it.
These values are included in the technical-static expert reports, which are necessary
for the status-determining model, and can be determined on that basis. On the basis

of the foregoing the required width of the strip foundations under the external main wall of the examined buildings was determined. Comparing this to the width of the applied strip foundation, the factor, depending on the conformance of the width of strip foundation, was obtained. If the width of the strip foundation is greater than the width of the idealized strip foundation, the value of μ_{Bf} may be between 0.05 and 0.40. If the width of the strip foundation is smaller than the idealized width of the strip foundation, the value of μ_{Bf} is 0 that is it has no impact on the value of μ_2.

7.2.3 The Factor Depending on the Year of Construction (μ_{Cf})

In 1914 Budapest introduced the Construction Rules and Regulations for all buildings in its territory. For all buildings built after this regulation in Budapest had been put into force, 0.10 was applied for the value of factor μ_{Cf}, while in case of buildings, built before 1914, the value of the factor μ_{Cf} is 0.

This factor takes two aspects into consideration. One is the question whether in the year of the construction the city had its regulations in effect or not, the second being simply the number of years that had past after construction because of the process of the natural impairment of the condition of buildings in terms of time.

7.2.4 The Factor Depending on the Detected Deteriorations of Strip Foundation (α_{Af})

Factor α_{Af} is determined by using the component featuring the status of the formerly determined membership value of foundation structure (μ_{1111}). The bigger the extent of the detected deteriorations is the closer the value of μ_{1111} is to 0. Membership values are determined on the basis of the fuzzy disjunction and the fuzzy conjunction, therefore in our case the bigger the extent of the deterioration is, the closer α_{Af} is to 1. Thus the complement value $\alpha_{Af} = 1 - \mu_{1111}$ was applied.

7.2.5 The Factor Depending on the Conformance of the Width of Strip Foundation (α_{Bf})

If the width of strip foundation is smaller than the ideal width, the value of α_{Bf} may be between 0.05 and 0.40 (in relation to w_f/w_{fi}).

7.2.6 The Factor Featuring Other Effects Deteriorating the Quality of the Structure (α_{Cf})

This factor takes into account the effect of vibrations impairing the status of the foundation structures. In case of buildings situated by roads with high traffic the value of α_{Cf} is 0.15, while in case of buildings situated over the subway train (Váci út) it is 0.30.
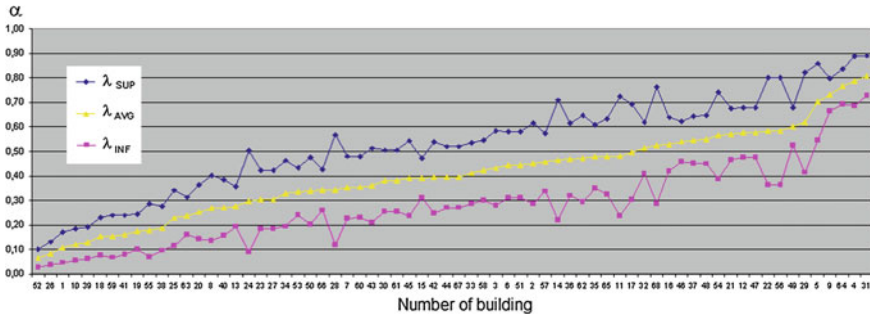
Fig. 7 Values of the membership functions in case of ranked buildings

In the close vicinity of buildings in side streets there is no considerable traffic, therefore in these cases the value of α_{Cf} is 0.00, that is, it has no impact on the value of α_2.

7.3 Results

To determine the membership values, featuring the foundation structures of the examined stock of residential buildings, factors influencing the membership value, were defined first for each examined building. Altogether six factors were defined: three status improving and three status deterioration factors. In the next stage the membership values featuring the status of the foundation structure of examined buildings were determined. λ_{SUP} and λ_{INF} are the two extreme values of the fuzzy interval values while the arithmetic mean of these two gives the estimated membership value (λ_{AVG}). Figure 7 includes the values of all three membership functions (λ_{SUP}, λ_{INF}, λ_{AVG}). The examined buildings were arranged in monotonically increasing sequence on the basis of the estimated overall value of membership functions, referring to the status of the foundation structures.

8 Summary

It was proposed that a fuzzy singleton signature based model would be suitable for evaluating and ranking of traditional residential buildings (e.g. in Budapest), so that the tested buildings be qualified on the basis of their respective conditions, and are ranked based on these qualification values.

As a results important conclusions can be drawn with regard to the condition of a given stock of buildings. The results of this study may make it easier to realize the rehabilitation ideas of similar residential areas.

A new method was elaborated for defining the membership values used for this fuzzy singleton signature-based model, formerly proposed by the authors, a model that is suitable for supporting decision-making related to residential buildings.

In addition to the deteriorations of the structures detected at the time of examination, this method is suitable for taking into account other parameters of the structures, and their respective effects exerted on the quality of the structure.

The proposed new method can be practically used evaluating the status of other built structures and infrastructural facilities, as well.

References

1. Bukovics, Á.: Building diagnostic and pathological analysis of residantial buildings of Budapest. PATORREB 2009, 3° Encontro Sobre Patologia E Reabilitacao de Edificios. Porto, Portugal, pp. 1025–1030 (2009)
2. Bukovics, Á.: Pathological analysis of suspension corridor and floor structures of residential buildings. CIB 2010 World Congress, University of Salford, CIB, Manchester, UK (2010)
3. Bukovics, Á., Kóczy, L.T.: Fuzzy signature-based model for qualification and ranking of residential buildings, XXXVIII. IAHS World Congress on Housing, Istanbul, Turkey, pp. 290–297 (2012)
4. Kóczy, L. T., Vámos, T., Biró, G.: Fuzzy signatures. Proceedings of EUROFUSE-SIC'99, Budapest, pp. 25–28 (1999)
5. Kóczy, L.T., Hajnal, M.A.: New attempt to axiomatize fuzzy algebra with an application example. Probl. Control Inf. Theory **6**(1), 47–66 (1977)
6. Kóczy, L.T.: Fuzzy graphs in the evaluation and optimization of networks. Fuzzy Set Syst. **46**(3), 307–319 (1992)
7. Mendis, B.S.U., Gedeon, T.D., Botzheim, J., Kóczy, L.T.: Generalised weighted relevance aggregation operators for hierarchical fuzzy signatures. Proceedings of the International Conference on Computational Intelligence for Modelling, Control and Automation, CIMCA (2006)

The Determination of the Bitrate on Twisted Pairs by Mamdani Inference Method

Ferenc Lilik and László T. Kóczy

Abstract   There are several methods for predicting the available maximal data transfer rate on dedicated telecommunication connections. This chapter presents some generally used techniques for prediction and some results of a Mamdani-type fuzzy reasoning system that is used in a telecommunication research aimed to create new predicting methods. At the end of the article the results of various methods are compared. All presented techniques are used for evaluation of the twisted-pair based local loops of the telecommunication access networks.

Keywords   Access networks · Performance evaluation · Fuzzy models

1 Introduction

Knowing the data communication service possibilities of a telephone line according to a defined transmission technology before the installation of the technological equipments has an importance. One of the main parameters of a data communication service is the data transfer rate, in other words the bitrate. There are several methods for predicting the available maximal data transfer rate of dedicated telecommunication connections. These techniques are inaccurate or expensive, and in some cases are kept private by the manufacturers.

Each evaluation technique is based on some physical parameters of the local loops. These physical parameters belong to the first layer of the Open System Interconnection (OSI) reference model [1] and have severe influence on the characteristics of higher layers.

F. Lilik (✉)
Department of Telecommunication, Széchenyi István University, Győr, Hungary
e-mail: lilikf@sze.hu

L.T. Kóczy
Department of Automation, Széchenyi István University, Győr, Hungary
e-mail: koczy@sze.hu

The differences between the techniques of evaluation may be found among these physical parameters and methods of prediction making. Necessarily, methods also differ from each other in accordance with the service types that are telephone lines predicted for.

This chapter deals with preliminary line evaluation for xDSL services. As DSL technology is used exclusively in access networks, evaluated telephone lines also belong to it.

Some currently used techniques are shortly presented and the predictions of two frequently used methods and a new approach are compared. The compared methods are in connection with Ethernet over SHDSL communication technology.

2 DSL Evaluation Technologies

Predicting systems are based on the physical parameters of the first layer of the OSI model. The way how they realize and use those physical parameters determine the complexity, precision and costliness of the systems.

Some methods use existing expert knowledge about the parts of access networks of technicians of telecommunication companies (telco). Other methods use registered data stored by telcos of networks as input. Most precise techniques make instrumental measurements in networks to get input data for evaluation. In this last case measurements can be carried out by human contribution or by automatic instruments and processes.

2.1 Evaluation by Human Contribution

Using Expert Knowledge. In the very early periods of the initiation of singular xDSL technologies telcos used this method in order to get information about the possibilities of individual telephone lines to give proper proposals to their respective customers. When customers go into the customer office to inquire about their possibilities of getting a DSL connection, the administrator sends an order to the suitable field technician to determine the available maximum bitrate. The technicians answer by their experiences about the given network. Sometimes the answer could be is imprecise or false depending on the knowledge of the technician.

This rather subjective method is still in use, mainly in case of lack of other prediction methods or if the prediction of other systems is evidently false or strange.

The only advantage of this method is its cheapness, but disadvantages—as e.g. its inaccuracy—are greater than its advantages.

Technological pre-survey. In certain cases, i.e. before submitting tenders or at the demand of e.g. VIP customers, telcos make technological pre-surveys. The presurvey needs, however, the selected service to be installed.

Temporarily a whole connection is made to the customer's place from the central office of the telco. The near end of the line is connected to a node at the central office, and a customer premises equipment (CPE) is connected to the end of the line at the customers' place. In this way the performance of the connection is accurately measurable.

Sometimes it happens that the customer does not know anything about the survey. This occurs mainly in case of tenders. If so, the CPE can not be placed at the customers place. For connecting the equipments the last distribution point is used. So, the measuring does not consider the last segment of the connection, however, the accuracy of the measure is good enough.

As this method gives results under the establishment of the technological equipments of the service, it is not a real preliminary evaluation. However, it is the most expensive way of the evaluation, because it needs the presence and installation of real technological equipments. Further, in some cases, e.g. if there is no empty node position for it, or there is no node at all, it is impossible to do that.

2.2 Evaluation by Location or Distance

Predictions based on location and distance parameters in fact use approximately the physical loss values of the telephone lines. The measurable parameters of the first layer of the OSI reference model are taken into consideration as average values of cable parameters in certain zones or in the same cable type. Methods of this type can be based on real locations of the endpoints or the estimated or proper length of telecommunication wire-pairs.

Evaluation by distance data from technical inventory. Telcos have technical inventory about their cable networks. This technical inventories contain structural data of networks e.g. topology, connections, etc., and dimensional data of cables in the networks among other things. In this way the length of each wire-pair is stored in the databases.

To have a prediction, the employee of the telecommunication company only has to set the line length against tables containing previously defined values. Tables contain the reachable value of maximal data transmission speed for various line lengths. The data of a certain table are referred to a unique diameter of wire-pair, so in fact it tries to consider the loss of line.

There are some problems with this method. First of all, it leaves out of consideration that maybe the quality of the inspected line is low, or the line is unusable. The line can be discontinuous between distribution points, or it can contain bridged taps. The real data transmission ability is eroded also by low quality connections. Finally, sometimes there are no data of some parts of the networks in the inventory, or stored data are old or incorrect.

Circles on Maps. A really swift and easy method for making preliminary evaluation is using geographic maps. On these maps concentric cylinders show the recommended bitrates for covered areas. In Fig. 1 the area of a town is depicted. The
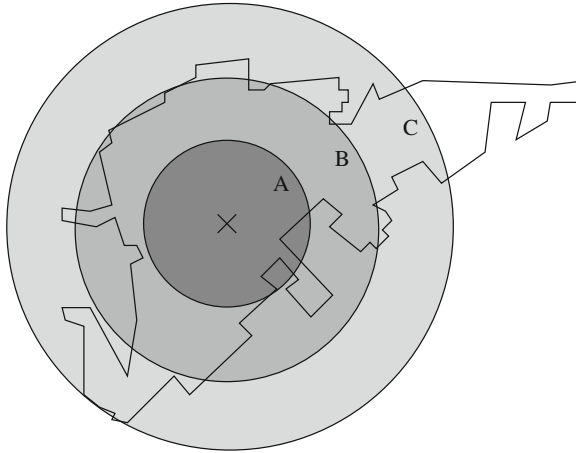
Fig. 1 An example of area dependent evaluation

location of the local exchange is signed by a cross (x). In this case within circle *A* data transmission rate of 15 Mb/s is said to be available and within circle *C* only 5 Mb/s is offered, as an example.

In this method the results of the prediction are not continuous. It provides discrete bitrate values, one for each cylinder. Generally the number and position of the concentric cylinders are in accordance with the telcos' bitrate offers. e.g. if a telecommunication supplier offers three packages of aDSL service by bitrate, the map contains three cylinders. As the length of the lines here are the shortest, the innermost disk (the darkest disk on Fig. 1) represents the area where the fastest aDSL package can be purchased. Moving into the outer cylinders, smaller and smaller bitrates are available. Finally, in the white area out of the last round the evaluation says that here the telephone lines are not able to serve aDSL connections.

The main problem of this method is that the line length is considered at a rough guess. As the cables are laid under the pavement, their real length depends on the topography of the roads. This is the reason why the diameter of the circles are much less than the cable length guaranteeing certain bitrates. However in the practice of telcos the wire-diameter of the cables closer to the central office (CO) is smaller, and the wire-diameter of the cables placed more distant from the CO is larger, this evaluation does not make allowance for this well known fact.

2.3 Instrumental Evaluation Techniques

Since various DSL technologies use different transmission techniques and different frequency bands, instrumental performance evaluation systems are also different from each other. However their theoretical bases are similar. All of them use the

physical parameters of the copper wire based telephone lines, but the methods for collecting these parameters and the evaluation techniques are variable.

As the DSL technology is worked out for copper-wire based access networks, instrumental measurements of local loops have to be made. The parameters can be e.g. insertion loss, line noise, attenuation, capacitance or symmetry. Some of them are taken into consideration by following methods as measured or as estimated values.

There are more different types of instrumental evaluation techniques. The differences between them are the place of measurement and the automation. One of them is called double-ended testing. In this method test units are connected to both ends of the line, one of them is connected to the loop at the central office (CO) while other at customer's premises (CP). If only one test unit is used during the evaluation method is called single-ended or one-ended testing. In this case test equipments can be connected to the line either at the CO or at the CP. Single-ended tests can be performed by a technician using test panels at the other side of the loop or automated. Automated tests are performed from the near end (CO) of the cables [2].

Generally, because they can test packets of lines during the same measurement, automated single-ended techniques are widely used.

2.4 Evaluation by Voltage and Capacitance Measurements

In this type of techniques voltage values between tip wire and ground (V_{TG}), ring wire and ground (V_{RG}) and between tip wire and ring wire (V_{TR}) are measured. The capacitances of C_{TG}, C_{RG} and C_{TR} are also measured. This V and C values are used to determine several characteristics of the loop. Average normalized line length and normalized noise level are calculated. In view of these parameters the evaluated bitrate is determined by using tables [3].

In several methods also the behaviour of various modems are calculated. This way models of modems are a part of the evaluation system. Such a system is described in US patents pat. no. 6,895,081 B1 [4] and in pat. no. 7,263,174 B2 [5]. The decision mechanism of the method described in US 6,895,081 B1 patent is depicted in Fig. 2.

The method takes load coils and bridged taps into consideration as disabling factors of DSL transmission. However these values, even line length and line noise are not measured but calculated values from measured capacitance and voltage.

2.5 Evaluation in Subchannels

Discrete multitone modulation (DMT) is used in various DSL technologies. The total band of the transmission of DMT is segmented into narrow frequency bands. In case of for example the aDSL the bandwidth of a lone subchannel is 4 kHz wide [6]. Each channel transmits several bits of the message, so in case of 256 subchannels the total number of the transmitted bits is $\sum_{i=1}^{256} n_i$ where the amount of transmitted bits of a
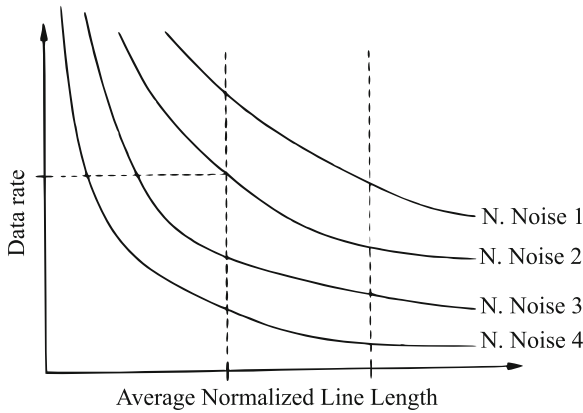
Fig. 2 Graphical representation of the method described in [4] (original in patent US 6,895,081 B1)

subchannel is represented by n_i and i is the subscript referring to a subchannel. The number of the bits transmitted in a subchannel depends on the frequency dependent attenuation and the line noises among others. This subchannel schema can be seen in Fig. 3.

A variant of the method described in Sect. 2.4 is when the frequency band of the xDSL transmission is divided into subchannels. Available bitrates are determined for all the subchannels under measured, calculated and recorded data of the line. For the final evaluation the data transmission capacities of the subchannels are added to each other [7].

2.6 Evaluation by Tones Generated by Customer Premises Equipments

This smart double-ended method can be used in case of lines connected to subscribers. It is based on measuring signals sent by customers, so the work of a field-technician is not needed.
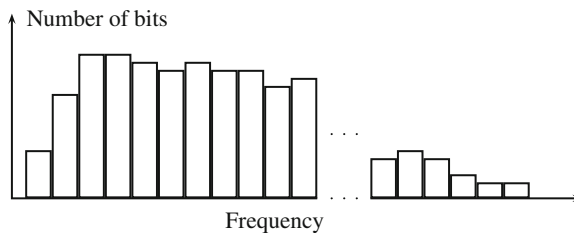
Fig. 3 Schematic view of DMT transmission

The method is roughly as follows. The subscriber is called by the network operator and is asked to send tone signals to the central office. The pattern of these signals can be pre-defined or random. The signals are produced by for example pushing buttons of the subset. The series of the signals are worked up by a measurement system activated by the operator. After A/D transformation the digital map of the original signal is used to determine physical parameters of the connection, for example loop length and capacitance. In accordance with these values a quantitative or qualitative evaluation can be made [8].

Tests can also be made in single-ended mode. In this case there is no customer to send tone signals to the CO. Signals are sent from CO and are reflected by some elements of the telecommunication connection [8].

As in the case of the method described in Sect. 2.4, bitrate influencing parameters are calculated also here.

3 Fuzzy Based System for SHDSL Evaluation Worked Out in Our Research

This method can be used for various DSL technologies, although it has been worked out for evaluation of telephone lines for SHDSL connections because this transmission technology is easily available and can be well elaborated. However statements are valid for other digital data communication technologies.

The method is double-ended and based on measured physical parameters of the first layer of the OSI reference model [1].

The selected transmission method is described by ITU-T Recommendation no. G.991.2 [9]. This recommendation lists the physical parameters of a connection that have influence on forming available data transmission speed. These parameters are insertion loss, line noise and return loss. As it is described in Rec. G.991.2, return loss is a calculated value of a reference impedance and the impedance of the equipment which is connected to the line. In this view the line noise and the insertion loss can give a real base for the evaluation. Lots of formerly mentioned methods use these two parameters, although those methods calculate these values. In our method these parameters are measured in real telecommunication access networks and are used as the input parameters of the evaluation system.

3.1 Reasoning Method

In the evaluation of telephone lines the task is to search the available maximal data transmission rate or data transmission speed. A telco is interested in the bitrates that can be available using certain lines and not in the unavailable transmission rates. In this case underestimation of the transmission capacity of a telephone line is better

than its overestimation. This behaviour needs a pessimistic-like approach. It is better to take into consideration the worst circumstances instead of any better one.

Using Zadeh's standard t-norm in the antecedent side of a reasoning system to implement the *AND* relations gives just this required pessimistic, but expressive approach. Mamdani's reasoning method [10] uses this *min* operator as logical *AND* in the antecedent side. Because of the usage of the *min* operator a single rule fires in the same way as the value of the observation's worst dimension takes membership in its antecedent set.

To implement this expressive approach, Mamdani's reasoning method has been chosen for this pre-qualification system. Evaluation the observation of a real line by one of the rule bases of the pre-qualification system is shown in Fig. 4. It can be seen that the second dimension's membership of the observation is the lowest. This means that this rule is surely true for this rate. In Fig. 5 another example can be seen worked out by another rule base. In Figs. 4 and 5 antecedent sets are denoted by $A_{r,d}$ where r is the number of the relevant rule and d is the dimension.

However other fuzzy reasoning systems, for example Larsen's reasoning method would give more smaller results, because of the use of the *multiplication* operator. As it has been shown by our results it is unnecessary to lower the weights of the rules under the minimal membership degree.

For such an experimental system, ranking the bitrate between a minimum and a maximum value is reasonable especially as the data transmission rate of some DSL services are provided exactly in this way. Therefore also this system evaluates bitrates
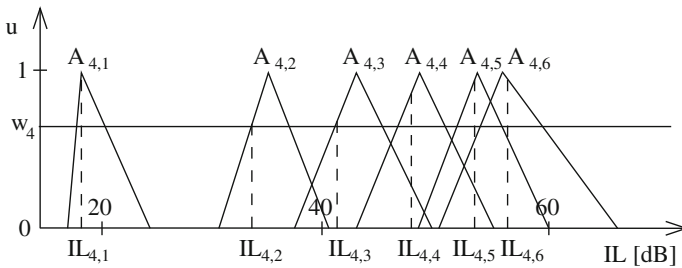
Fig. 4 The weight of the fourth rule from the rule base *A*
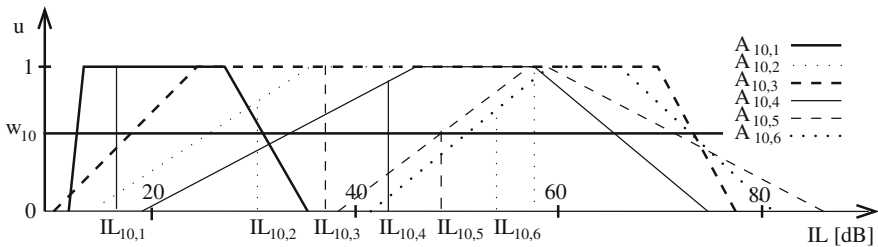
Fig. 5 The weight of the 10th rule from the rule base *B*
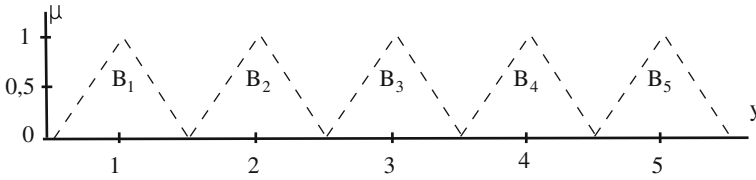
Fig. 6 Consequent sets separated by discrete output values
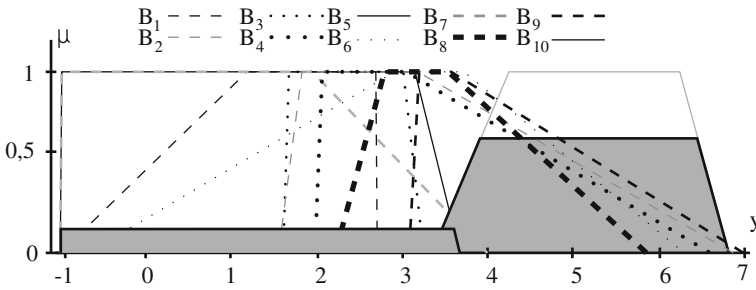
Fig. 7 Consequent sets of the rule base B

in five speed groups. It means that at the present state of the method there are five discrete values as outputs. (Certainly the output resolution can be higher up to the required level.) These outputs are separable in Fig. 6 and are described by triangle shaped fuzzy numbers. However the usage of another rule base (consequent sets are depicted in Fig. 7) gives more advantages as it will be described later. In Figs. 6 and 7 consequent sets are denoted as B_n, where n is the number of the relevant rule.

There are other physical systems with discrete outputs. One of them is the well known example of character recognition. In that case there are at least 26 values of the output namely the characters of the English alphabet. For these systems with discrete outputs not only Mamdani's reasoning method is suitable. This type of discrete output problems can be handled also by other methods, e.g. Takagi-Sugeno fuzzy modelling [11] is really effective in character recognition [12].

3.2 Crisp Conclusions

As the consequent sets of the rules are fuzzy sets, also the combined output of the Mamdani method is a fuzzy result. This (in some cases quite complex) fuzzy output cannot be used as the final result of the system. Also operators and technicians of telcos do not understand and interpret these fuzzy sets neither in graphical nor in numerical formats. Results have to be defuzzified.

Two defuzzification methods are used in our approach: COG and COM. Both results of rule bases A and B can be defuzzified by Center of Gravity defuzzification.

Center of Gravity defuzzification does not represent directly the expected number of a bitrate group. An approximate result is provided by this method. However also the nearest neighbour group is hidden in this result. As an example if the line's data transmission capacity is between 2.5 and 3.5 Mbits/sec and the crisp result is $y = 4.612$ than it means that the line is evaluated into the fourth bitrate group and it is closer to the fifth bitrate group than to the third. In other words, the line "strongly belongs" to the fourth group. For the final result using COG defuzzification this result can be rounded, or in another way the modulus of the COG result can be used. Figure 8 shows such an example. As the second rule base is created for COG, it can not be used for COM defuzzification.

The Consequent sets of the first rule base (A) describe directly the possible outputs (bit rate groups) by fuzzy numbers. These sets are triangle shaped and symmetrical. Here both Center of Gravity and Center of Maxima defuzzification methods are applicable. However there are differences between the use of these two.

It is in the nature of the observed system that using rule base A only two types of results can be produced. One of them occurres when only a single rule fires and the output is a lone symmetrical trapezoid. In this case the result of COG and COM defuzzification is the same, as it can be seen in Fig. 9. Both results give an accurate value for the right bitrate group.

The other case is when two neighbouring rules fire. In this case the measured line parameters have positive membership values in all of these two rules. It means that the telephone line belongs to the higher bitrate group, although its membership in
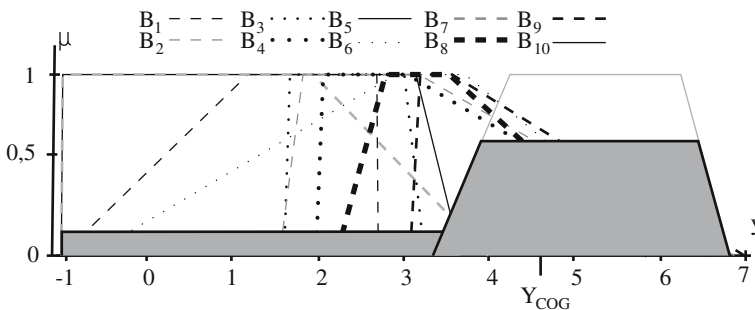
Fig. 8 Defuzzification of a fuzzy result of the rule base B
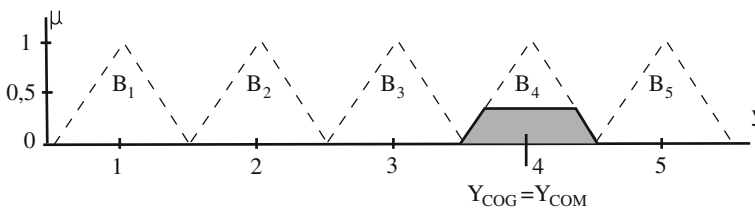
Fig. 9 Defuzzification of a fuzzy output of the rule base A
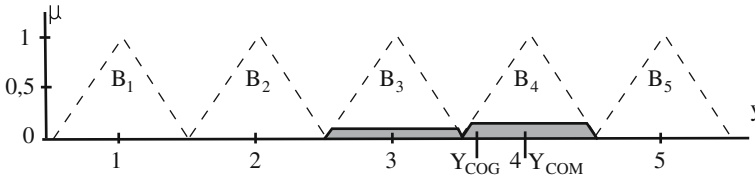
Fig. 10 Defuzzification of a fuzzy output of the rule base *A*

this group is quite low. The result of COG defuzzification in this case is a fraction which has to be rounded for getting the number of one of the bitrate groups.

The final consequence is immediately obtained from the COM defuzzification as it defuzzifies just the fuzzy number of the speed group that fits the best. In this case further processing is not needed (Fig. 10).

Theoretically there is a possibility for the case when two rules fire at the same rate. In this case neither COG nor COM defuzzification give integer results. Rounding the result or using a modulus can be a solution. In practice the probability of this case approximates to zero.

3.3 Different Rule Bases

For the performance evaluation in the presented research different rule bases are used. Each of them is based on measured physical parameters of real telecommunication lines used in several access networks. Input data are insertion loss and line noise. There are some technical and locational differences between them.

Technical differences mean that the method of their creation is different. The simpler rule base is made by the simple mathematical description of the input data sets and consists triangle shaped membership functions of antecedent and consequent sets. This rule base is sparse, there are uncovered areas in the antecedent side. Figure 11 shows an example of this rule base. *A* is used in this chapter to refer to this rule base.

Another type of rule base is also used in this pre-qualification method. This is referred to *B* in this chapter. In order to avoid the mistakes derived from the sparseness of rule base *A* it has been made by bacterial memethic algorithm [13]. Trapezoidal shaped fuzzy sets are used in this rule base and it contains ten rules instead of five in rule base *A*. A couple of the rules of rule base *B* can be seen in Fig. 12.

Detailed description of rule bases and their construction can be found in [14].

Locational differences are caused by the different noise climate of the different distribution areas. In the present state of the research these variances are handled by location-dependent rule bases. Also this is introduced in [14].
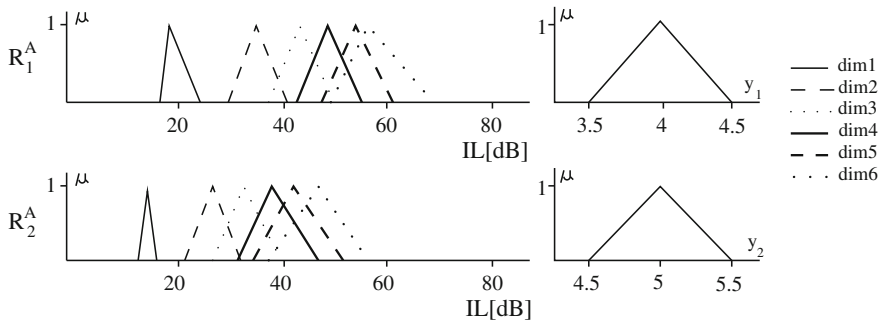
Fig. 11 Rules from rule base *A*
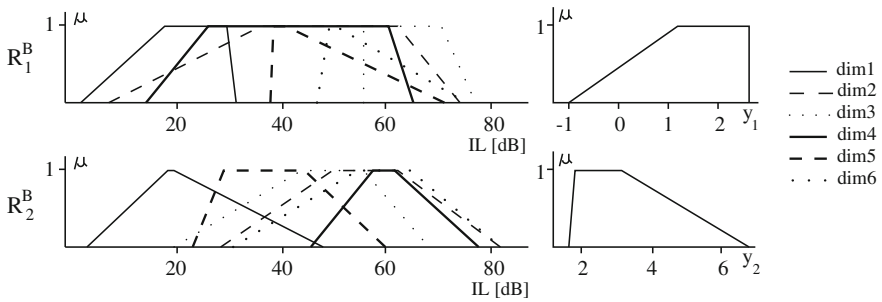
Fig. 12 Rules from rule base *B*

4 Comparison of the Results with Other Evaluation Methods

To test the presented evaluation technique physical parameters of several connections were measured and pre-qualified by our method. These results are presented and compared to the results of other evaluation methods in the next part of the paper. (Measured lines are identified by capital letters from *A* to *R*.) To discover the exact value of the available maximal bitrate, an SHDSL node and an SHDSL transceiver unit was installed to the observed lines. As evaluation by expert knowledge and evaluation by distance data are available for SHDSL transmission technology these two methods have been used in comparison.

All of the used evaluation methods apply bitrate ranges for the evaluation. These ranges are different in different evaluation systems. Narrower ranges are used by experts and quite wide ranges by length based evaluation. The ranges of our fuzzy based method is between these two extremes. Because of this in Table 1 the discrepancies of all methods are given in terms of their own ranges. i.e. 500 kbit/sec wide steps are used by experts. If the available bitrate of a line is 4616 kbit/sec and the expert's evaluation is 3000kbit/s then the difference is around 1500 kbit/sec, so the discrepancy of the evaluation is −3, as in case of line *R*.

Table 1 Measured values and discrepancies of evaluation systems

Telephone line	Real bitrate [kbit/sec]	Discrepancy by expert	Discrepancy by length from inventory	Discrepancy by fuzzy method (rule base A)	Discrepancy by fuzzy method (rule base B)
A	2376	−2	0	1	0
B	2056	−1	−1	0	0
C	4040	1	−1	−1	−2
D	4040	−1	−1	−1	−2
E	3144	0	−2	0	0
F	3144	0	−1	0	0
G	5704	−2	−2	inputs out of range	0
H	2056	−1	−1	0	0
I	3144	−1	0	inputs out of range	1
J	4936	−1	−2	0	0
K	4040	0	−1	−1	−2
L	4360	0	−1	−1	−1
M	1736	0	0	0	0
N	2056	0	−1	inputs out of range	0
O	4804	0	−1	0	0
P	4360	0	−1	0	0
R	4616	−3	−1	0	0

These data are graphically represented in Fig. 13. The vertical axis shows the error rate of the methods and the observed lines are represented on the horizontal axis. Hits are pictured by small diamonds on the vertical 0 and errors by positive or negative bars depending on the positive or negative value of the division from the real value. A positive bar can be seen if a line is overestimated and a negative one if it is underestimated. Naturally, positive deviation is the bigger problem.

Figure 13a shows the deviation of the method based on experts. It can be seen that the predictions of experts approximate both from above and from below the correct values. They try to guess the bitrate, and they are quite successful because of their experiences.

The efficiency of the method based on the comparison of technical inventory contained line length data with tables can be seen in Fig. 13b. Despite of preliminary hopes the results of this method are the worst. The proper value is almost completely missed. During the tests there were only three lines that could have been estimated well by this system.

Figure 13c, d show the results of the fuzzy based evaluation systems. The success rates differs from each other. In Fig. 13d there are holes in the graph. These holes are caused by the sparseness of the rule base (A) is used in this case. *As it is shown by this work, sparse rule bases can not be used in physical parameters based telecommunication pre-qualification purposed fuzzy systems.* Errors of rule base sparseness are corrected by using rule base B in Fig. 13c. It can be seen that in case of lines
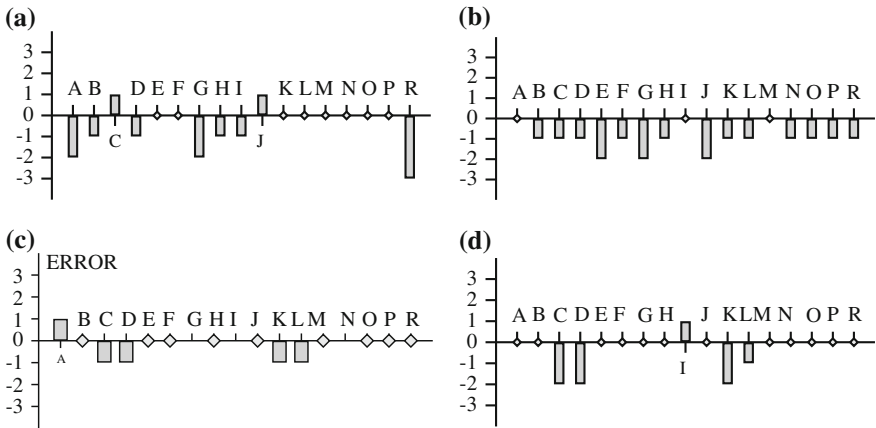
Fig. 13 Errors of different evaluation systems. **a** Error rate of evaluation by expert, **b** Error rate of evaluation by line length, **c** Error rate of evaluation by fuzzy system (rule base *A*), **d** Error rate of evaluation by fuzzy system (rule base *B*)

C, D, K and L both of them make mistakes. The noise environment of these lines are unknown for both of the rule bases. These lines were selected for tests randomly in order to test noise dependency. In known environments, which were considered during rule base construction, the fuzzy based method with rule base *B* works well. It fails the evaluation only in case of line I.

There are significant differences between the evaluation methods. The worst evaluation technique is the one based on line length data from technical inventory. Its success rate remains under 20 %. The best system is the fuzzy based evaluation using rule base *B*. It has been successful in more than 70 % of the cases. The success of other systems is around 50 %, however the fuzzy system with rule base *A* is better (if it hits) as it can be seen in Fig. 14.
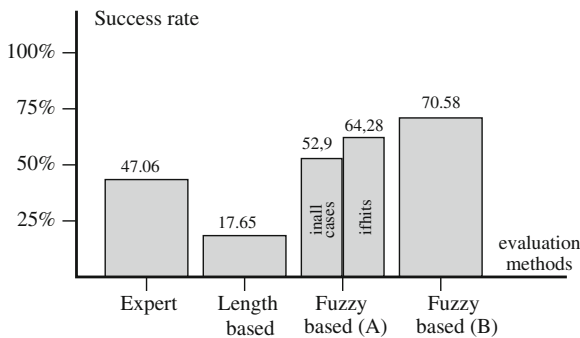
Fig. 14 Succes rates of different evaluation methods

5 Conclusions

In Sect. 2 various evaluation techniques were presented. Although there are numerous methods, only a few are used in evaluation for SHDSL. In this paper a new technique was presented that has been developed basically for SHDSL systems, but can be used also for the evaluation of other data transmission systems. In order to do this, only the rule bases have to be renewed, the set of physical input parameters can be the same.

As it comes from the nature of the telecommunication transmission systems the usage of sparse rule bases are not suitable. Some techniques have to be used to avoid the mistakes derived from rule base sparseness, e.g. fuzzy rule base interpolation should be investigated.

Tests and comparisons with other systems show that fuzzy methods can be used efficiently in performance evaluation of telecommunication systems, moreover our new method gives better and more exact results, than the ones presently in use.

References

1. ITU-T: Data Networks and Open System Communications, Open System Interconnection—Model and Notation, ITU-T Recommendation X.200, July 1994
2. Goralski, W.: DSL loop qualification and testing. IEEE Commun. Mag. **37**(5), 79–83 (1999)
3. Faulkner, R., Schmidt, K.E., Zhang, Y.: Method and apparatus for qualifying loops for data services, United States Patent, Patent No. US 6,385,297 B2, 7 May 2002
4. Schmidt, K.E., Groessl, D.J., Zhang, Y.: Predicting performance of telephone lines for data services, United States Patent, Patent No. US 6,895,081 B1, 17 May 2005
5. Schmidt, K.E., Groessl, D.J., Zhang, Y.: Predicting performance of telephone lines for data services, United States Patent, Patent No. US 7,263,174 B2, 28 Aug 2007
6. Cioffi, J., Silverman, P., Starr, T.: Digital subscriber lines. Comput. Netw. **31**, 283–311 (1999)
7. Liu, G., Campbell, M.A.: Single-ended subscriber loop qualification for xDSL service: United States Patent, Patent No. US 6,266,395 B1, 24 July 2001
8. Posthuma, C.R.: System to pre-qualify copper subscriber loops for high bandwidth access service using subscriber or network generated tones. United States Patent, Pat. No. US 6,459,773 B1, 1 Oct 2002
9. ITU-T: Single-pair high-speed digital subscriber line (SHDSL) transceivers, Transmission systems and media, digital systems and networks, Digital sections and digital line system—Access networks, ITU-T Recommendation G.991.2, Feb 2001
10. Mamdani, E.H., Assilian, S.: An expriment in linguistic synthesis with a fuzzy logic controller. Int. J. Man-Mach. Stud. **7**, 1–13 (1975)
11. Takagi, T., Sugeno, M.: Fuzzy identification of systems and its applications to modeling and control. IEEE Trans Syst Man Cybernet **SMC-15**, 116–132 (1985)

12. Tormási, A., Botzheim, J.: Single-stroke character recognition with fuzzy method. In: Balas V.L. et al (eds.) New concepts and applications in soft computing, SCI 417, pp. 27–46, Springer, Berlin (2012)
13. Botzheim, J., Cabrita, C., Kóczy, L.T., Ruano, A.E.: Fuzzy rule extraction by bacterial memetic algorithms. Int. J. Intell. Syst. **24**(3), 312–339 (2009)
14. Lilik, F., Kóczy, L.T.: The line noise as the optional antecedent parameter of performance evaluation. In: 13th IEEE international symposium on computational intelligence and informatics, Budapest (2012) (In press)

Construction Site Layout and Building Material Distribution Planning Using Hybrid Algorithms

Bence Kalmár, András Kalmár, Krisztián Balázs and László T. Kóczy

Abstract   Chapters have been written previously about how genetic algorithms and other evolution-based algorithms could aid construction site layout planning. These articles presented approaches that solved of the layout problem by applying costs on the moving of construction materials across the site. Our goal was to build an algorithm which is specialized in solving problems of distributing building materials—brick for example—on a site by placing their pallets at the optimal spots, for every unit built from a given material to be within optimal reach. This article describes a solution of this problem for the engineering practice and interprets the slow but accurate method of the Hungarian Algorithm, further it proposes a Memetic Algorithm as a faster but almost as accurate solution. Conclusions are drawn about the usability of this method.

Keywords   Construction layout planning · Genetic evolutionary algorithm · Bacterial evolutionary algorithm · Memetic evolutionary algorithm · Hungarian algorithm

B. Kalmár (✉)
Faculty of Architecture, Budapest University of Technology and Economics,
Budapest, Hungary
e-mail: bence.kalmar@gmail.com

A. Kalmár · K. Balázs · L. T. Kóczy
Department of Telecommunications and Media Informatics,
Budapest University of Technology and Economics, Budapest, Hungary
e-mail: kalmar@tmit.bme.hu

K. Balázs
e-mail: balazs@tmit.bme.hu

L. T. Kóczy
Department of Automation, Széchenyi István University, Győr, Hungary
e-mail: koczy@tmit.bme.hu; koczy@sze.hu

1 Introduction

At a construction site of a multi-storey building, especially in case of office and public buildings where several floors are structured from prefabricated or monolithic concrete structures, infilling walls are placed to separate the interior and exterior areas of the floors, as well as the rooms. These walls are made from blocks or bricks, which are placed by the construction workers piece by piece to build up the structure. On the construction site, these elements are stored in depots from where the workers can collect and move them to the wall where they are needed. Our intention is to find the spot (or spots) for the depot (or depots) from where any block or brick could be moved to its place on the shortest possible route. In civil engineering practice these kinds of problems are solved by heuristic methods because distributing various materials is a rather complex matter.

At a real scale construction site usually several different subcontractor companies are working simultaneously, and directing these workers usually takes up all the resources reserved for the organization. Furthermore, at a real scale construction, the incidents of time delays and setbacks in material supply are likely to happen, so these complex problem groups are far too difficult to handle by having all of them recalculated at each step of the construction. There are plenty of articles that provide different solutions on how to plan the whole construction site, some of them even use Evolutionary Algorithms [1–3]. Our intention is not to solve the whole problem, but to concentrate on a part of it, one that can be solved quickly. We limit our interest on the case where only one kind of material is distributed at a time. Furthermore we assume that there are no obstacles in the way when one piece or pack of material is moved from the depot to the wall.

With the method we seek one can calculate the optimal place for the depots of the chosen material and define which depot should serve which wall section, while showing the optimal amount of material to be stored in each depot. The method could have several uses, e.g. in the distribution of building material on construction sites, other problems dealing with goods in parcels, as well as an aid in planning layouts of networks that depend on costs or weights— corresponding to the scheme of this layout problem's distances. It is important to emphasize that most of the articles published so far use Genetic Algorithms. Relying on previous results comparing the efficiency of Genetic Algorithms and Bacterial Algorithms (e.g. [4, 5]), we recommend however the use of Bacterial Algorithms instead, because they have better convergence with a runtime similar to that of Genetic Algorithms.

In the next section a variety of usable algorithms will be explained briefly, namely the Bacterial Evolutionary Algorithm (BEA), the Memetic Evolutionary Algorithm (MEA), the Hungarian Algorithm and K-means Clustering. In Sect. 3, propositions on solving the matter and handling the algorithms mentioned are followed by the results of the simulations conducted on several differently sized and computationally intensive problems in Sect. 4. As a conclusion, applicability of the proposed algorithms is evaluated in the last section on the basis of process time and accuracy. Propositions in which direction to explore further are presented as a conclusion.

2 Overview of the Applied Methods

2.1 Bacterial Evolutionary Algorithm

This algorithm was introduced by Nawa and Furuhashi [6]. As the name suggests, Evolutionary Algorithms are iterative stochastic methods inspired by natural reproduction trying to optimise the given task using global optimisation steps. The population that evolves is made up of individuals that represent the potential solutions to the problem and are rated by their fitness values. The Bacterial Evolutionary Algorithm contains optimization steps similar to the reproduction cycle of bacteria. BEA consists of the following steps:

1. *Initialisation:* An initial population is created by selecting random elements of the search space according to some distribution, or by using an initial heuristic.
2. *Bacterial mutation:* All bacteria are mutated in all their genes, multiple times and in random orders. In case of each mutation step, if the original value was better, then it is restored, if the new one gives the individual a higher fitness value, then it is kept.
3. *Gene transfer:* The population is divided into two parts according to their fitness values. The individuals possessing higher fitness values form the superior and the ones having lower values form the inferior part of the population.

Then pairs are formed where the first members of the pairs are from the superior part (superior individuals) and the second members are from the inferior part (inferior individuals). For each pair a random point of the chromosome is selected and the value of the gene at the selected point in the inferior bacterium is overwritten with the value of the gene at the selected point in the superior bacterium.

The main iteration loop of the algorithm contains Steps 2 and 3. The algorithm stops if one of the termination criteria is fulfilled at the end of a generation (generation limit reached, time limit exceeded, etc.). After termination, the best individual represents the quasi-optimal solution.

2.2 Memetic Algorithms

The techniques cause minor modifications to the candidate solutions iteration by iteration and thus exploring only the 'neighbourhood' of particular elements of the search space are called local search methods.

As a result of these minor modification steps, the local search algorithms find the 'nearest' local minimum quite accurately after a sufficient number of iterations. However, these techniques are very sensitive to the location of the starting point. In order to find the global optimum, the starting point must be located close enough in the sense that no local optima separate the two points.

Evolutionary computation techniques explore the whole objective function because of their characteristics, so they find the global optimum but they approach it slowly. Local search based algorithms, on the other hand, find only the nearest local optimum, but they converge to it faster.

Avoiding the disadvantages of the two different technique types, evolutionary algorithms (including swarm intelligence techniques) and local search methods may be combined [7], for example, if one or more local search steps are applied in each iteration cycle for each individual. It is expected that the advantages of both local search and evolutionary techniques can be exploited this way: the local optima can be found quite accurately on the whole objective function, i.e. the global optimum can be obtained quite accurately.

2.3 Hungarian Algorithm

The Hungarian Algorithm proposed for the solution of this problem, published by Kuhn [8], solves the assignment problem in polynomial time [$O(n^3)$]. After creating the matrix of costs (in our case the distances) it is built up from 4 or 5 steps depending on the implementation. All these steps use the cost matrix in multiple sub-sequences and some of the steps need to be iterated several times to find the optimal assignment for the problem. This makes the runtime of the algorithm depending on the size of the matrix used.

2.4 K-means Clustering Algorithm

K-means clustering is one of the hard partitioning methods. It searches for an optimal partition of the data space by assigning n observations into k clusters, through iterative steps. In order to do this, it tries to minimize the so called sum-of-squared-error criterion in every step.

At the first step the algorithm selects k random locations to be the initial centroids for the clusters. Every observation is then assigned to one of these clusters, according to which cluster centroid is the nearest to it. (The distance function can be chosen freely) After this assignation, the centroids are recalculated using the mean value of assigned values. This process is repeated until the cluster centroids do not change anymore, or until the change stays under a given threshold [9].

3 The Proposed Methods

The problem consists of many parts, starting with the planning of the building, choosing the right material, defining the efficient number of depots, the capacity of each of these depots, and so on. In our presentation of the problem the walls to be

built are considered as input data, defined by coordinates of target points, where the building material should be transported to. These coordinates represent the sections of the walls. We decided to use the number and capacity of the depots as inputs as well, making our task this way easier, so we can focus on the speed and efficiency of finding the solution. What we are looking for are the coordinates of the depots.

From this point on we transformed the problem to another one which requires us to calculate coordinates from coordinates. Our output will be an unambiguous assignment among the walls and the depots, each wall point is served by one depot, and every depot has as much wall points assigned to it as its capacity allows.

Once both the wall and depot coordinates are given, one must only calculate the distances and find the combination of the distances where the compliance is assured as written above with the lowest accumulated distance value. This problem is a linear assignment task, which can be solved by polynomial time algorithms such as the Hungarian Algorithm, giving the optimal solution once all the coordinates are known.

We used this algorithm to give us the value of how good the solution offered by the current set of depot coordinates is. This value will be the fitness value of the Bacterial Evolutionary Algorithm in its fitness function.

3.1 Bacterial Evolutionary Algorithm with Heuristic Fitness Evaluation

Our aim was to first create a fast and moderately accurate solution that runs as quickly as possible. Using just BEA steps without local search is the fastest way, but the runtime is largely determined by the fitness evaluation. For shorter process time we used a heuristic method where the table of all distances between the depots and the wall points were calculated. The lowest distance values are determined by reading this table by its columns and assigning the smallest distances with the depots. The assignment depends on the sequence of reading the columns of this table. One can find the best solution by reading the columns in every possible sequence. For less computation time we decided to randomly switch the columns and try only a few of the possible sequences. The fitness value of one individual was determined by their average, thus an approximate value that turned out to be a good approximation at small sized problems.

Steps of the BEA:

1. Initialisation:

    (a) Initialising the population
        (i) one depot is defined by its coordinates
        (ii) one individual is defined by the given number of depots
    (b) Reading the wall coordinates and running parameters

2. Bacterial Mutation of the population as in BEA above Including multiple fitness evaluation with the heuristic algorithm

   (c) Creating the table of distances
   (d) Finding the smallest distances for the first depot by reading the columns in order
   (e) Randomly switch the columns and find the smallest distances
   (f) Repeat the switching and determine the average of the solutions as the fitness value

3. Gene Transfer as in BEA above

   (g) Multiple fitness evaluation

4. Continue iteration with Step 2

3.2 Bacterial Memetic Algorithm with Clustering Using Hungarian Algorithm in the Fitness Function

The usage of Bacterial EA is less accurate, but faster in convergence to the ideal arrangement in the beginning. To find the target points quickly and accurately, we proposed the use of the Bacterial Memetic Algorithm (BMA) which is more effective in time and processing, according to the literature. In our application it means, that every Bacterial Mutation and Gene Transfer step of the BEA is followed by a clustering algorithm that uses the best individual's depot coordinates as the cluster centre. Within a few iteration steps the algorithm finds the best assignment between the nearby wall points and the depots by moving the cluster centre around.

Steps of the BMA:

1. Initialisation:

   (a) Initialising the population
       (i) one depot is defined by its coordinates
       (ii) one individual is defined by the given number of depots
   (b) Reading the wall coordinates and running parameters

2. Bacterial Mutation of the population as in BEA above Multiple fitness evaluation with Hungarian Algorithm

   (a) Creating the table of distances
   (b) Running the HA on the distances
   (c) Defining the perfect fitness value

3. Local search: Clustering

   (a) Finding the depots' centre of gravity from the nearby wall points
   (b) Finding the nearest wall points for the new cluster centre

    (c) Finding the new centre of gravity
    (d) Iterating the steps for a given time or accuracy

4. Gene Transfer as in BEA above

    (a) Multiple fitness evaluation: Hungarian Algorithm

5. Local search like in Step 3
6. Continue iteration with Step 2

In the iterations of this EA a Hungarian Algorithm is executed to find the fitness value of the solution. This algorithm finds the lowest distance values in the distance table (described at the heuristic fitness evaluation). But the HA turned out to be very ineffective in time and process requirement. The processing time grows dramatically with the complexity of the problem. So the need arises for a better algorithm to solve this matter even for the price of less accuracy.

3.3 Bacterial Memetic Algorithm with Clustering Using Pre-clustering in the Fitness Function

In this approach the BEA iterations contain a full clustering algorithm as mentioned above. In the fitness function the fitness value is determined by a pre-clustering algorithm which uses the current individual's depot coordinates as a cluster centre. After a few iterations it finds the best assignment for the nearby wall points to each depot without moving the cluster centre. Then it adds up the distances and returns the summary of them as the fitness value of the solution.

Steps of the BMA:

1. Initialisation:

    (a) Initialising the population
        (i) One depot is defined by its coordinates
        (ii) One individual is defined by the given number of depots
    (b) Reading the wall coordinates and running parameters

2. Bacterial Mutation of the population as in BEA above Including multiple fitness evaluation with the pre-clustering algorithm

    (a) Finding the depots' centre of gravity from the nearby wall points
    (b) Finding the nearest wall points for the new cluster centre
    (c) Finding the new centre of gravity
    (d) Iterating the steps for a given time or accuracy
    (e) Calculating the distances with the new cluster centre

3. Local search: Clustering

    (a) Finding the depots' centre of gravity from the nearby wall points

    (b) Finding the nearest wall points for the new cluster centre
    (c) Finding the new centre of gravity
    (d) Iterating the steps for a given time or accuracy
    (e) Calculating the distances with the new cluster centre

4. Gene Transfer as in BEA above

    (a) Multiple fitness evaluation with pre-clustering algorithm as in Step 2

5. Local search like in Step 3
6. Continue iteration with Step 2

4 Comparing Solutions and Presenting Simulations

4.1 Simulations

In every approach we used the same running parameters. In the BEA one population had 20 individuals and one individual contained five pair of depot coordinates. In the Bacterial Mutation step of the BEA 50 mutated clones were made, selected and sent back to the population if their fitness values were adequate. We only mutated whole genes, not their particles. In the Gene Transfer step of the BEA 10 transfer took place to mix the population, select and send back the best mixes and only the same chromosomes of the individuals were transferred.

Several floor plans were tested but not every one of them with every algorithm. The different wall layouts used different number of wall points, so the detail of the depot-placing could be set to the scale of the floor plans. At higher detail or scale more runtime and computation was needed. The heuristic and the clustering algorithms are linearly related to the growth of the wall points in runtime but the HA uses the distance matrix in multiple steps. Thus at higher complexity problems the HA needed extreme computation time, and was found to be less adaptable at real scale layouts. Furthermore the heuristic fitness evaluation finds only strongly sub-optimal solutions when the problem complexity strikes high.

Figure 1 shows a small size problem where the wall layout is defined by 35 points. This gives us a rough approximation on where the depots should be placed while this problem is an easy task for all three algorithms. The solutions shown here are results of 100 iteration of each algorithm. It is easy to see that the BMA with pre-clustering and the BMA with Hungarian Algorithm gave the same coordinates for the depots to be placed. This is so because they both found the optimal solution using the same K-means Clustering local search. However the BEA produces a rather sub-optimal result. Table 1 shows the fitness values for the whole population.

In the first columns the absolute value of total distances from all the wall points to their depots are shown. The second columns contain the relative fitness value starting with 1.00 for the optimal solution and scaled to 0.00 for the starting positions of the population: uniformly 250 m in summarized distance. The BEA with heuristic
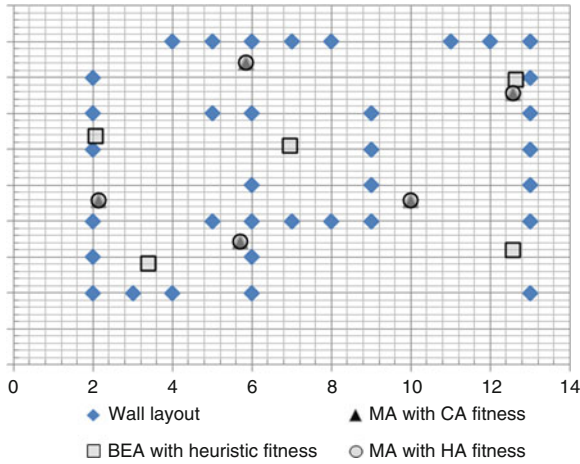
Fig. 1 Small sized problem layout

Table 1 Fitness values of the solutions

Individuals	BEA with heuristic fitness		BMA with CA fitness		BMA with HA fitness	
	Abs. distance	Rel. fitness	Abs. distance	Rel. fitness	Abs. distance	Rel. fitness
ind. 1	64.08	0.94	60.08	1.00	60.08	1.00
ind. 2	65.07	0.92	60.08	1.00	60.08	1.00
ind. 3	65.42	0.92	60.08	1.00	60.08	1.00
ind. 4	65.85	0.91	60.08	1.00	60.08	1.00
ind. 5	66.02	0.91	60.08	1.00	60.08	1.00
ind. 6	66.18	0.91	60.08	1.00	60.43	0.99
ind. 7	68.66	0.87	60.08	1.00	61.55	0.98
ind. 8	69.02	0.87	60.08	1.00	61.61	0.98
ind. 9	72.26	0.83	60.08	1.00	61.64	0.97
ind. 10	72.50	0.83	61.44	0.98	61.73	0.97
ind. 11	73.08	0.82	61.73	0.97	61.73	0.97
ind. 12	73.24	0.82	63.08	0.95	61.73	0.97
ind. 13	73.40	0.82	63.08	0.95	61.73	0.97
ind. 14	74.34	0.81	64.25	0.94	62.29	0.96
ind. 15	74.37	0.81	64.25	0.94	62.89	0.96
ind. 16	75.50	0.80	64.25	0.94	63.86	0.94
ind. 17	77.75	0.77	66.59	0.90	64.35	0.93
ind. 18	77.85	0.77	67.17	0.89	65.54	0.92
ind. 19	82.11	0.73	73.55	0.82	65.64	0.92
ind. 20	84.09	0.71	73.99	0.81	94.94	0.63
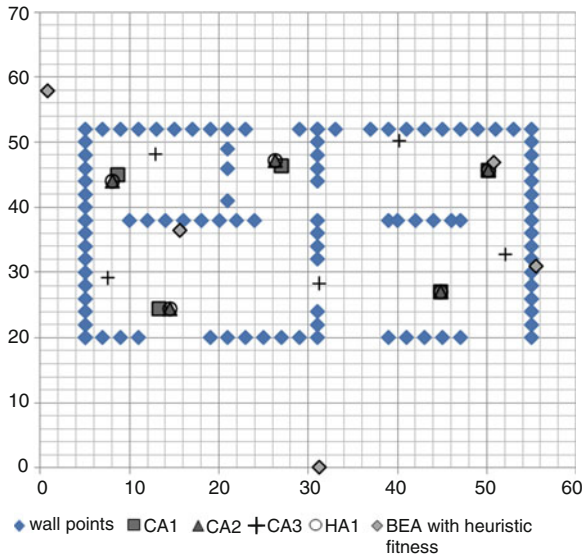
Fig. 2 Middle sized floor plan

fitness evaluation is not far from the optimum. In percentage of relative fitness value 6% difference is found and if the difference is measured in absolute distances: 60.08–64.08 m is 6.24%. The heuristic fitness evaluation seems to solve the matter surprisingly good taking the difference in accuracy between the BEA and the BMA into consideration.

Both Bacterial Memetic Algorithms have reached the maximum fitness but the one with clustering in fitness evaluation contains nine individuals with the highest rank. The BMA with Hungarian Algorithm in fitness evaluation has only five of them. Obviously the version using clustering had more iteration to spread the right genes in the population. Within the 100 iterations run by both algorithms the convergence to the right solution is evidently better at the version that uses clustering in fitness evaluation. Not to mention the difference in computation time what even at this easily solvable task is significantly higher at the BMA with Hungarian Algorithm.

The next example shows a more complex problem. The walls are represented by 100 points but all other running parameters are the same for the results to be comparable.

Figure 2 contains one solution per algorithm except for the BMA with clustering. At this amount of walls the Hungarian Algorithm needs significant computation time, thus even this middle sized problem's solution with BMA with HA took 3 days for an average computer. Meanwhile the BEA with the heuristic fitness evaluation stuck in local minimum values as this typical example shows.

The optimum for this problem is found as well but unlike the first presented problem (in Fig. 1) the BMA with clustering does not always find the same solution
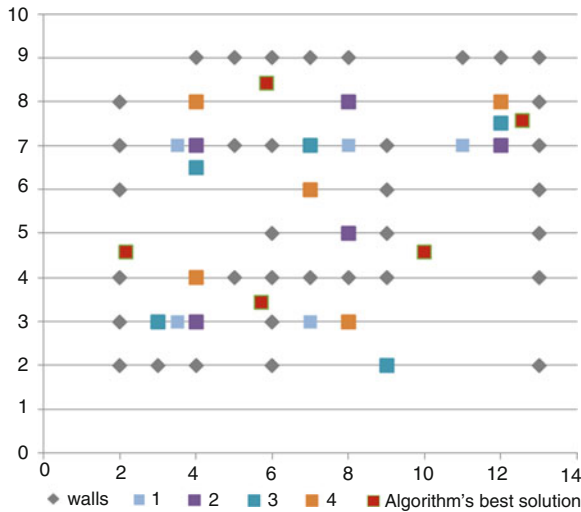
Fig. 3 Heuristics 1

Table 2 Fitness values of heuristics

	Problem 1		Problem2	
	Abs. distance	Rel. fitness	Abs. distance	Rel. fitness
Heuristic 1	70.10	0.86	956.24	0.91
Heuristic 2	65.59	0.92	947.08	0.92
Heuristic 3	73.89	0.81	1029.45	0.85
Heuristic 4	71,82	0.84	885.00	0.98
Algorithm	60.08	1.00	870.09	1.00

in the given 100 iteration. Instead it returns with different arrangements; shown in Fig. 2 by CA1, CA2 and CA3. By the 200th iteration the BMA with CA found the optimal solution for the first 10 times (considering that these algorithms run on randomly generated routes, the possibility of failing for the eleventh—or any other—time cannot be excluded, nevertheless, this approach may be unambiguously considered as success for one).

Meanwhile (just like in the first and second problems in Figs. 1 and 2) since the methods used so far in construction material distribution were based on heuristic placement of the depots; students of architecture were asked to place the depots as they think to be the best for serving the walls with building material. Even though the students were told not to think about the actual movements on the construction site and only focus on the absolute distances they could not find near optimal solutions. Figures 3 and 4 shows the heuristic placements suggested by the students (colours 1–4) for the problems presented in Figs. 1 and 2. The fitness values of the heuristics compared to the solution given by our algorithm are presented on Table 2.
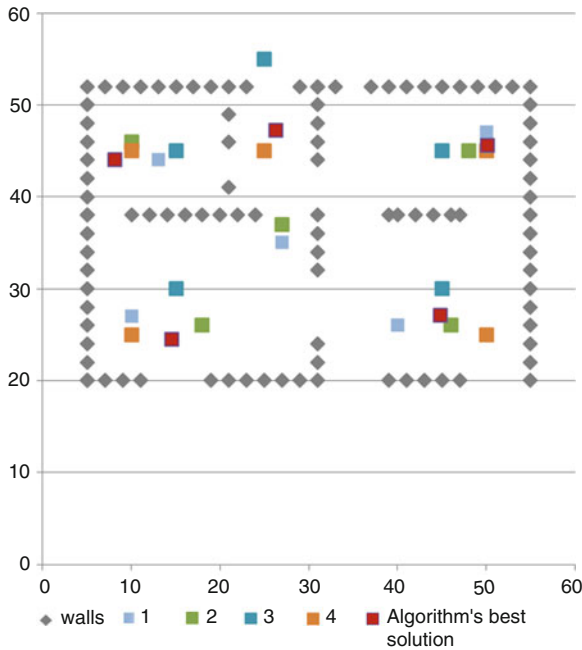
Fig. 4 Heuristics 2

For the reasons mentioned above solving large scale problems with the Hungarian Algorithm was stopped. The next example presented contains 830 wall points that is highly out of the range for this algorithm (in the aspect of computation time).

The example shown at Fig. 5 the BEA with heuristic algorithm was typically stuck after reaching local minimums and never got close to the optimal solution. This problem was planned to put the algorithm to a real test and the results were unexpected. Partition walls were defined by lower-, filling walls by higher density of wall points. Each colour initiates the walls assigned to each depot. The solutions of the BMA with clustering are mainly the same every time the algorithm is executed. Unfortunately the absolute fitness of the heuristics in this problem is unknown because the clustering algorithm finds sub-optimal assignments between the walls and depots. This is also the reason why the algorithm does not work properly with this example. Obviously the assignment shown in Fig. 5 is rather sub-optimal because the wall elements on the outside should not be assigned with the centrally placed depot.

4.2 Summary of the Simulations

In summary the heuristic solutions were misplaced in most examples but the average guesses of the students were not entirely wrong. The last problem was solved by the
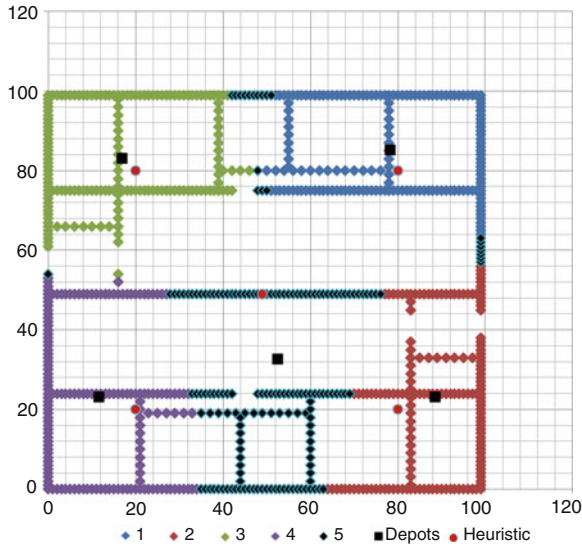
Fig. 5 High density problem with geometric complications

same method by every student; it is easy to notice that the wall layout is rotationally symmetric. They all placed one depot in every corner of the layout and the last depot was placed in the middle. It is an obvious solution but the algorithm did not find it. Although in the first and second case the students' heuristics were lagged behind, the third case proved the algorithm sub-optimal.

In the end the Bacterial Memetic Algorithm with clustering in fitness evaluation stuck after reaching a sub-optimal solution where the obvious choice for the depot placement (and the optimum of the problem) was easy to find for the human mind. The reason behind this failure was that the assignment between the walls and the depots were found by the K-means algorithm which mostly creates stabile clusters in the corners but cannot stay in the middle with the last depot's cluster.

5 Conclusion

After taking our algorithm to the test it is clear that despite the success in both low and middle sized problems the Bacterial Memetic Algorithm can come to a halt after finding sub-optimums if the task is—like the last one presented—showing geometric difficulties. In other greater scaled examples the algorithm finds the optimal solution if its process is not disturbed by geometric pitfalls. At lower scale problems the local minimums can be avoided by using Hungarian Algorithm or giving enough runtime for the clustering to proceed.

When we talk about real scale construction layout and material distribution problems the matter is much more complex than the simulations we run. A real solution should consider multiple materials to be placed and stored at the same time. Furthermore obstacles in the way of moving the materials and other real life problems of organising and layout planning could be relevant. We tend to give more details to the algorithm for more realistic material movement simulation and optimise for different depot sizes which would highly raise the realistic usability of the algorithm. We shall use the algorithm for other purposes like problems dealing with goods in parcels or planning layouts of networks that are depending on costs or weights in the future.

References

1. Soltani, A.R., Tawfik, H., Goulermas, J.Y., Fernando, T.: Path planning in construction sites: performance evaluation of the Dijkstra, A*, and GA search algorithms. Adv. Eng. Inform. **16**(4), 291–303 (2002)
2. Hegazy, T., Elbeltagi, E.: EvoSite: evolution-based model for site layout planning. J. Comput. Civ. Eng. **13**(3), 198–206 (1999)
3. Mawdesley, M., Al-jibouri, S., Yang, H.: Genetic algorithms for construction site layout in project planning. J. Constr. Eng. Manage. **128**(5), 418–426 (2002)
4. Balázs, K., Botzheim, J., Kóczy, L.T.: Comparison of various evolutionary and memetic algorithms. In: Proceedings of the International Symposium on Integrated Uncertainty Management and Applications, IUM 2010, Ishikawa, Japan, pp. 431–442 (2010)
5. Dányádi, Zs, Balázs, K., Kóczy, L.T.: A comparative study of various evolutionary algorithms and their combinations for optimizing fuzzy rule-based inference systems. Sci. Bull. Politech. Univ. Timisoara Rom. Transac. Autom. Control Comput. Sci. **55**(69), 247–254 (2010)
6. Nawa, N.E., Hashiyama, T., Furuhashi, T., Uchikawa, Y.: Fuzzy logic controllers generated by pseudo-bacterial genetic algorithm. In: Proceedings of the IEEE International Conference on Neural Networks, ICNN'97, Houston, pp. 2408–2413 (1997)
7. Moscato, P.: On evolution, search, optimization, genetic algorithms and martial arts: towards memetic algorithms. Technical Report Caltech Concurrent Computation Program, Report 826. California Institute of Technology, Pasadena, USA (1989)
8. Kuhn, H.W.: The Hungarian method for the assignment problem. Naval Res. Logist. Q. **2**(1–2), 83–97 (1955)
9. Xu, R., Wunsch, D.C.: Clustering. Wiley, New Jersey (2009)

Part III
Neural Network

Accuracy of Surrogate Solutions of Integral Equations by Feedforward Networks

Věra Kůrková

Abstract Surrogate solutions of Fredholm integral equations by feedforward neural networks are investigated theoretically. Convergence of surrogate solutions computable by networks with increasing numbers of computational units to theoretically optimal solutions is proven and upper bounds on rates of convergence are derived. The results hold for a variety of computational units, they are illustrated by examples of perceptrons and Gaussian radial units.

Keywords Surrogate modeling by neural networks · Approximate solutions of integral equations · Feedforward neural networks · Model complexity · Rates of approximation

1 Introduction

One of successful applications of feedforward neural networks is surrogate modelling of functional relationships. It has been successfully used for modelling of empirical functions, i.e., functions for which no mathematical formulas are known and thus their values can only be obtained experimentally. Often such experimental evaluations are too expensive or time consuming and so they are performed merely for samples of points in the domains of the empirical functions and the obtained values are used for training feedforward networks. The networks trained on such training sets play roles of surrogate models of these empirical functions. For example, input–output functions of feedforward networks have been used in chemistry as surrogate models of empirical functions assigning to compositions of chemicals measures of quality of catalyzers produced by reactions of these chemicals, in biology as models of

V. Kůrková (✉)
Institute of Computer Science, Academy of Sciences of the Czech Republic,
Pod Vodárenskou věží 2, 18207 Prague, Czech Republic
e-mail: vera@cs.cas.cz

empirical functions classifying structures of RNA, and in economy as models of functions assigning credit ratings to companies [1, 2]. It should be emphasized that results obtained by surrogate modelling of empirical functions can only be used as suggestions to be confirmed by additional experiments as no other than empirical knowledge of the functions is available. Also suitable types of network architectures and computational units have to be found experimentally.

In contrast to the case of empirical functions, for functions with known, although complicated, analytical descriptions, there is a potential for theoretical analysis of quality of surrogate models. When numerical computations of complicated analytical formulas are too time-consuming, relatively small samples of data obtained by such numerical computations can be sufficient for training feedforward networks. Investigation of mathematical properties of analytical formulas and their comparison with input-output functions of feedforward networks of various types can lead to estimates of accuracies of approximations and their dependence on types of computational units, their numbers, and input dimensions.

Many types of feedforward networks (including all standard types that are popular in applications as well as many others that may not have been considered by experimentalists) are known to be universal approximators. It means that it is possible to adjust their parameters so that they approximate to any desired accuracy a wide variety of mappings between subsets of multidimensional spaces. In particular, the universal approximation property has been proven for approximation of continuous functions on compact subsets of d-dimensional Euclidean spaces by one-hidden layer networks with almost all types of reasonable computational units (see, e.g., [3, 4]). It should be emphasizes that the universal approximation property requires potentially unlimited number of network units. Thus one can conclude that when a function with a complicated analytical description is continuous, surrogate models formed by input–output functions of networks of various types converge with increasing numbers of units to this function. However, a critical factor influencing whether a given type of network units is suitable for the task is the speed of the convergence. Such speed can differ considerably for various types of computational units. For some choices of network units, a sufficient accuracy can be achieved within a feasible bound on the number of network units, while for others, it might require numbers of units that are too large for a practical implementation. In particular for some high-dimensional tasks, the numbers of units of some types can grow with the input dimension exponentially, while choice of other types can lead to quadratic or even linear growth [5].

A large class of functions expressed by formulas, whose numerical calculations are difficult, is formed by solutions of Fredholm integral equations. These equations play an important role in many problems in applied science and engineering. They arise in image restoration, heat conduction, population modelling, potential theory and elasticity, etc. (see, e.g., [6–8]). Mathematical descriptions of solutions of Fredholm equations following from classical Fredholm theorem [9, p. 499] involve complicated expressions in terms of infinite Liouville–Neumann series with coefficients in the forms of integrals. Thus numerical calculations of these expressions are time consuming. Recently, several authors [10, 11] explored experimentally possi-

bilities of surrogate modelling of solutions of Fredholm equations by perceptron and
kernel networks. Motivated by these experimental studies, Gnecco et al. [12] initiated
a theoretical analysis of surrogate solutions of Fredholm equations computable by
neural networks. In Refs. [12, 13], estimates of rates of approximation with increas-
ing numbers of network units were derived for networks with kernel units induced
by the same kernels as the kernels defining the equations and extended to certain
smooth kernels.

   In this chapter, we investigate surrogate solutions of Fredholm integral equations
by networks with general computational units. Taking advantage of results from
nonlinear approximation theory and suitable integral representations of functions in
the form of "infinite" networks, we estimate how well surrogate solutions computable
by feedforward networks can approximate exact solutions of Fredholm equations.
We derive estimates of approximation errors measured in $\mathcal{L}^2$-norm. The estimates
depend on relationships of kernels of the equations to types of computational units.
We apply general results to networks with the most common computational units—
sigmoidal perceptrons and Gaussian radial units. A preliminary version of this chapter
appeared in a conference proceedings [14].

   The chapter is organized as follows. In Sect. 2, we describe approximation of
functions by feedforward neural networks. In Sect. 3, we introduce Fredholm integral
equations and recall theoretical approach to their solutions. In Sect. 4, we apply
some results from nonlinear approximation theory to approximation of solutions of
Fredholm equations by feedforward networks. We illustrate our results by examples
of surrogate solutions of Fredholm equations with the Gaussian kernel by networks
with perceptrons and with Gaussian radial units. Section 5 is a discussion.

2 Approximation of Functions by Feedforward Neural Networks

A traditional approach to approximation of functions known only by samples of data
points was based on linear methods such as polynomial interpolation. For suitable
points $x_1, \ldots, x_m$ from the domain $X \subset \mathbb{R}^d$ of a function ϕ to be approximated, sam-
ples of empirically or numerically obtained approximations $\bar{\phi}(x_1), \ldots, \bar{\phi}(x_m)$ of its
values $\phi(x_1), \ldots, \phi(x_m)$ are interpolated by functions from suitable n-dimensional
function spaces. Such spaces are often generated as *linear spans*

$$\text{span}\{g_1, \ldots, g_n\} := \left\{ \sum_{i=1}^{n} w_i g_i \mid w_i \in \mathbb{R} \right\}, \tag{1}$$

where the functions $g_1, \ldots, g_n$ are the first n elements from a set $G = \{g_n \mid n \in \mathbb{N}_+\}$ with a *fixed linear ordering*. Typical examples of linear approximators are
algebraic or trigonometric polynomials. They are obtained by linear combinations of
powers of increasing degrees or trigonometric functions with increasing frequencies,
respectively.

Feedforward neural networks have more adjustable parameters than linear models as in addition to coefficients of linear combinations of basis functions, also inner coefficients of computational units are optimized during learning. Thus they are sometimes called *variable-basis-approximation schemas* in contrast to traditional linear approximators which are called *fixed-basis-approximation schemas*. In some cases, especially in approximation of functions of large numbers of variables, it was proven that neural networks achieve better approximation rates than linear models with much smaller model complexities [15, 16].

One-hidden-layer networks with one linear output unit compute input–output functions from sets of the form

$$\text{span}_n\, G := \left\{ \sum_{i=1}^{n} w_i g_i \mid w_i \in \mathbb{R},\, g_i \in G \right\}, \tag{2}$$

where the set G is sometimes called a *dictionary* [17] and n is the *number of hidden computational units*. This number can be interpreted as a measure of *model complexity* of the network. In contrast to the case of linear approximation, the dictionary G has no fixed ordering.

Often, dictionaries are parameterized families of functions modeling computational units, i.e., they are of the form

$$G_F(X, Y) := \{F(\cdot, y) : X \to \mathbb{R} \mid y \in Y\}, \tag{3}$$

where $F : X \times Y \to \mathbb{R}$ is a function of two variables, an input vector $x \in X \subseteq \mathbb{R}^d$ and a parameter $y \in Y \subseteq \mathbb{R}^s$. When $X = Y$, we write briefly $G_F(X)$. So one-hidden-layer networks with n units from a dictionary $G_F(X, Y)$ compute functions from the set

$$\text{span}_n\, G_F(X, Y) := \left\{ \sum_{i=1}^{n} w_i F(x, y_i) \mid w_i \in \mathbb{R},\, y_i \in Y \right\}.$$

In some contexts, F is called a *kernel*. However, the above-described computational scheme includes fairly general computational models, such as functions computable by perceptrons, radial or kernel units, Hermite functions, trigonometric polynomials, and splines. For example, with

$$F(x, y) = F(x, (v, b)) := \sigma(\langle v, x \rangle + b)$$

and $\sigma : \mathbb{R} \to \mathbb{R}$ a sigmoidal function, the dictionary $G_F(X, Y)$ describes a set of functions computable by *perceptrons. Radial (RBF) units* with an activation function $\beta : \mathbb{R} \to \mathbb{R}$ are modelled by the kernel

$$F(x, y) = F(x, (v, b)) := \beta(v\|x - b\|).$$

Typical choice of β is the Gaussian function. *Kernel units* used in support vector machine (SVM) have the form $F(x, y)$ where $F : X \times X \to \mathbb{R}$ is a symmetric positive semidefinite function [9].

Various learning algorithms optimize parameters $y_1, \ldots, y_n$ of computational units as well as coefficients $w_1, \ldots, w_n$ of their linear combinations so that network input–output functions

$$\sum_{i=1}^{n} w_i \, F(., y_i)$$

from the set $\mathrm{span}_n \, G_F(X, Y)$ fit well to training samples $\{(x_i, \bar{\phi}(x_i)) \,|\, i = 1, \ldots, m\}$.

3 Fredholm Integral Equations

Solving an *inhomogeneous Fredholm integral equation of the second kind* on a domain $X \subseteq \mathbb{R}^d$ for a given $\lambda \in \mathbb{R} \setminus \{0\}$, $K : X \times X \to \mathbb{R}$, and $f : X \to \mathbb{R}$ is a task of finding a function $\phi : X \to \mathbb{R}$ such that for all $x \in X$

$$\phi(x) - \lambda \int_X \phi(y) K(x, y) \, dy = f(x). \tag{4}$$

The function ϕ is called *solution*, f *data*, K *kernel*, and λ *parameter* of the equation (4).

Fredholm equations can be described in terms of theory of inverse problems. Formally, an *inverse problem* is defined by a linear operator $A : \mathcal{X} \to \mathcal{Y}$ between two function spaces. It is a task of finding for $f \in \mathcal{Y}$ (called *data*) some $\phi \in \mathcal{X}$ (called *solution*) such that

$$A(\phi) = f.$$

Let T_K denotes the integral operator with a kernel $K : X \times X \to \mathbb{R}$ defined for every ϕ in a suitable function space $\mathcal{X}$ as

$$T_K(\phi)(x) := \int_X \phi(y) \, K(x, y) \, dy \tag{5}$$

and $I_{\mathcal{X}}$ denotes the identity operator. Then the Fredholm equation (4) can be represented as an inverse problem defined by the linear operator $I_{\mathcal{X}} - \lambda T_K$. So it is a problem of finding for a given data f a solution ϕ such that

$$(I_{\mathcal{X}} - \lambda T_K)(\phi) = f. \tag{6}$$

The classical Fredholm alternative theorem from 1903 proved existence and uniqueness of solutions of Fredholm equations for continuous one-variable functions on intervals. A modern version holding for general Banach spaces is stated in the next theorem from [9, p. 499]. Recall that an operator $T : (\mathcal{X}, \|.\|_{\mathcal{X}}) \to (\mathcal{Y}, \|.\|_{\mathcal{Y}})$ between two Banach spaces is called *compact* if it maps bounded sets to precompact sets (i.e., sets whose closures are compact).

Theorem 1 *Let $(\mathcal{X}, \|.\|_{\mathcal{X}})$ be a Banach space, $T : (\mathcal{X}, \|.\|_{\mathcal{X}}) \to (\mathcal{X}, \|.\|_{\mathcal{X}})$ be a compact operator, and $I_{\mathcal{X}}$ be the identity operator. Then the operator $I_{\mathcal{X}} + T :$ $(\mathcal{X}, \|.\|_{\mathcal{X}}) \to (\mathcal{X}, \|.\|_{\mathcal{X}})$ is one-to-one if and only if it is onto.*

A straightforward corollary of Theorem 1 guarantees existence and uniqueness of solutions of the inverse problem (6) when T is a compact operator and $1/\lambda$ is not its eigenvalue (i.e., there is no $\phi \in \mathcal{X}$ for which $T(\phi) = \frac{\phi}{\lambda}$).

Corollary 1 *Let $(\mathcal{X}, \|.\|_{\mathcal{X}})$ be a Banach space, $T : (\mathcal{X}, \|.\|_{\mathcal{X}}) \to (\mathcal{X}, \|.\|_{\mathcal{X}})$ be a compact operator, $I_{\mathcal{X}}$ be the identity operator, and $\lambda \neq 0$ be such that $1/\lambda$ is not an eigenvalue of T. Then the operator $I_{\mathcal{X}} - \lambda T$ is invertible (one-to-one and onto).*

If $1/\lambda$ is not an eigenvalue of T, then $I_{\mathcal{X}} - \lambda T_K$ is one-to-one and so by Theorem 1 it is also onto. Thus for any data f, there is a unique solution ϕ of the equation $I_{\mathcal{X}} - \lambda T_K)(\phi) = f$. Corollary 1 can be applied to a Fredholm integral equation with a kernel K inducing a compact operator T_K. The following proposition gives conditions guaranteeing compactness of operators T_K in spaces $(\mathcal{C}(X), \|.\|_{\sup})$ of bounded continuous functions on $X \subseteq \mathbb{R}^d$ with the supremum norm $\|f\|_{\sup} = \sup_{x \in X} |f(x)|$ and in spaces $(\mathcal{L}^2(X), \|.\|_{\mathcal{L}^2})$ of square integrable functions with the norm $\|f\|_{\mathcal{L}^2} = \left(\int_X f(x)^2 \, dx\right)^{1/2}$. The proof is well-known and easy to check (see, e.g., [18, p. 112]).

Proposition 1 *(i) If $X \subset \mathbb{R}^d$ is compact and $K : X \times X \to \mathbb{R}$ is continuous, then $T_K : (\mathcal{C}(X), \|.\|_{\sup}) \to (\mathcal{C}(X), \|.\|_{\sup})$ is a compact operator.*
(ii) If $X \subset \mathbb{R}^d$ and $K \in \mathcal{L}^2(X \times X)$, then $T_K : (\mathcal{L}^2(X), \|.\|_{\mathcal{L}^2}) \to (\mathcal{L}^2(X), \|.\|_{\mathcal{L}^2})$ is a compact operator.

So by Corollary 1, when the assumptions of the Proposition 1(i) or (ii) are satisfied and $1/\lambda$ is not an eigenvalue of T_K, then for every f in $\mathcal{C}(X)$ or $\mathcal{L}^2(X)$, resp., there exists a unique solution ϕ of the Eq. (4). It is known (see, e.g, [19]) that the solution ϕ can be expressed as

$$\phi(x) = f(x) - \lambda \int_X f(y) \, R_K^\lambda(x, y) \, dy \,, \tag{7}$$

where $R_K^\lambda : X \times X \to \mathbb{R}$ is called a *resolvent kernel*. However, the formula expressing the resolvent kernel is not suitable for efficient computation as it is expressed as an infinite Neumann series in powers of λ with coefficients in the form of integrals with iterated kernels [20, p. 140]. So numerical calculations of values of solutions of Fredholm equations based on (7) are quite computationally demanding. Thus various

methods of finding surrogate solutions of (4) have been used [10, 11]. Traditional methods employed polynomial interpolation. Recently, approximations of solutions by feedforward networks were explored experimentally. Such networks were trained on samples of input–output pairs $\{(x_1, \bar{\phi}(x_1)), \ldots, (x_m, \bar{\phi}(x_m))\}$, where $\{x_1, \ldots, x_m\}$ are selected points from the domain X and $\{\bar{\phi}(x_1), \ldots, \bar{\phi}(x_m)\}$ are numerically computed approximations of values $\{\phi(x_1), \ldots, \phi(x_m)\}$ of the solution ϕ. In these experiments, one-hidden-layer networks with perceptrons and Gaussian radial units were used. However, without a theoretical analysis, it is not clear how to choose a proper type and number n of network units to guarantee that input–output functions approximate well the solution and the networks are not too large to make their implementation unfeasible.

4 Rates of Convergence of Surrogate Solutions

Estimates of numbers of network units needed to guarantee a required accuracies of surrogate solutions of Fredholm equations by neural networks of various types can be obtained from inspection of upper bounds on rates of variable-basis approximation. Some such bounds have the form $\frac{\xi(h,G)}{\sqrt{n}}$, where n is the number of network units and $\xi(h, G)$ depends on a certain norm of the function h to be approximated and the dictionary G.

For our purposes we need a reformulation of this theorem in terms of a norm tailored to the dictionary G. The norm is defined quite generally for any bounded nonempty subset G of a normed linear space $(\mathcal{X}, \|.\|_\mathcal{X})$. It is called *G-variation*, denoted $\|.\|_G$, and defined for all $f \in \mathcal{X}$ as

$$\|f\|_{G,\mathcal{X}} := \inf\left\{c > 0 \mid f/c \in \mathrm{cl}_\mathcal{X}\, \mathrm{conv}\,(G \cup -G)\right\},$$

where the closure $\mathrm{cl}_\mathcal{X}$ is taken with respect to the topology generated by the norm $\|.\|_\mathcal{X}$ and conv denotes the *convex hull*. So G-variation depends on the ambient space norm, but when it is clear from the context, we write merely $\|f\|_G$ instead of $\|f\|_{G,\mathcal{X}}$.

The concept of variational norm was introduced by Barron [21] for sets of characteristic functions, in particular for the set of characteristic functions of half-spaces corresponding to the dictionary of functions computable by Heaviside perceptrons. Barron's concept was generalized in [22, 23] to variation with respect to an arbitrary bounded set of functions and applied to various dictionaries of computational units such as Gaussian RBF units or kernel units [24].

The following theorem on rates of approximation by sets of the form $\mathrm{span}_n G$ is a reformulation from [23] of results by Maurey [25], Jones [26], Barron [27] in terms of G-variation. For a normed linear space $(\mathcal{X}, \|.\|_\mathcal{X})$, $g \in \mathcal{X}$ and $A \subset \mathcal{X}$, we denote by

$$\|g - A\|_\mathcal{X} := \inf_{f \in A} \|g - f\|_\mathcal{X}$$

the *distance* of g from A.

Theorem 2 *Let $(\mathcal{X}, \|.\|_{\mathcal{X}})$ be a Hilbert space, G its bounded nonempty subset, $s_G = \sup_{g \in G} \|g\|_{\mathcal{X}}$, $f \in \mathcal{X}$, and n be a positive integer. Then*

$$\|h - \mathrm{span}_n G\|_{\mathcal{X}}^2 \leq \frac{s_G^2 \|h\|_G^2 - \|h\|_{\mathcal{X}}^2}{n}.$$

Theorem 2 guarantees that for every $\varepsilon > 0$ and n satisfying

$$n \geq \left(\frac{s_G \|h\|_G}{\varepsilon} \right)^2,$$

a network with n units computing functions from the dictionary G approximates the function h within ε. So the size of G-variation of the function h to be approximated is a critical factor influencing model complexities of networks with units from the dictionary G approximating h. Generally, it is not easy to estimate G-variation. However, the following theorem from [28] shows that for the special case of functions with integral representations in the form of "infinite networks", variational norms are bounded from above by the $\mathcal{L}^1$-norms of "output-weight" functions of these networks.

Theorem 3 *Let $X \subseteq \mathbb{R}^d$, $Y \subseteq \mathbb{R}^s$, $w \in \mathcal{L}^1(Y)$, $K : X \times Y \to \mathbb{R}$ be such that $G_K(X, Y) = \{K(., y) \mid y \in Y\}$ is a bounded subset of $(\mathcal{L}^2(X), \|.\|_{\mathcal{L}^2})$, and $h \in \mathcal{L}^2(X)$ be such that for all $x \in X$, $h(x) = \int_Y w(y) K(x, y) \, dy$. Then*

$$\|h\|_{G_K(X,Y)} \leq \|w\|_{\mathcal{L}^1}.$$

In experiments with surrogate solutions of Fredholm equations [10, 11], common computational units such as perceptrons and Gaussian RBFs were used to approximate solutions of Fredholm equations with a variety of kernels K. Thus to apply Theorem 3 to these cases, we need estimates of G-variations for dictionaries G of general computational units in terms of G_K-variations induced by various kernels K. The next proposition from [29] describes a relationship between variations with respect to two sets, G and F.

Proposition 2 *Let $(\mathcal{X}, \|.\|_{\mathcal{X}})$ be a normed linear space, F and G its bounded subsets such that $c_{G,F} := \sup_{g \in F} \|g\|_G \infty$. Then for all $h \in \mathcal{X}$, $\|h\|_G \leq c_{G,F} \|h\|_F$.*

Combining Theorems 2, 3, and Proposition 2, we obtain the next corollary on rates of approximation of functions which can be expressed as $h = T_K(w)$ by one-hidden-layer networks with units from a dictionary of computational units G.

Corollary 2 *Let $X \subseteq \mathbb{R}^d$, $K : X \times Y \to \mathbb{R}$ be a bounded kernel, and $h \in \mathcal{L}^2(X)$ such that $h = T_K(w) = \int_Y w(y) K(., y) \, dy$ for some $w \in \mathcal{L}^1(Y)$, where $G_K(X, Y)$*

is a bounded subset of $\mathcal{L}^2(X)$. Let G be a bounded subset of $\mathcal{L}^2(X)$ with $s_G = \sup_{g \in G} \|g\|_{\mathcal{L}^2}$ such that $c_{G,K} = \sup_{y \in Y} \|K(., y)\|_G$ is finite. Then for all $n > 0$,

$$\|h - \text{span}_n G\|_{\mathcal{L}^2} \leq \frac{s_G \, c_{G,K} \, \|w\|_{\mathcal{L}^1}}{\sqrt{n}}.$$

A critical factor in the estimate given in Corollary 2 is the $\mathcal{L}^1$-norm of the "output-weight function" w in the representation of the function h to be approximated as an "infinite network" with units from the dictionary G_K in the form $h(x) = T_K(w) = \int_Y w(y) K(x, y) \, dy$. We apply Corollary 2 to the representation

$$\phi - f = T_K(\lambda \phi) = \lambda \int_X \phi(y) K(x, y) \, dy,$$

where $\lambda \phi$ plays the role of the "output-weight" function in the infinite network $\int_X \lambda \phi(y) K(x, y) \, dy$.

Theorem 4 *Let $X \subset \mathbb{R}^d$ be compact, $K : X \times X \to \mathbb{R}$ be a bounded kernel such that $K \in \mathcal{L}^2(X \times X)$, $\rho_K = \int_X \sup_{y \in X} |K(x, y)| dx$ be finite, G be a bounded subset of $\mathcal{L}^2(X)$ with $s_G = \sup_{g \in G} \|g\|_{\mathcal{L}^2}$ such that $c_{G,K} = \sup_{y \in Y} \|K(., y)\|_G$ is finite, and $\lambda \neq 0$ be such that $\frac{1}{\lambda}$ is not an eigenvalue of T_K and $|\lambda| \rho_K < 1$. Then the solution ϕ of the Eq. (4) satisfies for all $n > 0$,*

$$\|\phi - f - \text{span}_n G\|_{\mathcal{L}^2} \leq \frac{s_G \, c_{G,K} \, |\lambda| \, \|f\|_{\mathcal{L}^1}}{(1 - |\lambda| \rho_K) \sqrt{n}}.$$

Proof As $\phi - f$ satisfies the Fredholm equation (4), we have for every $x \in X$,

$$|\phi(x)| \leq |\lambda| \, \|\phi\|_{\mathcal{L}^1} \sup_{y \in X} |K(x, y)| + |f(x)|.$$

Integrating over X we get

$$\|\phi\|_{\mathcal{L}^1} \leq |\lambda| \rho_K \|\phi\|_{\mathcal{L}^1} + \|f\|_{\mathcal{L}^1}$$

and so $\|\phi\|_{\mathcal{L}^1} (1 - |\lambda| \rho_K) \leq \|f\|_{\mathcal{L}^1}$. This inequality is non trivial only when $|\lambda| < \frac{1}{\rho_K}$. Thus we get $\|w\|_{\mathcal{L}^1} = |\lambda| \|\phi\|_{\mathcal{L}^1} \leq \frac{|\lambda| \|f\|_{\mathcal{L}^1}}{1 - |\lambda| \rho_K}$. The statement then follows from Corollary 2. $\qquad \square$

Theorem 4 estimates rates of approximation of the function

$$\phi - f = \lambda \int_X f(y) R_K^\lambda(x, y) \, dy$$

by functions computable by networks with units from a dictionary G. As f plays a role of a constant function, we can consider a surrogate solution formed by an input–output function of the network with n units from the dictionary G and one unit assigning to an input $x \in X$ the value $f(x)$.

With an increasing number of network units, the upper bound on rate of approximation decreases with $1/\sqrt{n}$. The speed of decrease depends on the $\mathcal{L}^1$-norm of the function f representing data in the Fredholm equation, bound $c_{G,K}$ on G-variations of functions from the dictionary G_K and ρ_X depending on the size of the domain X where the solution is approximated. For $|\lambda| < \frac{1}{\rho_K}$ and any bounded dictionary G with finite bound $c_{G,K}$ on $G_{K(X)}$-variations on its elements, input–output functions of networks with increasing numbers of units from G converge to the function $\phi - f$. When for a reasonable number n of network units, the upper bound from Theorem 4 is sufficiently small, the network can serve as a good surrogate model of the solution of the Fredholm equation.

Note that the $\mathcal{L}^1$-norm of the data f does not depend on the choice of a dictionary of computational units. Also $\rho_K = \int_X \sup_{y \in X} |K(x, y)| dx$ is determined by the Fredholm equation to be solved. It depends on the Lebesgue measure of the domain X and properties of the kernel K of the equation. For large dimensions d, choice of the domain has a strong effect on the upper bound from Theorem 4. For example, the Lebesgue measure of the unit cube $[0, 1]^d$ is equal to 1 for all dimensions d, while Lebesgue measures of cubes od sizes larger than 1 grow exponentially with d increasing, and Lebesgue measures of the d-dimensional unit balls decrease exponentially quickly to zero. The only factor that can be influenced by a choice of a type of computational units is $c_{G,K}$ expressing a bound on G-variations of functions induced by the kernel K of the equation.

To illustrate our results, consider approximation of Fredholm equations with the Gaussian kernel

$$K_b(x, y) = e^{-b\|x-y\|}$$

with the width b by surrogate solutions in the form of input–output functions of networks with two types of popular units: sigmoidal perceptrons and Gaussian radial units. Note that Fredholm equations with Gaussian kernels arise, e.g., in image restoration problems [8]. By μ is denoted the *Lebesgue measure* on $\mathbb{R}^d$ and by $P_d^\sigma(X)$ the *dictionary of functions on X computable by sigmoidal perceptrons*.

Corollary 3 *Let $X \subset \mathbb{R}^d$ be compact, $b > 0$, $K_b(x, y) = e^{-b\|x-y\|^2}$, $\lambda \neq 0$ be such that $\frac{1}{\lambda}$ is not an eigenvalue of T_{K_b} and $|\lambda| < 1$. Then the solution ϕ of the Eq. (4) with f continuous satisfies for all $n > 0$*

$$\|\phi - f - \operatorname{span}_n G_{K_b}(X)\|_{\mathcal{L}^2} \le \frac{\mu(X)\,|\lambda|\,\|f\|_{\mathcal{L}^1}}{(1 - |\lambda|\,\mu(X))\,\sqrt{n}}$$

and

$$\|\phi - f - \operatorname{span}_n P_d^\sigma(X)\|_{\mathcal{L}^2} \le \frac{\mu(X)\,2d\,|\lambda|\,\|f\|_{\mathcal{L}^1}}{(1 - |\lambda|\,\mu(X))\,\sqrt{n}}.$$

Proof It was shown in Ref. [30] that variation of the d-dimensional Gaussian with respect to the dictionary formed by sigmoidal perceptrons is bounded from above by $2d$ and thus by Proposition 2, $c_{P_d^\sigma, K_b} \leq 2d$. The statement then follows by Theorem 4, an estimate $s_{G_{K_b}} \leq \mu(X)$ and equalities $s_{P_d^\sigma} = \mu(X)$ and $\rho_{K_b} = \mu(X)$. □

5 Discussion

Taking advantage of results from mathematical theory of neurocomputing holding for functions representable as "infinite neural networks" we derived estimates of rates of convergence of surrogate solutions of Fredholm equations computable by feedforward neural networks. Our estimates decrease with increasing number of network units n, they are smaller than $\frac{1}{\sqrt{n}}$ multiplied by a product of two factors, the first one depending on the parameters of the equation f, K, λ and the domain X, and the second one depending on combination of the kernel K and the dictionary of computational units G. Thus our results show that a proper choice of a type of computational units can influence speed of convergence of surrogate solutions, however for high dimensions, a choice of the domain can have a stronger impact.

References

1. Forrester, A., Sobester, A., Keane, A.: Engineering Design via Surrogate Modelling: A Practical Guide. Wiley, Chichester (2008)
2. Baerns, M., Holeňa, M.: Combinatorial Development of Solid Catalytic Materials. Imperial College Press, London (2009)
3. Park, J., Sandberg, I.W.: Approximation and radial-basis-function networks. Neural Comput. **5**, 305–316 (1993)
4. Pinkus, A.: Approximation theory of the MLP model in neural networks. Acta Numerica **8**, 143–195 (1999)
5. Kainen, P.C., Kůrková, V., Sanguineti, M.: Dependence of computational models on input dimension: Tractability of approximation and optimization tasks. IEEE Trans. Inf. Theory **58**(2), 1203–1214 (2012)
6. Lovitt, W.V.: Linear Integral Equations. Dover, New York (1950)
7. Lonseth, A.T.: Sources and applications of integral equations. SIAM Rev. **19**, 241–278 (1977)
8. Lu, Y., Shen, L., Xu, Y.: Integral equation models for image restoration: high accuracy methods and fast algorithms. Inverse Prob. **26**, 045006 (2010)
9. Steinwart, I., Christmann, A.: Support Vector Machines. Springer, New York (2008)
10. Golbabai, A., Seifollahi, S.: Numerical solution of the second kind integral equations using radial basis function networks. Appl. Math. Comput. **174**, 877–883 (2006)
11. Effati, S., Buzhabadi, R.: A neural network approach for solving Fredholm integral equations of the second kind. Neural Comput. Appl. **21**(5), 843–852 (2012)

12. Gnecco, G., Kůrková, V., Sanguineti, M.: Bounds for approximate solutions of Fredholm integral equations using kernel networks. In: Honkela, T., et al. (eds.) Lecture Notes in Computer Science (Proceedings of ICANN 2011), vol. 6791, pp. 126–133. Springer, Heidelberg (2011)
13. Gnecco, G., Kůrková, V., Sanguineti, M.: Accuracy of approximations of solutions to Fredholm equations by kernel methods. Appl. Math. Comput. **218**, 7481–7497 (2012)
14. Kůrková, V.: Surrogate modeling of solutions of integral equations by neural networks. In: Iliadis, L., et al., (eds.), AIAI 2012—Artificial Intelligence Applications and Innovations, IFIP AICT 381, IFIP International Federation for Information Processing (2012), pp. 88-96
15. Gnecco, G., Kůrková, V., Sanguineti, M.: Some comparisons of complexity in dictionary-based and linear computational models. Neural Netw. **24**, 171–182 (2011)
16. Gnecco, G., Kůrková, V., Sanguineti, M.: Can dictionary-based computational models outperform the best linear ones? Neural Netw. **24**, 881–887 (2011)
17. Gribonval, R., Vandergheynst, P.: On the exponential convergence of matching pursuits in quasi-incoherent dictionaries. IEEE Trans. Inf. Theory **52**, 255–261 (2006)
18. Rudin, W.: Functional Analysis. McGraw-Hill, Boston (1991)
19. Atkinson, K.: The Numerical Solution of Integral Equations of the Second Kind. Cambridge University Press, Cambridge (1997)
20. Courant, R., Hilbert, D.: Methods of Mathematical Physics, vol. I. Wiley, New York (1989)
21. Barron, A.R.: Neural net approximation. In: Narendra, K. (ed.) Proceedings of 7th Yale Workshop on Adaptive and Learning Systems. Yale University Press, New Haven (1992)
22. Kůrková, V.: Dimension-independent rates of approximation by neural networks. In: Warwick, K., Kárný, M. (eds.) Computer-Intensive Methods in Control and Signal Processing. The Curse of Dimensionality, pp. 261–270. Birkhäuser, Boston (1997)
23. Kůrková, V.: High-dimensional approximation and optimization by neural networks. In: Suykens, J., Horváth, G., Basu, S., Micchelli, C., Vandewalle, J. (eds.), Advances in Learning Theory: Methods, Models and Applications (Chapter 4), pp. 69–88. IOS Press, Amsterdam (2003)
24. Kainen, P.C., Kůrková, V., Sanguineti, M.: Complexity of Gaussian radial-basis networks approximating smooth functions. J. Complexity **25**, 63–74 (2009)
25. Pisier, G.: Remarques sur un résultat non publié de B. Maurey. In: Séminaire d'Analyse Fonctionnelle 1980–1981, vol. I, no. 12, École Polytechnique, Centre de Mathématiques, Palaiseau, France (1981)
26. Jones, L.K.: A simple lemma on greedy approximation in Hilbert space and convergence rates for projection pursuit regression and neural network training. Ann. Stat. **20**, 608–613 (1992)
27. Barron, A.R.: Universal approximation bounds for superpositions of a sigmoidal function. IEEE Trans. Inf. Theory **39**, 930–945 (1993)
28. Kůrková, V.: Complexity estimates based on integral transforms induced by computational units. Neural Netw. **30**, 160–167 (2012)
29. Kůrková, V., Sanguineti, M.: Bounds on rates of variable-basis and neural-network approximation. IEEE Trans. Inf. Theory **47**, 2659–2665 (2001)
30. Kainen, P.C., Kůrková, V., Vogt, A.: A Sobolev-type upper bound for rates of approximation by linear combinations of Heaviside plane waves. J. Approx. Theory **147**, 1–10 (2007)

Vehicle Classification Using Neural Networks with a Single Magnetic Detector

Peter Šarčević

Abstract In this work, principles of operation, advantages and disadvantages are presented for different detector technologies. An idea of a new detection and classification method for a single magnetic sensor based system is also discussed. It is important that the detection algorithm and the neural network classifier needs to be easily implementable in a microcontroller based system.

Keywords Neural networks · Vehicle detection · Magnetic sensors · Vehicle classification · Vehicle detection technologies

1 Introduction

New vehicle detection technologies are constantly being developed and existing technologies improved, to provide speed monitoring, traffic counting, presence detection, headway measurement, vehicle classification, and weigh-in-motion data.

Vehicle count and classification data are important inputs for traffic operation, pavement design, and transportation planning. In traffic control, signal priority can be given to vehicles classified as bus or an emergency vehicle.

In this work, principles of operation, advantages and disadvantages are presented for different detector technologies. An idea of a new detection and classification method for a single magnetic sensor based system is also discussed. It is important that the detection algorithm and the neural network classifier needs to be easily implementable in a microcontroller based system.

P. Šarčević (✉)
Széchenyi István University, Egyetem tér 1., 9026 Győr, Hungary
e-mail: peter.sarcevic@gmail.com

2 Vehicle Detection Technologies

The need for automatic traffic monitoring is increasing, which urges the manufacturers and researchers to develop new technologies and improve the existing ones. Today a big number of detector technologies and methods are available.

Three categories of detector technologies exist: intrusive (in-roadway), non-intrusive (above or on the sides of roads) and off-roadway technologies [13, 14].

2.1 Intrusive Detector Technologies

These devices are installed directly on the pavement surface, in saw-cuts or holes in the road surface, by tunneling under the surface, or by anchoring directly to the pavement surface as is the case with pneumatic road tubes.

Intrusive detector technologies include inductive loops, magnetic detectors, pneumatic road tubes, piezoelectric detectors, and other weigh-in-motion (WIM) detectors.

Advantages and disadvantages for intrusive technologies are shown in Table 1.

Inductive Loop. When a vehicle stops on or passes over the loop, the inductance of the loop is decreased. The decreased inductance increases the oscillation frequency and causes the electronics unit to send a pulse to the controller, indicating the presence or passage of a vehicle. The data supplied by conventional inductive loop detectors are vehicle passage, presence, count, and occupancy. Although loops cannot directly measure speed, speed can be determined using a two-loop speed trap or a single loop detector and an algorithm.

Magnetic Detector. Magnetic sensors are passive devices that indicate the presence of a metallic object by detecting the perturbation (known as a magnetic anomaly) in the Earth s magnetic field created by the object.

Pneumatic Road Tube. Pneumatic road tubes sense vehicle pressure and send a burst of air pressure along a rubber tube when a vehicle's tires pass over them. The pulse of air pressure closes an air switch and sends an electrical signal that marks the passage of a vehicle. Pneumatic road tubes can detect volume, speed, and classification by axle count and spacing.

Piezoelectric. Piezoelectric is a specially processed material capable of converting kinetic energy to electrical energy. When a vehicle passes over a detector, the piezoelectric material generates a voltage proportionate to the force or weight of the vehicle. The material only generates a voltage when the forces are changing.

Piezoelectric detectors can detect traffic volume, vehicle classification, speed, and vehicle weight. They classify vehicles by axle count and spacing. A multiple-sensor configuration is required to measure vehicle speeds.

Weigh-in-Motion (WIM). WIM is a sensor system imbedded in a roadway to measure vehicle force on the pavement when vehicle axles pass over the sensors. WIM

Table 1 Advantages and disadvantages for intrusive technologies

Technology	Advantages	Disadvantages
Inductive loop	• Provides basic traffic parameters (volume, presence, occupancy, speed, headway, and gap) • High frequency excitation models provide classification data	• Installation requires pavement cut • Decreases pavement life • Installation and maintenance require lane closure • Wire loops subject to stresses of traffic and temperature
Magnetic detector	• Insensitive to inclement weather such as snow, rain, and fog • Less susceptible than loops to stresses of traffic • Some models transmit data over wireless RF link • Some models can be installed above roads, no need for pavement cuts	• Difficult to detect stopped vehicles • Installation requires pavement cut or tunneling under roadway • Decreases pavement life • Installation and maintenance require lane closure
Pneumatic road tube	• Quick installation • Low power usage • Low cost and simple to maintain	• Inaccurate axle counting • Temperature sensitivity of the air switch • Not suitable for permanent counting system
Piezoelectric	• High accuracy in classification because the output signals are proportional to the tire pressure	• Disruption to traffic during installation and repair • Sensitive to pavement temperature and vehicle speed

systems measure the weight proportions carried by each wheel assembly (half-axle with one or more tires), axle, and axle group on the vehicle. The primary WIM technologies are bending plate, piezoelectric, load cell, capacitance mat and fiber optic. They provide traffic data such as traffic volume, speed, and vehicle classification based on the number of and spacing of axles.

2.2 Non-intrusive Detector Technologies

Above ground sensors can be mounted above the lane of traffic they are monitoring or on the side of a roadway where they can view multiple lanes.

Non-intrusive detector technologies include active and passive infrared, microwave radar, ultrasonic, passive acoustic, and video image processing. Active in-

Table 2 Advantages and disadvantages for non-intrusive technologies

Technology	Advantages	Disadvantages
Active and passive infrared	• Active sensor transmits multiple beams for accurate measurement of vehicle position, speed, and class • Multizone passive sensors measure speed • Multiple lane operation available	• Operation of active sensor may be affected by fog or blowing snow • Passive sensor may have reduced sensitivity to vehicles in its field of view in rain and fog
Microwave radar	• Generally insensitive to inclement weather • Direct measurement of speed • Multiple lane operation available	• Antenna beamwidth and transmitted waveform must be suitable for the application • Doppler sensors cannot detect stopped vehicles
Ultrasonic and passive acoustic	• Multiple lane operation available	• Some environmental conditions such as temperature change and extreme air turbulence can affect performance • Large pulse repetition periods may degrade occupancy measurement on freeways with vehicles traveling at moderate to high speeds
Video image processing	• Monitors multiple lanes • Rich array of data available • Provides wide-area detection • Easy to add or modify detection zones	• Performance affected by many factors including fog, rain, snow, vehicle shadows, day to night transition • High installation and maintenance cost

frared, microwave radar, and ultrasonic are active detectors that transmit wave energy toward a target and measure the reflected wave. Passive infrared, passive acoustic, and video image processing are passive detectors that measure the energy emitted by a target or the image of the detection zone.

Table 2 shows the advantages and disadvantages of non-intrusive detectors.

Active and Passive Infrared. The detectors convert received energy into electrical signals that determine the presence of a vehicle by real time signal processing. There are active and passive infrared detector models. An active infrared detector emits invisible infrared low-energy by light-emitting diodes or high-energy by laser diodes to the detector zone and measures the time for reflected energy to return to the detector. A lower return time denotes the presence of a vehicle. The detectors measure vehicle speed by transmitting two or more beams and recording the times at which the vehicle enters the detection zone of each beam.

Any object that is not at absolute zero emits thermal radiation in the far infrared part of the electromagnetic spectrum. The amount of radiation depends on the object's surface temperature, size, and structure. Passive infrared detectors respond to thermal radiation changes in proportion to the product of emissivity difference (the difference between the emissivities of road surface and the vehicle) and temperature difference (the difference between the temperature of the road surface and the environment).

Two types of detectors exist: non-imaging and imaging. Non-imaging detectors use one or several energy-sensitive elements to collect infrared energy and cannot divide objects into pixels within the detection zone. Imaging detectors use two-dimensional arrays of energy-sensitive elements and can display pixel-resolution details.

Active infrared sensors can detect volume, presence, classification (length), and speed. Passive infrared sensors can detect volume, presence, occupancy and speed within multiple detection zones.

Microwave Radar. There are two types of microwave detectors: Doppler Microwave Detectors and Frequency-modulated Continuous Wave (FMCW) Detectors.

Doppler microwave detectors transmit low-energy microwave radiation at the detection zone. The Doppler effect is a frequency shift that results from relative motion between a frequency source and a listener. If both source and listener are not moving, no Doppler shift will take place. If the source and the listener are moving closer to each other, the listener will perceive a higher frequency. If the source and listener are moving farther apart, the listener will perceive a lower frequency. For traffic detection, motion of a vehicle causes a frequency shift in the reflected signal. Microwave detectors measure this shift to determine vehicle passage and speed.

FMCW detectors, sometimes referred to as true-presence microwave detectors, transmit continuous frequency-modulated waves at the detection zone. Frequency varies over time. Detectors measure the range from the detector to the vehicle to determine vehicle presence. To obtain speed, the distance between two range bins is divided by the time that the detected vehicle travels that distance.

Doppler microwave detects volume, occupancy, classification and speed. However it only recognizes vehicles above a minimum speed. True presence detectors can detect vehicle presence, volume, occupancy, classification, and speed.

Ultrasonic and Passive Acoustic. Ultrasonic detectors can detect volume, presence, classification and speed. They are active acoustic sensors and can transmit sound waves toward the detection zones. The detectors sense acoustic waves reflected by objects in the detection zones. Pulsed ultrasonic detectors and continuous wave

ultrasonic detectors are based on the different data-measurement methods. Pulsed ultrasonic detectors transmit a series of ultrasonic pulses. The detector measures the wave's travel time between the detection zone and the detector. The detectors differentiate between waves reflected from the road surface and waves reflected from the vehicles to determine vehicle presence. A continuous ultrasonic detector transmits a continuous wave of ultrasonic energy. The detector analyzes the acoustic sound reflected back from the detection zone based on the Doppler principle.

Passive acoustic detectors can detect volume, speed, occupancy, and classification. They measure the acoustic energy or audible sounds produced by a variety of sources within a passing vehicle. Sound energy increases when a vehicle enters the detection zone and decreases when it leaves. A detection threshold determines the termination of the vehicle presence signal.

Video Image Processing (VIP). VIP systems measure changes between successive video image frames. Passing vehicles cause variations in the gray levels of the black-and-white pixel groups. VIP systems analyze these variations to determine vehicle passage. Variations due to non-vehicle factors, such as weather and shadows, are excluded.

VIP systems detect a variety of traffic data. They classify vehicles by length and measure volume, presence, occupancy, and speed for each vehicle class. Other data include density, travel time, queue length, headway, and turning movements.

2.3 Off-Roadway Technologies

Off-Roadway Technologies refer to those that do not need any hardware to be setup under the pavement or on the roadside. It includes probe vehicle technologies with Global Positioning System (GPS) and mobile phones, Automatic Vehicle Identification (AVI), and remote sensing technologies that make use of images from aircraft or satellite.

Probe Vehicles with Global Positioning System (GPS). For traffic surveillance, probe vehicles equipped with GPS receivers are driven through the traffic sections of interest. Their position and speed information determined from the GPS is transmitted back to the Traffic Management Center (TMC) for travel time and section speed analysis. Drawbacks include lack of point traffic statistics at a fix location, and the fact that system coverage is limited by the number of probe vehicles.

Probe Vehicles with Mobile Phones. The localization technique is similar to that of a GPS system, with the satellites replaced by phone antenna base stations, and GPS receivers replaced by mobile phones. Because of the high penetration rate of mobile phones, at least one mobile phone can be found in a traveling vehicle.

Remote Sensing. Remote sensing refers to the technologies that collect traffic information without direct communication or physical contract with the vehicles or roads. Basically, high-resolution imagery from aircraft or satellite is used to extract traffic information like traffic count and speed.

3 Magnetic Sensor System

The used magnetic detector system is a HMC5843 based unit developed by "SELMA" Ltd. and "SELMA Electronic Corp" Ltd., companies from Subotica, Serbia. Two types of magnetic detectors have been developed, one with cable and one with wireless communication.

Wireless magnetic sensor networks offer an attractive, low-cost alternative to inductive loops, video and radar for traffic surveillance on freeways, at intersections and in parking lots.

Vehicles are detected by measuring the change in the Earth's magnetic field caused by the presence of a vehicle near the sensor. Two sensor nodes placed a few feet apart can estimate speed [6]. A vehicle's magnetic 'signature' can be processed for classification.

3.1 HMC5843

The Honeywell HMC5843 [10] is a small ($4 \times 4 \times 1.3$ mm) surface mount multi-chip module designed for low field magnetic sensing. The 3-Axis Magnetoresistive Sensors feature precision in-axis sensitivity and linearity, solid-state construction with very low cross-axis sensitivity designed to measure both direction and magnitude of Earth's magnetic fields, from tens of micro-gauss to 6 gauss. The highest sampling frequency is 50 Hz.

3.2 Detection Algorithm

Magnetic detectors are capable of very high, above 97 % [5, 11] detection accuracy with proper algorithms. Most of the algorithms use adaptive thresholds [5, 19].

It is known that HMC magnetic sensor measurements are affected by temperature. As the temperature on the pavement can change a lot in the course of a day, but the changes in the measured values are very slow [5], the detection algorithm has to change threshold values when no detection is available.

Currently an own algorithm using thresholds is being tested. It seems to be very accurate, but no exact detection rates are yet available. The main detection failures are caused by motorcycles with low metallic content.

The principles of the algorithm:

- During calibration the maximum and minimum values are determined in a period of time at all three axis (if even at one axis the difference between the maximum and minimum exceeds a previously defined value, the calibration starts from the beginning). After this stage, the range is equally stretched to a previously defined width, and the upper and lower thresholds are now determined at all three axis. This method makes the further algorithm immune to noise.

- If two or more axis have exceeded the range determined by the thresholds, a detection is generated (detection flag is "1").
- In case of a detection, if measures in all three axis are between thresholds for the time of ten measurements, the detection flag goes back to "0".
- If all three axis are in the range determined by the thresholds, and no detection is available, the algorithm calculates new thresholds.

The axis along the direction of travel can be used to determine the direction of the vehicle [2]. When there is no car present, the sensor will output the background earth's magnetic field as its initial value. As the car approaches, the earth's magnetic field lines of flux will be drawn toward the ferrous vehicle.

3.3 Vehicle Classification

Vehicle classification with other technologies. As with vehicle detection, a number of technologies were developed for classification. Vision-based, inductive loop, microwave, piezo-electric and acoustic-based classification technologies are the common ones in use nowadays.

The major limitation of vision-based classification is that the system's performance is greatly affected by the environmental and lighting conditions. In a simple single camera system, a vehicle may be categorized according to its length and height according to its two dimensional image. In [7], such a system is described, and the results show a classification rate of 70 % for classifying the vehicles into two classes (passenger and non-passenger).

In [17] also pixel-based vehicle length is used for classification but with uncalibrated video cameras. The classification rate was above 97 %, but vehicles were classified only into two classes (cars and trucks).

A new approach is presented to vehicle-class recognition from a video clip in [8]. The concept is based on probes consisting of local 3D curve-groups for recognizing vehicle classes in video clips, and Bayesian recognition based on class probability densities for groups of 3D distances between pairs of 3D probes. They achieved 88 % correct classification with only three vehicle classes.

Vehicle classification rate of over 92 % was obtained with a rule based classifier using range sensors in [9] (14 vehicle classes).

An algorithm, which performs line by line processing of laser intensity images, produced by laser sensory units, and extracts vehicle features used for the classification into five classes achieved 89 % efficiency [1]. The features include vehicle length, width, height, speed, and some distinguishable patterns in the vehicle profile.

Classification stations with highly calibrated inductive loops are also in use. However, the infrastructure and maintenance costs of such a vehicle classification station are high.

Reference [18] developed an artificial neural network method to estimate classified vehicle volumes directly from single-loop measurements. They used a simple three-layer neural network with back-propagation structure, which produced reliable

estimates of classified vehicle volumes under various traffic conditions. In this study four classes (by ranges of length) were defined, and all classes had an own ANN. All networks had 19 nodes in the input layer, 1 node for the time stamp input and 9 pairs of nodes for inputting single-loop measurements (volume and lane occupancy). All networks had one output node (each was one class bin), but the number of hidden neurons differed for each class (35 for class1, 8 for class2, 5 for class3 and 21 for class4).

In [15], Sun studied the use of existing infrastructure of loop detectors for vehicle classification with two distinct methods. The seven-class scheme was used for the first method because it targets vehicle classes that are not differentiable with current techniques based on axle counting. Its first method uses a heuristic discriminant algorithm for classification and multi-objective optimization for training the heuristic algorithm. Feature vectors obtained by processing inductive signatures are used as inputs into the classification algorithm. Three different heuristic algorithms were developed and an overall classification rate of 90 % was achieved. Its second method uses Self-Organizing Feature Maps (SOFM) with the inductive signature as input. An overall classification rate of 80 % was achieved with the four-class scheme.

Vehicle classification with magnetic detectors. In the last few years a big number of studies have been made with classification algorithms using magnetic detectors.

In [4] the rate of change of consecutive samples is compared with a threshold and declared to be $+1$ (-1) if it is positive and larger than (negative with magnitude larger than) the threshold, or 0 if the magnitude of the rate is smaller than the threshold. The second piece of information was the magnetic length of the vehicle. 82 % efficiency was achieved, with vehicles classified into five classes. Ref. [3] achieved a vehicle detection rate better than 99 % (100 % for vehicles other than motorcycles), estimates of average vehicle length and speed better than 90 %, and correct classification into six types with around 60 largest value of the samples and the also as in [4], rate of change of consecutive samples.

In [12], with x and z dimension data and without vehicle length information, a single magnetic sensor system, with a Multi-Layer Perceptron Neural Network, 93.5 % classification efficiency was achieved, but vehicles were only separated into two classes. In a double sensor system 10 classes were selected for development, and 73.6 % was achieved with length estimation and a methodology using K-means Clustering and Discriminant Analysis.

Classification algorithm. The basic idea is to gather data during and after the detection, and calculate the inputs of the neural network.

A three-layer back-propagation neural network (Fig. 1) will be used and implemented into a microcontroller. The neurons in the hidden layer will have logarithmic sigmoid transfer functions, while the output neurons will have saturating linear transfer functions.

Previously collected data should be used for network training. During the training process equal number of training and validation samples will be used for each class. Weight updating will be done after every sample. Mean squared errors and recognition rates will also be calculated. Weights will be saved during training when highest recognition rates on training samples, highest recognition rates on validation sam-
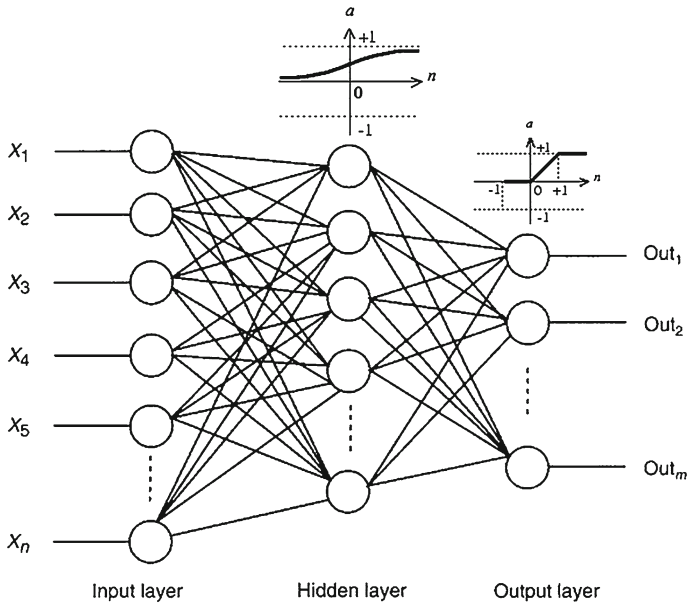
Fig. 1 Three-layer back-propagation neural network
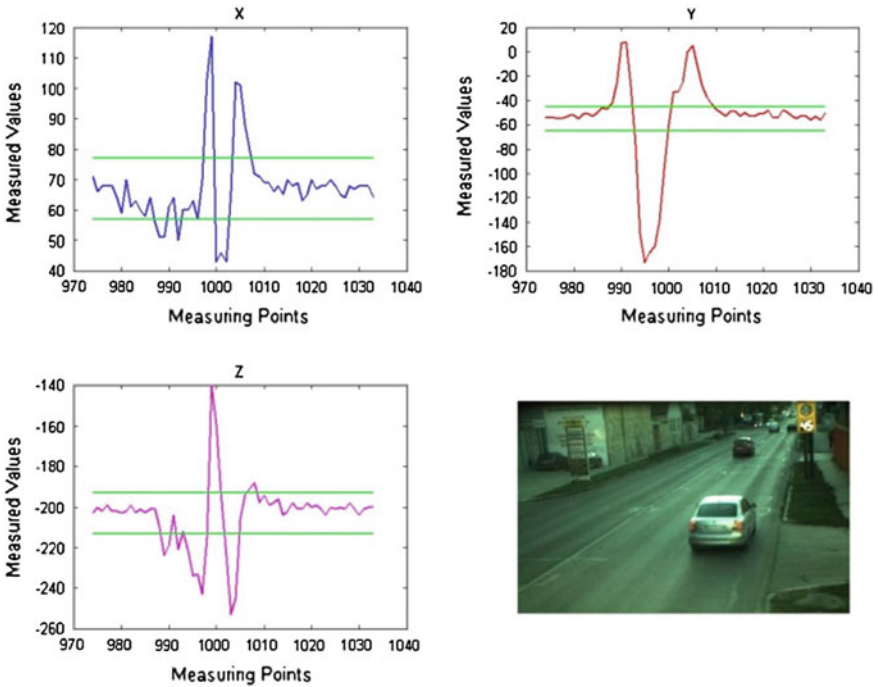
Fig. 2 Measurements of X, Y and Z axis, and a picture of the passing car
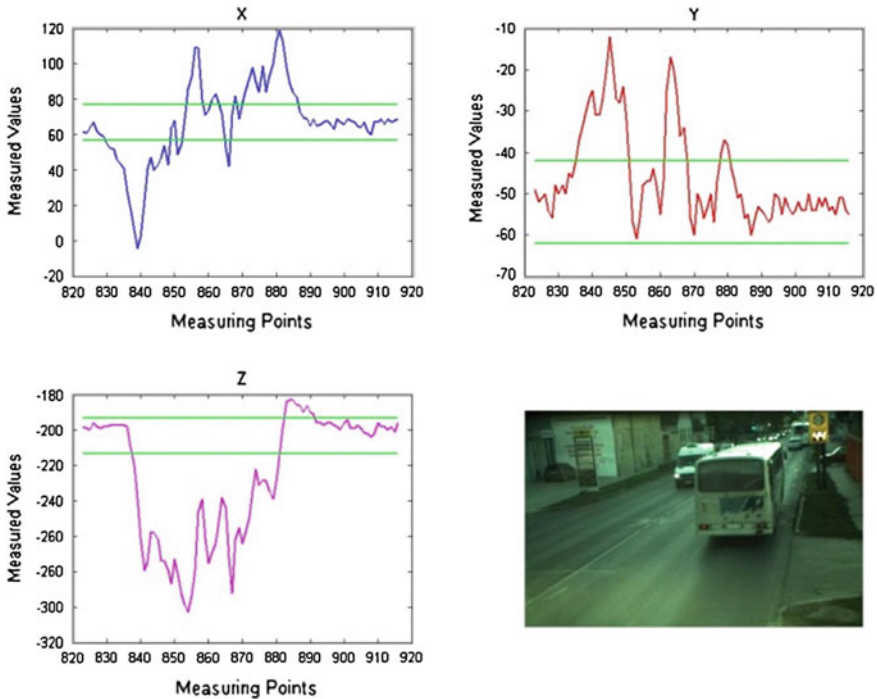
Fig. 3 Measurements of X, Y and Z axis, and a picture of the passing bus

ples, smallest mean squared errors on training samples and smallest mean squared errors on validation samples are found. The saved weights will be later tested on test samples.

Every vehicle class will have an assigned neuron in the output layer. The class with the biggest output will be declared as the class of the passed vehicle.

Possible input data:

- The biggest differences between measured values and thresholds (the difference between the highest measured value and the upper threshold, and the difference between the lower threshold and the smallest measured value) at all three axis should be applied to network.
- Detection length—the number of samples made during detection.
- Number of local maximums (if the measured values are above the upper threshold), and local minimums (if the values are under the lower threshold). These numbers could lead to the determination of axle numbers.

Figure 2 shows the measurement values of all three axis made during a car passing over the detector.

Measurement changes are shown in Fig. 3 during a bus passing over the detector.

The placement of the detector will be also important. The axis have to point always in the same direction as they pointed during the collection of training data.

4 Future Work

In the future data collection will be finished and used for neural network training. Two types of networks will be made, one for 5 and one for 9 vehicle classes. The training will be done with different number of neurons in the hidden layer, and with various input data (combinations of the previously discussed possible inputs will be tested, to find which are useful).

The measurements will be also processed via fuzzy grids [16], and tested for the same type of classifications, to compare efficiency of the neural network and fuzzy grid classification method.

References

1. Abdelbaki, H.M., Hussain, K., Gelenbe, E.: A laser intensity image based automatic vehicle classification system. In: Intelligent Transportation System Conference Proceedings, Oakland (2001)
2. Caruso M.J., Withanawasam L.S.: Vehicle Detection and Compass Applications using AMR Magnetic Sensors. Honeywell Inc, New York (2007)
3. Cheung S.-Y., Coleri S., Dundar B., Ganesh S., Tan C.-W., Varayra P.: Traffic measurement and vehicle classification with a single magnetic sensor. In: 84th Annual meeting of the Transportation Research Board, pp. 173–181 (2005)
4. Cheung S.-Y., Coleri S.E., Varayra P.: Traffic surveillance by wireless magnetic sensors. In: ITS World Congress, San Francisco, California (2005)
5. Cheung S.-Y., Varayra P.: Traffic Surveillance by wireless sensor networks: final report, California PATH Research Report (2004). UCB-ITS-PRR-2007-4
6. Deng X., Hu Z., Zhang P., Guo J.: Vehicle Class Composition Identification Based Mean Speed Estimation Algorithm using Single Magnetic Sensor. Beijing Transportation Research Center, China (2009)
7. Gupte, S., Masoud, O., Martin, R.F.K., Papanikolopoulos, N.P.: Detection and classification of vehicles. IEEE Trans. Intel.l Transp. Syst. **3**(1), 37–47 (2002)
8. Han D., Leotta M.J., Cooper D.B., Mundy J.L.: Vehicle class recognition from video based on 3D curve probes. In: Proceedings of IEEE International Workshop on Visual Surveillance and Performance Evaluation of Tracking and Surveillance, (2005). pp. 871–878
9. Harlow, C., Peng, S.: Automatic vehicle classification systems with range sensors. Transp. Res. Part C **9**, 231–247 (2001)
10. HMC5843 datasheet
11. Isaksson, M.: Vehicle detection using anisotropic magnetoresistors. Thesis for the degree of Master In Engineering Physics, Chalmers University Of Technology (2007)
12. Liu H., Jeng S.-T., Tok J.C.A., Ritchie S.G.: Commercial Vehicle Classification using Vehicle Signature Data. In: 88th Annual meeting of the Transportation Research Board (2009)

13. Martin P.T., Feng U., snd Wang X.: Detector Technology Evaluation, Mountain-Plains Consortium, Report No. 03–154 (2003)
14. Mimbala L.E.Y., Klein L.A.: A Summary of Vehicle Detection and Surveillance Technologies Used In Intelligent Transportation Systems. The Vehicle Detector Clearinghouse, Washington (2000)
15. Sun, C.: An Investigation in the Use of Inductive Loop Signature for Vehicle Classification. California PATH Research Report, California (2000)
16. Tormási A., Kóczy T.L.: Comparing the efficiency of a fuzzy single-stroke character recognizer with various parameter values. IPMU **1**, 260–269 (2012)
17. Zhang G., Avery R.P., Wang Y.: A video-based vehicle detection and classification system for real-time traffic data collection using uncalibrated video cameras. Annual meeting of the Transportation Research Board, Washington (2007)
18. Zhang G., Wang Y., Wei H.: An artificial neural network method for length-based vehicle classification using single-loop outputs. J. Transp. Res. Board **1945**, 100–108 (2007)
19. Zhang, W., Tan, G.-Z., Shi, H.-M., Lin, M.-W.: A distributed threshold algorithm for vehicle classification based on binary proximity sensors and intelligent neuron classifier. J. Inf. Sci. Eng. **26**, 769–783 (2010)

Part IV
Clustering and Image Processing

Exemplary Applications of the Complete Gradient Clustering Algorithm in Bioinformatics, Management and Engineering

Piotr Kulczycki, Malgorzata Charytanowicz, Piotr A. Kowalski and Szymon Łukasik

Abstract This publication deals with the applicational aspects and possibilities of the Complete Gradient Clustering Algorithm—the classic procedure of Fukunaga and Hostetler, prepared to a ready-to-use state, by providing a full set of procedures for defining all functions and the values of parameters. Moreover, it describes how a possible change in those values influences the number of clusters and the proportion between their numbers in dense and sparse areas of data elements. The possible uses of these properties were illustrated in practical tasks from bioinformatics (the categorization of grains for seed production), management (the design of a marketing support strategy for a mobile phone operator) and engineering (the synthesis of a fuzzy controller).

P. Kulczycki (✉) · M. Charytanowicz · P. A. Kowalski · S. Łukasik
Centre of Information Technology for Data Analysis Methods, Systems Research Institute,
Polish Academy of Sciences, Warsaw, Poland
e-mail: Piotr.Kulczycki@ibspan.waw.pl

M. Charytanowicz
e-mail: Malgorzata.Charytanowicz@ibspan.waw.pl

P. A. Kowalski
e-mail: Piotr.A.Kowalski@ibspan.waw.pl

S. Łukasik
e-mail: Szymon.Lukasik@ibspan.waw.pl

P. Kulczycki · P. A. Kowalski · S. Łukasik
Department of Automatic Control and Information Technology, Cracow University
of Technology, Cracow, Poland

M. Charytanowicz
Institute of Mathematics and Computer Science, John Paul II Catholic University of Lublin,
Lublin, Poland

1 Introduction

Clustering is becoming a fundamental procedure in exploratory data analysis [2, 20]. However it lacks natural mathematical apparatus, such as—for example—differential calculus for investigating the extremes of a function. In this situation the ambiguity of an interpretation (important mainly in practical applications) as well as particular factors of the definition itself (e.g. the meaning of "similarity" and consequently "dissimilarity" of elements) imply a huge variety of concepts and thus of clustering procedures. On one hand this significantly hinders the research, but on the other it allows to better suit the applied method to the specifics and requirements of an investigated task.

This publication aims to present the applicational properties of the so-called Complete Gradient Clustering Algorithm—abbreviated to CGCA in the following— illustrated in examples of practical problems of bioinformatics, management and engineering, concerning the categorization of grains for seed production, the design of a marketing support strategy for a mobile phone operator and the synthesis of a fuzzy controller for the reduction of a rule set, respectively.

Consider the m-elements data set comprised of n-dimensional vectors

$$x_1, x_2, \ldots, x_m \quad \in \mathbb{R}^n, \tag{1}$$

treated here as a sample obtained from an n-dimensional real random variable. In their now seminal paper [4], Fukunaga and Hostetler formulated a natural and effective concept of clustering, making use of the significant possibilities of statistical kernel estimators [8, 21, 23], which were becoming more widely applied at that time. The basis for this concept is accepting data set (1) as a random sample obtained from a certain n-dimensional random variable, calculating a kernel estimator for its distribution density and making a natural assumption that particular clusters are related to modes (local maxima) of the resulting estimator (in consequence "valleys" of the density function become borders for such-formed clusters). The method presented then was formulated as a general idea only, leaving detailed analysis to the user. In the paper [11], the Fukunaga and Hostetler algorithm was supplemented and finally given in its complete form, useful for application without the necessity of deeper statistical knowledge or laborious calculations and investigations. This is characterized by the following features:

1. all parameters can be effectively calculated using numerical procedures based on optimizing criteria;
2. the algorithm does not demand strict assumptions regarding the desired number of clusters, which allows the number obtained to be better-suited to a real data structure;
3. the parameter directly responsible for the number of clusters is indicated; it will also be shown how possible changes—e.g. with regard to values calculated using optimizing criteria (see point 1 stated above)—to this value, influence the

increase or decrease in the number of clusters without, however, defining their exact number;

4. moreover, the next parameter can be easily indicated, the value of which will influence the proportion between the number of clusters in dense and sparse areas of elements of data set (1); here also the value of this parameter can be assumed based on optimizing criteria (see again point 1); it will also be shown here that potential lowering of the value of this parameter results in a decrease in the number of clusters in dense regions of data as the number of clusters in sparse areas increases, while a potential raise in its value has the opposite effect—increasing the number of clusters in dense areas while simultaneously reducing or even eliminating them from sparse regions of data set (1);

5. the appropriate relation between the two above-mentioned parameters allows for a reduction, or even elimination of clusters in sparse areas, practically without influencing the number of clusters in dense areas of data set elements;

6. the algorithm also creates small, even single-element clusters, which can be treated as atypical elements (outliers) in a given configuration of clusters, which makes possible their elimination or assignation to the closest cluster by a change—described in points 3 and particularly 4 or 5—in the values of the appropriate parameters.

The features in point 4, and in consequence 5, are particularly worth underlining as practically non-existent in other clustering procedures. In practical applications it is also worth highlighting the implications of points 1 and 2, and potentially 3. Unusual possibilities are offered by the property expressed in point 6.

More details of the material presented in this publication is available in the paper [13].

2 Statistical Kernel Estimators

Let the n-dimensional random variable $X : \Omega \to \mathbb{R}^n$, with a distribution having the density f, be given. Its kernel estimator $\hat{f} : \mathbb{R}^n \to [0, \infty)$ is calculated on the basis of the m-elements random sample (1) experimentally obtained from the variable X, and is defined in its basic form by

$$\hat{f}(x) = \frac{1}{mh^n} \sum_{i=1}^{m} K\left(\frac{x - x_i}{h}\right), \qquad (2)$$

where the measurable function $K : \mathbb{R}^n \to [0, \infty)$, symmetrical with respect to zero and having a weak global maximum in this point, fulfils the condition $\int_{\mathbb{R}^n} K(x)\, dx = 1$ and is called a kernel, whereas the positive coefficient h is referred to as a smoothing parameter. Broader discussion and practical algorithms are found in the books [8, 21, 23]. Setting the quantities introduced in definition (1), i.e. choice of the form of the kernel K as well as calculation of the value for the

smoothing parameter h, is most often carried out according to the criterion of minimum of an integrated mean-square error. In particular, the choice of the kernel K form has no practical meaning and thanks to this it is possible to first take into account properties of the estimator obtained (e.g. its class of regularity, boundary of a support, etc.) or aspects of calculations, advantageous from the point of view of the applicational problem under consideration. On the contrary, the value of the smoothing parameter h has significant meaning for quality of estimation. Too small a value causes a large number of local extremes of the estimator $\hat{f}$ to appear; on the other hand, too big values of the parameter h result in overflattening of this estimator—this property will be successfully used here later.

Practical applications of kernel estimators may also use additional procedures, some generally improving the quality of the estimator, and others—optional—possibly fitting the model to an existing reality. For the first group one should recommend the modification of the smoothing parameter and a linear transformation, while for the second e.g. the boundaries of a support. The procedure of the modification of the smoothing parameter is outlined below, as it will be heavily used in the following.

Thus, in the case of the basic definition of kernel estimator (2), the influence of the smoothing parameter on particular kernels is the same. Advantageous results are obtained thanks to the individualization of this effect, achieved by introducing the positive modifying parameters $s_1, s_2, \ldots, s_m$ mapped to particular kernels, which value is given as

$$s_i = \left(\frac{\hat{f} * (x_i)}{\bar{s}} \right)^{-c}, \tag{3}$$

where $c \in [0, \infty)$, $\hat{f}*$ denotes the kernel estimator without modification, $\bar{s}$ is the geometrical mean of the numbers $\hat{f}*(x_1), \hat{f}*(x_2), \ldots, \hat{f}*(x_m)$, and finally, defining the kernel estimator with modification of the smoothing parameter in the following form:

$$\hat{f}(x) = \frac{1}{mh^n} \sum_{i=1}^{m} \frac{1}{s_i^n} K \left(\frac{x - x_i}{hs_i} \right). \tag{4}$$

Thanks to the above procedure, the areas in which the kernel estimator assumes small values are flattened and the areas connected with large values—peaked. The parameter c stands for the intensity of the modification procedure—the greater its value, the stronger (more distinct) the above procedure. Based on indications for the criterion of the integrated mean square error, the value

$$c = 0.5 \tag{5}$$

can be tentatively suggested.

Detailed information regarding kernel estimators can be found in the publications [8–10, 21, 23].

3 Complete Gradient Clustering Algorithm (CGCA)

Consider—as in the Sect. 1—the m-elements set of n-dimensional vectors (1). This will be treated as a random sample obtained from the n-dimensional random variable X, with distribution having the density f. Using the methodology described in Sect. 2, the kernel estimator $\hat{f}$ can be created. Take the natural assumption that particular clusters are related to its modes (i.e. the local maxima of the function $\hat{f}$), and elements of set (1) are mapped onto them by shifting in the gradient $\nabla \hat{f}$ direction, with the appropriate fixed step.

The above is carried out iteratively with the Gradient Clustering Algorithm [4], based on the classic Newtonian procedure ([6]—Sect. 3.2), defined as

$$x_j^0 = x_j \quad \text{for} \quad j = 1, 2, \ldots, m \tag{6}$$

$$x_j^{k+1} = x_j^k + b \frac{\nabla \hat{f}(x_j^k)}{\hat{f}(x_j^k)} \quad \text{for} \quad j = 1, 2, \ldots, m \quad \text{and} \quad k = 0, 1, \ldots, k^*, \tag{7}$$

where $b > 0$ and $k^* \in \mathbb{N}\backslash\{0\}$; in practice the value $b = h^2/(n + 2)$ can be recommended.

In order to refine the above concept to the state of a complete algorithm, the following aspects need to be formulated and analyzed in detail:

- formula of the kernel estimator $\hat{f}$;
- setting a stop condition (and consequently the number of steps k^*);
- definition of a procedure for creating clusters and assigning to them particular elements of set (1), after the last, k^*-th step;
- analysis of influence of the values of parameters on results obtained.

Respective procedures for each of the above aspects were given—following comprehensive research—in the form of the Complete Gradient Clustering Algorithm (CGCA) in the publications [11, 12]. Thanks to the appropriate utilization of specific features of kernel estimators, the properties 1–6 outlined in Sect. 1 are obtained.

4 Influence of the Values of Parameters on Results Obtained

It is worth summarizing that the CGCA does not require a preliminary, in practice often arbitrary, assumption concerning number of clusters—their size depends solely on the internal structure of data, given as set (1). When using its basic form, the values of the parameters used are effectively calculated taking optimizing reasons into account. However, optionally—if the researcher makes the decision—by an appropriate change in values of kernel estimator parameters it is possible to influence the size of number of clusters (still without defining their exact number), and also the

proportion of their appearance in dense areas in relation to sparse regions of elements in this set.

As mentioned in Sect. 2, too small a value of the smoothing parameter h results in the appearance of too many local extremes of the kernel estimator, while too great a value causes its excessive smoothing. In this situation lowering the value of the parameter h in respect to that obtained by procedures based on the criterion of the mean integrated square error creates as a consequence an increase in the number of clusters. At the same time, an increase in the smoothing parameter value results in fewer clusters. It should be underlined that in both cases, despite having an influence on the size of the cluster number, their exact number will still depend solely on the internal structure of data.

Next, as mentioned in Sect. 2, the intensity of modification of the smoothing parameter is implied by the value of the parameter c, given as standard by formula (5). Its increase smoothes the kernel estimator in areas where elements of set (1) are sparse, and also sharpens it in dense areas—in consequence, if the value of the parameter c is raised, then the number of clusters in sparse areas of data decreases, while at the same time increasing in dense regions. Inverse effects can be seen in the case of lowering this parameter value.

Practice, however, often prevents changes to the clusters in dense areas of data—the most important from an applicational point of view—while at the same time requiring a reduction or even elimination of clusters in sparse regions, as they frequently pertain to atypical elements commonly arising due to various errors. Putting the above considerations together, one can propose an increase of both the standard scale of the smoothing parameter modification (5) as well as the value of the smoothing parameter h calculated on the criterion of the mean integrated square error, to the value $h^* = (3/2)^{c-0.5}h$. The joint action of both these factors results in a twofold smoothing of the function $\hat{f}$ in the regions where the elements of set (1) are sparse. Meanwhile these factors more or less compensate for each other in dense areas, thereby having practically no influence on the detection of these clusters.

More details with illustrative examples can be found in the paper [11].

5 Applicational Examples

The CGCA was comprehensively tested both for random statistical data as well as generally available benchmarks. In comparison with other well-known clustering methods it is worth underlining that the CGCA allowed for greater possibilities of adjustment to the real structure of data, and consequently the obtained results were more justifiable to a natural human point of view. A very important feature for practitioners was the possibility of firstly using standard parameters values, and the option of changing them afterwards—according to individual needs—by the modification of two of them according to the suggestions made in Sect. 4. These properties were actively used in three projects from the domains of bioinformatics, management and engineering, which will be presented in detail in the following subsections.

5.1 Categorization of Grains for Seed Production

Bioinformatics—a discipline concerning the application of mathematical and IT tools to solve problems of biological science—is now growing on an exceptionally dynamic and diverse scale. Opportunities arising thanks to the development and prevalence of computer technology have resulted in a sudden increase in mutual understanding and cooperation in the frameworks of previously different research methods of hard and natural sciences. Below will be presented the results of investigations carried out as part of a larger project on the categorization of grains according to the geometric features of seeds, taken from X-ray images, for production purposes.

For an illustrative and comparative presentation of aspects of research using the CGCA, an analysis will be made of a sample of harvested wheat grain originating from experimental fields explored at the Institute of Agrophysics of the Polish Academy of Sciences in Lublin. The examined group consisted of grains of three strains of wheat—Kama, Rosa and Canadian—with 70 of each type selected randomly for testing. A high quality visualization of their internal structures was achieved using a soft X-ray technique, without destroying the subject material. After scanning the resulting pictures, the following seven geometric parameters of wheat kernels were obtained using the program GRAINS, specially created to this aim: area A, perimeter P, compactness $C = 4\pi A/P^2$, length, width, asymmetry coefficient, and length of kernel groove. Each was thus represented by a 7-dimensional vector ($n = 7$), while their set comprised a 210-elements sample (1). In the preliminary phase, the data dimensionality was reduced to two using Principal Components Analysis.

As a result of using the CGCA with the standard values of the smoothing parameter h and the intensity of its modification c, obtained by the mean-square criterion, seven clusters were found, of 76, 64, 57, 7, 3, 2, 1 elements each. It can be deduced that the first three represent the three used for the analysis investigated here, while the remaining four small clusters contain atypical elements, without excluding physically damaged. If one disregards the 13 units contained in these four small clusters (6 % of the entire population), the number of correctly classified grains was, in order 91, 97, 88 % for Kama, Rosa and Canadian, respectively. It is worth pointing out that the above results were obtained without the need for any a priori assumption as to required number of clusters, information which may be difficult or even impossible to obtain in practical problems in biology.

If, however, a necessity is assumed to map every element to one of the larger clusters, then this can be achieved by appropriately changing the values of the parameters h and c to those obtained with optimization criterions. Thus, in successively increasing the value of the former, the number of local extremes of the kernel estimator falls, while decreasing the latter makes it impossible to divide the large clusters created in this way. In doing so, three large clusters are obtained for h increased by 75 % and c decreased to the value 0.1. The number of correct classifications was for one strain slightly lower than that obtained earlier, and was 91, 96, 88 % for particular strains, respectively, and was still reached without any arbitrary assumptions as to number of clusters required.

In summary, use of the CGCA allowed the correct classification of the grains of three strains of wheat without a priori information about their number. What is more, with standard parameters values, the above algorithm also enabled the identification of atypical elements, e.g. physically damaged and—following their elimination from the sample—a slight reduction in the number of misclassifications in the remaining part.

The above illustratory example, concerning three strains of wheat, can be generalized for other categorization tasks of seed produce of similar conditioning. This research was carried out in cooperation with Jerzy Niewczas and Slawomir Zak. Detailed information is found in the publication [1].

5.2 Marketing Support Strategy for Mobile Phone Operator

The highly dynamic growth prevalent on the mobile phone network market naturally necessitates a company to permanently direct its strategy towards satisfying the differing needs of its clients, while at the same time maximizing its income. The uncontrollable nature of this kind of activity, however, can lead to a loss of coherence in treating particular clients, and their subsequent defection to competitors. To avoid this a formal solution of global nature must be found. Below are presented the results of research prepared for a Polish mobile phone network operator, concerning long term business clients, i.e. those with more than 30 SIM cards and an account history of at least 2 years.

In practice there is a vast spectrum of quantities characterizing particular subscribers. Following detailed analysis of the economic aspects of the task under investigation here, it was taken that basic traits of business clients would be shown by three quantities: average monthly income per SIM card, length of subscription and number of active SIM cards. Thus each of m-elements of a database $x_1, x_2, \ldots, x_m$ is characterized by the following 3-dimensional vector:

$$x_i = \begin{bmatrix} x_{i,1} \\ x_{i,2} \\ x_{i,3} \end{bmatrix} \quad \text{for} \quad i = 1, 2, \ldots, m, \tag{8}$$

where $x_{i,1}$ denotes the average monthly income per SIM card of the ith client, $x_{i,2}$—its length of subscription, and $x_{i,3}$—the number of active SIM cards.

In the initial phase, atypical elements of the set $x_1, x_2, \ldots, x_m$ (outliers) are eliminated, according to the procedure presented in the publication [17], based on kernel estimators methodology. The uniformity of the data structure is so increased, and it is worth underlining that the effect is obtained by canceling only those elements which would not be of importance further in the investigated procedure.

Next a grouping of the data set is performed using the CGCA. This results in a division of the data set representing specific clients, into groups of similar nature. The results obtained for typical intensity of smoothing parameter modification (5)

indicated that an excessive number of clusters of small sizes, located in areas of low density of sample elements, most often contain insignificant specific clients, and that an overly-numerous main cluster contains over half the elements. In accordance with the properties of the algorithm used, this value was increased to $c = 1$. This gave the desired effect: the number of "peripheral" clusters lowered significantly, and the main cluster was split. The obtained number of clusters was satisfying, which led to any possible change in the value of the smoothing parameter h becoming redundant. Finally the sample, considered at this stage, containing 1,639 elements was divided into 26 clusters of the following sizes: 488, 413, 247, 128, 54, 41, 34, 34, 33, 28, 26, 21, 20, 14, 13, 12, 10, two 4-elements clusters, three of 3-elements, two of 2-elements and two of 1-element. It is worth noting the four clearly drawn groups: the first of these comprises two numerous clusters of 488 and 413-elements, next two medium-sized 247- and 128-elements, followed by small—nine clusters containing from 20 to 54 and lastly 13 clusters of less than 20 elements. Next began the elimination of these last clusters, with the exception however of those containing key clients (clusters of 14, 13 and 10-elements) as well as one where at least half of its elements were prestige clients (12-elements cluster). In the end, 17 clusters remained for further analysis.

Next for each of the above defined clusters, an optimal—from the point of view of expected profit of the operator—strategy is created for treating subscribers belonging to it. With regard to the imprecise evaluation of experts used here, elements of fuzzy logic [5] and preference theory [3] have been used—details are however beyond the scope of this publication.

It is worth pointing out that none of the above calculations must be carried out at the same time as negotiating with the client, but merely updated (in practice once every 1–6 months).

The client being negotiated with is described with the aid—in reference to formula (8)—of a 3-dimensional vector with respective particular coordinates. This data can relate to the subscriber history to date in a given network, when renegotiating contract terms, or in a rival network if attempting to take them over. Mapping of the client being negotiated to the proper subscriber group, from those obtained as a result of earlier-performed clustering, was carried out using Bayes classification also applying kernel estimators methodology (for subject bibliography see [15]). Due to the fact that the marketing strategies for particular clusters have already been defined, this finally completes the procedure for the algorithm to support the marketing strategy for a business client, investigated here.

The above method, researched with the cooperation of Karina Daniel, was successfully implemented for the needs of a Polish network operator. Detailed information is found in the paper [14].

5.3 Synthesis of Fuzzy PID Controller

Fuzzy PID controllers are a valuable—from an applicational point of view—
generalization of commonly used, precisely examined and familiarized by practi-
tioners classical PID feedback-controllers. The fuzzy version is particularly useful
for challenging systems, e.g. containing strong nonlinearities and uncertainties, since
thanks to the greater degree of freedom, such controllers can better fit the specifics
of an object. On the other hand, however, too great a degree of freedom may cause
difficulties in appropriately fixing their functions and parameters, implying an incor-
rectly working system, and in the extreme case impossible excessive expansion of its
structure making it impossible to realize in practice. The problem of a suitably large,
but not lower quality, simplification of fuzzy PID controllers structures is therefore
fundamentally significant in applicational engineering.

Investigated below are the fuzzy PID controllers in Takagi-Sugeno sense [24].
Their concept is built on the set (base) of k fuzzy rules of the form

$$\text{IF } (x \text{ is } A_j) \text{ THEN } (y = f_j(x)) \quad \text{for} \quad j = 1, 2, \ldots, k. \tag{9}$$

If—according to the character of the fuzzy approach—the element x belongs to many
sets to a degree defined by values of their membership functions, i.e. with $\mu_{A_j}(x)$,
then finally y takes the form of the normalized mean

$$y = \frac{\sum_{j=1}^{k} \mu_{A_j}(x) f_j(x)}{\sum_{j=1}^{k} \mu_{A_j}(x)} \ . \tag{10}$$

In the case of fuzzy PID controllers, the coordinates of the vector x are connected
with an error and its integral and derivative, while the variable y constitutes a gen-
erated control. Even if one assumes the simple triangular or trapezoid membership
functions μ_{A_j}, and that the functions f_j are linear, then the large number of parame-
ters appearing in such a task may pose the threat of losing the possibility of correct
effective fixing of their values. The appropriate reduction in the size of the fuzzy
rules set (9) becomes therefore a fundamental problem, in particular for the complex
applicational cases. To solve the task of reducing fuzzy rules, many contemporary
IT methods are used, above all evolutionary algorithms, neuro-fuzzy systems or sta-
tistical approaches also, among which dominate concepts based on the clustering
technique. The CGCA was applied successfully to this aim.

Let then be given the vector $\begin{bmatrix} x \\ y \end{bmatrix}$ and m measurements of values obtained during
operation of the system with the fuzzy PID controller in its primary form, i.e. without
reducing the rules set:

$$\begin{bmatrix} x_1 \\ y_1 \end{bmatrix}, \quad \begin{bmatrix} x_2 \\ y_2 \end{bmatrix}, \dots, \quad \begin{bmatrix} x_m \\ y_m \end{bmatrix}. \tag{11}$$

Treating the above set as random sample (1) one can perform clustering with the use of the CGCA. Let

$$\begin{bmatrix} \tilde{x}_1 \\ \tilde{y}_1 \end{bmatrix}, \quad \begin{bmatrix} \tilde{x}_2 \\ \tilde{y}_2 \end{bmatrix}, \dots, \quad \begin{bmatrix} \tilde{x}_{\tilde{m}} \\ \tilde{y}_{\tilde{m}} \end{bmatrix} \tag{12}$$

represent centers of $\tilde{m}$ clusters obtained in this way. Each of the element $\tilde{x}_i$ for $i = 1, 2, \dots, \tilde{m}$ may be the basis of i-th fuzzy rule with the respective membership function

$$\mu_i(x) = \exp\left(-\left\|\frac{x - \tilde{x}_i}{d}\right\|^2\right), \tag{13}$$

where the "scaling" parameter $d > 0$ characterizes the generalization ability resulting from the fuzzy inference concerning the control system under design. The experimental research carried out indicates that the value $d = \tilde{m}/2$ can be successfully used. In consequence formula (10) takes the form

$$y = \frac{\sum_{i=1}^{\tilde{m}} \mu_i(x) f_i(x)}{\sum_{i=1}^{\tilde{m}} \mu_i(x)}, \tag{14}$$

while f_i are linear functions whose parameters may be calculated based on the classical least-squares estimation task.

This method was positively verified in numerous practical problems. Presented below are comparative results obtained for the control system of a hard-drive servo motor, presented in the paper [22]. Its following model was used:

$$\begin{bmatrix} \dot{s}(t) \\ \dot{v}(t) \end{bmatrix} = \begin{bmatrix} 1 & 1.664 \\ 0 & 1 \end{bmatrix} \begin{bmatrix} s(t) \\ v(t) \end{bmatrix} + \begin{bmatrix} 1.384 \\ 1.664 \end{bmatrix} u(t) \quad, \tag{15}$$

where u constitutes actuator input (in volts), s and v are the position (in tracks) and velocity of the disk drive's head. The problem of accurate positioning was analyzed with $s(t)$ as an output. Typically for such applications, a controller of PD type was considered [19].

First the standard PD fuzzy controller with 49-rules was tuned for quick response with the step reference signal. The 121-elements set (11) obtained in this way:

$$\begin{bmatrix} e_1 \\ \dot{e}_1 \\ u_1 \end{bmatrix}, \quad \begin{bmatrix} e_2 \\ \dot{e}_2 \\ u_2 \end{bmatrix}, \dots, \quad \begin{bmatrix} e_{121} \\ \dot{e}_{121} \\ u_{121} \end{bmatrix}, \tag{16}$$

where e represents error, was treated as random sample (1) and subjected to the CGCA. As a result the PD fuzzy controller with the base reduced to 38 rules was obtained.

To compare the results acquired using a classical PD feedback-controller, a fuzzy PD controller with full (unreduced) 49-elements rule base [19], and the above investigated fuzzy controller with base reduced to 38 rules, for each of them the values were obtained for the root-mean-square-error index and the percentage overshoot for a response with the step reference signal. For the first value the results were 0.291, 0.198, 0.111, respectively, for the second 78, 92, 15 %. For both, the best results were provided by the use of the fuzzy PD controller with the rule set reduced using the CGCA. Similar results were achieved for other conditions and performance indexes.

Further testing was carried out for the system with the fuzzy controller with the rule set reduced by the CGCA, for various—different from those obtained with the integrated mean-square error criterion—values of the smoothing parameter h and the intensity of modification c. The most advantageous results were achieved for the value of the latter, slightly lowered—with respect to optimal (5)—to $c = 0.25$. This effect can be interpreted by an increase in the number of peripheral clusters characterizing atypical states, "dangerous" from the point of view of correct behavior of the system. Moreover, the main cluster generally contained even 80 % elements of set (16), representing "safe" states, and its potential division did not bring any positive changes. As before it was not necessary to alter—with respect to optimal— the value of the smoothing parameter h. It proves once again that the CGCA adapts well to real data structures.

The presented concept was successfully implemented for the control of a robot under the authority of the Department of Automatic Control and Information Technology of the Cracow University of Technology. Detailed information is found in the publications [7, 18].

6 Summary

The results presented in this chapter, achieved by using the Complete Gradient Clustering Algorithm (CGCA), in particular the one investigated in the paper [11], confirmed its practical use, especially the six basic features dealt with in the Introduction. Noteworthy is the lack of necessity to significantly change the value of the parameter h, directly implying a number of obtained clusters, which points to the procedure being correctly adapted to the structure of real data. Particularly valuable in practice was the possibility to change the value of the parameter c, influencing the relation of the number of clusters in dense and sparse areas of random sample elements. In all three investigated problems this change enabled the creation of significantly better— from an applicational point of view—results. This is particularly worth underlining as the possibility of forming the above relation does not appear in other known clustering algorithms.

More details of the material presented in this publication is available in the paper [13]. It is also worth mentioning the procedure for reducing the dimension *n* and simple size *m* used to calculate the estimator, and based on the metaheuristics of simulated annealing, dedicated to the tasks applying kernel estimators, to be published in the work [16]. It can be very useful for practical problems of large magnitude, both in the sense of dimensionality and sample size.

References

1. Charytanowicz, M., Niewczas, J., Kulczycki, P., Kowalski, P.A., Łukasik, S., Zak, S.:gradient clustering algorithm for features analysis of X-ray images. In: Pietka, E., Kawa, J. (eds.) Information Technologies in Biomedicine, vol. 2, pp. 15–24. Springer, Berlin (2010)
2. Everitt, B.S., Landau, S., Leese, M.: Cluster Analysis. Arnold, London (2001)
3. Fodor, J., Roubens, M.: Fuzzy Preference Modelling and Multicriteria Decision Support. Kluwer, Dordrecht (1994)
4. Fukunaga, K., Hostetler, L.D.: The estimation of the gradient of a density function, with applications in pattern recognition. IEEE Trans. Inf. Theory **21**, 32–40 (1975)
5. Kacprzyk, J.: Multistage Fuzzy Control: A Model-Based Approach to Control and Decision-Making. Wiley, Chichester (1997)
6. Kincaid, D., Cheney, W.: Numerical Analysis. Brooks/Cole, Pacific Grove (2002)
7. Kowalski, P.A., Łukasik, S., Charytanowicz, M., Kulczycki, P.: Data-driven fuzzy modeling and control with kernel density based clustering technique. Pol. J. Environ. Stud. **17**, 83–87 (2008)
8. Kulczycki, P.: Estymatory jadrowe w analizie systemowej. WNT, Warsaw (2005)
9. Kulczycki, P.: Estymatory jadrowe w badaniach systemowych. In: Kulczycki, P., Hryniewicz, O., Kacprzyk, J. (eds.) Techniki informacyjne w badaniach systemowych, pp. 79–105. WNT, Warsaw (2007)
10. Kulczycki, P.: Kernel estimators in industrial applications. In: Prasad, B. (ed.) Soft Computing Applications in Industry, pp. 69–91. Springer, Berlin (2008)
11. Kulczycki, P., Charytanowicz, M.: A complete gradient clustering algorithm formed with kernel estimators. Int. J. Appl. Math. Comput. Sci. **20**, 123–134 (2010)
12. Kulczycki, P., Charytanowicz, M.: A complete gradient clustering algorithm. In: Deng, H., Miao, D., Lei, J., Wang, F.L. (eds.) Artificial Intelligence and Computational Intelligence, Lecture Notes in Artificial Intelligence, vol. III, pp. 497–504. Springer, Berlin (2011)
13. Kulczycki, P., Charytanowicz, M., Kowalski, P.A., Łukasik, S.: The complete gradient clustering algorithm: Properties in practical applications. J. Appl. Stat. **39**, 1211–1224 (2012)
14. Kulczycki, P., Daniel, K.: Metoda wspomagania strategii marketingowej operatora telefonii komorkowej, Przeglad Statystyczny, vol. 56, pp. 116–134 (2009)
15. Kulczycki, P., Kowalski, P.A.: Bayes classification of imprecise information of interval type. Control Cybern. **40**, 101–123 (2011)
16. Kulczycki, P., Łukasik, S.: An algorithm for reducing dimension and size of sample for data exploration procedures (2014) (in press)
17. Kulczycki, P., Prochot, C.: Wykrywanie elementow odosobnionych za pomoca metod estymacji nieparametrycznej. In: Kulikowski, R., Kacprzyk, J., Slowinski, R. (eds.) Badania operacyjne i systemowe: podejmowanie decyzji - podstawy teoretyczne i zastosowania, pp. 313–328. EXIT, Warsaw (2004)
18. Łukasik, S., Kowalski, P.A., Charytanowicz, M., Kulczycki, P.: Fuzzy models synthesis with kernel-density based clustering algorithm. In: Ma, J., Yin, Y., Yu, J., Zhou, S. (eds.) Fifth International Conference on Fuzzy Systems and Knowledge Discovery, vol. 3, pp. 449–453 Jinan (China), 18–20 Oct 2008

19. Mudi, R., Pal, N.R.: A robust self-tuning scheme for PI and PD type fuzzy controllers. IEEE Trans. Fuzzy Syst. **7**, 2–16 (1999)
20. Pal, S.K., Mitra, P.: Pattern Recognition Algorithms for Data Mining. Chapman and Hall, London (2004)
21. Silverman, B.W.: Density Estimation for Statistics and Data Analysis. Chapman and Hall, London (1986)
22. Tan, K.C., Sathikannan, R., Tan, W.W., Loh, A.P.: Evolutionary design and implementation of a hard disk drive servo control system. Soft Comput. **11**, 131–139 (2007)
23. Wand, M.P., Jones, M.C.: Kernel Smoothing. Chapman and Hall, London (1994)
24. Yager, R.R., Filev, D.P.: Foundations of Fuzzy Modeling and Control. Wiley, New York (1994)

A Hierarchical Approach for Handwritten Digit Recognition Using Sparse Autoencoder

An T. Duong, Hai T. Phan, Nam Do-Hoang Le and Son T. Tran

Abstract Higher level features learning algorithms have been applied on handwritten digit recognition and got more promising results than just using raw intensity values with classification algorithms. However, the approaches of these algorithms still not take the advantage of specific characteristics of data. We propose a new method to learn higher level features from specific characteristics of data using sparse autoencoder. The main key of our appoarch is to divide the handwritten digits into subsets corresponding to specific characteristics. The experimental results show that the proposed method achieves lower error rates and time complexity than the original approach of sparse autoencoder. The results also show that the more correlated characteristics we define, the better higher level features we learn.

Keywords Higher level features · Sparse autoencoder · Handwritten digit recognition · Specific characteristics

A. T. Duong (✉) · H. T. Phan · N. D.-H. Le · S. T. Tran
University of Science, HCMC, Ho Chi Minh, Vietnam
e-mail: 0912019@student.hcmus.edu.vn

S. T. Tran
e-mail: ttson@fit.hcmus.edu.vn

H. T. Phan
Advanced Program in Computer Science,
University of Science, HCMC, Ho Chi Minh, Vietnam
e-mail: pthai@apcs.vn

N. D.-H. Le
John von Neumann Institute, Vietnam National University HCMC,
Ho Chi Minh, Vietnam
e-mail: nam.le.ict@jvn.edu.vn

1 Introduction

Handwritten digit recognition is one of the main problems in recognition field. There are many common approaches to solve it such as K-Nearest neighbors, neural network and support vector machine. These algorithms do not achieve comparable error rates without preprocessing [3, 9]. Recently, some methods using higher representations instead of raw data have got promising results [5, 18].

Higher representations are more abstract representations of raw data [15]. For example, instead of raw pixel intensity values an image can be represented in term of edges. As we know that edges are not only primitive elements combined from a set of pixels but also basic elements comprising the content of an image. These higher representations contain more meaning and specific features than raw data. Thus, they can be seen as high level features representing for data than low-level features as raw pixel intensity values. Other features such as SIFT [12], HOG [2], MFCCs [7] are obtained by experts in computer vision and digital signal processing. Unlike those common features, higher representations are learned automatically regardless of type of learning data and knowledge of experts in specific fields [4, 15]. With this characteristic, higher level features can be applied in any kind of data such as images [11, 15], audio [4], text [16, 17].

However, the approach of higher level features from learning algorithms [6, 14, 15] still not take the advantage of specific characteristics of data. In this work, we utilize sparse autoencoder to learn higher level features from raw data. Specific characteristics of learning data are first clustered. After that, sparse autoencoders use these specific characteristics to learn higher level features from raw data. Our proposed method is based on achievements in neuroscience and unsupervised learning. Olshausen proposed sparse coding which shows that the receptive fields of simple cells in mammalian primary visual cortex can learn higher level representations from the outside input signals [14]. From the result of Olshausen et al. [14], many unsupervised learning algorithms such as autoencoder and Restricted Boltzmann Machine [5] are also proposed to learn higher level features. In addition, some researchers focus on improving learning algorithms by using weights optimization [13] or efficient solving algorithms [1, 10].

The rest of this paper is organized as follows. Section 2 describes sparse autoencoder for learning higher level features. Section 3 describes method of learning higher level features from specific characteristics of data. Finally experiments and interesting results are shown in Sect. 4.

2 Sparse Autoencoder

Higher representation learning is an unsupervised learning phase to obtain the features of the input data automatically. The higher representations retrieved from the autoencoder are used as the features for the supervised learning phase. Autoencoder [5]

Fig. 1 An example of simple
autoencoder
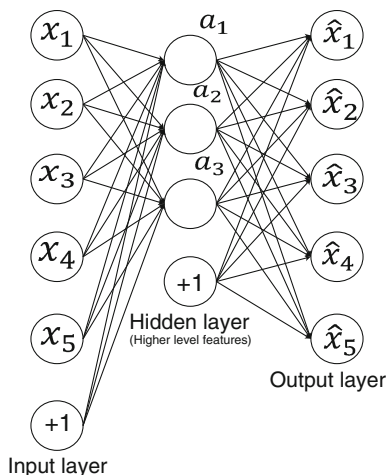
can learn higher representations from raw input data

$$D = \left\{ x^{(1)}, x^{(2)}, ..., x^{(m)} \right\}, \; x^{(i)} \in \mathbb{R}^n \tag{1}$$

where $x^{(i)}$ is the ith sample in dataset D. An autoencoder is a neural network with the special architecture: the number of input neurons is equal to the number of output neurons. Furthermore, the desired output of this neural network is also equal to the corresponding input. Thus, the term autoencoder means that it can encode automatically an input information to a representation and decode the representation to the original information. Figure 1 illustrates one example of an autoencoder with the 5-3-5 structure of input-hidden-output layers. Here we only consider one hidden layer autoencoder called shallow autoencoder. So we can denote that input layer is the 1st layer; hidden layer is the 2nd layer and output layer is the 3rd layer. With this special structure, the purpose of the autoencoder is to try to reconstruct the original information of the input data.

Let τ denote the number of hidden neurons of the network, $\Theta_{ij}^{(l)}$ denotes the weight matrix associated with the connection between jth neuron in lth layer and neuron ith in $(l + 1)$th layer and $\gamma_i^{(l)}$ denote the biased weight corresponding to the neuron ith in $(l + 1)$th layer. After unsupervised training phase, the value of $\Theta_{ij}^{(l)}$ is optimized so that for a given input $x^{(i)} \in \mathbb{R}^n$ the network gives the output as the approximation $\widehat{x}^{(i)}$.

Let $a^{(i)} = \{a_1, a_2, ..., a_\tau\} \in \mathbb{R}^\tau$ denote the value of hidden layer given the input $x^{(i)}$. Therefore, one can compute the hidden layer $a^{(i)}$ corresponding to the input $x^{(i)}$ using the weight matrix $\Theta_{ij}^{(1)}$ between the input and hidden layer. When we are given the computed $a^{(i)}$, the original $x^{(i)}$ is approximated to $\widehat{x}^{(i)}$ using the weight matrix $\Theta_{ij}^{(2)}$ of the hidden and output layer. As a result, we say that $a^{(i)}$ is another

representation of the input $x^{(i)}$. When the neuron number of the hidden layer is less than that of the input layer, $\tau < n$, $a^{(i)}$ can be considered as the compression of the input $x^{(i)}$ [5]. The lower dimensional information can be seen as the better representation of the original information.

But one can set the number neurons of the hidden layer greater than or equal to the number neurons of the input layer ($\tau \geq n$). Based on the good result of sparse representation on coefficients given by Olshausen [14], we can still obtain better representations by impose a sparse constraint (called sparsity for short) on the autoencoder in this case. Sparsity in autoencoder means we want the hidden neurons to be inactive most of the time. Specifically, a hidden neuron is active if its activation value close to 1 or it is inactive if its activation value close to 0 through the output of sigmoid function

$$\psi(z) = \frac{1}{1 + e^{-z}} \tag{2}$$

Imposing the sparsity on autoencoder changes the error function of autoencoder to a new error function.

$$J_{sparse} = J_{network} + \beta \sum_{j=1}^{\tau} KL(\rho \,||\, \widehat{\rho}_j) \tag{3}$$

where $J_{network}$ is the error function of the neural network without sparse constraint and β is the sparsity penalty term (i.e $\beta = 0.003$);

$$KL\left(\rho \,||\, \widehat{\rho}_j\right) = \rho \log \frac{\rho}{\widehat{\rho}_j} + (1 - \rho) \log \frac{1 - \rho}{1 - \widehat{\rho}_j} \tag{4}$$

where KL is Kull-back Leibler divergence [1] to control the sparsity of hidden neuron; ρ is a sparsity parameter (i.e $\rho = 0.1$) to keep the most number of hidden neurons being inactive and $\widehat{\rho}_j$ is an activated expectation of hidden neuron jth.

$$\widehat{\rho}_j = \frac{1}{m} \sum_{i=1}^{m} a_j^{(i)} \tag{5}$$

To learn the weights matrix $\Theta_{ij}^{(l)}$ of the sparse autoencoder we just implement the forward and backward propagation algorithm of neural network using error function J_{sparse} instead of original error function of neural network. After retrieving $\Theta_{ij}^{(l)}$, we can obtain higher level feature $a^{(t)} = \{a_1, a_2, ..., a_\tau\}$ from the input $x^{(t)}$ by computing

$$a_i^{(t)} = \psi \left(\sum_{j=1}^{n} \Theta_{ij}^{(1)} x_j^{(t)} + \gamma_i^{(1)} \right) \tag{6}$$

where $\psi(x)$ is an activation function, which can be sigmoid or threshold function. However, it is better to use characteristic learning to achieve higher level features instead of trivial learning raw data.

3 Learning Higher Level Features from Correlated Characteristic Data

We propose a new method at unsupervised learning phase to achieve higher level features having specific characteristics. Our proposed method is inspired by achievement in neuroscience. It shows that human brains have many different cortex areas to process the perceived outside world information. Each cortex area processes information which is highly correlated with each other [8]. Therefore we make an assumption that higher level features can be learnt better if data has highly correlated characteristics. Because in original method using sparse autoencoder, all data are used to train just one sparse autoencoder to get higher level features. This original approach is not taking the advantages of specific characteristics of data. Moreover our observation shows that handwritten digits are combined by primitive strokes such as straight strokes and curve. Each handwritten digit has specific characteristics which are different from other digits. For example, 1 and 7 digits are mostly combined by straight strokes. Meanwhile, 3 and 8 digits are mostly combined by curve strokes. So our proposed method has two phases:

- Clustering correlated characteristic of data.
- Learning higher level features.

The first phase is correlated characteristics data clustering. Let ξ be a characteristic set. In particular, with handwritten digit recognition problem, we can define three characteristic sets. ξ_1 is a characteristic set that digits are mostly combined by straight strokes. ξ_2 is a characteristic set that digits are mostly combined by curve strokes. ξ_3 is a characteristic set that digits are combined by both straight and curve strokes. Samples which satisfy one of characteristics in ξ belong to a same set described as follow

$$E_i = \{x \in D | \varphi(x) \in \xi_i\} \tag{7}$$

where E_i is an entity set containing samples which satisfy one of characteristics in ξ_i; D is our dataset and x is a sample of D. $\varphi(x) : \mathbb{R}^n \to \xi$ is a mapping function which maps a sample to characteristics. In this work, we define the mapping function based on statistic of human reception on straight and curve characteristics. This can help us verify that the method resembling human visual receptive fields. The experimental section (Sect. 4) describes how to define characteristic and entity sets in detail. Suppose we divide data into k entity sets, k sparse autoencoders need to be trained separately to learn weight matrix $\Theta_{ij}^{(l)}$ and biased weight $\gamma_i^{(l)}$ (mentioned in Sect. 2) from these entity sets. After weight matrix and biased weight are learnt, higher level features can be computed from data samples. Figure 2 visualizes this clustering phase generally.
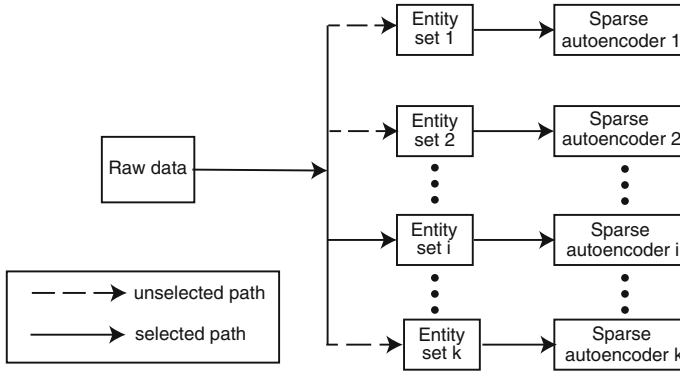
Fig. 2 Clustering correlated characteristic of data

After trained all sparse autoencoders, we move to higher level features learning phase as shown in Fig. 3. At this phase, one data sample is put into all trained sparse autoencoders to compute higher level features $a^{(t)} = \{a_1, a_2, ..., a_\tau\}$ (mentioned in Sect. 2). As a result, k sparse autoencoders output k higher level feature vectors. At last, the final higher level feature vector is generated by concatenating these k higher level feature vectors.

$$f_{final} = [f_1 f_2 ... f_k] \qquad (8)$$

where f_i, $i = 1, 2, ..., k$ is the τ dimensions higher level feature vector outputted by ith sparse autoencoder. f_{final} is the $k \times \tau$ dimensions higher level feature vector used for supervised learning and testing phase.

At supervised learning and testing phase, we first get the final higher level features described as above from raw data and then these feature vectors are inputs for softmax regression algorithm to classify digits.
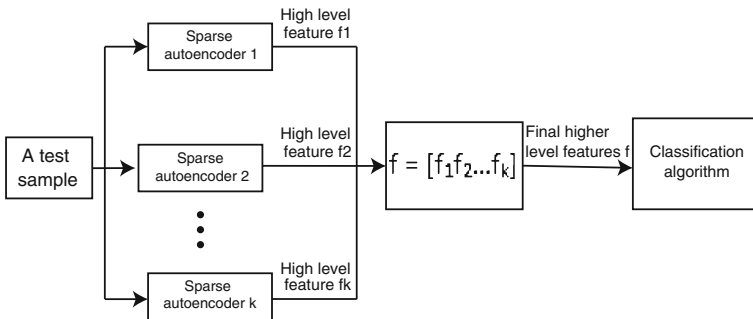

Fig. 3 Learning higher level features

4 Experiments and Results

We conduct two experiments on MNIST dataset to evaluate the classification error rates of our proposed method at many various definition ways of characteristic sets. In our two experiments, 60,000 samples are used for training and 10,000 samples for testing. As mentioned in Sect. 3, there are three basic characteristic sets such as ξ_1 is a characteristic set that digits are mostly combined by straight strokes; ξ_2 is a characteristic set that digits are mostly combined by curve strokes and ξ_3 is a characteristic set that digits are combined by both straight and curve strokes. Based on our observed characteristics of handwritten digits, we divide these digits into three basic entity sets corresponding to 3 characteristic sets above. The samples which have the labels {1, 4, and 7} belong to the first entity set. These digits satisfy characteristics of the characteristic set ξ_1. Similarly, the samples which have the labels {0, 2, 3, 6, and 8} belong to the second entity set because they satisfy characteristics of ξ_2. Lastly, the samples which have the labels {5 and 9} belong to the third entity set which corresponding to characteristic set ξ_3.

4.1 Evaluate the Performance on Two Characteristic Sets

In this experiment, we define only two characteristic sets and they are not as distinct as three characteristic sets above. Concretely, ξ_1 is a characteristic set that digits are mostly combined by straight strokes or both straight and curve strokes; ξ_2 is a characteristic set that digits are mostly combined by curve strokes or both straight and curve strokes. Thus, there are two entity sets satisfy these two characteristic sets. The first entity set contains the samples having the labels {1, 4, 7, 5, and 9} and the second entity set contains the samples having the labels {0, 2, 3, 6, 8, 5 and 9}. In our proposed method, we in turn set the number of hidden neurons of each sparse autoencoder (denoted as # HNeurons per SA) at various values $\tau = 50, 100, 200, 300$. The purpose is to evaluate the effect of the number of hidden neurons on classification performance. Because there are two trained sparse autoencoders corresponding to two entity sets so with each sample, we get the higher level feature with $2 \times \tau$ dimensions. On the other hand, the original method just uses one sparse autoencoder to learn higher level features. So we in turn set the number of hidden neurons $\tau = 100, 200, 400, 600$. As a result, the original method and our proposed method yield the higher level feature vectors as the same dimension such as 100, 200, 400 and 600.

Table 1 shows the comparison of the classification error rates between the original sparse autoencoder and our proposed method. Obviously, when the number of hidden neuron of each sparse autoencoder in our proposed method is still small (i.e $\tau = 50$) then the error rate higher than the error rate of original method at the same dimension. Particularly, when we use 100 dimensions final higher level feature vector, the error rate of our proposed method ($\tau = 50$) is 5.24 and it is higher than 4.67 which is the error rate of the original method ($\tau = 100$). However, when the number of hidden

Table 1 Error rates (%) of the original sparse autoencoder and our proposed method

Original sparse autoencoder		Our proposed method	
# HNeurons per SA	Error rates (%)	# HNeurons per SA	Error rates (%)
100	4.67	50 (100)	5.24
200	3.28	100 (200)	**3.25**
400	2.76	200 (400)	**2.59**
600	2.62	300 (600)	**2.37**

In this case, we use two sparse autoencoders corresponding two characteristic sets
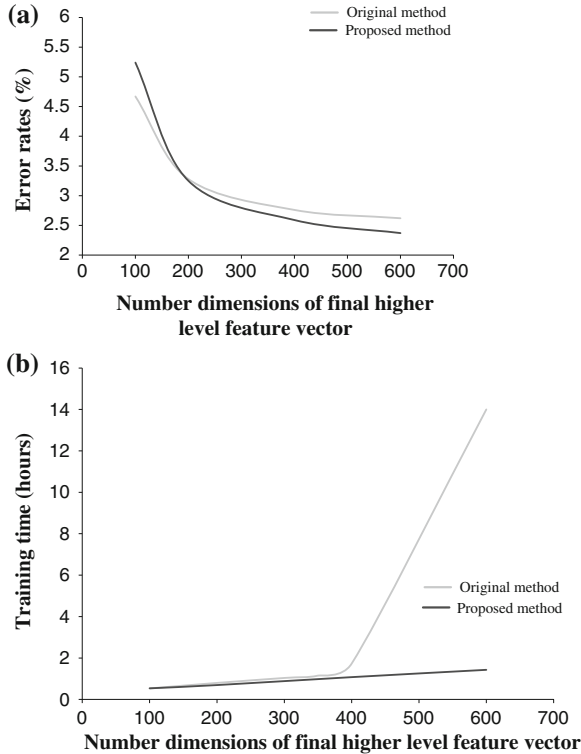
Fig. 4 Error rates (%) and training times (hours) of original method and proposed method in experiment 4.1. **a** Error rates (%). **b** Training time (hours)

neurons increases then the error rate of proposed method is lower than the original method (as shown in Fig. 4a).

Because of reducing the number of hidden neurons of each sparse autoencoder, our proposed method decreases the training time. Figure 4b and Table 2 shows that the training time of our proposed method is much more lower than the original method when we increase the number of hidden neurons. This experiment measures these time on computer CPU Intel core TM Quad CPU Q9400 2.66 GHz.

Table 2 Training time of original method and our proposed method with two characteristic sets

Original sparse autoencoder		Our proposed method	
# HNeurons per SA	Training time (hours)	# HNeurons per SA	Training time (hours)
100	0.532	50 (100)	0.37
200	0.789	100 (200)	**0.694**
400	1.429	200 (400)	**1.077**
600	14	300 (600)	**1.43**

4.2 Evaluate the Performance on Three Distinct Characteristic Sets

We define characteristic sets more distinct from each other than Sect. 4.1. We use three basic characteristic sets as described in Sect. 3. Recall shortly that three characteristic sets are straight, curve and "both straight and curve". Consequently, three entity sets are defined: entity set E_1 contains samples which have the labels {1, 4, and 7}; E_2 contains samples which have the labels {0, 2, 3, 6, and 8} and {5 and 9} for E_3.

As shown in Table 3 is the classification error rates in experiment 4.2. As the same with the result in the experiment 4.1, the error rates decrease gradually when the number of hidden neurons of each autoencoder increases. Table 4 shows that the error rates of three characteristic sets are lower than the error rates of two characteristic sets at the same dimension of final higher level features. It means that the more we define distinct characteristic sets, the more the error rates decrease.

Figure 5 visualizes the learnt weights from original method and Fig. 6 visualizes learnt weights from three sparse autoencoders corresponding to three characteristic sets in experiment 4.2. We can see that visualization of learnt weights in Fig. 6 have specific characteristics such as straight, curve and both straight and curve. On the other hand, the visualized weights of original method do not have any explicit characteristics. And Table 5 shows the comparison between other similar methods.

Table 3 Error rates (%) of proposed method with three characteristic sets in experiment 2

# HNeurons per SA	100 (300)	133 (399)	200 (600)	300 (900)	500 (1500)
Error rate (%)	2.79	2.52	2.32	2.2	1.94

Table 4 Error rates (%) of the original sparse autoencoder and our proposed method

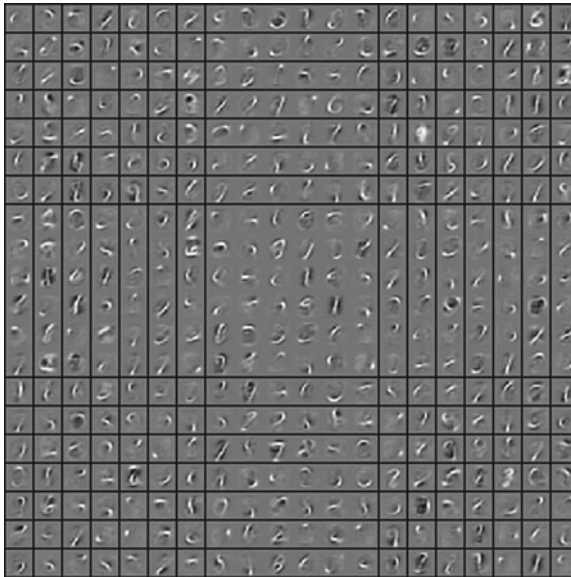| Our proposed method with 2 less distinct characteristic sets		Our proposed method with three more distinct characteristic sets	
# HNeurons per SA	Error rates (%)	# HNeurons per SA	Error rates (%)
200 (400)	2.59	133 (399)	**2.52**
300 (600)	2.37	200 (600)	**2.32**

Fig. 5 Visualization of learnt weights from original method

Table 5 Error rates (%) comparison with other similar methods

Error rates (%)		
Linear SVM + Sparse coding	Linear SVM + Local Coordinate coding [18]	Our proposed method for sparse autoencoder
2.16	2.08	1.94

Our method use less basic points (1,500) than these sparse coding and local coordinate coding (2,048) but it achieves lower error rates.

5 Conclusion

The proposed method takes the advantages of specific characteristics of data for learning higher level features using sparse autoencoder. Our proposed method achieves better performance and lower time complexity than the original method on MNIST dataset. The most notable thing is that the more we define distinct characteristic sets from each other, the more the error rates decrease. In future work, we will build an algorithm to learn specific characteristics of data automatically.
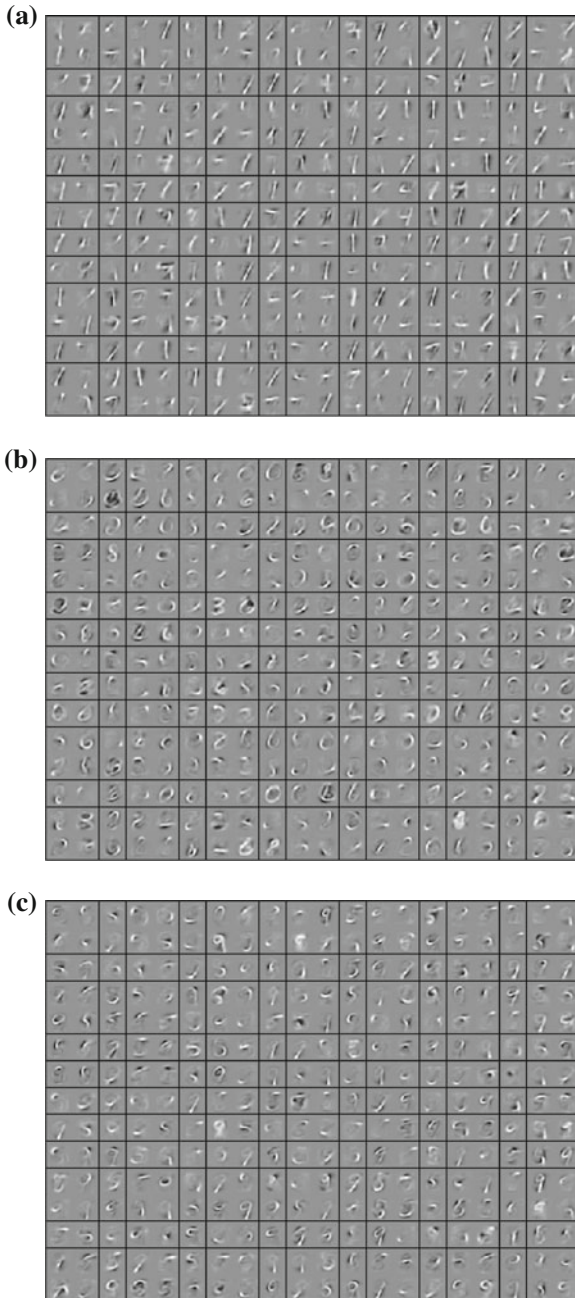
(a)

(b)

(c)

Fig. 6 Visualization of learnt weights from three sparse autoencoders corresponding to three characteristic sets in experiment 4.2. **a** Only straight strokes. **b** Only curve strokes. **c** Both straight and curve strokes

References

1. Bagnell, J.A., Bradley, D.M.: Differentiable sparse coding. In: NIPS. pp. 113–120 (2008)
2. Dalal, N., Triggs, B.: Histograms of oriented gradients for human detection. In: CVPR. vol. 1, pp. 886–893 (2005)
3. DeCoste, D., Schölkopf, B.: Training invariant support vector machines. Mach. Learn. **46**(1–3), 161–190 (2002)
4. Grosse, R., Raina, R., Kwong, H., Andrew, Y.Ng.: Shift-invariance sparse coding for audio classification. CoRR, abs/1206.5241, 2012.
5. Hinton, G., Salakhutdinov, R.: Reducing the dimensionality of data with neural networks. Science **313**(5786), 504–507 (2006)
6. Hinton, G.E., Osindero, S., Teh, Y.W.: A fast learning algorithm for deep belief nets. Neural Comput. **18**(7), 1527–1554 (2006)
7. Lennig M., Hunt, M., Mermelstein, P.: Experiments in syllable-based recognition of continuous speech. In: Proceedings of International Conference on Acoustics, Speech and, Signal Processing, pp. 880–883 (1996)
8. Huth, A.G., Gallant, J.L., Vu, A.T., Nishimoto, S.: A continuous semantic space describes the representation of thousands of object and action categories across the human brain. Neuron **76**(6), 1210–1224 (2012)
9. LeCun, Y., Bottou, L., Bengio, Y., Haffner, H.: Gradient-based learning applied to document recognition. In: Proceedings of the IEEE. vol. 86, pp. 2278–2324 (1998)
10. Lee, H., Battle, A., Raina, R., Andrew, Y.Ng.: Efficient sparse coding algorithms. In: Advances in Neural Information Processing Systems. vol. 19, pp. 801–808 (2007)
11. Lee, H., Grosse, R., Ranganath, R., Andrew, Y.Ng.: Convolutional deep belief networks for scalable unsupervised learning of hierarchical representations. In: ICML. p. 77 (2009)
12. Lowe, D.G.: Distinctive image features from scale-invariant keypoints. Int. J. Comput. Vision **60**(2), 91–110 (2004)
13. Martens, J.: Deep learning via hessian-free optimization. In: Fürnkranz, J., Joachims, T.,(eds.) Proceedings of the 27th International Conference on Machine Learning (ICML-10), Haifa, Israel, pp. 735–742 June 2010
14. Olshausen, B.A., Field, D.J.: Emergence of simple-cell receptive field properties by learning a sparse code for natural images. Nature **381**, 607–609 (1996)
15. Raina, R., Battle, A., Lee, H., Packer, B., Andrew Y.Ng.: Self-taught learning: Transfer learning from unlabeled data. In: ICML '07: Proceedings of the 24th International Conference on, Machine learning (2007)
16. Simard, P., Steinkraus, D., Platt, J.C.: Best practices for convolutional neural networks applied to visual document analysis. In: ICDAR, pp. 958–962 (2003)
17. Socher, R., Eric, H., Pennin, J., Andrew, Y.Ng, Manning, C.D.: Dynamic pooling and unfolding recursive autoencoders for paraphrase detection. In: Shawe-Taylor, J., Zemel, R.S., Bartlett, P., Pereira, F.C.N., Weinberger, K.Q., (eds.) Proceeding of 24th Advances in Neural Information Processing Systems, pp. 801–809 (2011)
18. Kai. Y., Zhang, T., Gong, Y.: Nonlinear learning using local coordinate coding. In: Bengio, Y., Schuurmans, D., Lafferty, J.D., Williams, C.K.I., Culotta, A. (eds.) Proceeding of 24th Advances in Neural Information Processing Systems, NIPS, pp. 2223–2231 (2009) (Curran Associates Inc.)

Fuzzy Single-Stroke Character Recognizer with Various Rectangle Fuzzy Grids

Alex Tormási and László T. Kóczy

Abstract In this chapter we introduce the results of a formerly published FUBAR character recognition method with various fuzzy grid parameters. The accuracy and efficiency of the handwritten single-stroke character recognition algorithm with different sized rectangle ($N \times M$) fuzzy grids are investigated. The results are compared to other modified FUBAR algorithms and known commercial and academic recognition methods. Possible applications and further extensions are also discussed. This work is the extended and fully detailed version of a previously published abstract.

Keywords Fuzzy logic · Fuzzy systems · Fuzzy grid · Single-stroke character recognition

1 Introduction

These days' tablets, netbooks and notebooks with touch screen are more popular than any other types of computers. In some cases the use of physical keyboards in portable devices are circumstantial or not possible at all. Handwriting recognition systems may replace keyboards. Processing written text by computers nevertheless has a long history. In this field there are still many ongoing research and development projects aiming to achieve more accurate and efficient recognition of handwriting. In her study LaLomia determined 97 % as the general user acceptance rate for handwriting recognizers [1].

A. Tormási (✉) · L. T. Kóczy
Department of Automation, Széchenyi István University, Györ, Hungary
e-mail: tormasi@sze.hu

L. T. Kóczy
Department of Telecommunications and Media Informatics, Budapest University
of Technology and Economics, Budapest, Hungary
e-mail: koczy@sze.hu; koczy@tmit.bme.hu

After the introduction in this chapter the basic steps of the original FUBAR (Fuzzy Based Recognition) algorithm [2] with various parameter optimizations [3] will be shown. The results of the study on rectangle fuzzy grids are detailed in Sect. 3 [4]. Formerly published versions of the FUBAR method based on the optimal sized rectangle fuzzy grid are shortly summarised in Sect. 4 [5, 6]; which is followed by the comparison of the results with previous versions of FUBAR character recognizer and other known recognition algorithms with the planned further works in Sect. 5 [7–10].

2 Basic Concept of the Original Recognition Algorithm

2.1 Overview

Creating a personalized (user-dependent), accurate, fast and extensible recognition engine was the main goal during the design of the FUBAR method. The segmentation of multiple strokes was not considered as part of the designed method to simplify the problem universe and focus only on the recognition engine itself. This decision led to the use of a modified version of Palm's Graffiti [11] single-stroke alphabet. The concept of Graffiti symbols is simple: each English letter is assigned to a single-stroke gesture which is a simplified version of the symbol (Fig. 1).

Since the design of Graffiti is based on mainly English users, we decided to change the strokes for the letter "G" and "U" in order to have a stroke-set more similar to Hungarian writing style (Fig. 2).

Fig. 1 The original Graffiti alphabet

Fig. 2 Changes applied to Graffiti symbols in FUBAR
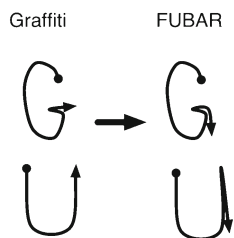
To define minimal constraints regarding the representation (e.g. size and angle) of the strokes a decision was made to use such methods which are able to handle the variance of the writing-styles of the symbols.

The number of sampled points is not fixed in the designed algorithm, it may vary for the same symbol for different samples, which means that a method based on point-to-point comparison of the input symbol with the stored etalon letter are not eligible solutions.

Extracting complex stroke-features such as loops, circles and turns could be time and resource consuming and may return in a less responsive system. Too long response time may also have effect on the user's performance. The use of parameters which are easy to calculate was favoured during the design of the algorithm. This consideration led to use stroke-features extracted from properties of grids drawn around the strokes.

The use of artificial neural networks was ruled out because the symbol-set must be fixed or the addition or removal of a given symbol may change the complete structure of the network.

With fuzzy sets and systems [12] it is easy to represent stroke-parameters mentioned previously and store the "knowledge" describing the alphabet.

To adopt and learn user-specific writing-style the method uses an evolutionary method [13], namely bacterial evolutionary algorithm [14] extended to handle problem-specific constraints. During the tests the adaptation phase was disabled, because its stochastic behaviour could influence the results.

The concept of the designed recognition method with feature extraction grid and fuzzy rule-based inference mechanism is shown in Fig. 3.
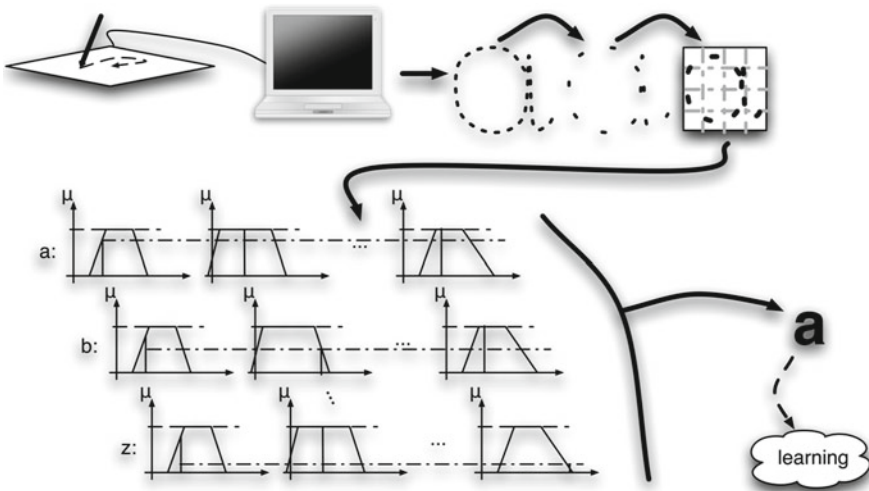

Fig. 3 Basic concept of the designed method
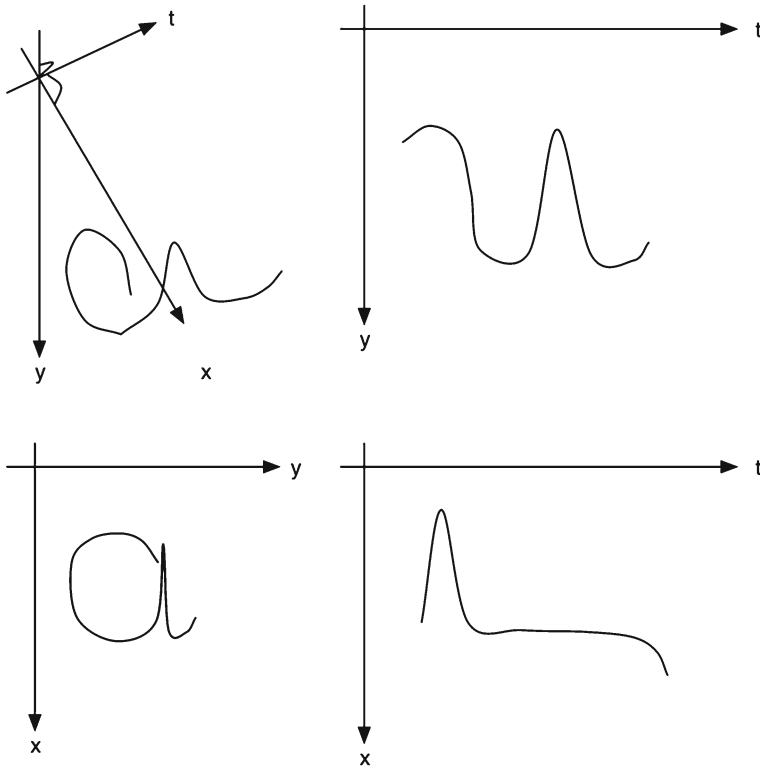
Fig. 4 Example: signal of lowercase letter "a"

2.2 Input

Each individual stroke could be represented as a three-dimensional continuous signal sampled by the digitizer tablet (Fig. 4).

The system collects all the coordinates in chronological order representing the pen movement (digital ink). The application is not able to collect each point of the signal causing gaps between the sampled points. The distance between the collected points depends on the writing speed and the available resources (CPU, BUS speed etc) in the computer.

The varying distance between points or stroke-parts renders more difficulty in recognizing the stroke by the average density of points in the extraction grid.

2.3 Pre-processing

Before further steps are taken to the input, it has to be conditioned by re-sampling in order to achieve an almost equal distance between the sampled points of the input signal. In a previously presented chapter it has been shown that the optimal

minimum Euclidean distance between the neighbour sampled points in our testing environment is 6 pixels. The first and last elements of the strokes are also stored (as reference points).

Another advantage of re-sampling process is its anti-aliasing functionality; it is capable to decrease the level of the noise (arose during the writing) or even remove it from the stroke.

Some pre-calculations are also made in order to calculate the aspect ratio of the stroke and to determine the size and position of the fuzzy grid drawn around it.

2.4 Feature Extraction

The algorithm uses two kinds of features; the first kind is the width/height ratio of the input stroke; the second kind of parameters is the average fuzzified number of points in a given row or column of the fuzzy grid.

The very first version of the algorithm used simple grid (with sharp borders), but the italic writing style of the letters decreased the accuracy of the system. Most of other known recognition methods are rotating the stroke, which is resource consuming. As a solution to the oblique writing problem a grid with blurred boundaries has been developed, which will be referred to as fuzzy grid (each grid column and row is defined by a fuzzy set). Assuming a situation where a stroke-point is located close to a border of the grid, it will be counted as a member of either columns or rows with different membership degrees (Fig. 5).

Fig. 5 Fuzzy grid example with lowercase letter "a"
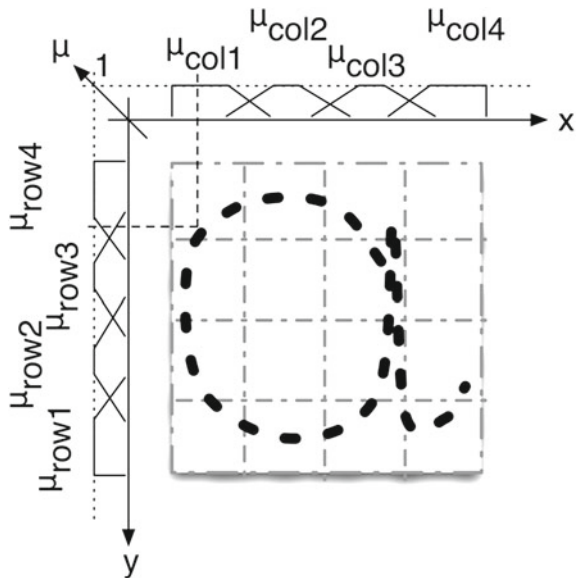
2.5 Inference

Each symbol in the alphabet is represented by only one single fuzzy rule [15, 16]. Previously collected stroke-features are used as input parameters for the fuzzy rules. The consequent part of the rules represents the degree of matching the parameters of the input stroke and the parameters of the symbol represented by the given rules. For inference a Takagi-Sugeno method was used with discrete outputs. The rule with the highest matching value will be chosen as the result of the system.

The trapezoid fuzzy sets of the rule input parameters are calculated statistically from 60 previously collected samples.

The algorithm has the capability of learning the user-specific writing via a modified bacterial evolutionary algorithm with "punish/reward" extension, but due to its nondeterministic effects on the recognition rate it has been disabled during the tests.

2.6 Various Parameter Optimizations for N × N Fuzzy Grids

In a formerly published work the study of various parameters were investigated in order to reach higher accuracy or lower computational time [3]; the search for optimal size of N × N fuzzy grids was also part of this work. The results showed that the recognition rate for the 5×5 fuzzy grid with minimum 6 pixels point-distance was 97.67 %, which is less than the results of the method with 4×4 and 6×6 fuzzy grids with the same minimum distance. This is caused by the characteristics of the re-sampled points and the fuzzy grids; the optimal size of the fuzzy grid based on the average recognition rate is not the optimal grid size for individual symbols.

The best average recognition rate (99.42 %) was achieved with a 6×6 fuzzy grid and minimum 6 pixels distance between points. The average recognition rates of FUBAR with various parameter values (N_g stands for number of rows and columns in grid, N_d is the minimal distance between re-sampled points) are presented in Table 1.

3 Size Optimization for N × M Fuzzy Grids

3.1 Concept

The main goal of this study was to find the optimal row and cell number for fuzzy grids to collect parameters from the input stroke. Previous results for N × N fuzzy grids showed that some symbols may reach higher individual accuracy using fuzzy grids with a size different from the overall optimal size. According to a detailed analysis of the parameter variance of sample-strokes the system may reach a higher recognition rate and lower computational time by the use of fuzzy grids with rectangular cells (rectangle fuzzy grids).

Table 1 Average recognition rates of FUBAR with various parameter values

Symbol	Recognition rate (%)					
	$N_g = 4, N_d = 6$	$N_g = 5, N_d = 6$	$N_g = 6, N_d = 6$	$N_g = 8, N_d = 6$	$N_g = 10, N_d = 6$	$N_g = 16, N_d = 6$
a	100	99.4444	100	98.3333	99.4444	77.2222
b	90.5555	94.4444	95.5555	95.5555	97.7777	93.3333
c	99.4444	97.2222	99.4444	99.4444	92.7777	98.8888
d	82.2222	98.8888	98.3333	100	99.4444	96.6666
e	96.6666	98.8888	99.4444	100	97.7777	98.8888
f	100	100	100	100	100	100
g	100	100	100	100	100	100
h	100	100	100	100	100	100
i	97.777	97.777	97.7777	97.7777	97.7777	97.7777
j	100	100	100	100	100	100
k	98.8888	99.4444	100	100	99.4444	99.4444
l	98.8888	100	100	100	100	100
m	100	100	100	100	100	100
n	100	100	100	100	100	100
o	91.6666	96.1111	97.7777	89.4444	80	94.4444
p	100	100	100	100	100	97.7777
q	96.6666	95.5555	98.8888	98.8888	97.7777	97.7777
r	96.6666	96.1111	98.3333	98.3333	87.7777	87.7777
s	96.6666	79.4444	100	96.1111	98.8888	98.3333
t	100	100	100	100	100	100
u	100	100	100	100	100	100
v	100	100	100	100	100	94.4444
w	100	99.4444	100	100	98.8888	100
x	96.1111	93.3333	99.4444	96.6666	96.1111	97.2222
y	100	100	100	100	100	100
z	100	93.3333	100	100	100	98.8888
Average	97.7778	97.6709	**99.4231**	98.8675	97.8419	97.2649

For the modified method the same data were used as in the original system tests. The 180 samples per symbol were collected from 12 test subjects selected from the students of the Széchenyi István University. The initial rule-base was built from the first 60 samples (per symbol) using statistical methods to construct the fuzzy sets describing the rule input parameters.

The system is designed to process and learn user-specific handwriting, but we decided to use a more general symbol set to calculate the initial rule-base; during the first run of the system it does not have a personalized model of the alphabet, so the algorithm could recognize various handwriting styles with a good-enough initial accuracy before the learning process optimizes the parameters to describe the user-specific parameters.

The results of this optimization were originally presented as a short abstract at The Eighth Conference of Ph.D. Students in Computer Science [4].

3.2 Accuracy

The average recognition rates for is different N × M fuzzy grids are shown in Table 2.

Average letter-wise recognition rates are listed in Table 3.

The highest average recognition rate of the system is 99.23 % with rectangle (6 columns and 4 rows) fuzzy grids. It is 0.19 % less than the recognition rate achieved by the method with squared cells (99.42 %, 6 rows and 6 cells).

3.3 Efficiency

The computational cost of the system during the rule evaluation was decreased due to the reduced number of rule input parameters. The system with a 6 × 6 fuzzy grid recognizes 9,942 from 10,000 input symbols (99.42 %) for the cost of 3,380,000 fuzzifications, the same system with a fuzzy grid containing 6 columns and 4 cells recognizes only 9,923 from 10,000 symbols; but considering the results from the point of view of the computational cost, the modified system with rectangular cells recognizes 11,727 letters from 11,818 for 3,379,948 fuzzifications; which is less computation and more recognized symbols, than seen in the original method.

4 Results of Previous Versions of FUBAR

4.1 Rule Input Parameter Weighting

There are numerous works on different fuzzy rule and antecedent weighting methods and applications with promising results especially in classification problems [17–19]. The results introduced in the previously mentioned chapters showed that

Table 2 Average recognition rates of FUBAR for various NxM fuzzy grids

Number of rows in fuzzy grid	Number of columns in fuzzy grid							
	3 (%)	4 (%)	5 (%)	6 (%)	7 (%)	8 (%)	9 (%)	10
3	x	95.09	98.14	98.74	98.61	98.57	98.44	98.61
4	97.82	x	98.31	99.23	99.08	98.87	98.50	98.38
5	97.05	96.99	x	98.70	98.72	98.57	98.18	98.50
6	97.54	96.62	97.97	x	98.53	98.53	97.99	98.38
7	96.69	96.00	97.63	97.98	x	97.80	97.65	97.99
8	96.11	96.35	97.22	98.21	97.54	x	97.48	97.26
9	96.62	96.54	97.71	98.21	98.29	98.08	x	98.29
10	94.98	95.81	96.88	98.38	97.71	97.78	97.65	x

Table 3 Average accuracy of FUBAR for the optimal NxN and NxM sized fuzzy grids

| Symbol | Recognition rate (%) | |
	6 × 6 FUBAR	6 × 4 FUBAR
A	100	98.3333
B	95.5555	95.5555
C	99.4444	99.4444
D	98.3333	100
E	99.4444	100
F	100	100
G	100	100
H	100	100
I	97.7777	97.7777
J	100	100
K	100	100
L	100	100
M	100	100
N	100	100
O	97.7777	89.4444
P	100	100
Q	98.8888	98.8888
R	98.3333	98.3333
S	100	96.1111
T	100	100
U	100	100
V	100	100
W	100	100
X	99.4444	96.6666
Y	100	100
Z	100	100
Average	***99.42 %***	99.23 %

the accuracy of the designed recognition method could be increased by the weighting of the different input-parameters for each rule according to their reliability value.

Considering the previous researches, the computational complexity and the accuracy of the method, a recognizer with a 6 × 4 fuzzy grid have been chosen as the basic system for the improvement. With weighted rule input parameters the same system with a 6 × 4 fuzzy grid has a 99.49 % average recognition rate. The symbol-wise average recognition rates of FUBAR with a weighted "D", "K", "O" and "X" symbols are shown in Table 4.

4.2 Hierarchical Rule-Base

The number of evaluated rules during the inference phase in fuzzy systems could be decreased by the use of hierarchical rule-bases [20–22].

Table 4 Comparing the accuracy of FUBAR algorithms with 6x4 fuzzy grid after rule weighting

Symbol	Recognition rate (%)		
	6×6 FUBAR	6×4 FUBAR	6×4 FUBAR weighted
A	100	100	100
B	95.5555	92.7778	92.7778
C	99.4444	97.7778	97.7778
D	98.3333	98.8889	99.4444
E	99.4444	98.8889	98.8889
F	100	100	100
G	100	100	100
H	100	100	100
I	97.7777	100	100
J	100	100	100
K	100	99.4444	100
L	100	100	100
M	100	100	100
N	100	100	100
O	97.7777	93.8889	98.8889
P	100	100	100
Q	98.8888	100	100
R	98.3333	100	99.4444
S	100	100	100
T	100	100	100
U	100	100	100
V	100	100	100
W	100	100	100
X	99.4444	98.3333	99.4444
Y	100	100	100
Z	100	100	100
Average	99.42 %	99.23 %	***99.49 %***

The 98.82 % recognition rate was achieved by FUBAR with a hierarchical rule-base which is lower than the average accuracy of the original system but it still reaches the user acceptance threshold and the decrease in the computational costs of the recognition was more than the decrease in the recognition rate [6]. The average recognition rates of FUBAR with a hierarchical rule base built from Row3 parameter are shown in Table 5.

5 Conclusions and Future Work

With 6×4 (optimal sized rectangle) fuzzy grids the average recognition rates were decreased. The accuracy of the system dropped to 99.23 %; but as we have shown in Sect. 3 the system has a lower computational time, which was also a main goal

Table 5 Comparing the accuracy of various FUBAR algorithms

Symbol	Recognition rate (%)			
	6 × 6 FUBAR	6 × 4 FUBAR	6 × 4 FUBAR weighted	6 × 4 FUBAR hierarchical
A	100	98.3333	99.4444	77.2222
B	95.5555	95.5555	97.7777	93.3333
C	99.4444	99.4444	92.7777	98.8888
D	98.3333	100	99.4444	96.6666
E	99.4444	100	97.7777	98.8888
F	100	100	100	100
G	100	100	100	100
H	100	100	100	100
I	97.7777	97.7777	97.7777	97.7777
J	100	100	100	100
K	100	100	99.4444	99.4444
L	100	100	100	100
M	100	100	100	100
N	100	100	100	100
O	97.7777	89.4444	80	94.4444
P	100	100	100	97.7777
Q	98.8888	98.8888	97.7777	97.7777
R	98.3333	98.3333	87.7777	87.7777
S	100	96.1111	98.8888	98.3333
T	100	100	100	100
U	100	100	100	100
V	100	100	100	94.4444
W	100	100	98.8888	100
X	99.4444	96.6666	96.1111	97.2222
Y	100	100	100	100
Z	100	100	100	98.8888
Average	99.42%	99.23%	***99.49%***	***98.82%***

during the design. The results also revealed that the individual accuracy of symbols could be increased with the use of rectangle fuzzy grids. With this information in our minds we decided to use 6×4 fuzzy grids as default grid size as the basis of further works.

The first extended version of the FUBAR method with rectangle fuzzy grids used weighted rule antecedents to improve the average recognition rate of the algorithm. The system with 6×4 fuzzy grid and 4 symbols with weighted antecedents reached 99.49 % accuracy, which is higher than the average recognition rate achieved by the algorithm with 6×6 fuzzy grid. The weights were fixed and calculated according to the data extracted from the same sample set used to build the initial rule-base. This means that, the use of weights did not increase the computational complexity of the algorithm.

Another study was investigating the effects to accuracy and efficiency of the same system with hierarchical rule-base instead of linear. The algorithm used 6×4 fuzzy

grids and a hierarchical rule-base constructed according to only one feature. The best results were achieved by the system with a rule-base based on parameter "*Row3*". The average recognition rate was decreased to 98.82 %, which is still over the 97 % user acceptance threshold [ct. 1], but much lower than the previous results of the system. Despite the low recognition rate, the algorithm needed much less computational time due to the reduced number of the rules to evaluate.

The results of other known commercial system, academic algorithms and FUBAR methods with various modifications applied to the algorithm are shown in Fig. 6.

Each version of the FUBAR algorithm is handling 26 different single-stroke symbols without the use of dictionaries, learning or predictive methods.

The results for Palm's Graffiti single-stroke recognition algorithm are from the study of Fleetwood et al. [7]. They stated that the average recognition rate for Palm's Graffiti was 91 %; and 98 % for the virtual keyboard of the same device.

Graffiti 2 was the extended version of Graffiti in which the letters "i", "t" and "x" could be written with multiple strokes. The accuracy of Graffiti 2 was investigated in the study of Költringer and Grechenig [8] in which the algorithm reached 86.03 % recognition rate.

The $1 algorithm was presented by Wobbrock et al. [9]. The method reached 97 % average recognition rate for 16 different single-stroke gestures.

As an improved, multi-stroke version of $1 algorithm Anthony and Wobbrock presented $N method, which reached 93.7 % average recognition rate for 20 multi-stroke symbols [10].

The FUBAR system with different modifications in most cases reached recognition rates which are well over 97 % user acceptance threshold defined by LaLomia [ct. 1] and in most of the cases it has outstanding results in recognition rate and computational complexity compared to other recognizers.

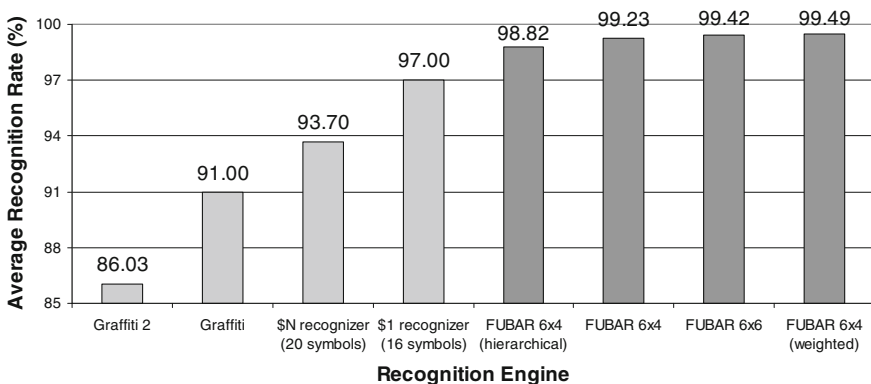We have plans to create rule-base for different alphabets such as old Hungarian runes and Greek letters.

Fig. 6 Average recognition rates of various recognition algorithms

Another extension for the system is under development to optimize the rule-base and the shape of fuzzy grids with evolutionary algorithms to improve the accuracy of the system.

Advantages will be also investigated for the application of different dictionary-like and predictive methods to give the system a capability of context-based decision making.

References

1. LaLomia, M.J.: User acceptance of handwritten recognition accuracy. Companion Proceedings CHI '94, New York, p. 107 (1994)
2. Tormási, A., Botzheim, J.: Single-stroke character recognition with fuzzy method. In: Balas, V.E. et al. (eds.) New Concepts and Applications in Soft Computing SCI, vol. 417, pp. 27–46 (2012)
3. Tormási, A., Kóczy, L.T.: Comparing the efficiency of a fuzzy single-stroke character recognizer with various parameter values. In: Greco, S. et al. (ed.) Proceedings of IPMU, : Part I. CCIS, vol. 297, pp. 260–269 (2012)
4. Tormasi, A., Kóczy, L.T.: Efficiency and accuracy analysis of a fuzzy single-stroke character recognizer with various rectangle fuzzy grids. In: Proceedings of CSCS '12, Szeged, pp. 54–55 (2012)
5. Tormási, A., Kóczy, L.T.: Improving the accuracy of a fuzzy-based single-stroke character recognizer by antecedent weighting. In: Proceedings of 2nd World Conference on Soft Computing, Baku, pp. 172–178 (2012)
6. Tormási, A., Kóczy, L.T.: Improving the efficiency of a fuzzy-based single-stroke character recognizer with hierarchical rule-base. In: Proceedings of 13th IEEE International Symposium on Computational Intelligence and Informatics, Óbuda, pp. 421–426 (2012)
7. Fleetwood, M.D. et al.: An evaluation of text-entry in palm OS–Graffiti and the virtual keyboard. In: Proceedings of HFES '02, Santa Monica, CA, pp. 617–621 (2002)
8. Költringer, T., Grechenig, T.: Comparing the immediate usability of graffiti 2 and virtual keyboard. In: Proceedings of CHI EA '04, New York, pp. 1175–1178 (2004)
9. Wobbrock, J.O., Wilson, A.D., Li, Y.: Gestures without libraries, toolkits or training: a 1 recognizer for user interface prototypes. In: Proceedings of UIST '07. ACM Press, New York, pp. 159–168 (2007)
10. Anthony, L., Wobbrock, J.O.: The N multi-stroke recognizer. In: Proceedings of GI'10, Ottawa, pp. 245–253 (2010)
11. Butter, A., Pogue, D.: Piloting Palm: The Inside Story of Palm, Handspring, and the Birth of the Billion-Dollar Handheld Industry. Wiley, New York (2002)
12. Zadeh, L.A.: Fuzzy sets. Inf. Control **8**, 338–353 (1965)
13. Holland, J.H.: Adaption in Natural and Artificial Systems. The MIT Press, Cambridge (1992)
14. Nawa, N.E., Furuhashi, T.: Fuzzy system parameters discovery by bacterial evolutionary algorithm. IEEE Trans. Fuzzy Syst. **7**(5), 608–616 (1999)
15. Mamdani, E.H., Assilian, S.: An experiment in linguistic synthesis with a fuzzy logic controller. Int. J. Man Mach. Stud. **7**(1), 1–13 (1975)
16. Takagi, T. Sugeno, M.: Fuzzy identification of systems and its applications to modeling and control. IEEE Trans. Syst. Man Cybern. SMC-15, 116–132 (1985)

17. Ishibuchi, H., Nakashima, T.: Effect of rule weights in fuzzy rule-based classification systems. IEEE Trans. Fuzzy Syst. **9**(4), 506–515 (2001)
18. van den Berg, J., Kaymak, U., van den Bergh, W.M.: Fuzzy classification using probability-based rule weighting. In: Proceedings of 11th IEEE International Conference on Fuzzy Systems, Hawaii (2002)
19. Ishibuchi, H., Yamamoto, T.: Rule weight specification in fuzzy rule-based classification systems. IEEE Trans. Fuzzy Syst. **13**(4), 428–435 (2005)
20. Sugeno, M., Griffin, F.M., Bastian, A.: Fuzzy hierarchical control of an unmanned helicopter. In: Proceedings of IFSA '93, Seoul, pp. 1262–1265 (1993)
21. Sugeno, M., Park, K.G.: An approach to linguistic instruction based learning. Int. J. Uncertainty Fuzziness Knowl. Based Syst. **1**(1), 19–56 (1993)
22. Kóczy, L.T., Hirota, K.: Approximate inference in hierarchical structured rule bases. In: Proceedings of IFSA '93, Seoul, pp. 1262–1265 (1993)

Part V
Robotic Systems

Delay and Stiffness Dependent Polytopic LPV Modelling of Impedance Controlled Robot Interaction

József Kuti, Péter Galambos and Péter Baranyi

Abstract Impedance/admittance control algorithms are considered as key technologies in human–robot interaction and other fields of advanced robotics where complex physical interaction plays role. In this chapter, we utilize a Tensor Product (TP) Model Transformation based method to derive the delay and stiffness dependent polytopic LPV representation of the impedance controlled physical interaction. The applied transformation method is feasible with bounded delay that is the non-linear function of the environmental stiffness. Thus, the ideal transformation space is non-rectangular that makes it improper for the TP model transformation. We propose a dimensionless parametrisation to define a rectangular grid upon witch the transformation is viable. The resulted model form is promptly appropriate for the modern multi-objective LMI based control design techniques.

Keywords Interaction robotics · LPV/qLPV modelling · Impedance control · Admittance control · Time delay systems · Telemanipulation · Haptics

1 Introduction

In advanced robotics, the importance of impedance and admittance control (hereafter referred to as impedance control) is unarguable since it is appearing in many applications from dexterous manipulation to telerobotics. In this chapter, we deal with the stability problem that is caused by the communication time delay when

J. Kuti (✉) · P. Galambos · P. Baranyi
Institute for Computer Science and Control, Hungarian Academy of Sciences, Budapest, Hungary
e-mail: kuti.jozsef@sztaki.mta.hu

P. Galambos
e-mail: galambos@sztaki.mta.hu

P. Baranyi
e-mail: baranyi@sztaki.mta.hu

the impedance control scheme is used in bilateral telemanipulation. This problem is thoroughly investigated by Gil et al. in [1] for haptics scenario but their conclusions are valid for bilateral control with common impedance model as well.

In [2], the convex TP type polytopic representation of the impedance controlled robotic interaction is derived considering the varying time delay as the parameter of the model but the environmental stiffness was treated as constant. Based on that work, in this chapter we extend the model taking the environmental stiffness as a second parameter into consideration.

The theoretical contribution of this chapter is based on the Tensor Product (TP) model transformation. The mathematical background of these methodology was introduced and elaborated in [3, 4]. To study the direct antecedents of the results discussed here, please be referred to the paper [2].

The chapter is structured as follows: In Sect. 2, the notations and abbreviations used along the chapter are explained. Section 3 contains the definitions of the mathematical concepts that are concerned here. Section 4 formulates the modelling problem then the HOSVD-based TP form of the model is derived in Sect. 5. In Sect. 6 the derivation of the convex TP model is discussed, while Sect. 7 validates the resulted TP type polytopic model. Finally, Sect. 8 concludes the chapter.

2 Nomenclature

In this section, the terms and notations are defined:

LPV	Linear Parameter Varying
qLPV	quasi Linear Parameter Varying
LTI	Linear Time Invariant
LMI	Linear Matrix Inequality
SVD	Singular Value Decomposition
HOSVD	Higher-Order Singular Value Decomposition
TP model	Tensor Product model
CNO	Close to NOrmal

F_h	Interaction force/torque with the operator $[N]$
F_e	Interaction force/torque with the remote environment $[N]$
x	Position of the impedance model $[m]$
m	Mass in the impedance model $[kg]$
b	Viscous damping in the impedance model $[Ns/m]$
k	Stiffness of the environment $[N/m]$
τ	Time delay $[s]$
$a, b, \ldots$	scalar values
$\mathbf{a}, \mathbf{b}, \ldots$	vectors
$\mathbf{A}, \mathbf{B}, \ldots$	matrices
$\mathcal{A}, \mathcal{B}, \ldots$	tensors

$$\mathcal{A} \underset{n=1}{\overset{N}{\boxtimes}} \mathbf{U}_n \qquad \text{multiple tensor product as } \mathcal{A} \times_1 \mathbf{U}_1 \times_2 \mathbf{U}_2 \cdots \times_N \mathbf{U}_N$$

3 Basic Concepts

The mathematical background of the TP model transformation and TP model transformation based LMI controller design was introduced and elaborated in [3, 5, 6]. Let us recall some of the related theorems and definitions:

Definition 1 *(qLPV model): Consider the Linear Parameter Varying State Space model:*

$$\dot{\mathbf{x}}(t) = \mathbf{A}(\mathbf{p}(t))\mathbf{x}(t) + \mathbf{B}(\mathbf{p}(t))\mathbf{u}(t) \tag{1}$$

$$\mathbf{y}(t) = \mathbf{C}(\mathbf{p}(t))\mathbf{x}(t) + \mathbf{D}(\mathbf{p}(t))\mathbf{u}(t),$$

with input $\mathbf{u}(t) \in \mathbb{R}^m$, *output* $\mathbf{y}(t) \in \mathbb{R}^l$ *and state vector* $\mathbf{x}(t) \in \mathbb{R}^k$. *The system matrix*

$$\mathbf{S}(\mathbf{p}(t)) = \begin{pmatrix} \mathbf{A}(\mathbf{p}(t)) & \mathbf{B}(\mathbf{p}(t)) \\ \mathbf{C}(\mathbf{p}(t)) & \mathbf{D}(\mathbf{p}(t)) \end{pmatrix} \tag{2}$$

is a parameter-varying object, where $\mathbf{p}(t) \in \Omega$ *is a time varying* N-*dimensional parameter vector, and* $\Omega = [a_1, b_1] \times [a_2, b_2] \times \cdots \times [a_N, b_N] \in \mathbb{R}^N$ *is a closed hypercube.* $\mathbf{p}(t)$ *can also include some elements of* $\mathbf{x}(t)$. *In this case,* (2) *is referred to as a quasi LPV (qLPV) model. This type of model is considered to belong to the class of non-linear models. The size of the system matrix* $\mathbf{S}(\mathbf{p}(t))$ *is* O *times* I, *where* $O = l + k$ *and* $I = m + k$.

A wide class of LMI based control design techniques are available for convex polytopic model representations. The finite element convex polytopic form of (1) is defined as:

Definition 2 *(Finite element polytopic model):*

$$\mathbf{S}(\mathbf{p}(t)) = \sum_{r=1}^{R} w_r(\mathbf{p}(t))\mathbf{S}_r, \tag{3}$$

where $\mathbf{p}(t) \in \Omega$. $\mathbf{S}(\mathbf{p}(t))$ *is given for any parameter vector* $\mathbf{p}(t)$ *as the parameter varying combinations of LTI system matrices* $\mathbf{S}_r \in \mathbb{R}^{O \times I}$ *called LTI vertex systems. The combination is defined by weighting functions* $w_r(\mathbf{p}(t)) \in [0, 1]$. *The term finite means that* R *is bounded.*

Definition 3 *(Finite element TP type polytopic model):* $\mathbf{S}(\mathbf{p}(t))$ *in* (3) *is given for any parameter as the parameter-varying combination of LTI system matrices* $\mathbf{S}_r \in \mathbb{R}^{O \times I}$.

$$\mathbf{S}(\mathbf{p}(t)) = \sum_{i_1=1}^{I_1} \sum_{i_2=1}^{I_2} \cdots \sum_{i_N=1}^{I_N} \mathbf{S}_{i_1,i_2,\cdots,i_N} \prod_{n=1}^{N} w_{n,i_n}(p_n(t)), \tag{4}$$

applying the compact notation based on tensor algebra (Lathauwer's work [7]) one has:

$$\mathbf{S}(\mathbf{p}(t)) = S \underset{n=1}{\overset{N}{\boxtimes}} \mathbf{w}_n\,(p_n\,(t)) \tag{5}$$

where the (N+2) dimensional coefficient tensor $\mathbf{S} \in \mathbb{R}^{I_1 \times I_2 \times \cdots \times I_N \times O \times I}$ *is constructed from the LTI vertex systems* $\mathbf{S}_{i_1,i_2,\ldots,i_N}$ *(5) and the row vector* $\mathbf{w}_n\,(p_n\,(t))$ *contains one variable and continuous weighting functions* $w_{n,i_n}(p_n(t))$, $(i_n = 1, \ldots, I_N)$.

Remark 1 *TP model (5) is a special class of polytopic models (3), where the weighting functions are decomposed to the Tensor Product of univariate functions.*

Definition 4 *(TP model transformation): TP model transformation is a numerical method that transforms qLPV models given in the form of (1) to the form of (5), so that a large class of LMI based control design techniques can be applied to the resulting model. Detailed description of TP model transformation and application examples can be found in [3]. The TP model transformation gives a trade-off between the accuracy of the resulting model and the number of vertexes required for the LMI control design. The TP model transformation is also capable of providing a convex hull manipulation tool during execution. For further details please consult the papers [4] and [8].*

Definition 5 *(HOSVD-based canonical form of qLPV models) The direct result of the TP model transformation when no complexity trade-off neither convex hull manipulation is done is the numerical reconstruction of the HOSVD of a given function. It is like the HOSVD of tensors, but for functions where instead of singular matrices we have singular functions in an orthonormal structure and the core tensor contains the higher order singular values. In case of systems where matrix functions are used the HOSVD canonical form has the same structure, only difference is that the core tensor contains the system vertices assigned to the higher order singular values. For further details please be referred to papers [9, 10].*

Definition 6 *(Convex TP model) The TP model is convex if the weighting functions satisfy the following criteria:*

$$\forall n, i_n,\, p_n(t) : w_{n,i_n}(p_n(t)) \in [0, 1]; \tag{6}$$

$$\forall n,\, p_n(t) : \sum_{i_n=1}^{I_n} w_{n,i_n}(p_n(t)) = 1. \tag{7}$$

Different convex hulls for TP type polytopic qLPV models can be defined. Some of the basic types are defined as follows:

Definition 7 (SN type TP function) *The convex TP function is SN (Sum Normalized) if the sum of the weighting functions for all $x \in \Omega$ is 1.*

Definition 8 (NN type TP function) *The convex TP function is NN (Non-Negative) if the values of the weighting functions for all $x \in \Omega$ are non-negative.*

Definition 9 (NO/CNO, NOrmal type TP function) *The convex TP function is a NO (Normal) type model if its $w(p)$ weighting functions are Normal, that is, if it satisfies (6) and (7), and the largest value of all weighting functions is 1. Also, it is CNO (close to normal), if it is satisfies (6) and (7) and the largest value of all weighting functions is 1 or close to 1.*

Definition 10 (IRNO, Inverted and Relaxed NOrmal type TP function) *The TP function is IRNO type if the smallest values of all weighting functions are 0, and the largest values of all weighting functions are the same.*

Examples on the utilisation of TP model transformation can be found in [11–15].

4 Specification of the Modelling Problem

Along this chapter a single degree of freedom impedance model will be discussed but the results can be extended to multidimensional cases. Impedance model is understood as the desired dynamic relationship between the external forces and the resulted velocity or displacement which is usually specified by a mass-spring-damper mechanical system. Consider the mechanical system depicted by Fig. 1a as a simplified model of the impedance controlled robot interaction. Mass m and viscous damping b are virtual properties defining the desired dynamics of the manipulator, while k denotes the stiffness of the robot's environment. In bilateral telemanipulation where the impedance model at the master site and the slave site are connected via computer network, varying time delay occurs whilst the motion command is received and the force response is sent back to the master (Fig. 1b).

Considering the varying time delay $(\tau(t))$ in the bilateral control and the varying environmental stiffness $(k(t))$ the equation of motion is as follows:

$$\ddot{x}(t) = \frac{F_h(t) + F_e(t)}{m} - \frac{b}{m}\dot{x}(t), \tag{8}$$
$$dF_e(t) = -k(t)dx(t - \tau(t)).$$

One can see that the equation represents a mass-spring-damper system where the elastic effect is delayed by $\tau(t)$. Figure 1b illustrates this model.

We search the representation of the investigated delayed dynamical system in TP type polytopic form, wherein the time delay τ and the environmental stiffness k are
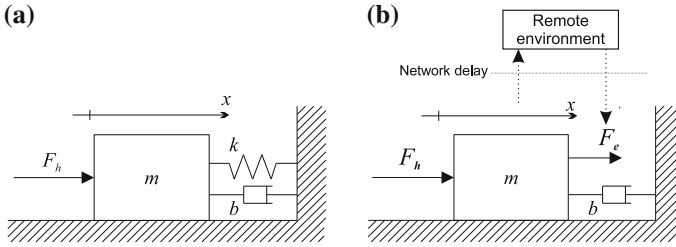
Fig. 1 a Mass-Spring-Damper system as the simplified model of impedance controlled robot interaction, **b** Mass-Spring-Damper model where the effect of the spring is delayed Introducing the time-delay in the measurement of the interaction force between the robot and its environment

a parameters of the model and which is appropriate for LMI-based multi-objective synthesis methods.

5 Derivation of the HOSVD-Based TP Form

As the first step of the model creation we apply a modified version of the TP model transformation to derive the so called HOSVD based form of the investigated system. Compared to the one-parameter model derived in [2] we face a difficulty when considering the environmental stiffness (k) as a second variable, since the critical τ—up till the transformation can be done with the given reidentification method— depends on the environmental stiffness as $\tau_{crit} = \frac{b}{k}c$, where $c = 1.566$ for $m = 1$ kg and $dT = 1$ ms sampling time of the control system [1, 16]. Therefore, the so called transformation space $\Omega = [k_{min}, k_{max}] \times [\tau_{min}, \tau_{max}]$ is not rectangular regarding the valid area on $k - \tau$ plane 2a. As the TP model transformation supports only rectangular transformation space we propose the $\vartheta = \frac{\tau}{\tau_{crit}}$ dimensionless time delay parameter to get rid of this barrier 2b.

Using the dimensionless parametrisation the following two dimensional TP model form can be derived executing the first and second step of the modified TP model transformation as applied in [2]:

$$\mathbf{S}(k, \vartheta) = \mathcal{S}^D \overset{2}{\underset{n=1}{\boxtimes}} \mathbf{w}_n(p_n) = \sum_{i_k=1}^{R_k} \sum_{i_\vartheta=1}^{R_\vartheta} w_{i_k}(k) w_{i_\vartheta}(\vartheta) \mathbf{S}_{i_k, i_\vartheta}, \tag{9}$$

where R_k and R_ϑ equals the ranks of the $\mathcal{S}^D$ tensor. Along this chapter, a numerical example will be discussed using the parameters $m = 1$ kg, $b = 120$ Ns/m, $k = [1000..8000]$ N/m and $\vartheta = [0..0.65]$. The two dimensional discretisation grid M is defined over these intervals containing 137 and 97 equidistant points respectively.

Executing the Higher Order SVD (HOSVD) on the discretised LTI system tensor resulted from the first step of the modified TP model transformation the number of
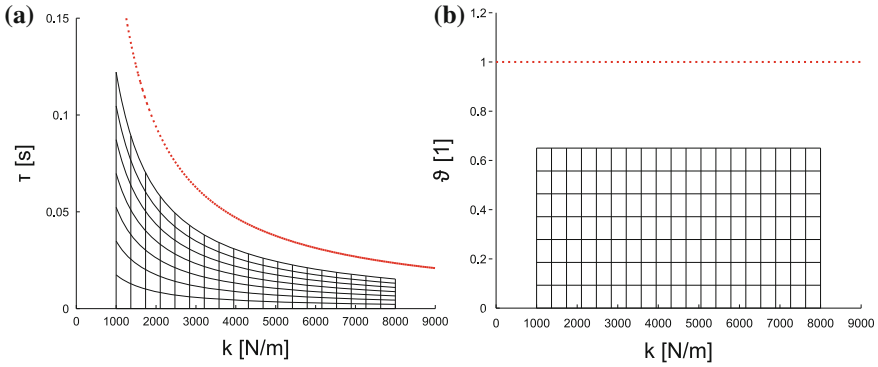
Fig. 2 **a** The non-rectangular grid in $k - -\tau$ plane. **b** The rectangular grid in $k - -\vartheta$ plane The shape of transformation space and grid
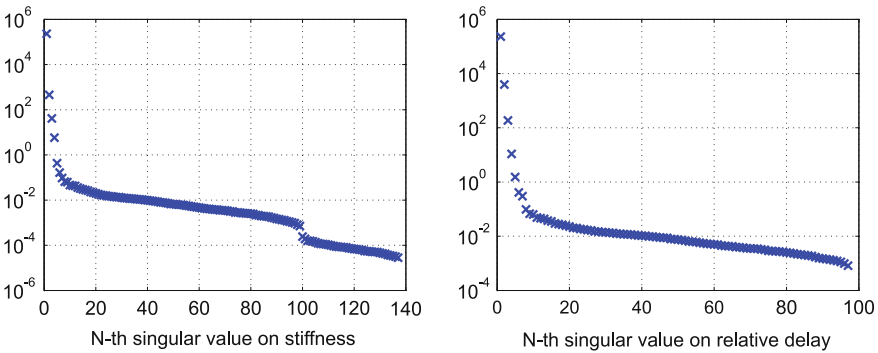

Fig. 3 Singular values of the HOSVD based canonical form

non-zero singular values (ranks) are 137 and 97, which means that $\mathcal{S}^D$ is full rank in mathematical sense. Figure 3 shows the singular values along the dimensions of k and ϑ.

Please note that in many cases the full rank $\mathcal{S}^D$ has only mathematical meaning because the re-identification based discretisation may leads to noisy result. As one can see in this example, the singular values are decreasing non-uniformly and the contribution of the smallest singular values to the whole system is negligible in most cases. Neglecting the smallest non-zero singular values we get the so called best matching reduced rank model that approximates the original system in $\mathcal{L}_2$ sense. In the rest of the chapter, we make use of this approximation capability of TP model transformation.
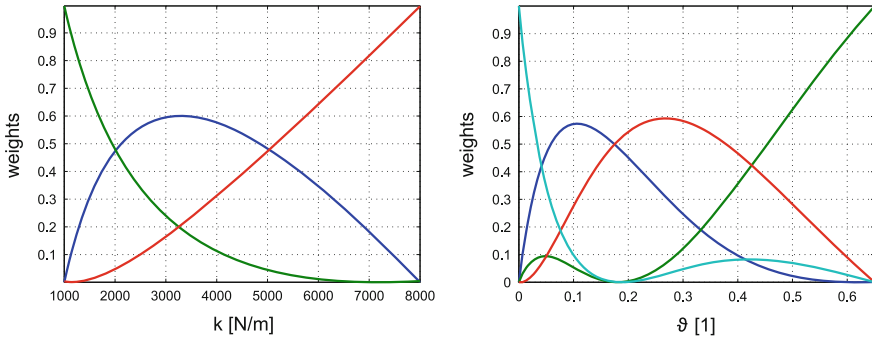
Fig. 4 Weighting functions of CNO type convex hull of the reduced TP model

6 Derivation of the Convex TP Model for Control Design Purposes

The LMIs are very sensitive for the shape of the convex hull that defines the polytopic LPV/qLPV representation. Different type of convex hulls of the impedance model can be generated utilizing the hull manipulation capabilities of TP model transformation. For the sake of brevity, only the non-exact, CNO type convex model with 3–3 vertices is detailed here. Performing a trade-off between the accuracy and the complexity of the resulted TP model the 3–3 largest singular values were kept while the others were neglected then the CNO type convex hull has been generated. The shape of the resulted reduced CNO type convex polytopic representation is depicted in Fig. 4 by its weighting functions. In the dimension of relative delay ϑ the numerical algorithm of hull generation [17] automatically added one more weighting function in order to reach the normalised criterion as close as possible.

7 Validation of the Resulted Model

As the first stage of the model validation, we have tested the model accuracy with constant parameters. Figure 5 shows the results of a sequence of numerical simulations comparing the original delayed model, the re-identified system and the reduced TP model. In this figure, 9 test cases are presented: the stiffness (k) is a constant in each row $k = 1200, 3000$ and 7800 [N/m] respectively, while the relative delay (ϑ) is constant by columns $\vartheta = 0, 0.3$ and 0.6. Each plot contains the responses of the different models for step input of F_h. The comparison shows that both the re-identification based TP model and the reduced TP model reproduce the dynamical behaviour of the original system with high accuracy even though the complexity of the TP model has been drastically reduced via the complexity trade-off mechanism of the TP model transformation.
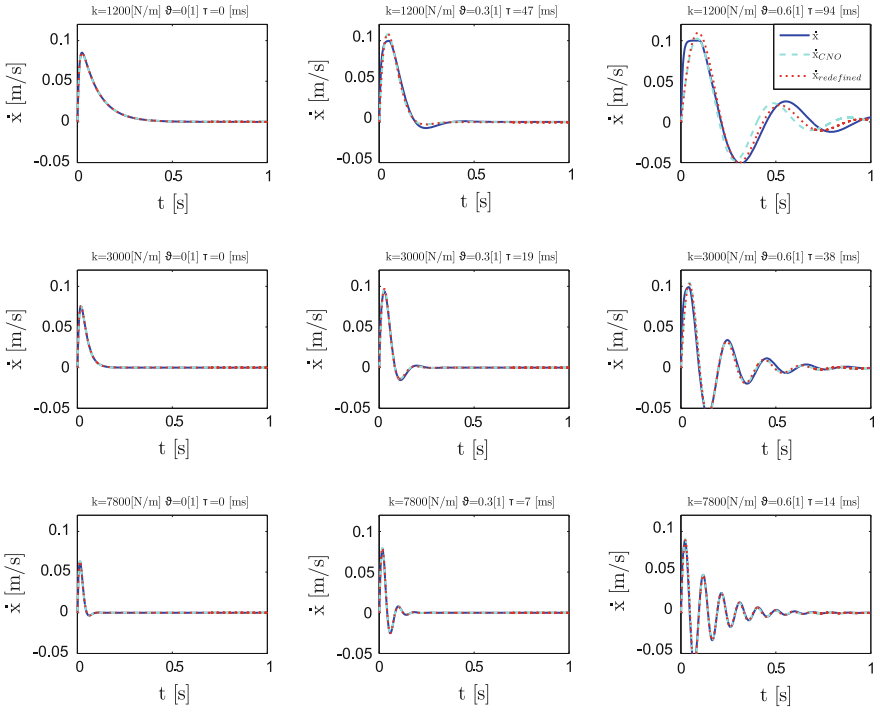
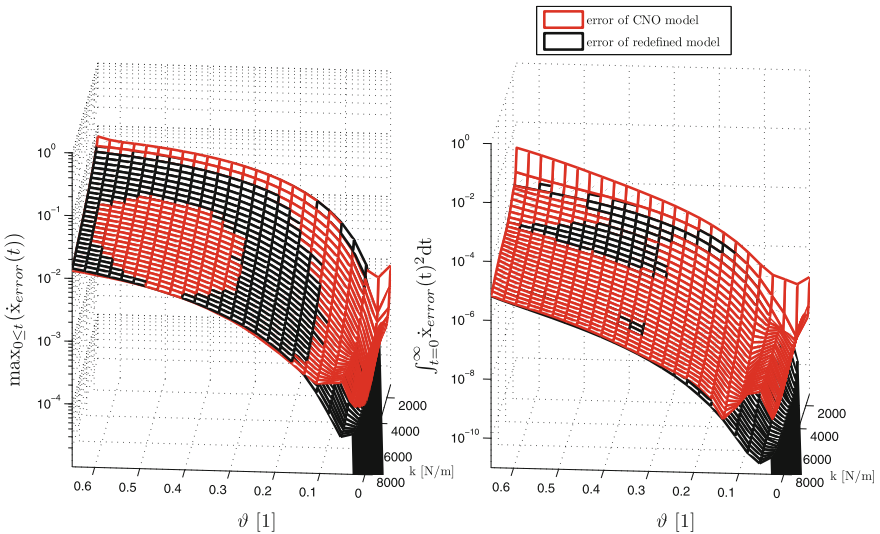**Fig. 5** Validation of the model with constant time delay and stiffness

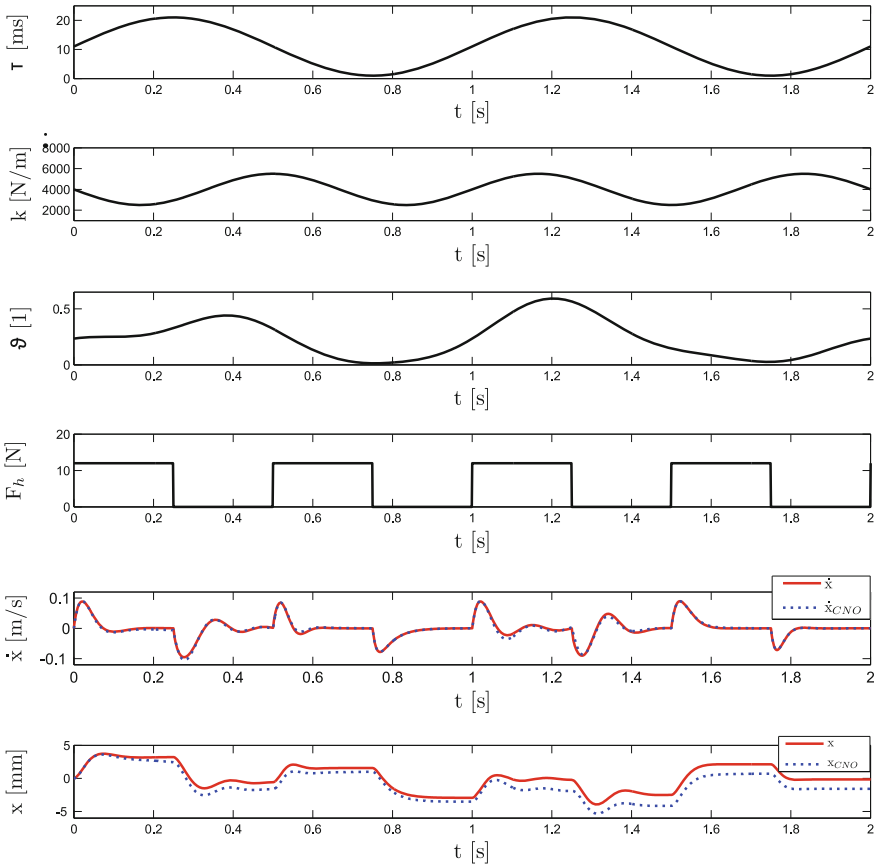**Fig. 6** Modelling error with constant time delay and stiffness

Fig. 7 Validation of the model with varying time delay and time-dependent stiffness

To give a better view the same test were executed in 25×27 parameter pairs. Characterising the modelling accuracy, the maximum error of $\dot{x}$ and the integrated squared error are displayed in Fig. 6 over each tested grid point. One can see that both these measures increase by the relative delay and in cases with no delay the modelling error tends to zero.

The second stage of the validation has been carried out with varying time delay and time-dependent environmental stiffness. Figure 7 displays the result of the numerical simulation wherein the original model and the reduced TP model are compared.

These comparisons show that the TP model generates the velocity response very similarly to the original delayed model. This observation implies that the accuracy of the derived reduced TP type polytopic model is appropriate for control design purposes.

8 Conclusion

In this chapter, the TP type convex polytopic representation of the impedance controlled robot interaction under time delay was presented where the time delay and the environmental stiffness are the parameters of the model. A modified version of the TP model transformation was applied to derive the HOSVD-based TP form, then performing complexity trade-off and convex hull manipulation provided by TP model transformation, a reduced CNO-type polytopic TP model was generated. Since the maximum time delay whereby the applied transformation methodology works is the nonlinear function of the environmental stiffness the discretisation grid would be non-rectangular and non equidistant on the $\tau - k$ plane. To overcome this problem, a dimensionless parametrisation of the time delay has been proposed that makes the transformation space rectangular, and thus, the transformation became feasible. The presented TP model was compared to the original delayed system via numerical simulations. The fine accuracy of the proposed model let us to conclude that it is appropriate for control design purposes. The tight, CNO type convex hull indirectly supports the feasibility of optimal control performance under the LMI based control design concept.

References

1. Gil, J.J., Sanchez, E., Hulin, T., Preusche, C., Hirzinger, G.: Stability boundary for haptic rendering: Influence of damping and delay. J. Comput. Inf. Sci. Eng. **9**(1), 1–8 (2009)
2. Galambos, P., Baranyi, P.: Representing the model of impedance controlled robot interaction with feedback delay in polytopic lpv form: Tp model transformation based approach. Acta Polytech. Hung. **10**(1), 139–157 (2013)
3. Baranyi, P.: TP model transformation as a way to LMI based controller design. IEEE Trans. Industr. Electron. **51**(2), 387–400 (2004)
4. Baranyi, P.: Convex hull generation methods for polytopic representations of LPV models, in Applied Machine Intelligence and Informatics, SAMI 2009. 7th International Symposium on IEEE 2009, pp. 69–74 (2009)
5. Baranyi, P.: Tensor-product model-based control of two-dimensional aeroelastic system. J. Guidance Control Dyn. **29**(2), 391–400 (2005)
6. Baranyi, P.: Output feedback control of two-dimensional aeroelastic system. J. Guidance Control Dyn. **29**(3), 762–767 (2005)
7. Lathauwer, L.D., Moor, B.D., Vandewalle, J.: A multilinear singular value decomposition. SIAM J. Matrix Anal. Appl. **21**(4), 1253–1278 (2000)
8. Gróf, P., Baranyi, P., Korondi, P.: Convex hull manipulation based control performance optimisation. WSEAS Trans. Syst. Control **5**, 691–700 (2010)
9. Baranyi, P., Szeidl, L., Várlaki, P., Yam, Y.: Definition of the HOSVD-based canonical form of polytopic dynamic models. In: 3rd International Conference on Mechatronics (ICM 2006), pp. 660–665. Budapest, Hungary, 3–5 July 2006

10. Szeidl, L., Várlaki, P.: HOSVD based canonical form for polytopic models of dynamic systems. J. Adv. Comput. Intell. Intell. Inf. **13**(1), 52–60 (2009)
11. Kolonic, F., Poljugan, A., Petrovic, I.: Tensor product model transformation-based controller design for gantry crane control system—an application approach. Acta Polytech. Hung. **3**(4), 95–112 (2006)
12. Precup, R., Dioanca, L., Petriu, E.M., Radac, M., Preitl, S., Dragos, C.: Tensor product-based real-time control of the liquid levels in a three tank system. In: 2010 IEEE/ASME International Conference on Advanced Intelligent Mechatronics, Montreal, QC, Canada, http://ieeexplore.ieee.org/lpdocs/epic03/wrapper.htm?arnumber=5695727. Accessecd July 2010, pp. 768–773
13. Szabó, Z., Gáspár, P., Bokor, J.: A novel control-oriented multi-affine qLPV modeling framework. In: 18th Mediterranean Conference on Control Automation (MED), June 2010, pp. 1019–1024 (2010)
14. Ilea, S., Matusko, J., Kolonic, F.: Tensor product transformation based speed control of permanent magnet synchronous motor drives. In: 17th International Conference on Electrical Drives and Power Electronics, EDPE 2011 (5th Joint Slovak-Croatian Conference), 2011
15. Precup, R., Dragos, C., Preitl, S., Radac, M., Petriu, E.M.: Novel tensor product models for automatic transmission system control. IEEE Syst. J. **6**(3), 488–498 (2012)
16. Galambos, P.: Stability boundary of impedance controlled robots: effect of stiffness, damping, friction and delay. In: Proceedings of the 15th WSEAS International Conference on Systems. World Scientific and Engineering Academy and Society (WSEAS), pp. 247–252. (2011)
17. TP Toolbox for matlab, http://tptool.sztaki.hu (2011)

Local Center of Gravity Based Gathering Algorithm for Fat Robots

Kálmán Bolla, Zsolt Csaba Johanyák, Tamás Kovács and Gábor Fazekas

Abstract Swarm intelligence has become an intensively studied research area in the last few years. Gathering of mobile robots is one of its basic topics that aims the assembly of the scattered robots on the smallest possible area. In this chapter, we present a new and effective algorithm for this task supposing an obstacle-free plan, limited visibility, and synchronous, fat (disc-like) robots without global navigation, communication, or memory. The key idea of the algorithm is that in case of each robot after detecting the visible neighbouring robots it sets the target of the next step based on the encountered visible robots' center of gravity. The new algorithm was successfully tested using computer simulations for several parameter and swarm size values and it achieved similar or better performance as the studied previously published algorithms in all of the cases.

Keywords Mobile robot swarm · Gathering problem · Fat robots

1 Introduction

Gathering of identical autonomous robots on a plane without global navigation tools became a highly studied theoretical problem in the last decade. In the present state of

K. Bolla (✉) · Z. Csaba Johanyák · T. Kovács · G. Fazekas
Kecskemét College, Department of Information Technologies, Izsáki út 10,
Kecskemét 6000, Hungary
e-mail: bolla.kalman@gamf.kefo.hu
http://www.kefo.hu

Z. Csaba Johanyák
e-mail: johanyak.csaba@gamf.kefo.hu

T. Kovács
e-mail: kovacs.tamas@gamf.kefo.hu

G. Fazekas
e-mail: fazekas.gabor@inf.unideb.hu

the art, the algorithms aiming the solution of this task are too theoretical to use them in practice: the robots are considered as points in the plane (i.e. without physical extent) and they do not block the movement of each other in any situation. Though, there are proposed solutions for the gathering problem for robots with extent as well, but these suppose global navigation or limit the number of the robots, as it will be treated below.

To be more specific, the gathering problem means that the robots have to gather in one point starting from an arbitrary initial condition under a finite time. A weaker version of the problem is the convergence task when we require that the diameter of the area enclosing all of the robots tends to zero with the increasing time. It was necessary to introduce the convergence task, because the gathering problem is not solvable in numerous cases [1]. The solution, i.e. the algorithm of the individual robots, depends highly on the properties of the robots. In order to classify the problem we have to decide whether the robots:

- have memory or not,
- synchronize their acts to each other or not (synchronous or asynchronous case),
- have global navigation tool with common coordination system or not,
- have limited or unlimited radius of visibility,
- can communicate with each other or not,
- are point-like or have an extent (fat robots).

According to the thought of using as simple individuals as possible, most of the gathering algorithms are based on memory-less (oblivious) robots without global navigation. This means that the robots cannot use backtracking steps and common coordinate system. In a typical gathering algorithm each robot repeats the steps of:

- "look" (determining the positions of all visible robots),
- "calculate" (the position in the next time-step for itself),
- "move" (to the calculated position),

in this order. In a synchronous model the robots execute these steps at the same time providing some synchronizing signal. In an asynchronous model, however, the starting times and the durations of the steps above can be different for the individual robots, and, in addition to this, a wait phase can be added between the move and the next look phase. There is also a semi-synchronous model, where the starting times and durations of the different phases are synchronized, but an arbitrary number of robots can skip one or more moving cycles. It is easy to see that the solution for the asynchronous case is the strongest, that is, it gives solution for the semi-synchronous and synchronous cases too, and not reverse; and similarly, the solution for the semi-synchronous case solves the synchronous case.

One straightforward solution is to calculate and move toward the center of gravity (COG) of the robots in each moving step, since it is the same in each local coordinate system. Cohen and Peleg [2] proved the correctness of the COG algorithm for point-like, oblivious robots with unlimited visibility for arbitrary number of robots in the semi-synchronous (and the synchronous) case. The same correctness could be proven only for two such robots in the asynchronous case.

Cieliebak et al. [3] used the center of the smallest enclosing circle (SEC) of all robots instead of the COG, and with this SEC algorithm solved the asynchronous gathering problem for arbitrary number of point-like, oblivious robots with unlimited visibility.

With these algorithms, the gathering problem is solved for point-like robots with unlimited visibility; however, it is necessary to step towards more realistic models. Ando et al. examined the synchronous gathering problem with limited visibility and point-like oblivious robots. Here the concept of the visibility graph arises. This graph contains all robots as vertices, and there is an edge between two vertices (robots), if and only if the two robots see each other. Ando et al. [4] gave solution to the gathering problem with the condition, that the visibility graph is connected. They, too, applied the SEC algorithm, but in this case, the robots calculated and moved towards the center of SEC of the group robots visible by the robot at hand, so each robot had a different center of SEC as purpose at each step cycle. In addition to this the calculated movement of each robot was limited by the condition, that any edge of the visibility graph must not be broken by the step of the robot, so the vector of the planned move was shortened according to this condition. They proved the correctness of their local SEC algorithm in the synchronous case.

Later Flocchini et al. [5] and Soussi et al. [6] introduced algorithms to solve the asynchronous limited visibility problem. However, here the robots could determine the directional angle of a common and global polar coordinate system (with a compass, for example), so, partly, they provided a global navigational tool.

Recently Degener et al. [7] proposed an algorithm for the synchronous limited visibility problem that is based on the local convex hull of the visible robots instead of the COG or the SEC. In this algorithm no global navigation but communication abilities were supposed, since the robots could share coordinates local the moving strategy with each other.

Another step towards the realistic models is to work with no point-like but fat robots, where all of the robots are supposed to be solid discs on a plane with radius R_s. This modification of the problem has serious consequences: it is impossible to gather in a single point, so the original purpose should be modified. Another problem is that the robots now can hinder or totally block the movement of each other; moreover, this is true for the visibility too, since the robots are not transparent in a realistic case.

How should we define the gathering in the case of the fat robots? Czyzowicz et al. [8] defined the gathering so that

- the contact graph of the disks are connected, and
- each robot sees all of the others.

(The contact graph contains the center of the disks as vertices, and two vertices are connected if and only if the two disks are in contact.) Starting out from this definition, they solved the gathering problem for at most four robots. It is obvious, however, that the condition of seeing the other robots at the gathered position cannot be satisfied if there are a numerous robots. Therefore, we define the minimum requirement of gathering as the connectivity of the contact graph.
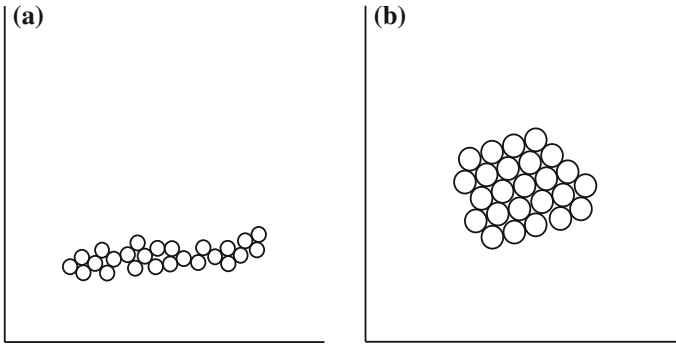
Fig. 1 **a** COG based gathering without randomness in the goal definition ($c_r = 0$); **b** COG based gathering with randomness in the goal definition ($c_r = 0.020$)

Cord-Landwehr et al. [9] and later Chaudhuri et al. [10] invented algorithms to gather arbitrary number of disk-like robots around a given point so that the contact graph, and, beyond this, in the gathered state the robot-disks should be as closely packed as possible. In these models, the robots had global navigation tools and total visibility, which meant, in this case, that the robot disks were transparent.

In the present chapter, we deal with problem of oblivious, fat robots with limited visibility, but with no global navigation and no communication capabilities at all. We test the local COG based algorithm applied for fat robots, and propose some improvements of the basic algorithm according to the problems caused by the fat property of the robots. The two main elements of the improvement are that a random noise is added to the movement of the robots, and a get-around behavior is also added to the algorithm to solve the deadlock situations caused by the extent of the robots. In the next section, we give the details of the algorithms at hand. In Sect. 3, the results of the computer simulation tests are introduced, and in the last section we conclude.

2 Gathering Algorithm

2.1 Goal Point Definition

The key idea of the center of gravity based gathering algorithm (COGGA) is that each robot tries to move towards the center of gravity of the visible robots. However, using only the COG as goal point usually results in an elongated shape of the robot swarm (see e.g. Fig. 1a). In order to facilitate a more compact final shape (see e.g. Fig. 1b) we intruded a small random value in the formula of the goal point.

Thus the coordinates of the goal point for the current robot are determined by

$$g_x = \frac{1}{n} \sum_{j=1}^{n} RV_{j,1} \cdot (1 + c_r \cdot R_1), \qquad (1)$$

$$g_y = \frac{1}{n} \sum_{j=1}^{n} RV_{j,2} \cdot (1 + c_r \cdot R_2), \qquad (2)$$

where n is the number of the visible robots, RV is a $n \times 2$ matrix containing the coordinates of the centers of the visible robots, $R1, R2 \in [-0.5, 0.5]$ are random numbers, c_r is the randomness coefficient that controls in which measure the random numbers influence the position of the goal point.

2.2 Step Length

The step length of each robot is limited in order to keep the visibility graph connected. If the visibility graph is broken, there is no guarantee of successfully gathering and the robot swarm might be flocking. To satisfy the connected visibility graph condition in each robot step we use Ando's [4] step limitation algorithm.

2.3 Handling the Blocking Situation

A robot cannot always complete its calculated step because it can be blocked by one or more other robots. To alleviate this problem we used basically the solution called slip introduced in [11] by Bolla et al. The only modification was an additional step that deals with the case when the center of the blocking robot falls on the line connecting the center of the current robot and the goal point. Thus the applied algorithm is the following.

> **if** There are more blocking robots **then**
>> Do not move the robot.
> **else**
>> **if** The goal vector goes through the
>> center of the blocking robot **then**
>>> Set a new goal in a perpendicular direction to the original one
>>> choosing from the possible two directions randomly.
>>> Calculate the new step length by multiplying the original step
>>> length by an arbitrary coefficient $c_s \in [0, 1]$.
>> **else**
>>> Define a new tangential goal vector with length equal to the
>>> projection of the original vector to the tangential direction
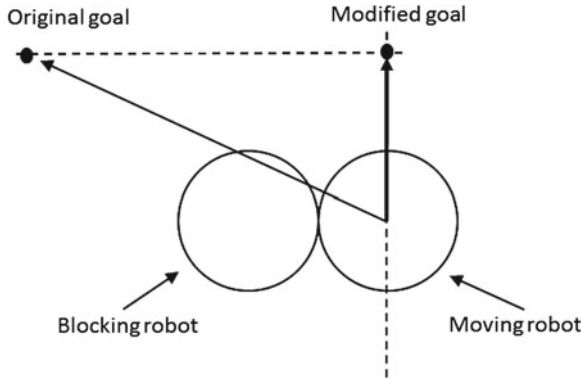>>> (see Fig. 2).
>> **end if**
> **end if**

Fig. 2 Solution to the blocking problem

3 Evaluation of the Robot Group's Formation

The application of different gathering algorithms and parameter values can result in diverse distributions of the robot swarm. Evaluation criteria of the algorithms could be for example the fulfilment of the demand on connectivity of the contact graph, the elapsed time as well as the compactness of the formation. For the measurement of compactness we used a formula that expresses how close the robots to a given point are. It is the mean square distance to the robot swarm's center of gravity. To get an easy-to-understand and comparable indicator value we divided this value by the area of the rectangle-shaped surface used to distribute the robots and multiplied the resulting number by 1,000. Thus the final performance indicator is

$$PI = \frac{\sum_{i=1}^{N}\left(x_i - \frac{\sum_{i=1}^{N} x_i}{N}\right)^2 + \sum_{i=1}^{N}\left(y_i - \frac{\sum_{i=1}^{N} y_i}{N}\right)^2}{N \cdot H \cdot W} \cdot 1,000, \qquad (3)$$

where N is the number of the robots, x_i, y_i are the coordinates of the center of the ith robot, H, W are the height and width of the rectangle-shaped area. The type of this indicator is the lower the better, which means that when an algorithm has a lower *PI* than another algorithm then it ensures a more compact formation of the robots. Further on we will use this indicator as primary performance measure in course of the comparison of the proposed algorithm and the previously studied two other algorithms.

Table 1 Performance indicator values in case of different robot swarm size values (N) and in case of different algorithms/parameter values

Method/N	12	25	50	100
SEC	0.3725	0.2441	0.6884	1.0166
BKF	0.0655	0.1743	0.3447	0.9835
COGGA—$c_r = 0.000$	0.0887	0.7518	1.7038	5.0391
COGGA—$c_r = 0.005$	0.1006	0.6589	0.6909	1.9295
COGGA—$c_r = 0.010$	0.0886	0.2862	0.4757	1.3562
COGGA—$c_r = 0.015$	0.0695	0.2446	0.3417	1.3010
COGGA—$c_r = 0.020$	0.0602	0.1476	0.2763	0.8703
COGGA—$c_r = 0.025$	0.0552	0.1239	0.2542	0.5490

4 Experimental Results

In order to test the proposed algorithm we created an implementation in Matlab and we defined four random start positions (distributions) for four robot groups ($N = 12, 25, 50, 100$) so that the initial visibility graph was connected. We defined six values for the randomness coefficient ($c_r = 0.000, 0.005, 0.010, 0.015, 0.020, 0.025$) and we chose the value 0.01 for the step coefficient c_s.

We compared in case of all robot groups the proposed algorithm to the one proposed by Ando (SEC) [4] and the one proposed by Bolla et al. [11] (BKF). The number of iteration cycles was limited by two factors. First, an upper limit was set to $n = 1,000$. Besides, the iteration also stopped when the robots did no more movements. This approach resulted in quite different gathering-time values for the three algorithms.
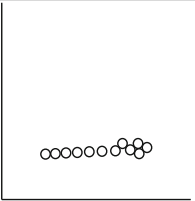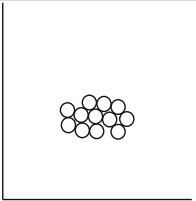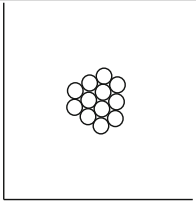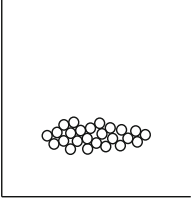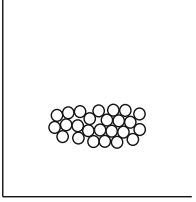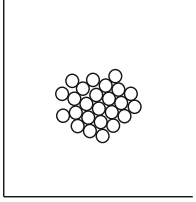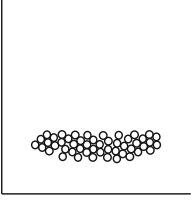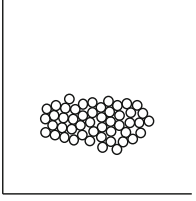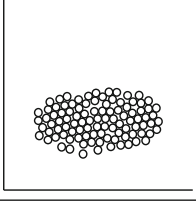
However, we considered the most important evaluation factor the performance indicator *PI* introduced in the previous section. Table 1 summarizes the obtained test results in case of COGGA and the two reference methods. In case of the new method Table 1 contains average values of the performances measured by the four different starting positions. Table 2 contains the figures of the obtained swarm shapes. In case of COGGA for each swarm size the shapes with the best average *PI* values were included. In all of the four cases (four swarm size values) $c_r = 0.025$ ensured the best average performance.
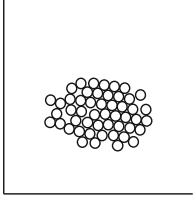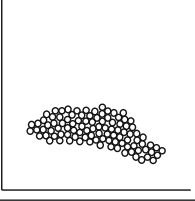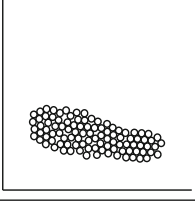
In case of some test runs the final contact graph was not connected in case of COGGA or SEC. However, in most of the cases the COGGA algorithm with a proper parameter selection ensured the most compact swarm shape.

5 Conclusions

In this chapter we proposed a new algorithm for the robot swarm gathering problem that in case of the applied simulation situations ensured good results. Further

Table 2 Final swarm shapes

N/Method	SEC	BKF	COGGA
12			
25			
50			
100			

research will concentrate on the analysis of the parameters' effects and finding their optimal values using evolution based methods (e.g. [12]), the application of obstacle avoidance methods [13], robot control strategies [14] as well as other computational intelligence based techniques (e.g. [15–17]).

References

1. Prencipe, G.: Impossibility of gathering by a set of autonomous mobile robots. Theoret. Comput. Sci. **384**, 222–231 (2007)

2. Cohen, R., Peleg, D.: Robot convergence via center-of-gravity algorithms. In: Kralovic, R., Sykora, O. (eds.) SIROCCO 2004. LNCS, vol. 3104, pp. 79–88. Springer, Heidelberg (2005)

3. Cieliebak, M., Flocchini, P., Prencipe, G., Santoro, N.: Solving the robots gathering problem. In: Baeten, J.C.M., Lenstra, J.K., Parrow, J., Woeginger, G.J. (eds.) ICALP 2003. LNCS, vol. 2719, pp. 1181–1196. Springer, Heidelberg (2003)

4. Ando, H., Suzuki, I., Yamashita, M.: Formation and agreement problems for synchronous mobile robots with limited visibility. In: Proceedings of the 1995 IEEE International Symposium on Intelligent Control, pp. 453–460. IEEE Press, New York (1995)

5. Flocchini, P., Prencipe, G., Santoro, N., Widmayer, P.: Gathering of asynchronous robots with limited visibility. Theoret. Comput. Sci. **337**, 147–168 (2005)

6. Souissi, S., Défago, X., Yamashita, M.: Using eventually consistent compasses to gather oblivious mobile robots with limited visibility. In: Datta, A. K., Gradinariu, M. (eds.) SSSS 2006. LNCS, vol. 4208, pp. 484–500. Springer, Heidelberg (2006)

7. Degener, B., Kempkes, B., auf der Heide, F.M.: A local O(n^2) gathering algorithm. In: SPAA '10 Proceedings of the 22nd ACM symposium on Parallelism in algorithms and architectures, pp. 224–232. ACM, New York (2010)

8. Czyzowicz, G.J., Gasieniec, L., Pelc, A.: Gathering few fat mobile robots in the plane. Theoret. Comput. Sci. **410**, 481–499 (2009)

9. Cord-Landwehr, A., Degener, B., Fischer, M., Hüllmann M., Kempkes, B., Klaas, A., Kling, P., Kurras S., Märtens M., auf der Heide, F. M., Raupach, C., Swierkot, K., Warner D., Weddemann, C., Wonisch, D.: Collisionless gathering of robots with an extent. In: Cerná, I., Gyimóthy, T., Hromkovic, J., Jefferey, K., Královic, R., Vukolic, M., Wolf, S. (eds.) SOFSEM 2011. LNCS, vol. 6543, pp. 178–189. Springer, Heidelberg (2011)

10. Chaudhuri, S.G., Mukhopadhyaya, K.: Gathering asynchronous transparent fat robots. In: Janowski, T., Mohanty, H. (eds.) ICDCIT 2010. LNCS, vol. 5966, pp. 170–175. Springer, Heidelberg (2010)

11. Bolla, K., Kovacs T., Fazekas G.: Gathering of fat robots with limited visibility and without global navigation. Swarm and Evolutionary Computation, LNCS, vol. 7269, pp. 30–38. Springer, Heidelberg (2012)

12. Gál, L., Botzheim, J., Kóczy, L.T.: Advanced bacterial memetic algorithms. In: First Győr Symposium on Computational Intelligence, pp. 57–60. Győr, Hungary (2008)

13. Pozna, C., Troester, F., Precup, R.-E., Tar, J.K., Preitl, S.: On the design of an obstacle avoiding trajectory: method and simulation. Math. Comput. Simul. **79**(7), 2211–2226 (2009)

14. Klančar, G., Matko, D., Blažič, S.: A control strategy for platoons of Differential-drive wheeled mobile robot. Robot. Auton. Syst. **59**(2), 57–64 (2011)

15. Vaščák, J.: Approaches in adaptation of fuzzy cognitive maps for navigation purposes. In: SAMI-8th International Symposium on Applied Machine Intelligence and Informatics, pp. 31–36. Herany, Slovakia (2010)

16. Vincze, D., Kovács, S.: Incremental rule base creation with fuzzy rule interpolation-based Q-learning. Stud. Comput. Intell. Comput. Intell. Eng. **313**, 191–203 (2010)

17. Perfilieva, I., Wrublova, M., Hodakova, P.: Fuzzy interpolation according to fuzzy and classical conditions. Acta Polytech. Hung. **7**(4), 39–55 (2010)

18. Cohen, R., Peleg, D.: Local spread algorithms for autonomous robot systems. Theoret. Comput. Sci. **399**, 71–82 (2008)

19. Valdastri, P., Corradi, P., Menciassi, A., Schmickl, T., Crailsheim, K., Seyfried, J., Dario, P.: Micromanipulation, communication and swarm intelligence issues in a swarm microrobotic platform. Robot. Auton. Syst. **54**, 789–804 (2006)

20. Nouyan, S., Alexandre Campo, A., Dorigo, M.: Gathering path formation in a robot swarm self-organized strategies to find your way home. Swarm Intell. **2**(1), 1–23 (2008)

21. Kovács, L.: Rule approximation in metric spaces. In: Proceedings of 8th IEEE International Symposium on Applied Machine Intelligence and Informatics SAMI, pp. 49–52. Herl'any, Slovakia (2010)

Intelligent Robot Cooperation with Fuzzy Communication

Á. Ballagi, L. T. Kóczy and C. Pozna

Abstract Designing the decision-making engine of a robot which works in a collaborative team is a challenging task. This is not only due to the complexity of the environment uncertainty, dynamism and imprecision, but also because of the coordination of the team has to be included in this design. The robots must be aware of other robots' actions in order to cooperate and to successfully achieve their common goal. In addition, decisions must be made in real-time and using limited computational resources. In this chapter we propose some novel algorithms for action selection in ambiguous tasks where the communication opportunities among the robots are very limited.

Keywords Fuzzy signatures · Fuzzy communication · Robot cooperation

1 Introduction

Intelligent cooperation is a new research field in autonomous robotics. If one would plan or build a cooperating robot system which has intelligent behaviors, one could not program the all scenarios which may appear in the life of the robots. The problem is more complicated if the robots have to cooperate with a human, where appear some special difficulties i.e. the imperfection of the communication.

Á. Ballagi (✉)
Department of Automation, Széchenyi István University, Győr, Hungary
e-mail: ballagi@sze.hu

L. T. Kóczy
Department of Telecommunications and Media Informatics, Budapest University
of Technology and Economics, Budapest, Hungary
e-mail: koczy@sze.hu

C. Pozna
Department of Informatics, Széchenyi István University, Győr, Hungary
e-mail: pozna@sze.hu

We are investigating such cooperation problems where are not any explicit communication channel between the participants thus there are very weak common communication opportunities. In practical point of view the machine–machine or man–machine cooperative working is a typical case of it if not a special trained person stays on human side.

One of our aims in this research project is to work out soft-computing algorithms that cope with this communication gap and can be a base of an effective working machine–machine or man–machine (man–robot) cooperative group. A challenging strategy is to extract information from observations [1–3]. This strategy is one of the most important cornerstones of a high-end cooperating system. In order to build such a system it is necessary to build up contextual knowledge base which grows by learning from observations. It appears to be very important in the cooperation and communication of intelligent robots or physical agents that the information exchange among them is as effective and compressed as possible [4].

In this chapter we propose a strategy of context understanding on Fuzzy Communication base and information extraction based on an original data structure named the fuzzy signature and on a priori knowledge data base, named the robot codebook. By context we understand the goal of the human and robot activity which involve cooperation, the state of the environment where the cooperation takes place and the task involved in the goal realization.

After an overview of this type of fuzzy communication the chapter will deal with some real scenarios of autonomous mobile robot cooperation.

Research towards extending this fuzzy communication method to more complex robot cooperation is going on currently.

2 Fuzzy Communication of Cooperating Robots

One of the most important parameters of effective cooperation is the efficient communication. Because communication itself very expensive, it is much more advisable to build up as large as possible contextual knowledge bases and codebooks in robot controllers in order to shorten their communication process [5]. That is, if it essentially reduces the amount of information that must be transmitted from one to another, than to concentrate all contextual knowledge in one of them and then to export its respective parts whenever they are needed in other robot(s). It appears to be very important in the cooperation and communication of intelligent robots or physical agents that the information exchange among them is as effective and compressed as possible [4].

2.1 The System in Hand

Let us examine a subset of our overall robot cooperation problem work in practice. There is a warehouse where some square boxes wait for ordering. Various configurations can be made from them, based on their color and tags. We have a group of autonomous intelligent robots which try to build the actual order of boxes according to the exact instructions given to the R0 (foreman) robot. The other robots have no direct communication links with R0, but they are able to observe the behavior of R0 and all others, and they all possess the same codebook containing the base rules of storage box ordering. Every box has an identity color and tag on one side of it. The individual boxes can be shifted or rotated, but always two robots are needed for actually moving a box, as they are heavy. If two robots are pushing the box in parallel the box will be shifted according the joint forces of the robots. If the two robots are pushing in opposite directions positioned at the diagonally opposite ends, the box will turn around the center of gravity. If two robots are pushing in parallel, and one is pushing in the opposite direction, the box will not move or rotate, just like when only a single robot pushes. Under these conditions the task can be solved, if all robots are provided with suitable algorithms that enable intention guessing from the actual movements and positions, even though they might be unambiguous.

Figure 1 presents an example of how five boxes can be arranged. There are just a few essentially different robot positions allowed. Because two robots are needed for pushing or turning a box, at each side of the boxes, two spaces are available for the robots manipulating them: the "counterclockwise position" and the "clockwise position" (see Fig. 2).

Eventually "stopping combination" is mentioned where two robots intend to do a move operation (shift or rotate), and another robot that has recognized the goal box configuration positions itself to prevent a certain move. $C_{1,2,3}^{i} = ST$ is essentially a three robot combination, where either R_1 and R_2 are attempting a shift and R_3 positions itself to prevent it, or R_2 and R_3/R_1 and R_3 are starting a rotation and R_1 and R_2 prevent it, knowing that the intended move is wrong from the point of view of the goal configuration. However, in $C_{1,2,3}^{i} = ST$ it is sufficient that R_1
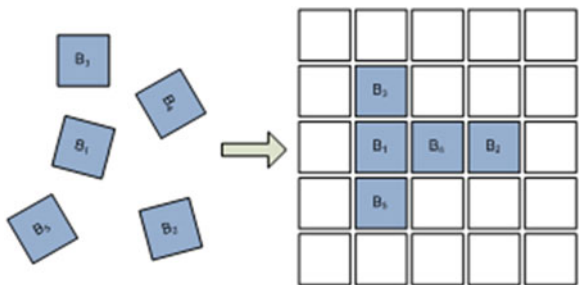

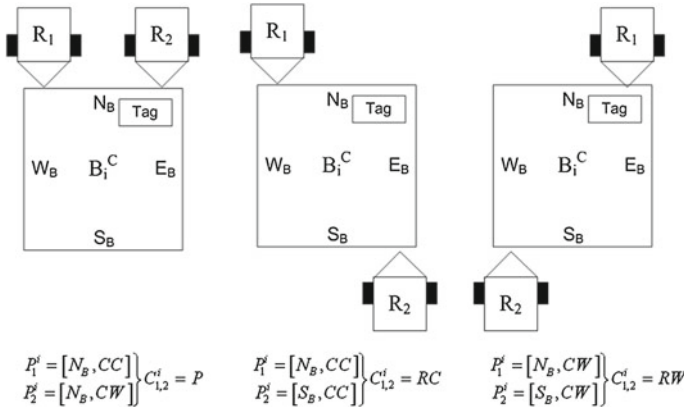**Fig. 1** An example of box arrangement

Fig. 2 Allowed combinations of two robots

takes up its $P_1^i = [N_B, CC]$ position if R_3 is aware that both the shift and the rotate counterclockwise combinations would be wrong from the point of view of the goal, thus R_3 immediately stops the maneuver by assuming the $P_3^i = [S_B, CW]$ position, thus preventing both shift and clockwise rotation. This is an exception where a two robot combination other than the ones listed in Fig. 2 is legal as a temporary combination, clearly signalizing "stop this attempt as it is in contrary to the goal".
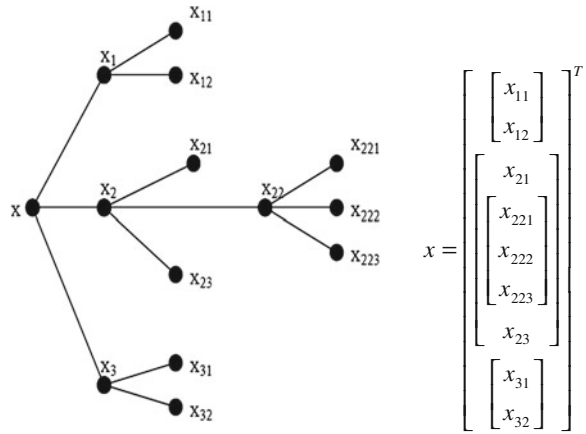
2.2 Fuzzy Signatures

The original definition of fuzzy sets was $A : X \rightarrow [0, 1]$, and was soon extended to *L-fuzzy sets* by Goguen [6]

$A_L : X \rightarrow L$, L being an arbitrary algebraic lattice. A practical special case, *Vector Valued Fuzzy Sets* was introduced by Kóczy [7], where $A_{V,k} : X \rightarrow [0, 1]^k$, and the range of membership values was the lattice of k-dimensional vectors with components in the unit interval. A further generalization of this concept is the introduction of fuzzy signature and signature sets, where each vector component is possibly another nested vector (right).

Fuzzy signature can be considered as special multidimensional fuzzy data. Some of the dimensions are interrelated in the sense that they form sub-group of variables, which jointly determine some feature on higher level [8, 9]. Let us consider an example. Figure 3 shows a fuzzy signature structure.

Here $[x_{11}\ x_{12}]$ from a sub-group that corresponds to a higher level compound variable of x_1. $[x_{221}\ x_{222}\ x_{223}]$ will then combine together to form x_{22} and $[x_{21}\ [x_{221}\ x_{222}\ x_{223}]\ x_{23}]$ is equivalent on higher level with $[x_{21}\ x_{22}\ x_{23}] = x_2$. Finally, the fuzzy signature structure will become $x = [x_{221}x_{222}x_{223}]$ in the example.

Fig. 3 A fuzzy signature structure

$$x = \begin{bmatrix} \begin{bmatrix} x_{11} \\ x_{12} \end{bmatrix} \\ \begin{bmatrix} x_{21} \\ \begin{bmatrix} x_{221} \\ x_{222} \\ x_{223} \end{bmatrix} \\ x_{23} \end{bmatrix} \\ \begin{bmatrix} x_{31} \\ x_{32} \end{bmatrix} \end{bmatrix}^{T}$$

The relationship between higher and lower level is govern by the set of fuzzy aggregations. The results of the parent signature at each level are computed from their branches with appropriate aggregation of their child signature.

Let a_1 be the aggregating associating x_{11} and x_{12} used to derive x_1, thus $x_1 = x_{11}a_1x_{12}$.

2.3 Fuzzy Signature Classes

On basis of the features of the boxes the robot can build a fuzzy signature for each box [10]. This signature built up on a template or class, and every box has its own instance of the Box fuzzy Signature Class (BSC). This signature records the position, the arrangement, the dynamic and the robots working on the actually box. Let us see the construction of this fuzzy signature class. As can be seen in (1), the main signature has three sub-signatures.

$$B_i^c = \begin{bmatrix} P \\ AR \\ DY \end{bmatrix} \tag{1}$$

The first is the position (P) sub-signature which describes the actual fuzzy position of the box (e.g.: Nearly North). It has four leaves namely the points of the compass, North, East, South and West. The box is "in direction" if its reference side lays near to any main compass direction.

It is important that the real position of a box has two other parameters: the latitude and the longitude of its reference point, but it does not have any importance to decision making only in navigation, so we abandon these parameters here.

The second branch of box fuzzy signature is the arrangement that describes the box's connections to other boxes. As it was described above, a box can connect to
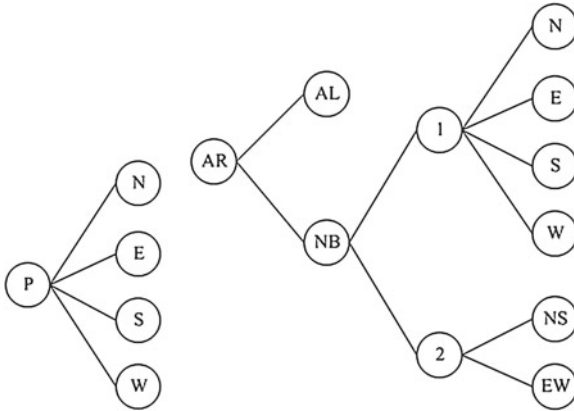
Fig. 4 Box position arrangement fuzzy signature

none, one or two other boxes. Therefore the signature has two main branches for the no connection case, and for the connected case, which has two other branches for connect to one, connect to two boxes.

The leaves describe the side of connection. As we see this signature we can observe that there are some surprising permitted connect positions in it (e.g.: North or tag side). These are very useful for decision making about wrong positions and wrong dynamic of the box. The Fig. 4 presents the arrangement signature (*AR*) where *AL* is the "alone" (no connection) branch, *NB* are the neighbor boxes: one or two and the direction of the join.

The next branch is the dynamic feature (*DY*) of the box, which is valid if robots work on the box and records what the robots are doing: push or rotate, and in which direction. This signature includes all the valid combinations of robots, and all valid movements of boxes.

These three output fuzzy signatures are able to describe the actual states of the box and give a basis for the fuzzy decision process in the robot control. Every robot builds its actual knowledge-base from the fuzzy signature classes and then boxes are assigned individual signatures in each individual robot controller.

The second necessary fuzzy signature class is the Robot state fuzzy Signature Class (RSC), which describes the state of each robot. This represents the dynamic and working behavior of the robot. In this chapter we do not consider the robot signatures in detail because they do not have an important role in the primary decision making.

2.4 Fuzzy Situational Maps

We propose a novel approach to support difficult decision-making and depict situation or context dependent structured data. A special form of fuzzy signatures [8, 11–13] are used, namely the Fuzzy Situational Map (FSM).

The FSM as a two dimensional signature has in each node a fuzzy membership value or a whole fuzzy set. The membership values are changed dynamically by results of some fuzzy observation of environmental situations (context) and inner process states. This map can write down the situation of a complex system in very compact form as shows the Fig. 5.

The most challenging question is how should the node values are changed which moreover depend each other? We investigate more approaches to answer this question.

The results of our solutions are presented on a complex cooperative box pushing assignment where a group of autonomous intelligent mobile robots is supposed to solve transportation problems according to the exact instructions given to the Robot Foreman (RF). The other robots have no direct communication links with the RF and each other, but can solve the task by intention guessing from the actual movements and positions of other robots, even though these simulation might be ambiguous [5, 10, 14]. The basic idea of this application came from the partly unpublished research projects at LIFE [15].

In the above mentioned cooperative robot task some FSMs are used as "Box Settling Map" (SM). The SM depicts the fuzzy plausibility value of a box in each position at goal-area.

The settling-map is a lattice with fuzzy data in each node where each position depicts a fuzzy box-settling plausibility value in [0, 1]. These nodes are as long and wide as a box so each of them is a possible position of a box. The measure of the settling-map is equal to the area of the working arena.

Each robot has the own settling-map which works as a trigger for action and behaviour selection. This settling-map is formed dynamically based on the a priori knowledge and actual observation of the state of the workplace. The Fig. 6 shows a common settling-map in our robot controller.

Fig. 5 A fuzzy situational map

0	0.6	0.7	0	0
0	0.7	1	0.7	0
0.7	1	0.7	0.6	0
0	0	0.6	0	0
0	0	0	0	0

$PV = 0 \rightarrow$ "A box in this position is not to be suffered"

⋮

$PV = 0.5 \rightarrow$ "A box in this position is not my bussines"

⋮

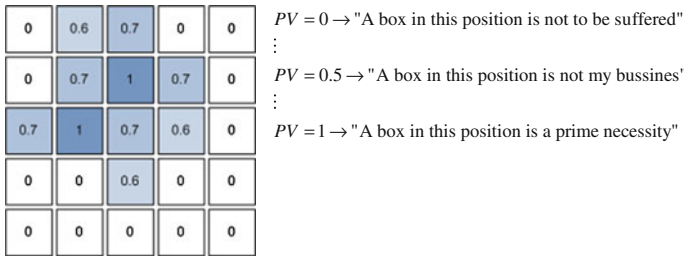$PV = 1 \rightarrow$ "A box in this position is a prime necessity"

Fig. 6 The settling map

2.5 Fuzzy Decision Making

The above described fuzzy signatures enable robots to recognize a situation in the warehouse, and then the robots use their codebooks to take action accordingly. Let us see the codebook, namely a hidden fuzzy decision tree, in the robot controller. For simplicity we have cut the decision tree to sub-trees, and then arranged them in a logical sequence. The robot takes decisions from some simple cases to more complex ones. The Fig. 7 shows the entry point of the decision process. This figure depicts the steps of decision making based on fuzzy signatures, where the diamond shaped objects denote the elementary decisions (decision milestones) and hide the fuzzy signatures that are used. The used and hidden signatures are presented by a grey arrow with the signature name.

It is important to mention here this is only a local task and the final decision making needs the global signatures and other robot signatures, but these are beyond the scope of this chapter. The first step in the local decision is to search for the nearest box, after which the box signature is built up or updated. In the next level, the position of the box is investigated which is described by the P signature. If the membership value of any good direction (N, E, S or W) is high enough, then the decision process steps to the next level and takes the arrangement (AR) and dynamic (DY) signatures of the box, if not then there is a simple decision: the box must rotate. Which direction? This is dependent on the global state of system, which is described by global signatures.

The arrangement and dynamic signatures are used in a partially parallel way. The Fig. 8 shows the whole decision task from this point. The robot analyzes the arrangement and dynamic of the box. If three robots work on it then there is a Stop combination and our robot (Ri) does not have any task on this box, it must search the next box. If two robots work on it and the guessed result points to higher order then Ri leaves it and searches the next near box. If the box has one or two neighbors in a good combination then the membership degree of "on the place" is raised and any dynamic (shift or rotate) is forbidden so if there any robot combination the Ri should go to the Stop position. Of course, if the neighbors of the box are not in a good place then more analysis is necessary to take the appropriate decision. If one robot waits for help there, then Ri decides which is a good position for pushing or turning the
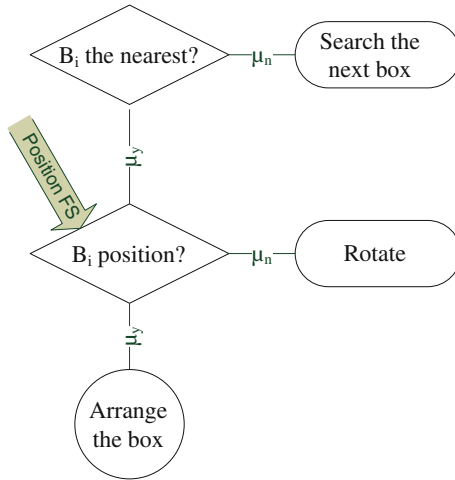
Fig. 7 The entry point of decision task
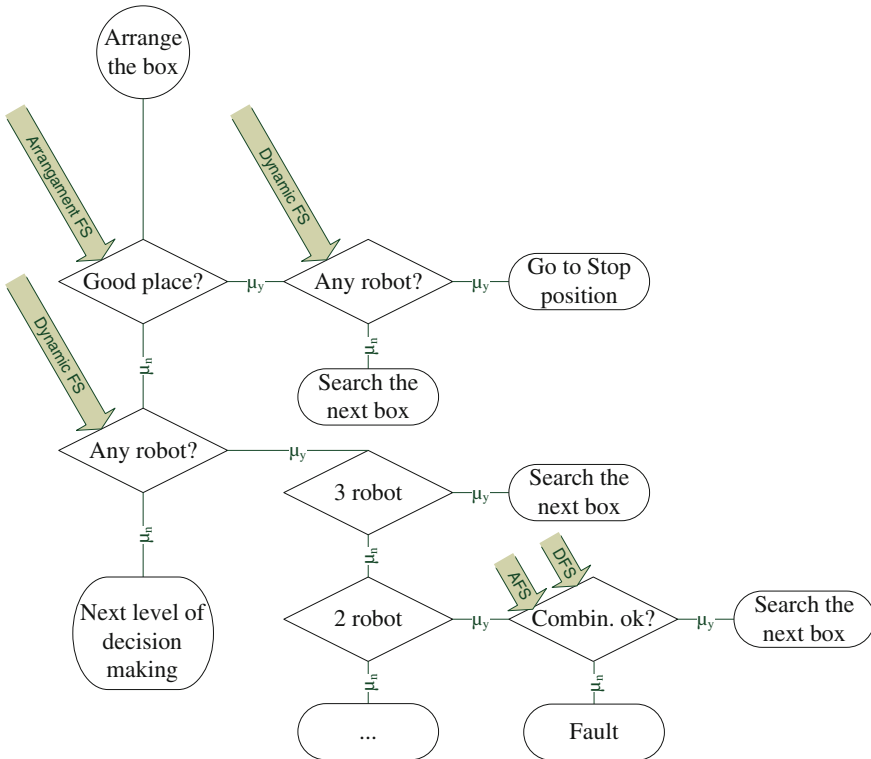
Fig. 8 The decision task
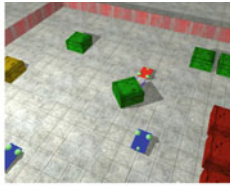
Step 1: The R0 (red) takes a rotating position at one side of a box.
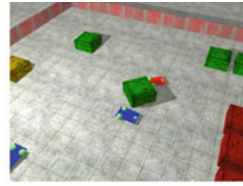
Step 2: The R1 (blue) assistant robot guess the intention of R0 and goes to the rotating position.
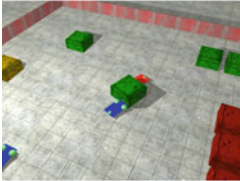
Step 3: The box is rotating.
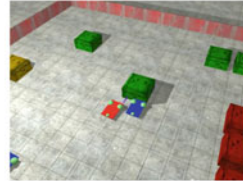
Step 4: The robots take the pushing combination.
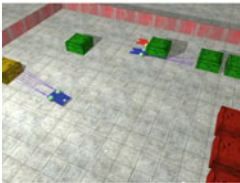
Step 5: The R2 robot, who stayed and collect information about the task as far as here, start to move to the next box in a guessed pushing position.
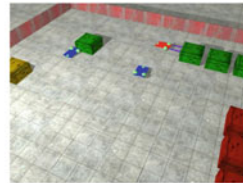
Step 6: The R2 is waiting in its position for a feedback on its intention guessing.
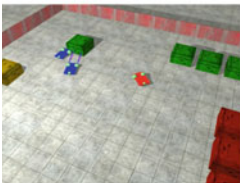
Step 7: The positive feedback is arrived, the R1 takes the combination.

Step 8: The box is pushed, the foreman R0 robot from this point plays only a supervisor role.

Step 9: The two robots get a perpendicular pushing combination and push the box.
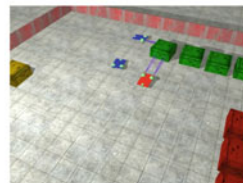
Step 10: The task is finished.

Fig. 9 The settling scenario

box and goes to this position. The most complex decision problem appears when any robot is not at the box; in this case Ri needs to take a decision about the box alone. This higher level problem is not covered in this chapter.

Based on the above considerations it is possible to build some elements of the context and codebook for cooperating robots. It takes the form of a decision tree, where the inputs are the fuzzy signatures of the observations, the first level outputs are intention guesses and the second level outputs the concrete actions of the corresponding robot.

3 A Simulated Scenario

A 3D simulator framework was built where the arena, the boxes and the robot team can be dynamically simulated like in the real box-settling system. This is a physical simulator so the features of elements are very close to substantive parts. The pictures in Fig. 9 depict some steps of a simulated box-settling scenario.

4 Future Works

Our aim is to achieve totally autonomy of robots, which also covers the sensors. Currently, the arena is viewed an overhead camera which broadcast the actual status of the system. Of this replacement to an onboard camera brings with it problems of covering, i.e. no continuous visual information about the events. Such state with incomplete information is need knowledge extrapolation. We investigate using of cognitive extrapolation for these situations, for now being in simulated environment (Fig. 10).

Fig. 10 Master robot with onboard camera

5 Conclusion

In this chapter we presented the usage of fuzzy signature based algorithms on field of mobile robotics. These methods were used in totally other level of robot control. Fuzzy communication contains vague or imprecise components and it might lack abundant information. If two robots are communicating by a fuzzy channel, it is necessary that both ends possess an identical part within the codebook. The codebook might partly consist of common knowledge but it usually requires a context dependent part that is learned by communicating.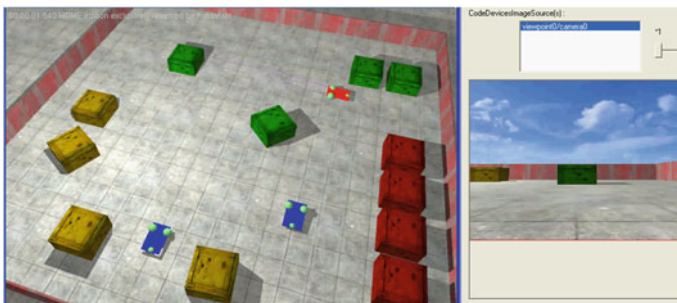 Possibly it is continuously adapting to the input information. If such a codebook is not available or it contains too imprecise information, the information to be transmitted might be too much distorted and might lead to misunderstanding, misinterpretation and serious damage. If however the quality of the available codebook is satisfactory, the communication will be efficient i.e. the original contents of the message can be reconstructed. At the same time it is cost effective, as fuzzy communication is compressed as compared to traditional communication. This advantage can be deployed in many areas of engineering, especially where the use of the communication channels is expensive in some sense, or where there is no proper communication channel available at all.

Here we illustrate clearly that the communication among intelligent robots by intention guessing and fuzzy evaluation of the situation might lead to effective cooperation and the achievement of tasks that cannot be done without collaboration and communication.

References

1. Ballagi, Á., Kóczy, L.T.: Fuzzy communication and cooperation of intelligent mobile robots. In: Proceedings of the Workshop on Cognitive and Eto-Robotics in iSpace (CERiS'10). Budapest (2010)
2. Ballagi, Á., Kóczy, L.T.: Robot cooperation by fuzzy signature sets rule base. In: Proceedings of the 8th IEEE International Symposium on Applied Machine Intelligence and Informatics, (SAMI 2010), pp. 37–42. Herlany, Slovakia (2010)
3. Ballagi, Á., Kóczy, L.T., Pozna, C.: Context recognition in mobile robots cooperation using fuzzy signature. In: Proceedings of the International Conference on Theoretial and Mathematical Foundations of Computer Science (TMFCS), pp. 110–114. Orlando (2010)
4. Kóczy, L.T., Gedeon, T.D.: Context dependent reconstructive communication. In: Proceedings of the International Symposium on Computational Intelligence and Intelligent Informatics, ISCIII, pp. 13–19. Agadir (2007)
5. Ballagi, Á., Kóczy, L.T.: Fuzzy communication in a cooperative multi-robot task. In: Proceedings of the 10th International Carpathian Control Conference, ICCC'2009, pp. 59–62. Zakopane(2009)
6. Goguen, J.A.: L-fuzzy sets. J. Math. Anal. Appl. **18**, 145–174 (1967)
7. Kóczy, L.T.: Vectorial I-fuzzy sets. In: Gupta M.M., Sanchez E. (eds.) Approximate Reasoning in Decision Analysis, pp. 151–156. North Holland, Amsterdam (1982)

8. Wong, K.W., Chong, A., Gedeon, T.D., Kóczy, L.T., Vámos, T.: Hierarchical fuzzy signature structure for complex structured data. In: Proceedings of the International Symposium on Computational Intelligence and Intelligent Informatics (ISCIII), pp. 105–109. Nabeul, Tunisia (2003)
9. Mendis, B.S.U., Gedeon, T.D., Kóczy, L.T.: Investigation of aggregation in fuzzy signatures. In: Proceedings of the 3rd International Conference on Computational Intelligence, Robotics and Autonomous Systems, CIRAS 2005. Singapore (2005)
10. Ballagi, Á., Kóczy, L.T., Gedeon, T.D.: Local codebook construction for fuzzy communication in cooperation of mobile robots. Acta Technica Jaurinensis **1**, 547–560 (2008)
11. Vámos, T., Bíró, G., Kóczy, L.T.: Fuzzy signatures. In: Proceedings of the SIC-EUROFUSE'99, pp. 210–217. Budapest (1999)
12. Gedeon, T.D., Kóczy, L.T., Wong, K.W., Liu, P.: Effective fuzzy systems for complex structured data. In: Proceedings of the IASTED International Conference on Control and Applications (CA 2001), pp. 184–187 (2001)
13. Vámos, T., Kóczy, L.T., Bíró, G.: Fuzzy signatures in data mining. In: Proceedings of the IFSA World Congress and 20th NAFIPS International Conference, pp. 2842–2846. Vancouver (2001)
14. Ballagi, Á., Kóczy, L.T.: Fuzzy signature based mobile robot motion control system. In: Proceedings of the 5th Slovakian—Hungarian Joint Symposium on Applied Machine Intelligence, SAMI: Herlany, pp. 29–33. Slovakia (2008)
15. Terano, T. et al.: Research projects at LIFE, presented at the Laboratory for International Fuzzy Engineering Research, Yokohama (1993)

Indoor Pose Estimation Using 3D Scene Landmarks for Service Robotics

Tiberiu T. Cocias, Sorin M. Grigorescu and Florin Moldoveanu

Abstract In this paper, a markerless approach for estimating the pose of a robot using only 3D visual information is presented. As opposite to traditional methods, our approach makes use of 3D features solely for determining a relative position between the imaged scene (e.g. landmarks present on site) and the robot. Such a landmark is calculated from stored 3D map of the environment. The recognition of the landmark is performed via a *3D Object Retrieval* (3DOR) search engine. The presented pose estimation technique produces a reliable and accurate pose information which can be further used for complex scene understanding and/or navigation. The performance of the proposed approach has been evaluated against a traditional marker-based position estimation library.

Keywords 3DOR · Shape matching · Convexity · 3D descriptors · Indoor robot navigation · Service robotics

1 Introduction

In the last few years, cost attractive and affordable 3D scanning technology has spawned a large number of algorithms developed for the purpose of analyzing 3D visual information. As a consequence, the amount of 3D models and shapes available for benchmarking, both on the internet and in domain-specific databases, has increased significantly [1]. For the common case of robotic navigation, the precise

---

T. T. Cocias (✉) · S. M. Grigorescu · F. Moldoveanu
Departament of Automation, Transilvania University of Brasov, Brasov, Romania
e-mail: tiberiu.cocias@unitbv.ro

S. M. Grigorescu
e-mail: s.grigorescu@unitbv.ro

F. Moldoveanu
e-mail: moldof@unitbv.ro

pose of the robot is mandatory for achieving different imposed goals. Thus, navigation, grasping or obstacle avoidance rely exclusively on the estimated poses [2, 3]. Starting from the presumption that the robot uses only machine vision as a perception mechanism, its pose can be estimated using either 2D features [4], 3D landmarks, or a combination of both [5]. Considering strictly the image domain, the *Pose from Video* (PfV) approach tries to determine the robot's pose by observing the change in image features from subsequent frames. From another point of view, in the same image domain, using a special marker placed in the scene, the pose of the robot can be determined relative to the observed marker [6]. The dimension and the pattern of the marker needs to be a priori established. Further, multiple markers can be used for complex scene understanding or for different robotic tasks. Nevertheless, such a system has little chance to cope with new situations since it is based on artificial visual markers.

In our approach, the issue of pose estimation addresses only 3D features extracted from the imaged scene. In this sense, the problem can be splitted in two main phases. Firstly, the perceived scene is *searched* for similarities against a series of pre-stored scenes scans. Further, in the second phase, using the previously determined similarities, the position and perspective of the robot is estimated. The search process is tackled from the *3D Object Retrieval* (3DOR) point of view. Tasks like 3D object recognition, complex model segmentation or scene reconstruction are investigated from the 3DOR perspective [7, 8]. The main issue related to the 3D object retrieval engines is reduced to the problem of determining the similarity of two given shapes, or surfaces. In literature, there are several methods that deals with 2D contours, 3D surfaces and volumes or shape statistics [9, 10]. To produce correct correspondences, the object retrieval process must follow a validation step. In [11], the validation occurs based on a ratio between two distance samples, whereas in [12], a fast and simple validation algorithm based on the slope of the line connecting the corresponding points is presented. For a more accurate correspondence validation approaches, methods such as the one presented in [13] must be used. The main contribution of our paper is the usage of a 3DOR search engine for retrieving the pose of a robot relative to 3D landmarks.

The rest of the paper is organized as follows. In Sect. 2, the overall machine vision apparatus is presented. In Sect. 3, the proposed pose estimation approach is described, followed by the performance evaluation results given in Sect. 4.

2 Machine Vision Apparatus

The need for robotic *pose* estimation is mandatory for complex scene understanding or for any other further interaction with the environment. The presented approach makes use of previous detected landmarks and their known locations for determining a relative position of the robot with respect to the environment. The block diagram in Fig. 1 depicts the main components of a robotic pose estimation and object modelling
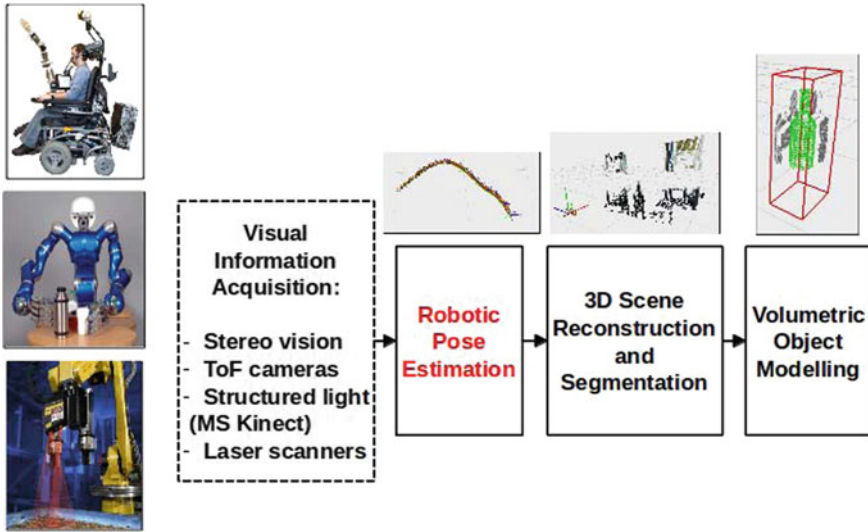
Fig. 1 Processing flow for robotic 3D pose reconstruction and object volumetric modelling in mobile manipulation

flow used in mobile manipulation. The pose of the robot is essential for achieving an easy and secure robotic grasp configuration.

2.1 Shape Recognition Framework

The main objective of the approach is to find the viewed perspective of the scene inside a large scan representation of the location in which the robot navigates. One reliable search method, with the main aim of finding the similarity between two given surfaces, is represented by the *3D Object Retrieval* - 3DOR mechanism [14]. Conceptually, the 3D Object Retrieval method (see Fig. 2) tries to identify a template model (*query*) among a large number of shapes (*targets*). The origin of the technique lies in the abundance of available 3D object representations on the internet. It is used mainly for object recognition and surface reconstruction.

For a large objects database, the algorithm cannot offer real-time model extraction, but it compensates with precision and reliability. As depicted in Fig. 2, the overall structure is coarse divided into two sections: on-line and off-line. The first sub-structure is used to process only variable information, such as templates descriptors extraction, or correspondence identification and validation, whereas the second sub-structure deals with static data such as database models or database descriptors computation. Because a scene is represented by large models, the on-line computation of the scene's descriptors is not feasible. Thus, in pur work, we have calculated
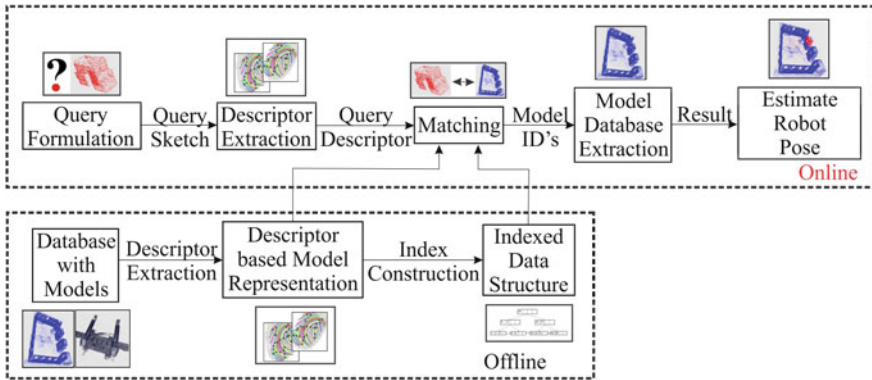
Fig. 2 Generic 3D object retrieval search engine framework

the descriptors off-line. The similarity between the 3D shape models can occur only in the direction of partial matching because the robot cannot perceive the entire backbone structure of the scene's landmarks. Finally, the database target shape with the highest confidence (similarity) is used to estimate the relative pose of the robot.

2.2 Surface Description

The main objective of the 3DOR search engine is to establish valid correspondences between surfaces. Simple and direct point to point surface comparison, based on Euclidean points coordinates, is impossible because of the variable sampling rate or precision of different depth sensors. To overcome this, a *descriptor* can be used to represent the complex surface of each model involved in the process. The *descriptor* has as main purpose the embedment of the surface's geometry in a unique representation [10]. The output description is a histogram which maps a certain surface to a high-dimensional, yet finite, vector space preserving in the same time as much information as possible. In the end, a low-dimension vector (histogram) is constructed.

Shape descriptors can be roughly divided in three main categories: (1) feature based; (2) graph based and (3) other descriptors types. Because of the large occluded regions of the perceived scene, the robot can make use only of feature based descriptors. Further, the feature based descriptors can be divided in the following subcategories: (1) global features; (2) local features; (3) distribution based and (4) spatial maps. For a reliable similarity estimation, only the local features can be used, since in some scenarios, the global structure of the landmark cannot be fully observed by the robotic platform [12]. In this sense, the specific literature points out several local descriptors such as: Signature of Histograms of OrienTations (SHOT) [11], Spin Images [15], Fast Points Features Histograms [16], Spherical harmonics [17], etc.

The descriptor can describe a surface through *signatures* and/or *histograms*. The firs category represents the 3D surface neighborhood of a given point by dening an invariant local *Reference Frame* (RF) and encoding, according to the local coordi-
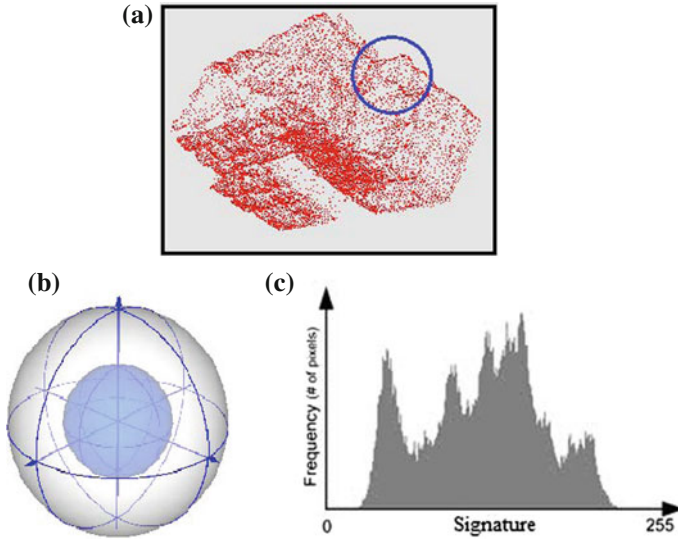
Fig. 3 Encoding a particular local surface using compact *reference frame* and histograms. **a** Input surface. **b** Signature structure. **c** Output histogram

nates, one or more geometric measurements computed individually on each point of a subset of the support. The second category, the local geometry or topology (point count, mesh triangles etc.) is accumulated into a histogram according to a specific quantized domain (e.g. point coordinates, curvatures) which requires the definition of either a *Reference Axis* (RA) or a local RF. For the case of SHOT descriptor [11], the method makes use of both approaches, that is *signatures* and *histograms*, for creating a reliable local surface descriptor. Given the robust RF proposed by the authors and the proper combination of *signatures* and *histograms*, the SHOT descriptor is one of the best choice for representing incomplete surface models. In our work we have used the SHOT descriptor for representing both templates and targets. In Fig. 3, the definition of the RF and histogram generation for a particular surface is presented.

2.3 Shape Similarity by Partial Matching

The robotic platform can perceive the scene from only one perspective. Because of this, a particular landmark can contain large occluded regions, thus making impossible the extraction of any global structural information. By using the local feature based descriptors presented in 2.2, the similarity between two given *point distribution models* (PDM), that is a template and a target, can be evaluated using partial matching.

Table 1 Quality measurements for histogram matching

Distance measure $d(H_1, H_2)$	Mathematical formulation	Exact match	Half match	Total miss-match
Correation coeff.	$d = \dfrac{\sum_i H_1{}^{\cdot}(i) \cdot H_2{}^{\cdot}(i)}{\sqrt{H_1{}'^2(i) \cdot H_2{}'^2(i)}}$ $H_k{}' = H_k(i) - \dfrac{1}{N}(\sum_j H_k(j))$	1.0	0.7	-1.0
ChiSqr	$d = \sum_i \dfrac{(H_1(i) - H_2(i))^2}{H_1(i) + H_2(i)}$	0.0	0.67	2.0
Histogram intersection	$d = \sum_i \min(H_1(i), H_2(i))$	1	0.5	0.0
L1-Norm	$d = \sum_i H_1(i) - H_2(i)$	0.0	–	1.0
L2-Norm	$d = \sqrt{\sum_i (H_1(i) - H_2(i))^2}$	0.0	–	1.0
Battacharyya	$d = \sqrt{1 - \sum_i \dfrac{\sqrt{H_1(i) \cdot H_2(i)}}{\sqrt{\sum_i H_1(i) \cdot \sum_i H_2(i)}}}$	0.0	0.55	1.0

For each point of the model $\mathbf{M} = \{p_0, p_1, \ldots p_i\}$, where $i = 0 \ldots nr\,Points$, a histogram $\mathbf{H}(i)$ describing the neighbor point distribution information is generated. By comparing two given histograms, a similarity measure between the regions can be determined. Further, to compute an overall shape similarity measure, a *brute force matching* technique can be used. The approach searches for each histogram of the *template* model, namely the *target*, which is the most similar histogram inside the second model. The amount of similarity is given by a similarity quality measure, described in the next paragraphs.

Different types of similarity measures can be found in literature. From those we mention the *correlation* coefficient, *ChiSqr* distance, histogram *intersection*, the L1- and L2-*Norm* and the *Battacharyya* distance [18]. Table 1 centralizes the mathematical formulation of each measurement technique.

In Table 1, d is the measured distance, H_1 is a histogram from the template shape, while H_2 is the histogram of the target shape.

Considering the mathematical complexity and the computation time, the L2-Norm is one of the most computational efficient. If the computational time is not an impediment, the Battacharyya distance can be chosen for best precision. The result of the matching process is represented by a vector $\mathbf{C}$ in which the *template* points, represented through histograms, are linked by correspondences (in terms of indexes) with
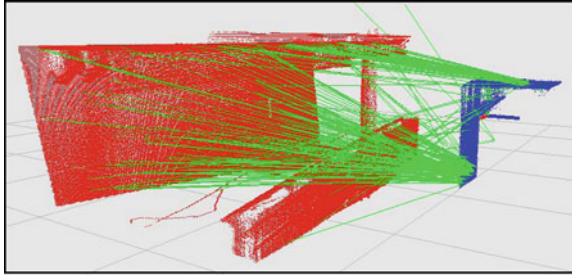
Fig. 4 Correspondences matching example. The *red* points highlight the *target* surface, the *blue* ones the *template* surface, whereas the lines depicting the computed correspondences are *green* (best viewed in color)

the points from the *target* model. Thus, a correspondence *c* is defined as follows:

$$c(i) = \{IDx_{H_1}, IDx_{H_2}\}, \; IDx_{H_1} = 0 \ldots N_{max_{H_1}} \; and \, IDx_{H_2} = 0 \ldots N_{max_{H_2}}, \; (1)$$

where N is the number of points defining each shape (target and template).

Depending on the size of the *reference frame*, defined by the descriptors given in Sect. 2.2, the number of correspondences varies. For regular surfaces the number of correspondences is low. This is because of the ambiguity of the linking process. Figure 4 illustrates the established correspondences for the case of an university lobby scene, where large flat surfaces are present.

As depicted in Fig. 4, not al correspondences are correct. Many of them are pointing to wrong surfaces. This happens because of the flat walls present in the scene. In order to reject all these bad correspondences, special filters, such as the ones described in the next subsection, need to be used.

2.4 Correspondence Validation

The aim of the validation process is to filter out the correspondences pointing to wrong connections between local regions. For a given scene cloud **M**, it is almost impossible to have only discriminative surfaces. The amount of ambiguity is controlled by the size of the RF, which, for the case of a small RF, the number of bad correspondences is high, whereas for a large RF the number is much lower but with the cost of altering the similarity measure. In this paper, two sequential filters are addressed for solving this issues: (1) *neighbour distance validation* and (2) *probabilistic slope filter*.

The first filter aims at keeping only discriminative correspondences. A correspondence $c(i)$ is considered to be discriminative (e.g. *unique*) if, its description $H_1(i)$ produces a *ratio* factor below 0.7 in the target description. This ratio, described by Eq. 2, is formed using the measured similarities with respect to the target model. Since all histograms are normalized, the *ratio* is defined within the interval [0, 1].
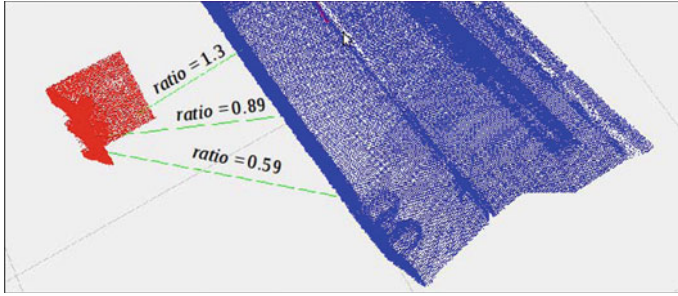
Fig. 5 Different ratio factors for a series of correspondent regions

$$ratio = \frac{dist_{NN}}{dist_{secondNN}}. \tag{2}$$

The two distances involved in the ratio computation are determined as follows. Considering a given template description $H_1(i)$, the question is: which is the most similar correspondent description $H_2(j)$ within all target descriptions. This correspondence $c(i)$ is considered to have the smallest distance (the highest similarity) $dist_{NN}$. Next, hiding the previous correspondent description $H_2(j)$, the $dist_{secondNN}$ is computed by determining which is the next most similar correspondent $H_2(k)$ within all targets, where $j, k = 0 \ldots sizeOf(target)$. Fig. 5 shows the computed target ratios for different regions of the model.

Using this approach, if a given template description, $H_1(i)$, can be found in two different regions, $H_2(j)$ and $H_2(k)$ of the target model, the resulted correspondence will be rejected from the correspondence vector C because the surface is considered ambiguous.

Again, not all remaining correspondences can be considered trustful. Further, the *probabilistic slope filter*, tries to eliminate all cross correspondences. The principle uses the slope attribute to filter out any bad correspondences. The slopes are thus computed using the following equations:

$$m_1 = \frac{[p_1(x) - p_2(x)]}{[p_1(x) - p_2(x)]}, m_2 = \frac{[p_1(z) - p_2(z)]}{[p_1(x) - p_2(x)]} \tag{3}$$

where, m_1 and m_2 are the 2D slopes of the $c(i)$ that respects $m_1, m_2 \in \mathbf{M}$, p_1 is a point in the template model and p_2 is a point belonging to the target model (see Fig. 6). The slope is computed from two 2D perspectives, namely xOy and zOy, as presented in Eq. 3. Using this slopes, a *probabilistic density function* (PDF), as described in Eq. 4 and used to estimate a *pattern* of the slope correspondences. The core of the PDF is actually a *maximum likelihood estimator* (MLE) as the one in Eq. 5
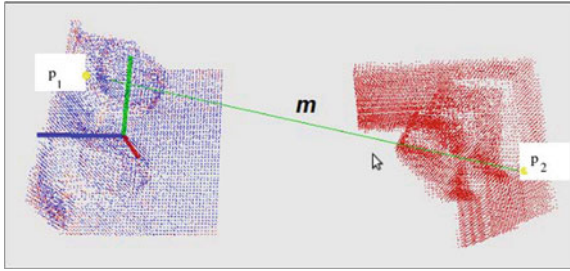
Fig. 6 Correspondence matching example
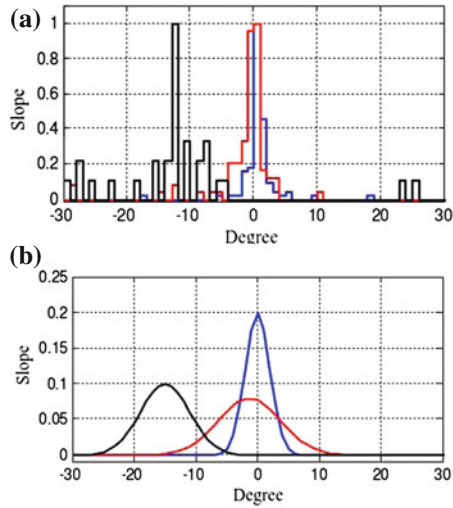
Fig. 7 Probabilistic density function based filtering. **a** Slope data examples. **b** Estimated slope models

$$p(\mathbf{M}|\theta_\mu, \theta_\sigma) \qquad (4)$$

$$\theta = \arg\max_{\theta \in \Theta} L(\theta|\mathbf{M}) \qquad (5)$$

Any correspondence slope exceeding a certain threshold of the standard deviation from the determined Gaussian distribution will be rejected. In order to be able to use this filter the two input shapes, template and target, must be registered in the same coordinate system. In Fig. 7, the extraction of the slope patterns for a given series of three slope distributions can be observed.

The combination of the presented filters produces in the end, only reliable correspondences which can be trustworthy use for further robot pose estimation.

3 *Pose* Estimation Using 3D Landmarks

The position and orientation of the view point focusing the landmark provides all the information needed to estimate the robot's pose. Thus, by relating the pose of the camera sensor to the scene object, an estimated robot position inside a large scene environment can be determined (e.g. the robot is situated at the first room of the 3'rd floor. The goal is to determine the camera pose $\mathbf{C}$ using a set of correspondence points P_i and the camera's intrinsic and extrinsic parameters.

Firstly, the transformation matrix (*homography*) $\mathbf{H}_{R-L}$ between the camera sensor (robot) and the perceived scene (containing the landmark) is used to estimate the rotation $\mathbf{R}_{R-L}$ and the translation $\mathbf{T}_{R-L}$. A transformation $\mathbf{H}_{L-S}$ (see Eq. 6) relating the perceived scene and the global scene is determined from set of minimum 4 points $\mathbf{H}_{L-S}$ [19].

$$\mathbf{H} = \begin{pmatrix} s\mathbf{R} & t \\ 0^{\mathbf{T}} & 1 \end{pmatrix} \tag{6}$$

where $\mathbf{s}$ is the scale factor, $\mathbf{R}$ is the matrix rotation and $\mathbf{t}$ is the translation matrix.

For reducing the search space dimensionality the *Normal Aligned Radial Feature* (NARF) key point extractor is used [20]. The correspondences between the input clouds are computed using the measures from Table 1. Once the pairs of correspondent key points are determined using the *Perspective-N-Point* (PNP) algorithm, the homography $\mathbf{H}_{L-S}$ between the visible part of the scene and the scene itself is obtained. This is actually a rough transformation used to align the robot's perspective to the overall scene. An *Iterative Closest Point* (ICP) determines next a fine clouds alignment. Thus, the robot's pose is obtained from three homography matrices (see Eq. 7), namely, the homography between the robot and the imaged surface, the one between the seen surface and the overall scene and, in the end, the homography $\mathbf{H}_{ICP}$ generated by the ICP alignment.

$$\mathbf{H}_{robot} = \mathbf{H}_{R-L} * \mathbf{H}_{L-S} * \mathbf{H}_{ICP} \tag{7}$$

4 Experimental Results

4.1 Scene Set-up

For evaluation purposes, different indoor robot navigation scenarios have been considered. For imaging the scene, the robot was equipped with a Kinect® RGB-D sensor. To create the *target* models, e.g virtual scans of different chambers scenes, a SICK LMS500 laser scaner was used. Two target models were used in this sense: a chamber from the *Machu Picchu* temple (see Fig. 8) and a lobby from a public building, e.g. university building (see Fig. 9).
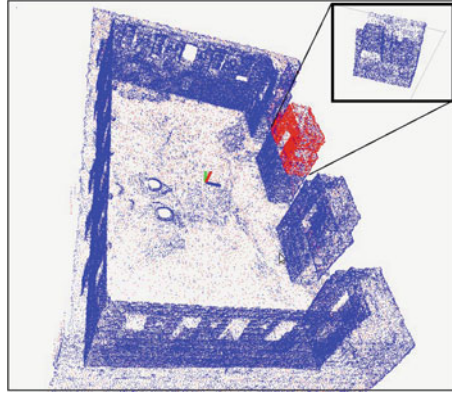
Fig. 8 Identifying a specific region inside a target. The corresponding points between the template and the target are marked with *red*, whereas the target points are *blue*
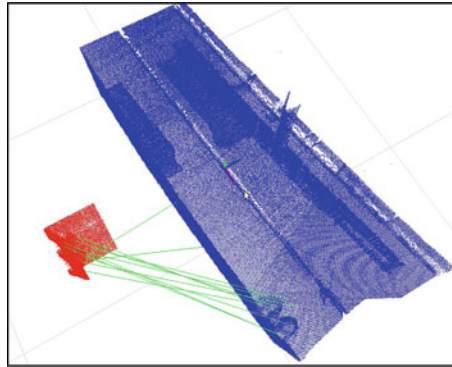
Fig. 9 Identifying a specific region inside a target. The template model (air-vents) is shown in *red* whereas the lobby target model is *blue*. The *green lines* depict the correspondences between the presented models (best viewed in color)

The similarity between the scene perspective and the database targets was performed using the L2-Norm, while the correspondences were validated via the neighboring distance quality measure and probabilistic slope filter, were used. Each surface was represented by a SHOT descriptor. For evaluation purposes, an ARToolKIT® based marker detection approach was used for obtaining a parallel estimate of the robot's pose with respect to artificial ARToolKIT landmarks.

A particular region was cropped for a known position inside the *Machu Picchu* temple chamber. Next, using the proposed approach, the cropped region (now considered to be the *template*) was searched inside all defined *targets* (monument chambers stored in a database). In terms of correspondences dimensionality, the template, or query, was represented by 12.721 points, whereas the target model was defined by 245.685 points. Figure 9 illustrates the result of the first matching scenario.

Table 2 Measured errors for different robot pose estimation scene

Scene	Method	Pose errors					
		x (mm)	y (mm)	z (mm)	pitch (○)	yaw (○)	roll (○)
Machu Picchu	Our approach	8.89	33.58	15.12	2.54	1.39	3.78
	ARToolKit	–	–	–	–	–	–
Lobby	Our approach	11.25	32.79	21.35	3.98	2.69	3.36
	ARToolKit	10.64	28.56	15.25	2.25	1.97	2.78

The highest density of valid correspondences defined the visible part of the landmark, which was used for estimating robot's pose. Numerical error results are given in Table 2.

Considering the case of a real robotic scenario, a particular region, depicting two distinctive air-vents, were perceive inside an university lobby. The algorithm's configuration was identical to one used in the *Machu Picchu* test scenario. From a total of 4897 searched points, describing the template model, 8 valid correspondences and 2 outliers were found inside of 2.798.245 scene points, as shown in Fig. 9.

As seen in Table 2, the presented approach outputs an overall error below 5 % for any measured parameter. Because the *Machu Picchu* dataset is a standard evaluation scene [21], no ARToolKit ground truth information could be provided. The position of the robot was determined relative to the closest landmark sensed by the sensor.

5 Conclusions

In this paper, a 3DOR engine based robotic pose estimation technique has been proposed. The goal of the approach is to enable accurate pose estimation using only 3D visual information extracted directly from the imaged scene. Along with this approach, two correspondence filters were integrated within the 3DOR method. The filters produce dense and accurate correspondences which can be further used for 3D shape recognition or pose estimation. As future work the authors consider the enhancement of the computation time through parallel computational devices (e.g. Graphic Processors), as well as the application of the method to other computer vision areas, such as 3D medical imaging.

References

1. Shilane, P., Min, P., Kazhdan, M., Funkhouser, T.: The Princeton Shape Benchmark. Shape Modeling International June (2004)
2. Grigorescu, S.M., Macesanu, G., Cocias, T.T., Puiu, D., Moldoveanu, F.: Robust camera pose and scene structure analysis for service robotics. Robot. Auton. Syst. **59**, 899–909 (2011)

3. Grigorescu, S.M.: On robust 3D scene perception and camera egomotion estimation. In: Proceedings of the 33rd Colloquium of Automation, Leer, Germany (2011)
4. Grinstead, B., Koschan, A., Gribok, A., Abidi, M.A., Gorsich, D.: Outlier rejection by oriented tracks to aid pose estimation from video. Pattern Recogn. Lett. **27**(1), 37–48 (2006)
5. Grigorescu, S.M., Pangercic, D., Beetz, M.: 2D–3D Collaborative tracking (23CT): towards stable robotic manipulation. In: Proceedings of the 2012 IEEE International Conference on Intelligent Robots and Systems IROS, Workshop on Active Semantic Perception, Vilamoura, Algarve, Portugal (October 7–12, 2012)
6. Malbezin, P., Piekarski, W., Thomas B.: Measuring ARToolKit accuracy in long distance tracking experiments. 1st International Augmented Reality Toolkit Workshop, Darmstadt, Germany (2002)
7. Sebastian, T.B., Klein, P.N., Kimia, B.B.: Recognition of shapes by editing shock graphs. ICCV. **1**, 755–762 (2001)
8. Hartley, R.I.: An object-oriented approach to scene reconstruction. IEEE International Conference on Systems, Man, and Cybernetics, New York, **4**, 2475–2480 (1996)
9. Zhang, H., Fiume, E.: Shape matching of 3-D contours using normalized fourier descriptors. Proceedings of the Shape Modeling, international (SMI02), 261–268 (2002)
10. Tangelder, J.W., Veltkamp, R.C.: A survey of content based 3D shape retrieval methods. Multimedia Tools Appl. **39**(3), 441–471 (September 2008)
11. Tombari, F., Salti S., Di Stefano, L.: Unique signatures of histograms for local surface description. 11th European Conference on Computer Vision (ECCV), Hersonissos, Greece, 356–369 (September 5–11, 2010)
12. Heider, P., Pierre-Pierre, A., Li, R., Grimm, C.: Local shape descriptors, a survey and evaluation. Eurographics Workshop on 3D Object Retrieval, 49–57 (2011)
13. Cech, J., Matas, J., Perdoch, M.: Efficient sequential correspondence selection by cosegmentation. IEEE Trans. PAMI **32**(9), 1568–1581 (2010)
14. Min, P., Halderman, J.A., Kazhdan, M., Funkhouser, T.A.: Early experiences with a 3D model search engineering. Web3D, Symposium, 7–18 (2003)
15. Johnson, A.E.: Using spin images for efficient object recognition in cluttered 3D scenes. IEEE Trans. PAMI **21**(5), 433–449 (1999)
16. Rusu, R.B., Blodow, N., Beetz, M.: Fast point feature histograms (FPFH) for 3D registration. In: Proceedings of the IEEE international conference on Robotics and Automation (ICRA'09) IEEE Press. Piscataway, NJ, USA, 1848–1853 (2009)
17. Sajjanhar, A., Lu, G., Zhang, D., Hou, J., Zhou, W., Chen, P.: Spectral shape descriptor using spherical harmonics. Integr. Comput.-Aided Eng. **17**(2) 167–173 (April 2010).
18. Bhattacharyya, A.: On a measure of divergence between two statistical populations defined by their probability distributions. Bull. Calcutta Math. Soc. **35**, 99–109 (1943)
19. Hartley, R., Zisserman, A.: Multiple View Geometry in Computer Vision. Cambridge University Press, Cambridge (2004)
20. Steder, B., Rusu, R.B., Konolige, K., Burgard, W.: NARF: 3D range image features for object recognition. International Conference on Intelligent Robots and Systems (2010).
21. Computer Modelling of Heritage [online] Available: http://www.cast.uark.edu/home/research/archaeology-and-historic-preservation/archaeological-geomatics/archaeological-laser-scanning/laser-scanning-at-machu-picchu.html (2012)

Part VI
Data Manipulation

A Novel View of Bipolarity in Linguistic Data Summaries

Janusz Kacprzyk, Sławomir Zadrożny and Mateusz Dziedzic

Abstract The problem of data summarization of a set of (numeric) data, notably a (relational) database is dealt with. We are concerned with how to devise a short, (quasi) natural language summary, in the form of a sentence, which would best grasp the very content of the set of data. For instance, for a personnel database with records corresponding to particular employees who are described by attributes like age, sex, salary, etc., such a linguistic summary with respect to age may be "most employees are middle aged". We use as a point of departure a fuzzy logic based approach to linguistic summarization originated by Yager, and then developed by Kacprzyk and Zadrożny who have also indicated—first—an intrinsic connection between linguistic summarization and fuzzy querying, and—second—a crucial role of protoforms in Zadeh's sense. The second point of departure is the concept of a bipolar query in the sense that the querying criteria may be mandatory and optional, i.e. those which must be satisfied and those which should be satisfied if possible, as initiated by Zadrożny, and then developed by Zadrożny, Kacprzyk and De Tré. In this paper we present the concept of a bipolar linguistic summary that combines the very concepts of a linguistic summary with that of bipolarity in the above sense, and also an analogous relation between the linguistic summaries and bipolar queries.

J. Kacprzyk (✉) · S. Zadrożny · M. Dziedzic
Systems Research Institute, Polish Academy of Sciences, ul. Newelska 6, 01-447 Warsaw, Poland
e-mail: kacprzyk@ibspan.waw.pl

S. Zadrożny
Warsaw School of Information Technology, ul. Newelska 6, 01-447 Warszawa, Poland
e-mail: zadrozny@ibspan.waw.pl; zadrozny@wit.edu.pl

J. Kacprzyk
PIAP–Industrial Research Institute of Automation and Measurements, Warsaw, Poland

M. Dziedzic
Department of Electrical and Computer Engineering, Cracow University of Technology, Cracow, Poland

1 Introduction

In a general quest for an effective and efficient inclusion of elements of natural language in all kinds of ICT related tasks, which is related to a wide acceptance and proliferation of the idea of human centric (centered) systems, an important role within data mining (knowledge discovery) is played by *linguistic data summarization*, introduced by Yager [1, 2], and in particular in its implementable version proposed by Kacprzyk and Yager [3], and Kacprzyk et al. [4].

Data querying and data mining may be seen as closely related but somehow opposite paradigms. The former is concerned with the retrieval of pieces of data satisfying the user's interests, intentions and preferences while the latter is concerned with the finding of non-trivial, interesting to the user, regularities in data that are exhibited in general by the pieces of data. In a specific data mining technique of *linguistic data summarization* there is an essential conceptual and algorithmic overlap in the structure of summaries and *fuzzy linguistic queries*.

A characteristic feature of both linguistic data summaries and fuzzy linguistic queries is their use of elements of natural language. The essence of the former is the use of natural language to describe characteristic features of a data set. The latter makes it possible for the user to express his or her preferences (conditions) as to the data sought using terms of natural language what is arguably often more convenient than using artificially and inadequately precise constraints. In our previous work, cf. e.g. [5–7], we have been trying to find ways to exploit this close relationship between both techniques, and within this framework we have notably proposed an interactive approach to deriving the linguistic data summaries [8, 9].

Recently [10] some attempts have been undertaken to make fuzzy linguistic queries even more human consistent in their representation of user preferences through the concept of *bipolar queries* in order to grasp the positive and negative assessments of data which are not necessarily complements of each other and expose strong attitudinal aspects. The bipolar queries may be considered in their most general form as consisting of two conditions separately accounting for these positive and negative assessments, the so-called *pros* and *cons*. However in the literature a specific interpretation of bipolar queries seems to prevail so far in which the negative and positive conditions correspond to a *wish* and *constraint*, respectively.

In this paper, we look for an extension of the concept of linguistic summaries which would exploit a relation to bipolar queries in the vein of a conceptually similar relation of linguistic summaries to fuzzy linguistic queries.

Basically, we introduce some new types of bipolar linguistic summaries of the following main types;

- Simple bipolarity-related summaries as, e.g.: "There are *young* employees earning a *high* salary",
- Bipolar circumstantial linguistic summaries as, e.g.: "Most employees are *young* and *if realistic, with respect to their department mates*, earn a *high* salary",
- Bipolar multilevel linguistic summaries as, e.g.: Most departments employ *young and possibly highly paid* employees".

We provide an in depth analysis of the determination of truth value of such classes of linguistic data summaries, as well as a logical and aggregation focused analysis of them.

Therefore, the purpose of the paper is to propose a novel concept of a bipolar linguistic summary with the "and possibly" operator, dealt with in the context of an intrinsic relation between the linguistic summaries and bipolar fuzzy querying. For clarity we propose here only qualifier-free versions of the bipolar linguistic summaries but an extension by including qualifiers is relatively straightforward. Basically, due to space limitations, we concentrate on a more general and conceptual analysis leaving a more technical discussion to forthcoming papers.

2 Fuzzy Querying and Linguistic Data Summaries: An Intrinsically Close Relationship

As we have already mentioned in Sect. 1, a key feature that has been proposed and advocated by us for years has been an intrinsic relationship between the essence, and derivation of linguistic data summaries and fuzzy querying (with fuzzy linguistic quantifiers). These issues will now be briefly discussed.

2.1 Fuzzy Linguistic Queries

The beginning of the process of database querying is when the user's expresses preferences and intentions are specified as to what is intended, or is interesting to be found. In our context, when a relational database model is employed, these are expressed in terms of preferred or intended values and/or relations of data. As it is normal in any human centric process, i.e. when a human being is a key element, those preferences/intentions are initially expressed in the form that is the only fully natural for a human being, i.e. in natural language. Of course, some conditions may be precise and then they may easily be expressed in a standard database querying language, notably in SQL.

However, in virtually all cases concerning human specific, non-trivial issues, this may be difficult. For instance, a request like: "give me all points in the watershed of a river with a *serious pollution*" may require some non-standard aggregation of conditions that go beyond the standard conjunction or disjunction of a number of

some elementary conditions, e.g. the exceeding of threshold values of some basic water pollution indicators. As proposed by Kacprzyk, Zadrożny and Ziółkowski [11, 12], fuzzy logic can come here to the rescue, and can provide tools and techniques to represent and process linguistic terms such as "cheap", "low" or "most", and then to extend a query language so as to allow for the use of these linguistic terms. Basically, the terms such as "cheap" are represented by fuzzy predicates while the terms such as "most" are represented by *linguistic quantifiers* [13]. The fuzzy linguistic query interfaces are based on the dictionaries of such linguistic terms, cf., e.g. [14].

2.2 Linguistic Data Summaries

The idea of linguistic data summarization has been originally proposed by Yager [1, 2] and further developed notably by Kacprzyk and Yager [3], and Kacprzyk, Yager and Zadrożny [4, 15]. The essence of linguistic data summaries is that a set of data, for instance concerning employees, with (numeric) data on their age, sex, salaries, etc., can be linguistically summarized with respect to a selected attribute or attributes, say age and salaries, by *linguistically quantified propositions* in the sense of Zadeh [13] exemplified by

$$\textit{Almost all} \text{ employees are } \textit{well qualified} \tag{1}$$

or

$$\textit{Most young} \text{ employees earn } \textit{high salary} \tag{2}$$

For our purposes it is expedient to consider the linguistic summaries in the following relational database related context (cf. Kacprzyk and Zadrożny [4, 14]) :

- $R = \{t_1, \ldots, t_n\}$ is a set of the tuples (a relation R) in a database, representing, e.g. a set of employees;
- $A = \{A_1, \ldots, A_m\}$ is a set of attributes characterizing relation R, e.g. salary, age, etc. in a database of employees, and $A_j(t_i)$ denotes a value of attribute A_j for tuple t_i.

Then, a linguistic summary of set R is a linguistically quantified proposition such as (1) or (2) which may be treated as instantiations of an abstract Zadeh's [16] *protoform* (cf. Kacprzyk and Zadrożny [14] for details), respectively:

$$Q_{t \in R} \ S(t) \tag{3}$$

and

$$Q_{t \in R} \ (U(t), S(t)) \tag{4}$$

where the predicates S and U correspond to conditions (preferences/intentions of the user) formed using some (combination of) attributes from A.

A linguistic summary is composed in general of:

- A summarizer S, a fuzzy predicate representing an expression like "an employee is well qualified";
- A qualifier U, optionally, another fuzzy predicate determining a fuzzy subset of R (e.g. a set of "young employees") further restricting the scope of the summarizer;
- A linguistic quantifier Q, e.g. "most", representing the proportion of tuples satisfying the summarizer (optionally, among those satisfying a qualifier);
- truth (validity) T of the summary, i.e. a number from the interval [0, 1] assessing the truth (validity) of the summary (e.g. 0.7); it can be determined using many different models of linguistic quantifiers, notably that proposed by Zadeh [13].

Using Zadeh's fuzzy logic based calculus of linguistically quantified propositions, a (proportional, nondecreasing) linguistic quantifier Q is assumed to be a fuzzy set in [0, 1] and then

$$\text{truth}(Q_{t \in R} S(t)) = \mu_Q \left[\frac{1}{n} \sum_{i=1}^{n} \mu_S(t_i) \right] \tag{5}$$

and

$$\text{truth}(Q_{t \in R}(U(t), S(t)) = \mu_Q \left(\frac{\sum_{i=1}^{n} (\mu_U(t_i) \wedge \mu_S(t_i))}{\sum_{i=1}^{n} \mu_U(t_i)} \right) \tag{6}$$

Protoforms, in the sense of Zadeh [17], are more or less abstract prototypes (templates) of a linguistically quantified proposition. The most abstract protoforms correspond to (3) and (4), while (1) and (2) are examples of fully instantiated protoforms. Thus, protoforms form a hierarchy, where higher/lower levels correspond to more/less abstract protoforms. Going down this hierarchy one has to instantiate particular components of (3) and (4), i.e., Q, and S and U.

A protoform may provide a "stepping stone" (guiding paradigm) for an interactive user interface for the mining of linguistic summaries as proposed by Kacprzyk and Zadrożny [8, 9] who assume that the user provides a protoform of a summary intended. The system is meant as an extension of a fuzzy linguistic querying interface and is equipped with a dictionary of linguistic terms, mentioned in Sect. 2.1. Then, the system generates and tests linguistic summaries in the context of a given database which result in various instantiations of the protoform provided, using different combinations of linguistic terms from the dictionary.

The user is presented with those summaries which verify the validity to a degree higher than some threshold. The more abstract protoform the more instantiations are possible and the resulting summaries are potentially more interesting while the computation costs are higher.

The linguistic summaries, such as (1, 2), are easily comprehensible for a human being in their "raw" form and may be potentially highly informative. Their linguistic sophistication may be still further enhanced with the use of natural language generation (NLG) techniques as proposed by Kacprzyk and Zadrożny [7].

3 Bipolar Queries: A Way to Handle Bipolarity in User Preferences/Intentions

The user's preferences (and intentions), which are the crucial elements any querying process is based upon, may be complex and difficult to formalize even with the use of fuzzy tools and techniques as summarized in Sects. 2.1, 2.2. Some studies, cf. Dubois [18], show that while expressing preferences a human being is separately considering *positive* and *negative* aspects of a given option (here: a piece of data). Thus, in general a query should be considered as a combination of two conditions whose essence is: the satisfaction of one of them makes a piece of data desired, or to be accepted, while the satisfaction of the second makes it to be undesired, i.e. to be rejected. The former is termed a positive and the latter a negative condition. We will refer to such a query as a *bipolar query*—for a general approach to such bipolar queries, cf. [19]).

To be more specific, here we consider a special class of bipolar queries in which the positive and negative conditions are interpreted in a specific way. Namely, the data items sought have to satisfy the complement of the latter conditions unconditionally, while the former conditions are of a somehow secondary importance. For example, a house the user is looking for may have to be cheap, and then among such houses those which are close to a bus stop may be preferred. The negative condition is here "not cheap" while the positive condition is "close to a bus stop". The complement of the negative condition (denoted C) may therefore be interpreted as a *required* condition while the positive condition is expressed directly, referred to as a *desired* condition (denoted P); the whole query is denoted (C, P). Both conditions are generally fuzzy and may be identified with fuzzy sets, with the membership functions denoted μ_C and μ_P, respectively.

The evaluation of a bipolar query results therefore in two membership (matching, satisfaction,…) degrees $(\mu_C(t), \mu_P(t))$ for each tuple t, and to make the concept of bipolar queries operational we have to adopt or devise some method to compare such pairs of membership degrees. Following Lacroix and Lavency [20], Yager [21, 22] and Bordogna and Pasi [23], we model the interaction between the required and desired conditions using the "and possibly" operator casting the whole bipolar query condition in the following form:

$$C \text{ and possibly } P \tag{7}$$

which may be exemplified, referring to the previous example, by:

$$cheap \text{ and possibly } close\,to\,a\,bus\,stop \tag{8}$$

The essence of the "and possibly" operator consists in taking into account the whole dataset while combining the matching degrees related to the required and desired conditions. Yager [22] refers to P as a *possibilistically qualified criterion* which is intuitively characterized as one which should be satisfied unless it *interferes*

with the satisfaction of C. This is in fact the essence of the aggregation operator "and possibly" as we understand it here. Namely, if there is a piece of data which satisfies both conditions, then and only then it is actually *possible* to satisfy both of them and each piece of data has to meet both of them. Thus, the (C, P) query reduces to the usual conjunction $C \wedge P$. On the other hand, if there is no such a piece of data, then it is *not possible* to satisfy both conditions and the desired one can be disregarded. Thus, the (C, P) query reduces to C.

These are however two extreme cases and actually it may be the case that the two conditions may be simultaneously satisfied to some degree lower than 1. Then, the matching degree of the (C, P) query against a piece of data is between its matching degrees of $C \wedge P$ and for C which may be formally written, for the crisp case, as [20]:

$$C(t) \, and \, possibly \, P(t) \equiv C(t) \wedge (\exists s (C(s) \wedge P(s)) \Rightarrow P(t)) \tag{9}$$

and for the fuzzy case as [24, 25]:

$$\text{truth}(C(t) \, and \, possibly \, P(t))$$
$$= \min(\mu_C(t), \max(1 - \max_{s \in R} \min(\mu_C(s), \mu_P(s)), \mu_P(t))) \tag{10}$$

where R denotes the whole dataset (relation) being queried.

The value of

$$\max_{s \in R} \min(\mu_C(s), \mu_P(s)), \text{ denoted as } \exists CP \tag{11}$$

which expresses the truth of $\exists s(C(s) \wedge P(s))$, may be treated as a measure of the above mentioned interference of P with C.

The formula (10) is derived from (9) using the classic fuzzy interpretation of the logical connectives via the maximum and minimum operators. In Zadrożny and Kacprzyk [25] we analyze the properties of the counterparts of (10) obtained by using a broader class of the operators modeling logical connectives.

4 Bipolarity in Linguistic Summaries: A Rationale

First, notice that a straightforward use of (7) to instantiate the summarizer in the protoforms (3)–(4), and its interpretation via (9), does not make much sense because (7) may be appropriate to represent preferences of the user (as exemplified by (8)) but not properties of the data in a summary. Obviously, the user may be unaware of an interference between C and P with respect to the content of a database queried but the system generating a summary is "aware" if such an interference occurs.

For instance, "*Most* of the employees are *young* and possibly earn a *high* salary" is meaningless as a summary if it is known that there is or is not such an interference. However, we will show that knowledge of such an interference may often

be interesting, and that a slight modification to (9) may give rise to some forms of bipolar type linguistic summaries related to the "and possibly" operator.

4.1 Simple Bipolarity-Related Summaries

We assume an *interactive* approach to the generation of linguistic summaries, as mentioned in Sect. 2.2, possibly augmented with some additional statistics obtained from the database management system. In case of bipolar queries these statistics can easily yield the $\exists C P$ coefficient (11) so that the system can immediately generate a summary of the form:

It is possible to satisfy simultaneously conditions C and P

which may be phrased by the postulated use of the NLG techniques (cf. Sect. 2.2) of the system in a slightly different way depending on the semantics of the predicates C and P what may be exemplified for the personnel database as follows:

There are *young* employees earning a *high* salary.

This shows that it makes sense to instantiate Q in the protoform of linguistic summaries $Q_{t \in R} S(t)$ (in $Q_{t \in R}(U(t), S(t))$, too) also with the existential quantifier $\exists$. This makes sense particularly in the case of semantically "conflicting" C and P. By the way, it should be observed that the lack of such a summary among those generated by the system (due to its low validity degree) may also be valuable by showing such a conflict which need not be obvious to the user.

4.2 Bipolar Circumstantial Linguistic Summaries: The Case of a Local "and possibly" Operator

In this subsection we will propose a novel type of a bipolar linguistic summary called a *bipolar circumstantial linguistic summary*. Its essence and rationale may be related to what we have noticed in the beginning of Sect. 4 that the assumed interpretation of the proposition "C and possibly P" does not make it a good candidate for a summarizer. This can be alleviated by introducing another version of the "and possibly" operator such that "possibly" in the "and possibly" interpretation, refers to a *part* of the database rather than the whole database and, moreover, let us make this part dependent on the tuple considered.

To decide if the simultaneous satisfaction of both C and P is possible, we now check only a subset of the tuples and this subset will be defined locally, separately for each tuple. For instance, assume that a company is divided into departments and each employee is assigned to one of them. Then, in the linguistic summary:

> Most employees are *young* and possibly *with respect to their*
> *department mates* earn *high* salary $\qquad(12)$

the summarizer "*young* and possibly *with respect to their department mates* earns *high salary*" should be meant satisfied by an employee if:

1. he or she is young (to a high degree) and earns a high salary (to a
   high degree), or $\qquad(13)$
2. he or she is young (to a high degree) and there is no other employee
   in his or her department who is both young and earns a high salary.

Such a summary is now clearly meaningful and potentially useful.

In general, such a circumstantial bipolar linguistic summary may be written as

$$C \text{ and, circumstances permitting, } P \qquad(14)$$

in which the term "and, circumstances permitting" is equal to "and possibly, with respect to their department mates" in the summary (12).

This new version of the "and possibly" operator, the circumstantial 'and possibly' operator, may also be referred to as a "local 'and possibly' operator" (cf. Dziedzic et al. [26]). It now involves three arguments C, P and W, i.e.:

$$C \text{ and possibly } P \text{ with respect to } W \qquad(15)$$

where the predicates C and P should be interpreted, as previously, as representing the required and desired conditions, respectively, while the predicate W denotes the set of tuples relevant/similar/…to a given tuple and establishes a reference set to decide if the simultaneous satisfaction of C and P is possible.

Then, the formula (15) is interpreted as:

$$C(t) \, and \, possibly \, P(t) \text{ with respect to } W$$
$$\equiv C(t) \land \exists s (W(t, s) \land C(s) \land P(s)) \Rightarrow P(t) \qquad(16)$$

In the case of our example, C and P represent the properties of being young and earning high salary, respectively, while W denotes the relation of working in the same department, i.e., $W(t, s)$ is true if both tuples represent employees working in the same department. Here W is a crisp predicate but may be fuzzy too, e.g. we could modify example summary (12) in the following way:

> Most employees are *young* and possibly *with respect*
> *to similarly educated colleagues* earn *high* salary.

and then W may be a fuzzy relation based on the attribute representing the level of education of the employees and expressing to which degree they are similar (e.g. M.Sc. may be treated as similar to B.Sc. to a degree 0.6 etc.).

And, again, it should be stressed that we follow here an interactive approach to linguistic summarization which seems to be the most promising in the case of bipolar linguistic summaries, too. Thus, the choice of C, P and W is up to the user.

4.3 Bipolar Linguistic Summaries with a Grouping Based "and possibly" Operator

In general both the traditional (non-bipolar) linguistic summaries and bipolar linguistic summaries introduced in the preceding subsections, concern individual tuples, that is, capture properties shared by a majority of tuples in the database.

However, it may be even more interesting to form summaries concerning some sets of tuples as, for instance, in:

Most departments employ *young* and earning *high* salaries employees.   (17)

or

In almost all Asian cities most of the hotels are *moderately priced* and *comfortable*.
(18)

in which we have an "outer", concerning the groups of the tuples, and an "inner", related to the tuples in a group, linguistic quantifier.

Here, a new protoform is employed:

$$Q_y^1 Q_{x \in y}^2 S(x) \tag{19}$$

which, in the examples presented, is instantiated as:
for (17)

$Q^1 =$ "most", $Q^2 =$ "all", $Y = \{y_i\}$ is a set of departments, $X_y = \{x_i\}$ is a set of employees of a department y, and $S(x) =$ "x is young and highly paid (earns high salary)",

for (18)

$Q^1 =$ "almost all", $Q^2 =$ "most", $Y = \{y_i\}$ is a set of cities in Asia, $X_y = \{x_i\}$ is a set of hotels located in a city y, and $S(x) =$ "x is moderately priced and comfortable".

The truth degree of a summary represented by the protoform (19) is computed using a modified version of formula (5) used for the standard linguistic summaries of the protoforms (3):

$$\text{truth}(Q_y^1 Q_{x\in y}^2 S(x)) = \mu_{Q^1}\left(\sum_{i=1}^{|Y|} \frac{\mu_{Q^2}\left(\frac{\sum_{j=1}^{|y_i|}\mu_S(x_j)}{|y_i|}\right)}{|Y|}\right) \qquad (20)$$

where $|A|$ denotes the cardinality of set A.

In the case of the new protoform (19) the use of the "and possibly" connective becomes reasonable and interesting. For instance, a good example may be a modified version of (17) like:

Most departments employ *young and possibly* earning *highly paid* employees.

(21)

to be understood as follows: it is true (to a high degree) for most departments that they employ only young people and, moreover, if such a department employs an employee who is young and earns a high salary (i.e., *it is possible* to be young and earn a lot *in this department*), then all its employees are young and earning a high salary.

Thus, if a summarizer in (19) contains the "and possibly" connective then the notion of possibility is interpreted in the context of a set y rather than in the context of the *whole database*. Formally, this is expressed for a linguistic summary:

$$Q_y^1 Q_{x\in y}^2 \ C(x) \text{ and possibly } P(x) \qquad (22)$$

by the following form of $\mu_S(x_j)$ in the formula (20) for its truth value:

$$\mu_S(x_j) = \text{truth}(C(x_j) \wedge \exists_{x_k\in y_i}(C(x_k) \wedge P(x_k)) \rightarrow P(x_j))) \qquad (23)$$

In this context it is worthwhile to mention the case of linguistic summaries of time series as proposed by Kacprzyk et al. [27, 28]. In this approach database tuples, representing a time series data, are also first grouped (subjected to segmentation, i.e. determination of trends) and only then summarized. The difference with our case of a bipolar summary is however that each group of tuples, corresponding to a segment (trend), is viewed as a new individual tuple characterized by some properties exemplified by the dynamics of change of the trend). Thus, the summaries generated follow the general protoform (3) or (4) with some slight variation related to its specific time series related interpretation.

5 Discussion and Related Work

Some similarity between the bipolar linguistic summaries with local "and possibly" operator (bipolar circumstantial linguistic summaries) and bipolar linguistic summaries with the grouping based "and possibly" operator is worth noting and

discussing. Namely, both types of summaries are characterized by the interpretation of the "and possibly" operator in a restricted context: the possibility of the satisfaction of both arguments of this operator is defined in terms of a subset of the tuples rather than the whole database. In the former case a relation W is introduced to form the context—in general, separately for each tuple. In the latter case a partitioning $Y = \{y_i\}$ of the set of tuples is assumed which is fixed for the whole database. Both, relation W and partitioning Y, may be fuzzy what makes the modeling of the context more realistic and slightly more complicated computationally, at the same time.

Let us now consider, for the sake of simplicity, the case of the crisp: relation W and partitioning Y. Then, the latter case seems to be a special case of the former for W being an equivalence relation. However, we should notice that the protoform (3) with the summarizer (15) is essentially different from the protoform (19). The latter makes use of two level linguistic quantifier guided aggregation and concerns groups of tuples while the former concerns individual tuples. Thus even apparently very similar summaries of these two types convey different information and should in general have different truth degrees. This may be observed comparing two summaries (12) and (21). Let there are 5 departments employing the numbers of young workers shown in Table 1. For the sake of simplicity we assume that the predicates "young" and "earns high salary" are both crisp. Then, the summary (12) will have a low truth degree as even if most of the employees are young (90 out of 100) still for almost a half of them it is not true that they earn high salary while they have young department mates who do (cf. department I). On the other hand, in most of the departments (4 out of 5) there are working only young employees and in each of these departments they all earn high salaries or no one of them earns high salary, thus the summary (21) will have a high truth degree.

This comparison well illustrates a need for new measures of quality in case of bipolar linguistic summaries. Namely, the validity T corresponding to the truth of a summary, (5) or (6), is the basic measure of the quality for regular linguistic summaries. There are several other quality measures proposed, cf., e.g. [4, 15] which take into account different aspects of the summary. In case of bipolar linguistic summaries still another measure is needed which, roughly speaking, takes into account how often the summarizer "C and possibly P" operator involved turns into "$C \wedge P$" or into "C"; cf. Sect. 4. Namely, if it happens for a high majority of tuples (in case

Table 1 Comparison of two types of bipolar linguistic summaries: An example of a database content

Dept. No.	Total No. of employees	No. of young employees	No. of young employees earning high salary
I	60	50	2
II	10	10	10
III	10	10	0
IV	10	10	0
V	10	10	10

of a linguistic summary with local "and possibly" operator) or for a high majority of groups of tuples (in case of a grouping based "and possibly" operator), then the bipolar summarizer may be more often satisfied than its corresponding "standard summarizers" ("$C \wedge P$" or "C") while the resulting summary is less interesting than the standard one. A basic component of such a measure is the $\exists C P$ coefficient which should always be taken into account when deciding the quality measure of a bipolar linguistic summary.

Bipolar linguistic summaries with the grouping based "and possibly" operator are easier to integrate with the standard SQL queries, and thus also with their fuzzy linguistic extensions. Namely, the partitioning Y may be defined by the GROUP BY clause of the SELECT command. In case of a fuzzy partitioning things get more complex but the general idea is still in line with the well-known syntax of the SQL and related intuitions of the users of this language.

Concerning a related research we are not aware of any other extensions of the concept of linguistic summaries which take into account the bipolarity of the constituent conditions, in the sense assumed here. Maybe, the work of Niewiadomski [29] should be mentioned here. Niewiadomski introduces the concept of Type-2 linguistic summary where all the linguistic terms in a summary, i.e., linguistic quantifiers and fuzzy predicates in summarizers and qualifiers, may be in general represented using Type-2 fuzzy sets instead of "regular" fuzzy sets. Some links with bipolar linguistic summaries proposed here by us become evident especially when compared with interval-valued fuzzy sets based summaries which are proposed by Niewiadomski as a special case of Type-2 fuzzy sets. Interval-valued fuzzy sets may be in turn interpreted in terms of Atanassov intuitionistic fuzzy (A-IFS) sets which are one of the possible theoretical foundations of the bipolar queries; cf., e.g. [18, 30]. However, there is a fundamental difference between our approach and that of Niewiadomski. Namely, in the latter the interval-valued fuzzy sets are used to model individual linguistic terms in the domains of particular attributes. When interpreted in terms of A-IFS it makes it possible to, e.g. indicate the ranges of prices which are to some extent *cheap* (positive, desired) and *not cheap* (negative, complement of required), separately—not requiring that one range is the complement of another. In our approach bipolarity of a summarizer or a qualifier may be more subtle: the definitions of desired and required components may refer to different attributes what seems to lead to more interesting summaries in some practical scenarios. The links between both approaches surely deserve a further study and the difference indicated above is related to the structural aspects of bipolarity expression discussed in our earlier paper [31].

6 Conclusion

We proposed a novel concept of a bipolar linguistic summary with the "and possibly" operator. We have employed as points of departure a couple of our ideas presented in our previous papers concerned with traditional (not bipolar) linguistic summaries,

notably: a close relation between the derivation of linguistic summaries and fuzzy querying of relational databases, an interactive approach to the derivation of linguistic summaries, and a protoform based analysis and derivation of linguistic summaries. All these issues have been reformulated in terms of bipolar preferences/intentions of the user, and a concept of a bipolar linguistic summary has been proposed. Some classes of bipolar linguistic summaries have been formulated and analyzed, notably the simple, circumstantial and multi-level ones.

The new class of linguistic summaries can greatly improve our ability to better reflect preferences and intentions of the human user with respect to the data to be summarized.

As to some further research directions, some non-standard views of bipolar queries exemplified by the approach based on modal logic, as proposed by Kacprzyk and Zadrożny [32], or using Grabisch et al. [33] bipolarity based multicriteria decision making model, can lead to relevant novel forms of linguistic summaries.

References

1. Yager, R.R.: A new approach to the summarization of data. Inf. Sci. **28**, 69–86 (1982)
2. Yager, R.R.: On linguistic summaries of data. In: Frawley, W., Piatetsky-Shapiro. G., (eds.) Knowledge Discovery in Databases, pp. 347–363. AAAI/MIT Press (1991)
3. Kacprzyk, J., Yager, R.R.: Linguistic summaries of data using fuzzy logic. Int. J. Gen. Syst. **30**, 33–154 (2001)
4. Kacprzyk, J., Yager, R.R., Zadrożny, S.: A fuzzy logic based approach to linguistic summaries of databases. Int. J. Appl. Math. Comput. Sci. **10**, 813–834 (2000)
5. Kacprzyk, J., Zadrożny, S.: Computing with words: towards a new generation of linguistic querying and summarization of databases. In: Sinčak, P., Vaščak, J. (eds.) Quo Vadis Computational Intelligence?, pp. 144–175. Springer, Heidelberg and New York (2000)
6. Kacprzyk, J., Zadrożny, S.: Linguistic database summaries and their protoforms: towards natural language based knowledge discovery tools. Inf. Sci. **173**(4), 281–304 (2005)
7. Kacprzyk, J., Zadrożny, S.: Computing with words is an implementable paradigm: fuzzy queries, linguistic data summaries, and natural-language generation. IEEE Trans. Fuzzy Syst. **18**(3), 461–472 (2010)
8. Kacprzyk, J., Zadrożny, S.: Data mining via linguistic summaries of data: an interactive approach. In: Yamakawa, T., Matsumoto, G. (eds.) Methodologies for the Conception, Design and Application of Soft Computing, pp. 668–671. Proceedings of IIZUKA'98, Iizuka, Japan (1998)
9. Kacprzyk, J., Zadrożny, S.: Data mining via linguistic summaries of databases: an interactive approach. In: Ding, L. (ed.) A New Paradigm of Knowledge Engineering by Soft Computing, pp. 325–345. World Scientific, Singapore (2001)
10. Dubois, D., Prade, H.: Bipolarity in flexible querying. In: Andreasen, T., Motro, A., Christiansen, H., Larsen, H. L. (eds.) FQAS 2002, LNAI, vol. 2522, pp. 174–182. Springer, Heidelberg (2002)

11. Kacprzyk, J., Ziółkowski, A.: Database queries with fuzzy linguistic quantifiers. IEEE Trans. Syst. Man Cybern. **16**(3), 474–479 (1986)
12. Kacprzyk, J., Zadrożny, S., Ziółkowski, A.: FQUERY III+: a "human consistent" database querying system based on fuzzy logic with linguistic quantifiers. Inf. Syst. **14**(6), 443–453 (1989)
13. Zadeh, L.A.: A computational approach to fuzzy quantifiers in natural languages. Comput. Math. Appl. **9**, 149–184 (1983)
14. Kacprzyk, J., Zadrożny, S.: Computing with words in intelligent database querying: standalone and internet-based applications. Inf. Sci. **134**(1–4), 71–109 (2001)
15. Kacprzyk, J., Yager, R.R., Zadrożny, S.: Fuzzy linguistic summaries of databases for an efficient business data analysis and decision support. In: Abramowicz, W., Żurada, J. (eds.) Knowledge Discovery for Business Information Systems, pp. 129–152. Kluwer, Boston (2001)
16. Zadeh, L.A.: From search engines to question answering systemsthe problems of world knowledge relevance deduction and precisiation. In: Sanchez, E. (ed.) Fuzzy Logic and the Semantic Web, p. 163210. Elsevier (2006)
17. Zadeh, L.A.: A prototype-centered approach to adding deduction capabilities to search engines - the concept of a protoform. In: Proceedings of the Annual Meeting of the North American Fuzzy Information Processing Society (NAFIPS 2002), pp. 523–525. New Orleans, USA (2002)
18. Dubois, D., Prade, H.: Handling bipolar queries in fuzzy information processing. In: Galindo, J. (ed.) Handbook of Research on Fuzzy Information Processing in Databases, pp. 97–114. Information Science Reference, New York (2008)
19. Matthé, T., De Tré, G., Zadrożny, S., Kacprzyk, J., Bronselaer, A.: Bipolar database querying using bipolar satisfaction degrees. Int. J. Intell. Syst. **26**(10), 890–910 (2011)
20. Lacroix, M., Lavency, P.: Preferences: Putting more knowledge into queries. In: Proceedings of the 13 International Conference on Very Large Databases, pp. 217–225. Brighton, UK (1987)
21. Yager, R.R.: Higher structures in multi-criteria decision making. Int. J. Man Mach. Stud. **36**, 553–570 (1992)
22. Yager, R.R.: Fuzzy logic in the formulation of decision functions from linguistic specifications. Kybernetes **25**(4), 119–130 (1996)
23. Bordogna, G., Pasi, G.: Linguistic aggregation operators of selection criteria in fuzzy information retrieval. Int. J. Intell. Syst. **10**(2), 233–248 (1995)
24. Zadrożny, S.: Bipolar queries revisited. In: Torra, V., Narukawa, Y., Miyamoto, S. (eds.) Modelling Decisions for Artificial Intelligence (MDAI 2005), vol. 3558, pp. 387–398. LNAI, Springer, Heidelberg (2005)
25. Zadrożny, S., Kacprzyk, J.: Bipolar queries: an aggregation operator focused perspective. Fuzzy Sets Syst. **196**, 69–81 (2012)
26. Dziedzic, M., Zadrożny, S., Kacprzyk, J.: Towards bipolar linguistic summaries: a novel fuzzy bipolar querying based approach. In: Fuzzy Systems (FUZZ-IEEE), 2012 IEEE International Conference on, p. 1–8, june 2012
27. Kacprzyk, J., Wilbik, A., Zadrożny, S.: Linguistic summarization of time series using a fuzzy quantifier driven aggregation. Fuzzy Sets Syst. **159**(12), 1485–1499 (2008)
28. Kacprzyk, J., Wilbik, A., Zadrożny, S.: An approach to the linguistic summarization of time series using a fuzzy quantifier driven aggregation. Int. J. Intell. Syst. **25**(5), 411–439 (2010)
29. Niewiadomski, A.: A type-2 fuzzy approach to linguistic summarization of data. IEEE Trans. Fuzzy Syst. **16**(1), 198–212 (2008)
30. De Tré, G., Zadrożny, S., Bronselaer, A.: Handling bipolarity in elementary queries to possibilistic databases. IEEE Trans. Fuzzy Sets **18**(3), 599–612 (2010)
31. Zadrożny, S., De Tré, G., Kacprzyk, J.: Remarks on various aspects of bipolarity in database querying. In: DEXA Workshops, IEEE Computer Society (2010)
32. Kacprzyk, J., Zadrożny, S.: Bipolar queries, and intention and preference modeling: synergy and cross-fertilization. In: Proceedings of the World Conference on Soft Computing, San Francisco, CA, USA, 23/05/2011-26/05/2011 (2010)
33. Grabisch, M., Greco, S., Pirlot, M.: Bipolar and bivariate models in multicriteria decision analysis: descriptive and constructive approaches. Int. J. Intell. Syst. **23**, 930–969 (2008)

On Reduction of Data Series Dimensionality

Maciej Krawczak and Grażyna Szkatuła

Abstract In this paper we introduce a complex procedure of reducing dimensionality of multidimensional data series. The procedure consists of several steps, and each step gives a new data series representation as well as dimension reduction. The approach is based on the concept of data series aggregated envelopes, and principal components called here 'essential attributes' generated by a multilayer neural network. The essential attributes are generated by outputs of hidden layer neurons. Next, all differences of the essential attributes are treated as new attributes. The real values of the new attributes are nominalized in order to obtain a nominal representation of data series. The approach creates a nominal representation of the original data series and considerably reduces their dimension. Practical verification of the proposed approach was verified for classification and clustering of time series problems, the results are set out in different papers of the authors. Here, the short summarization confirms utilities of time series dimension reduction procedure.

Keywords Data series · Nominal attributes · Dimension reduction · Envelopes · Essential attributes · Data series mining

1 Introduction

In many areas such as medicine, finance, industry, climate etc. data series mining problems arise often. The obtained data is registered, stored, transmitted and then analyzed. The majority of data series mining research focuses on the following problems: *indexing* (e.g. [12]), *clustering* (e.g. [12, 19, 32]), *classification* (e.g. [17, 18, 24]), *summarization* (e.g.[21]), and *anomaly detection* [27].

M. Krawczak (✉) · G. Szkatuła
Systems Research Institute, Polish Academy of Sciences, Newelska 6, Warsaw, Poland
e-mail: krawczak@ibspan.waw.pl

G. Szkatuła
e-mail: szkatulg@ibspan.waw.pl

Due to a huge amount of data, different kinds of data series representations were developed. In the literature we can find specialized algorithms for such problems, including decision trees [26], neural networks [24], bayesian classifiers [32], etc. Some representations are general and some are rather specialized for prescribed applications. It should be mentioned that there is an increasing interest in data series mining, e.g. Xi, Keogh, Shelton, Wei, Ratanamahatana, 2006. It is said that time series or data series mining is considered as one of the tenth challenging problems in data mining [4, 33].

In most of the above listed data series mining problems there are necessity of reducing dimensionalities and creating new data series representations. It is required that the new representation must preserve sufficient information for solving data series mining problems with gratifying accuracy. In literature we can find several data series representations which include the discrete Fourier transform [3], the discrete wavelet transform [1], the piecewise constant models [12], the singular value decomposition models [12], the symbolic aggregate approximation [22], and the upper/lower envelopes and principal component analysis [5, 17, 25].

In the present paper we propose a new complex procedure of reducing the dimensionality of the original data series thereby a new representation of data series is obtained (Sect. 2).

The propose methodology consists of several steps realized by separate modules. We recall the idea of upper and lower envelopes of data series, first introduced by Krawczak and Szkatuła [17, 18]. The upper and/or lower envelopes give a first new data series representation, as well as the aggregated envelopes—another new data series representation, this way first reduction of dimensionality is obtained. Based on aggregated envelopes (upper or lower, or both) essential attributes are introduced. The essential attributes constitute another new representation, with additional dimension reduction of the data series [2, 15]. In order to generate the essential attributes a multilayer neural network is applied. A three-layer neural network with one hidden layer allows to encode aggregated envelopes data series representation (e.g. [13, 14]), and the outputs of the hidden layer neurons constitute just the essential attributes. A set of essential attributes constitutes another representation of the considered data series, and another reduction of dimensionality. Next, on the base of the essential attributes a new set of the attributes can be created, as some function of the essential attributes (e.g. differences between essential attributes). In the next step, during a nominalization process, nominal values are assigned for real values of the essential attributes. This way a simple symbolic representation of the original data series is obtained.

Practical presentation of the proposed methodology was carried out for the database available at the Irvine University of California (in Sect. 3). Validation of practical use of the proposed approach was carried out for classification and clustering of the essential attributes with symbolic values. Calculations were performed to verify whether the proposed methodology of reducing the dimensionality still retains important features of the original data series to classify and to cluster them in proper way. In this paper only the results of the methodology validation is quoted.

2 Description of Methodology

The aim of this paper is to propose a new complex procedure for reduction of dimension of multidimensional data series. Consequently, after application of the proposed reduction of dimension, each data series is represented by nominal values. The developed methodology consists of five steps, called here modules:

(1) *Normalization module* The original data series are normalized and have the following vector form $[x_1(n), x_2(n), \ldots, x_M(n)], n = 1, \ldots, N$.
(2) *Aggregation envelopes module* The upper and/or lower envelopes are developed, and then aggregated, the step $m \ll M$ of aggregation is adjusted, and the aggregated envelopes (upper or lower) are denoted as follows $[y_1(n), y_2(n), \ldots, y_{\lfloor \frac{M}{m} \rfloor}(n)], n = 1, \ldots, N$.
(3) *Essential attributes generation module* The essential attributes are generated and the number of them is adjusted $E \ll \lfloor \frac{M}{m} \rfloor$, and now the data series representation described by the essential attributes has a set form $\{b_1(n), b_2(n), \ldots, b_E(n)\}$, $n = 1, \ldots, N$.
(4) *Attributes transformation module* The functions of the essential attributes are generated creating the new set of attributes denoted by $\{c_1(n), c_2(n), \ldots, c_K(n)\}$, $n = 1, \ldots, N$, where the number of new attributes is adjusted as $K \geq E$.
(5) *Attributes nominalization module* The real values of the attributes are replaced by nominal values constituting the new symbolic data series representation $\{a_1(n), a_2(n), \ldots, a_K(n)\}, n = 1, \ldots, N$.

In next section each module of the developed data series dimension reduction is described in details for the particular database available at the Irvine University of California.

3 Case Study

Practical presentation of the proposed approach for reduction of dimension of data series was carried out for the database available at the Irvine University of California (http://kdd.ics.uci.edu/databases/synthetic_control/synthetic_control.data.html).

The database consists of data series synthetically generated by proper equations. Each equation represents a different type of data series pattern. Each pattern was taken as a time series of 60 data points. The following equations were used to create the data points $z(t)$, where $1 \leq t \leq 60$, for the various patterns:

pattern E:	$z(t) = v + rs + kx$	(upward shift)
pattern F:	$z(t) = v + rs - kx$	(downward shift)
pattern A:	$z(t) = v + rs$	(normal)

where, for each pattern, v is the mean value of the process variable under observation ($v = 80$), s is the standard deviation of the process variable ($s = 5$), r is a random number between -3 and 3, x is the magnitude of the shift (x takes a value between 7.5 and 20), k indicates the shift position in E and F ($k = 0$ before the shift and $k = 1$ at the shift and thereafter).

We considered the following learning data series, where introduced classes correspond to the respective patterns:

> 25 time series belonging to Class 1 (pattern E),
>
> 25 time series belonging to Class 2 (pattern F) and
>
> 25 time series belonging to Class 3 (pattern A).

Each learning data series has 60 values, below there are first seven values of four beginning data belonging to pattern E:

28.7812	34.4632	31.3381	31.2834	28.9207	33.7596	25.3969	…
24.8923	25.7410	27.5532	32.8217	27.8789	31.5926	31.4861	…
31.3987	30.6316	26.3983	24.2905	27.8613	28.5491	24.9717	…
25.7740	30.5262	35.4209	25.6033	27.9700	25.2702	28.1320	…

In Figs. 1, 2 and 3 there are depicted time series belonging to Class 1, Class 2 and Class 3, respectively. Based on these figures one can justify that each of the considered class of time series is characterized by different pattern. The patterns correspond to one of three different generating expressions (written above) as well as different characteristic movement, namely: upward shift, downward or normal.

Next picture, Fig. 4, shows all 75 training times series together, the shapes overlap and it seems that no one is able to disentangle not only separate data but even an accurate class affiliation.

In the same mentioned above website there also available different time series which we consider as the **testing data series**, see Fig. 5. These data are completely different from those treated as learning data, and the testing data are characterized as follows
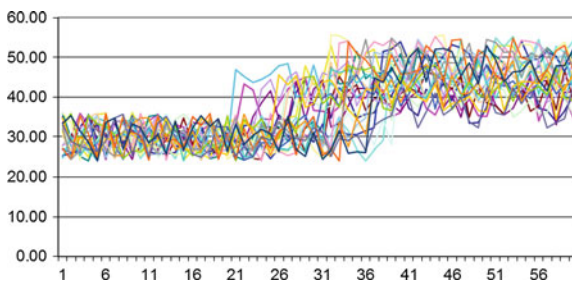

Fig. 1 The time series belonging to the pattern E
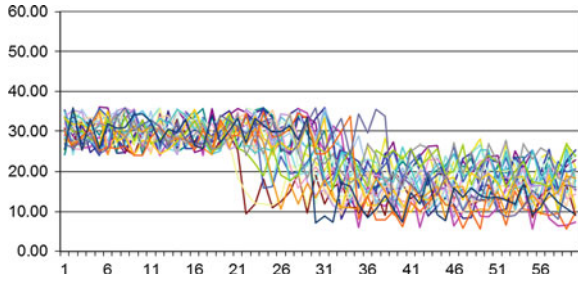
Fig. 2 The time series belonging to the pattern F
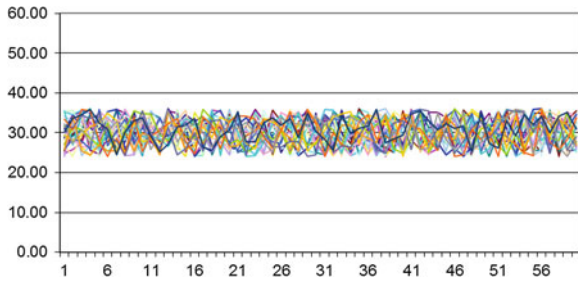

Fig. 3 The time series belonging to the pattern A
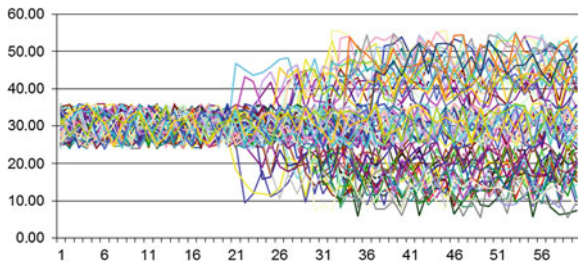

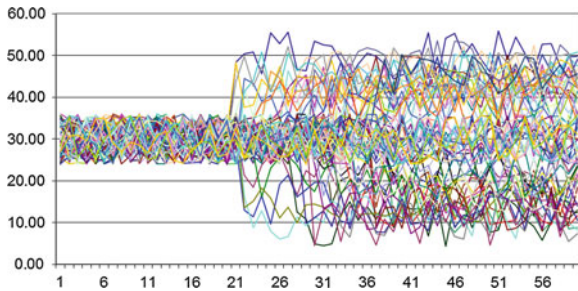**Fig. 4** The time series belonging to one of the pattern E, F and A

Fig. 5 Testing time series belonging to patterns E or F or A

      25 time series belonging to Class 1 (pattern E),

      25 time series belonging to Class 2 (pattern F) and

      25 time series belonging to Class 3 (pattern A),

and they are used only for testing purposes.

3.1 Data Normalization Module

Before starting the dimension reduction of the data series, each series is normalized to have mean equal zero and standard deviation equal one, because it is obvious that it is meaningless to consider data series with different offsets and amplitudes. As a result we obtained normalized data series described by the following data ($M = 60$):

$$\{x_k(n)\}_{k=1}^{k=60} = [x_1(n), x_2(n), \ldots, x_{60}(n)] \tag{1}$$

where for $n = 1, 2, \ldots, 75$, as shown in Figs. 6, 7 and 8—there are learning data series. In Fig. 9 there are drown all 75 normalized time series representing one of the three classes. These data are used only for learning purposes.

    For testing another different time series are used and they are described by formula (1) where $n = 76, 77, \ldots 150$.

    In Table 1 there are shown exemplary values of selected time series of the considered normalized data series.

    Now, the dimension reduction methodology for data series described in the previous section will be applied step by step. The methodology is based on the concept of envelopes, aggregation of the envelopes and extracting essential attributes, and nominalization of the attributes.

    Having normalized all available time series, both learning for $n = 1, 2, \ldots, 75$ and testing for $n = 76, 77, \ldots 150$, now we will generate *upper* as well as *lower* *time series envelopes*. The envelopes must be obtained for all considered time series, both training and testing, it means for all $n = 1, 2, \ldots, 150$.
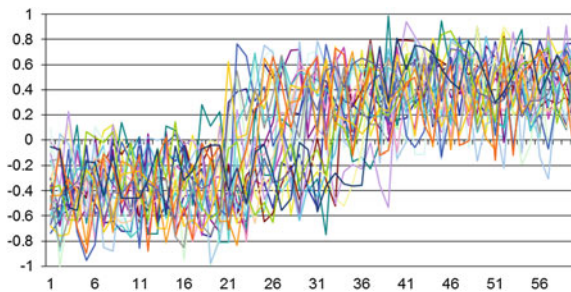
Fig. 6 The normalized time series $\{x_k(n)\}_{k=1}^{k=60}$, $n = 1, 2, \ldots, 25$, belonging to the pattern E

Fig. 7 The normalized time series $\{x_k(n)\}_{k=1}^{k=60}$, $n = 26, 27, \ldots, 50$, belonging to the pattern F
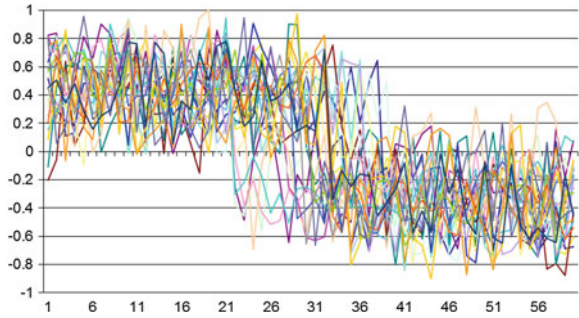
Fig. 8 The normalized time series $\{x_k(n)\}_{k=1}^{k=60}$, $n = 51, 52, \ldots, 75$, belonging to the pattern A
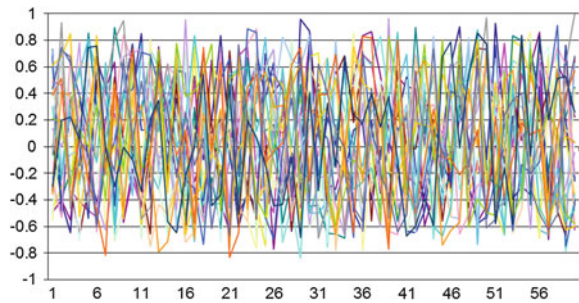
Fig. 9 The normalized time series $\{x_k(n)\}_{k=1}^{k=60}$, $n = 1, 2, \ldots, 75$, belonging to the patterns E, F, A
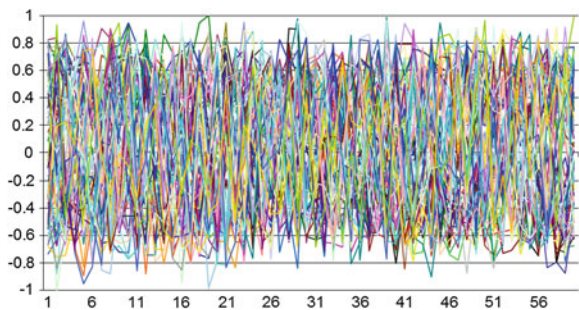
The developed procedure for reducing the dimensionality of data series by using the *upper envelopes* and/or *lower envelopes* requires adjusting values of required parameters. The only required procedure parameters are: the step of aggregation m and the number of generated essential attributes E. Here, due to performing many computer experiments we selected the following values of the parameters: the aggregation step $m = 4$ and the number of essential attributes $E = 5$. Selection of the proper values of these parameters is of crucial importance because their values have strong influence on quality of time series representations. Let us mention that the aggregated envelopes are used to create five attributes representing the data series of 60 data points.

Table 1 The learning time series

n	$x_1(n)$	$x_2(n)$	$x_3(n)$	$\cdots$	$x_{58}(n)$	$x_{59}(n)$	$x_{60}(n)$	Pattern
1	−0.30	−0.60	−0.55	$\cdots$	0.26	0.12	0.33	E
15	−0.10	−0.36	0.23	$\cdots$	0.27	0.91	0.18	E
40	0.26	0.35	0.22	$\cdots$	−0.73	−0.64	−0.20	F
48	0.80	0.06	0.18	$\cdots$	−0.51	−0.44	−0.41	F
55	−0.49	−0.40	−0.55	$\cdots$	0.62	0.48	0.22	A
75	−0.30	0.20	0.22	$\cdots$	0.51	0.53	0.26	A

3.2 Reducing of the Data Series Dimensionality Using Aggregated Envelopes

The main aim to introduce envelopes of data series is to find a new representation of them characterized by prescribed reduction of dimension compare to the original representation. The parameter m describes the rank of time series dimension reduction. The idea of envelopes is borrowed from the signal processing theory and in our case is partially similar known piecewise constant approximations of time series, and in principle relies on dividing the range of the original time series K into m equal parts. Within each part there are taking in account either the highest values—for the upper envelopes, or the lowest values—for the lower envelopes. It means that within each part we assign the same value for m succeeding samples. Here we consider $m = 4$ step approximation of the original time series, and for considered number of samples $M = 60$ we have $\lfloor \frac{M}{m} \rfloor = 15$ parts of the original time series. The idea of the upper and lower envelopes is illustrated by the following picture, Fig. 10.

Next, as is shown in Fig. 11, within each part of the original range, the equal four values of the envelopes are replaced by a single value, respectively for upper as well for lower envelopes. Such a process is called here as aggregation of the envelopes,
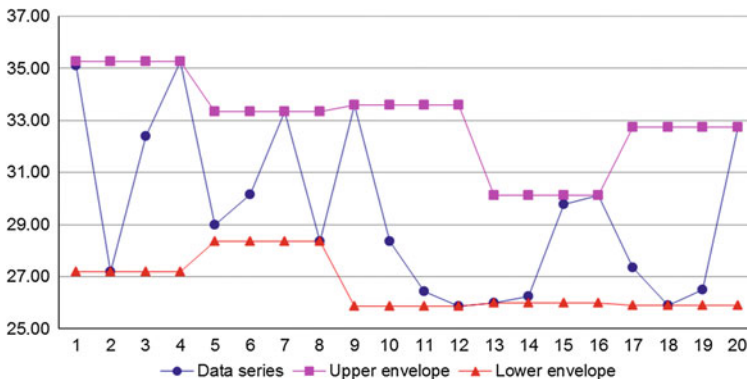
Fig. 10 *4*-step upper and lower envelopes for the first 20 values of an exemplary data series
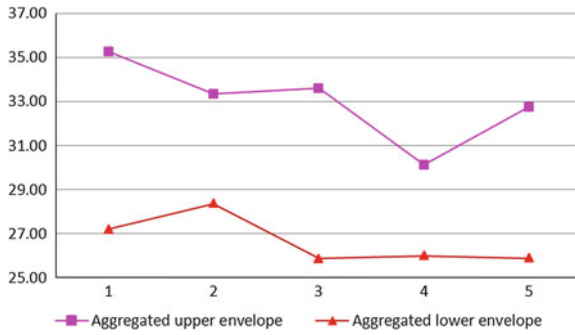
Fig. 11 The aggregated *4*-step upper and lower envelopes

and in result in subsequent text we will use so called the aggregated upper or lower envelopes.

This way we obtain another new representation of the original time series, where dimension is reduces $m = 4$ times, and now the dimension of this representation is equal to $\lfloor \frac{M}{m} \rfloor = 15$. Details of this part of the dimension reduction are described as follows.

The *4*-step upper envelopes

The *4*-step upper approximation (upper envelope) of a data series of (1) is denoted by $\{x_k^U (n)\}_{k=1}^{k=15}$, and has the following form:

$$x_1^U (n) = \max\{x_1 (n), x_2 (n), x_3 (n), x_4 (n)\}$$
$$\cdots$$
$$x_4^U (n) = \max\{x_1 (n), x_2 (n), x_3 (n), x_4 (n)\}$$
$$x_5^U (n) = \max\{x_5 (n), x_6 (n), x_7 (n), x_8 (n)\}$$
$$\cdots \tag{2}$$
$$x_{57}^U (n) = \max\{x_{57} (n), x_{58} (n), x_{59} (n), x_{60} (n)\}$$
$$\cdots$$
$$x_{60}^U (n) = \max\{x_{57} (n), x_{58} (n), x_{59} (n), x_{60} (n)\}.$$

Next, the envelopes (2) can be aggregated. We can replace each 4 sequential equal values of the envelope with a single value, see Figs. 12, 13, 14 and 15. The aggregated upper envelopes yield a new data series representations, for $n = 1, 2, \ldots, 150$, formally represented as follows

$$\{y_k(n)\}_{k=1}^{k=15} = [y_1(n), y_2(n), \ldots, y_{15}(n)]. \tag{3}$$

For the data from Table 1 the aggregated *4*-step upper envelopes look like in Table 2.

Fig. 12 The aggregated *4*-step upper envelopes $\{y_k(n)\}_{k=1}^{k=15}$, $n = 1, 2, \ldots, 25$, of data series E

Fig. 13 The aggregated *4*-step upper envelopes $\{y_k(n)\}_{k=1}^{k=15}$, $n = 26, 27, \ldots, 50$, of data series F
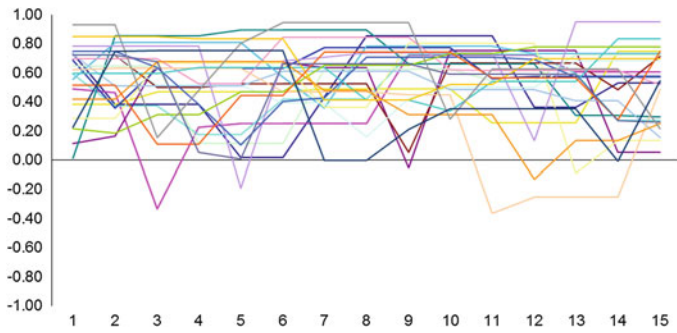
Fig. 14 The aggregated *4*-step upper envelopes $\{y_k(n)\}_{k=1}^{k=15}$, $n = 51, 52, \ldots, 75$, of data series A

For the sake of entirety, below, we will repeat the detailed description for the aggregation of lower envelopes of the considered time series.

Fig. 15 The aggregated *4*-step upper envelopes of data series $\{y_k(n)\}_{k=1}^{k=15}$, $n = 1, 2, \ldots, 75$, of data series E, F and A

Table 2 The 4-step upper envelopes

n	$y_1(n)$	$y_2(n)$	$y_3(n)$	$\cdots$	$y_{13}(n)$	$y_{14}(n)$	$y_{15}(n)$	Pattern
1	-0.30	-0.33	-0.33	$\cdots$	-0.44	-0.43	-0.43	E
15	0.23	0.23	0.23	$\cdots$	0.06	0.06	0.06	E
40	0.35	0.35	0.50	$\cdots$	0.68	0.28	0.36	F
48	0.80	0.96	0.96	$\cdots$	0.71	0.71	0.71	F
55	0.11	0.16	0.67	$\cdots$	0.75	0.05	0.05	A
75	0.22	0.74	0.75	$\cdots$	0.35	-0.01	0.55	A

The *4*-step lower envelopes

Similarly, the *4*-step lower approximations (lower envelopes) of a data series (1), is denoted by $\{x_k^L(n)\}_{k=1}^{k=15}$ and has the following form:

$$x_1^L(n) = \min\{x_1(n), x_2(n), x_3(n), x_4(n)\}$$

$$\ldots$$

$$x_4^L(n) = \min\{x_1(n), x_2(n), x_3(n), x_4(n)\}$$

$$x_5^L(n) = \min\{x_5(n), x_6(n), x_7(n), x_8(n)\}$$

$$\ldots \tag{4}$$

$$x_{57}^L(n) = \min\{x_{57}(n), x_{58}(n), x_{59}(n), x_{60}(n)\}$$

$$\ldots$$

$$x_{60}^L(n) = \min\{x_{57}(n), x_{58}(n), x_{59}(n), x_{60}(n)\}$$

Next aggregated $[y_1(n), y_2(n), \ldots, y_{15}(n)]$ were calculated, and in this way we obtained the new representation of the data series with reduced dimensionalities, for $n = 1, 2, \ldots, 150$, see Figs. 16, 17, 18 and 19.

In Table 3 there are shown exemplary values of six selected aggregated *4*-step lower envelopes of data series E, F and A.
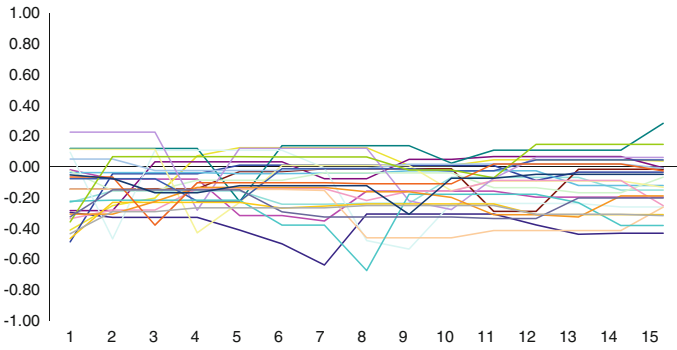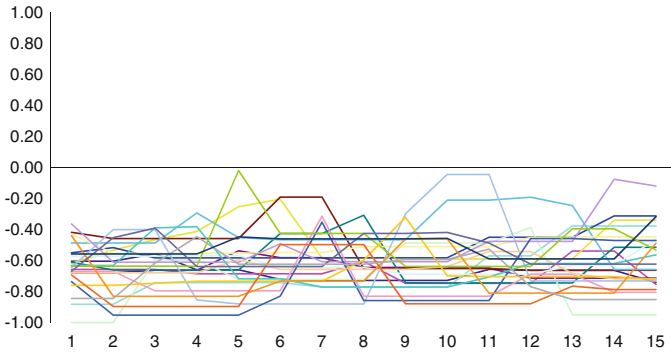
Fig. 16 The aggregated *4*-step lower envelopes $\{y_k(n)\}_{k=1}^{k=15}$, $n = 1, 2, \ldots, 25$, of data series E
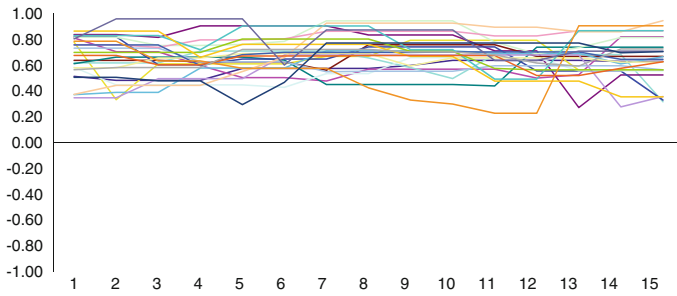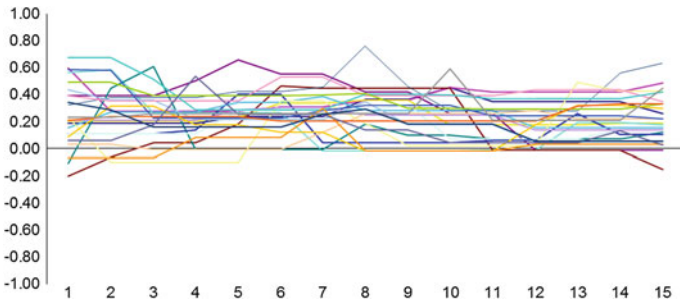

Fig. 17 The aggregated *4*-step lower envelopes $\{y_k(n)\}_{k=1}^{k=15}$, $n = 26, 27, \ldots, 50$, of data series F
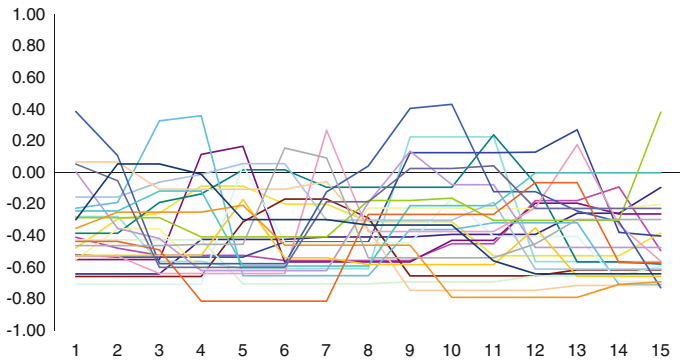
Fig. 18 The aggregated *4*-step lower envelopes $\{y_k(n)\}_{k=1}^{k=15}$, $n = 51, 52, \ldots, 75$, of data series A

In this way we obtained the new representation of the data series (1); the new representation is described by either upper or lower envelopes, or by both kinds of the envelopes.
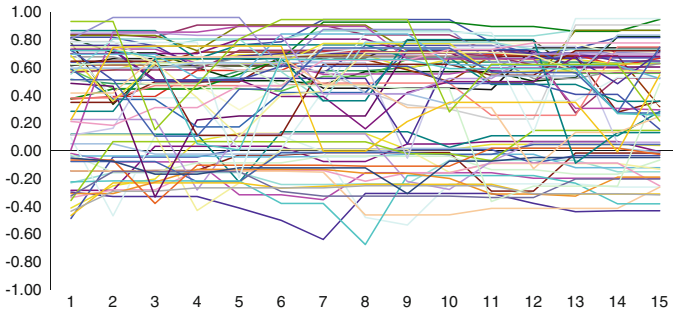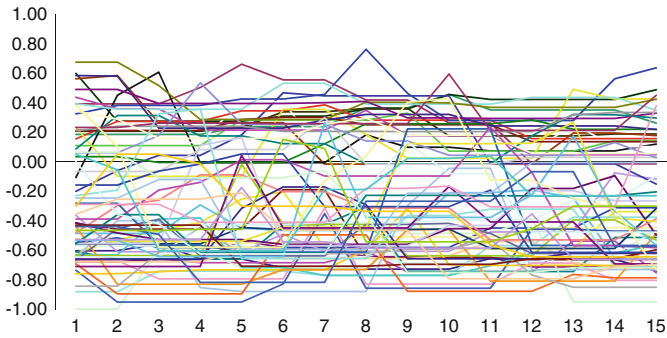
Fig. 19 The aggregated 4-step lower envelopes $\{y_k(n)\}_{k=1}^{k=15}$, $n = 1, 2, \ldots, 75$ of data series E, F, A

Table 3 The 4-step lower envelopes

n	$y_1(n)$	$y_2(n)$	$y_3(n)$	$\cdots$	$y_{13}(n)$	$y_{14}(n)$	$y_{15}(n)$	Pattern
1	−0.60	−0.60	−0.55	$\cdots$	−0.66	−0.66	−0.74	E
15	−0.36	−0.61	−0.61	$\cdots$	−0.48	−0.07	−0.12	E
40	0.21	0.21	0.21	$\cdots$	0.14	0.14	0.14	F
48	0.06	0.06	0.18	$\cdots$	0.04	0.13	0.03	F
55	−0.55	−0.55	−0.55	$\cdots$	−0.20	−0.27	−0.27	A
75	−0.30	0.05	0.05	$\cdots$	−0.64	−0.64	−0.64	A

3.3 Generation of the Essential Attributes

In this paper for obtaining the essential attributes the heteroassociation memory implemented by a feedforward neural network is applied. Such a multi layer neural network consists of one distinguished hidden layer; see Krawczak, Szkatuła [16].

A multi layer feedforward neural network was applied with different numbers of neurons within the hidden layer. All neurons have sigmoidal activation functions. The brief architecture of the designed neural network is as follows:

- The input layer in which the number of inputs is equal to 15 due to the number of samples of new time series representation—the 4-step aggregated envelopes (upper or lower),
- The output layer consisting of 15 neurons (the same as the number of inputs),
- The hidden layer consisting of E neurons representing the essential attributes.

For learning of the neural networks we applied the backpropagation algorithm with momentum, but even the standard backpropagation algorithm gives sufficiently good results. Completing the learning process using learning time series, for $n = 1, 2, \ldots, 75$, the outputs of the neural network are able to emulate the inputs.

It is assumed that neurons of the hidden layer represent "principle components" of the aggregated envelopes. These principal components we named *essential*
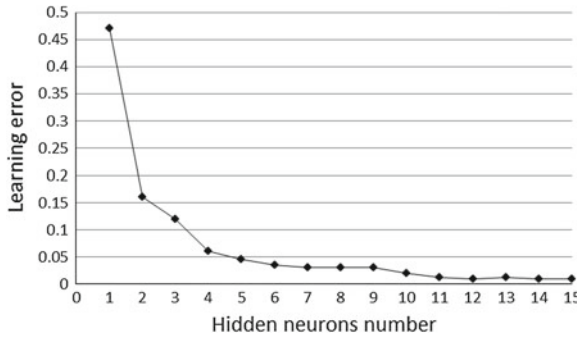
Fig. 20 Values of learning error versus the number of hidden neurons

attributes. The number of hidden neurons, it means the number of essential attributes must be accepted in result of a computational experiment, and in Fig. 20 there is a plot describing the neural network learning error versus the number of hidden neurons. In the experiment the number of hidden neurons was changed, between 1 and 15.

We should be emphasized that original data as well as the aggregated envelopes have a form of series of time where the order of samples is natural and of crucial importance. Meanwhile the essential attributes generated by the designed neural network have a set form where the order of elements is meaningless. However the essential attributes for all data must be generated for one chosen permutation of elements of the set of the essential attributes, and we denote the new representation of time series as a vector.

Here we selected the neural network architecture with five hidden neurons as rationally sufficient, meaning that five essential attributes conserve the information about the data series patterns, the architecture of the used neural network is shown in Fig. 21, and the hidden neurons generate the essential attributes.

It must be emphasized that for the learning process of the described neural network were used only aggregated envelopes indexed by $n = 1, 2, \ldots, 75$. Having the neural network with adjusted connection weights the essential attributes were calculated for all considered time series, that means for the learning data $n = 1, 2, \ldots, 75$ as well as for the testing data $n = 76, 77, \ldots, 150$.

Fig. 21 Schematic neural network generating the essential attributes
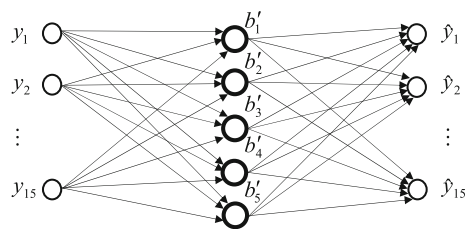
In Fig. 21 the inputs are denoted as $[y_1(n), y_2(n), \ldots, y_{15}(n)], n = 1, \ldots, 75$, the outputs emulating as $[\hat{y}_1(n), \hat{y}_2(n), \ldots, \hat{y}_{15}(n)], n = 1, \ldots, 75$ and the essential attributes as $[b_1(n), b_2(n), b_3(n), b_4(n), b_5(n)], n = 1, \ldots, 75$.

In the next step of our procedure we normalized the data describing the essential attributes, and the outputs of the hidden layer were multiplied by 1000.

The essential attributes for the aggregated *4*-step upper envelopes

The exemplary values of the essential attributes for the aggregated *4*-step upper envelopes are shown in Table 4.

It is worth mentioning that in Fig. 22 there are plots of the five essential attributes for one chosen permutation of the numbers of the attributes $\{1, 2, 3, 4, 5\}$, and under such assumption the attributes form a vector $[b_1(n), b_2(n)\ b_3(n), b_4(n), b_5(n)]$.

For each class the shapes of the plots are meaningfully different, it means that the composition of the essential attributes in some sense describes (remembers) the class of each data series. For a different permutation of the attributes we could observe a similar effect. Thus, the original learning data series can be represented by a set of these five essential attributes $\{b_1(n), b_2(n), \ldots, b_5(n)\}$, see Figs. 22, 23, 24 and 25.

The testing data series can be represented by a set of these five essentials attributes $[b_1(n), b_2(n), b_3(n), b_4(n), b_5(n)], n = 76, \ldots, 150$, for upper envelopers, see Fig. 26.

Table 4 The attributes for the upper envelopes

n	$b_1(n)$	$b_2(n)$	$b_3(n)$	$b_4(n)$	$b_5(n)$	Class
1	74	400	71	470	834	1
15	46	354	46	736	866	1
40	24	761	613	414	63	2
48	25	700	587	628	50	2
55	33	485	194	675	451	3
75	23	283	119	682	558	3

Fig. 22 The values of the attributes $\{b_j(n)\}_{j=1}^{j=5}, n = 1, 2, \ldots, 25$, describing the learning data from Class 1—for upper envelopers
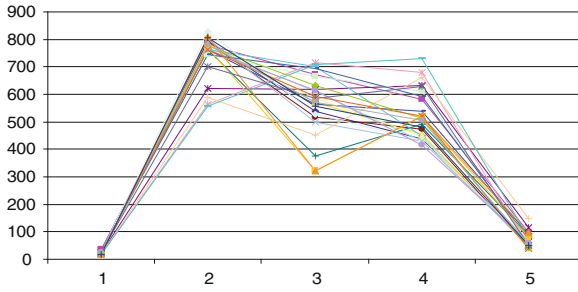
Fig. 23 The values of the attributes $\{b_j(n)\}_{j=1}^{j=5}$, $n = 26, 27, \ldots, 50$, describing the learning data from Class 2—for upper envelopers

Fig. 24 The values of the attributes $\{b_j(n)\}_{j=1}^{j=5}$, $n = 51, 52, \ldots, 75$, describing the learning data from Class 3—for upper envelopers
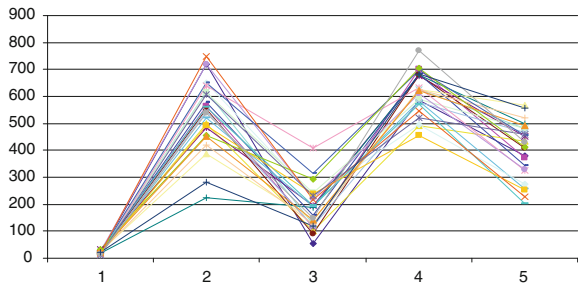
Fig. 25 The values of the attributes $\{b_j(n)\}_{j=1}^{j=5}$, $n = 1, 2, \ldots, 75$, describing the learning data from Class 1, 2 and 3—for upper envelopers
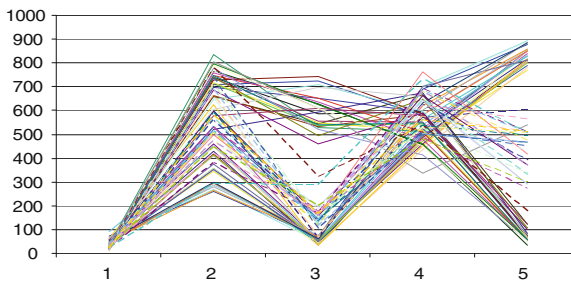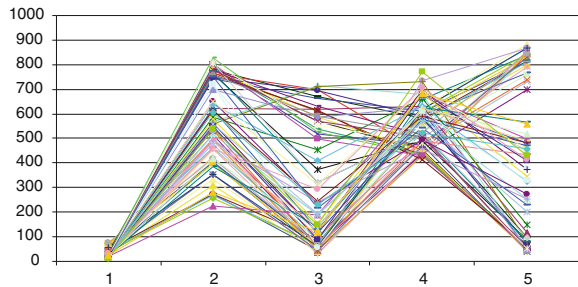
Fig. 26 The values of the essential attributes $\{b_j(n)\}_{j=1}^{j=5}$, $n = 76, 77, \ldots, 150$, describing the testing data from Class 1, 2 and 3—for upper envelopers

The essential attributes for the aggregated *4*-step lower envelopes

The exemplary values of the essential attributes for the aggregated *4*-step lower envelopes are shown in Table 5, Figs. 27, 28, 29 and, 30.

The original testing data series can be represented by a set of this five essentials attributes $\{b_1(n), b_2(n), \ldots, b_5(n)\}$ generated by the developed neural network, for lower envelopers, see Fig. 31.

Table 5 The attributes for the lower envelopes

n	$b_1(n)$	$b_2(n)$	$b_3(n)$	$b_4(n)$	$b_5(n)$	Class
1	372	454	559	214	946	1
15	288	395	691	195	956	1
21	412	316	253	335	944	2
48	249	713	787	934	228	2
55	475	487	468	695	848	3
75	732	387	762	645	865	3
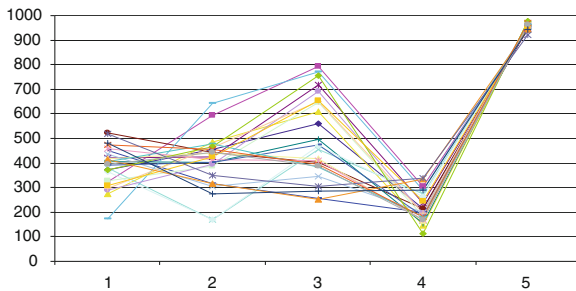
Fig. 27 The values $\{b_j(n)\}_{j=1}^{j=5}$, $n = 1, 2, \ldots, 25$, describing the learning data from Class 1—for lower envelopers
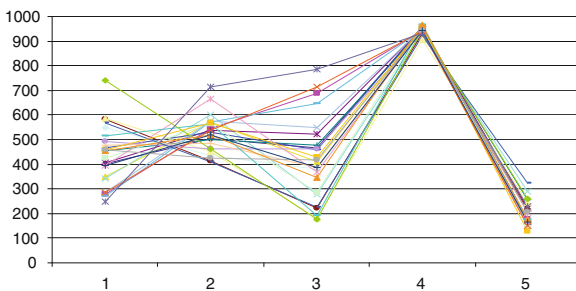
Fig. 28 The values $\{b_j(n)\}_{j=1}^{j=5}$, $n = 26, 27, \ldots, 50$, describing the learning data from Class 2—for lower envelopers
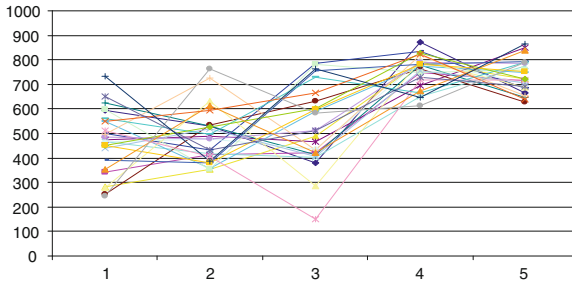
Fig. 29 The values $\{b_j(n)\}_{j=1}^{j=5}$, $n = 51, 52, \ldots, 75$, describing the learning data from Class 3—for lower envelopers
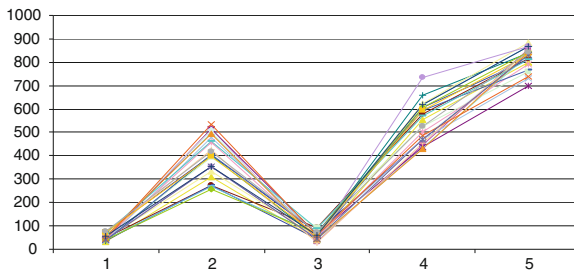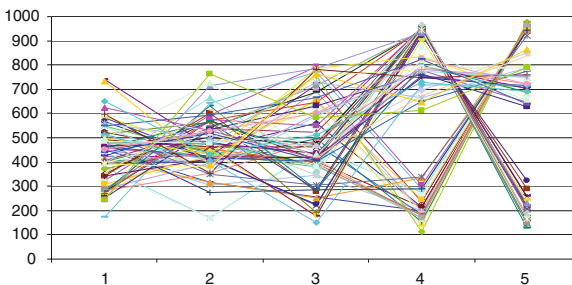

Fig. 30 The values of the attributes $\{b_j(n)\}_{j=1}^{j=5}$, $n = 1, 2, \ldots, 75$, describing the learning data from Class 1, 2 and 3—for lower envelopers

Fig. 31 The values of the attributes $\{b_j(n)\}_{j=1}^{j=5}$, $n = 76, 77, \ldots, 150$, describing the testing data from Class 1, 2 and 3—for lower envelopers
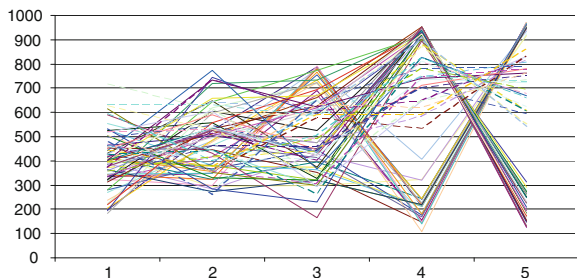
3.4 Transformation of the Essential Attributes

The essential attributes can be used directly or can be modified, and on the base of the essential attributes it is possible to generate a new set of attributes.

These new attributes can be obtained in various ways, generally it is said that the new attributes are some functions of the original essential ones [23, 32]. The main reason to generate the new attributes is to express tacit relationships between individual essential attributes. There are possible to use functions like maximum

value, minimum value, average value, etc. or some arithmetic operators including: $+, -, *$ and integer division, and so on.

In the paper two following cases are considered:

1. *The use of original essential attributes,* $\left\{c_j(n)\right\}_{j=1}^{j=5} := \left\{b_j(n)\right\}_{j=1}^{j=5}, n = 1, 2, \ldots, 150.$
2. *To generate a new set of attributes.*

The new attributes $\{c_j(n)\}_{j=1}^{j=10}, n = 1, 2, \ldots, 150,$ can be calculated as rearrangements of the essential attributes. This way we slightly enlarge dimensionality of the data series representation, but in the same time we provided in some sense the distances between the essential attributes. Now, there are $K = \begin{pmatrix} 5 \\ 2 \end{pmatrix} = 10$ new attributes, which are generated as combinations without repetitions of differences $b_i(n) - b_j(n), i, j \in \{1, 2, \ldots, 10\}, i > j,$ for $n = 1, 2, \ldots, 150.$ The new essential attributes have the following form:

$$
\begin{aligned}
\{c_j(n)\}_{j=1}^{j=10} \\
= \{ & b_2(n) - b_1(n), b_3(n) - b_2(n), b_4(n) - b_3(n), b_5(n) - b_4(n), \\
& b_3(n) - b_1(n), \quad b_4(n) - b_2(n), \quad b_5(n) - b_3(n), \\
& b_4(n) - b_1(n), \quad b_5(n) - b_2(n), \\
& b_5(n) - b_1(n)\}
\end{aligned} \tag{5}
$$

For both described cases, in the succeeding part of the paper, we will denote the attributes by $\{c_j(n)\}_{j=1}^{j=5}$ or by $\{c_j(n)\}_{j=1}^{j=10}, n = 1, 2, \ldots, 150,$ as new representation of the data series. Meanwhile in details we will describe the second case for the aggregated upper envelopes.

The new attributes for the aggregated *4* -step upper envelopes

Figures 32, 33, 34 and 35 show the attributes $\{c_j(n)\}_{j=1}^{j=10}, n = 1, 2, \ldots, 150,$ for a fixed permutation of the attributes for the aggregated *4*-step upper envelopes as well as lower envelopes.
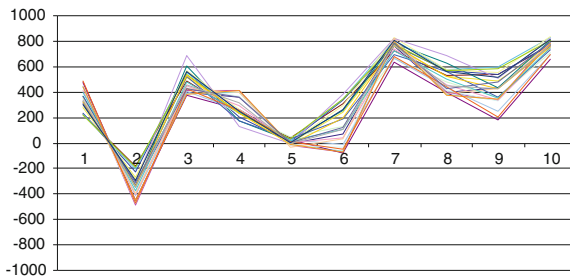
Fig. 32 The new attributes $\{c_j(n)\}_{j=1}^{j=10}, n = 1, 2, \ldots, 25,$ for Class 1—for the upper envelopes
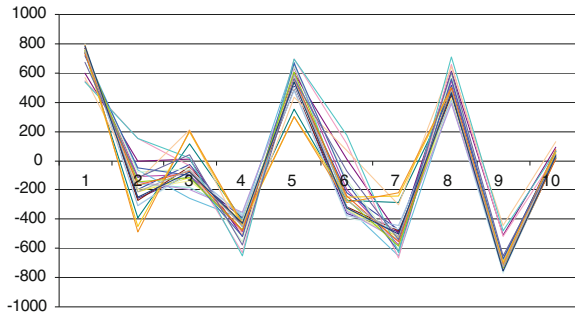
Fig. 33 The new attributes $\{c_j(n)\}_{j=1}^{j=10}$, $n = 26, 27, \ldots, 50$, for Class 2—for the upper envelopes

Fig. 34 The new attributes $\{c_j(n)\}_{j=1}^{j=10}$, $n = 51, 52, \ldots, 75$, for Class 3—for the upper envelopes
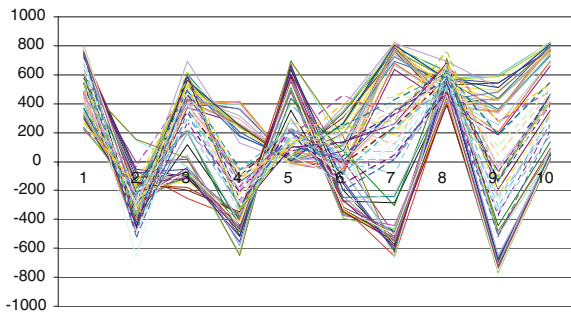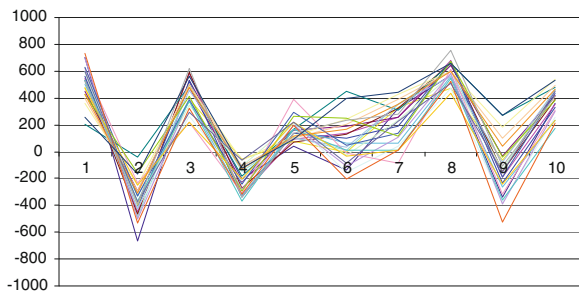
Fig. 35 Plots of new attributes $\{c_j(n)\}_{j=1}^{j=10}$, $n = 1, 2, \ldots, 75$—for the upper envelopes

Exactly in the same way we prepared the rest of data, it means the testing data $\{c_j(n)\}_{j=1}^{j=10}$, $n = 76, 77, \ldots, 150$.

The new attributes for the aggregated *4*-step lower envelopes

Figures 36, 37 and 38 show the attributes $\{c_j(n)\}_{j=1}^{j=10}$, $n = 1.2.\ldots, 75$, for a fixed permutation of the attributes for the aggregated *4*-step lower envelopes.
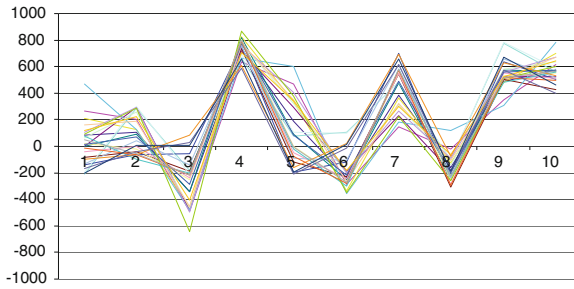
Fig. 36 The new attributes $\{c_j(n)\}_{j=1}^{j=10}$, $n = 1, 2, \ldots, 25$, for Class 1—for the lower envelopes
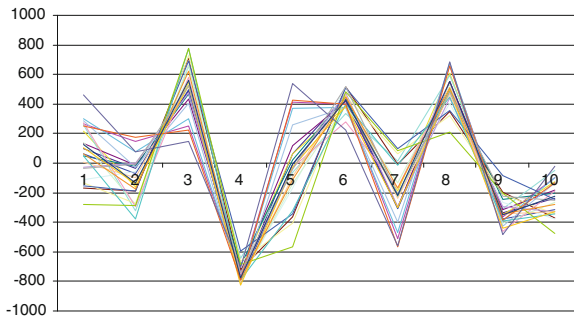
Fig. 37 The new attributes $\{c_j(n)\}_{j=1}^{j=10}$, $n = 26, 27, \ldots, 50$, for Class 2—for the lower envelopes
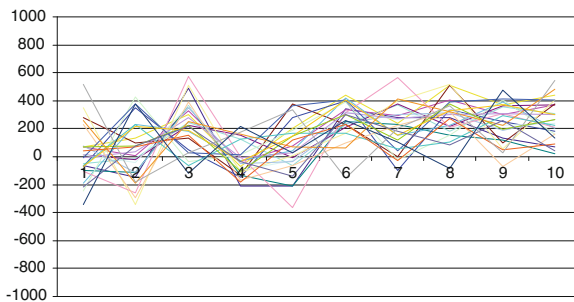
Fig. 38 The new attributes $\{c_j(n)\}_{j=1}^{j=10}$, $n = 51, 52, \ldots, 75$, for Class 3—for the lower envelopes

The new attributes $\{c_j(n)\}_{j=1}^{j=10}$, $n = 1, 2, \ldots, 150$, very within a range $[-1000, 1000]$ and before their nominalization they should be fixed in a new range $[0, 1000]$, in order to unify the nominalization process. The following simple formula changes the attributes values ranges:

$$c_j(n) := \frac{1}{2}c_j(n) + 500, \quad j = 1, 2, \ldots, 10 \quad \text{and} \quad n = 1, 2, \ldots, 150.$$

3.5 Nominalization of the Attributes

In order to simplify actual representation of the time series, denoted by $\{c_j(n)\}_{j=1}^{j=10}$, $n = 1, 2, \ldots, 150$, let us replace the real values of the attributes ranging from 0 to 1000 by the following nominal values $[a, b, c, d, e, f, g, h, i, j]$. The replacement is done in such a way that the common range of the all attributes is divided into ten elements (subranges). In the paper we apply a particular and simple method (often used) called equal width interval discretization. In general the method involves determining the domain of observed values of the attributes and dividing this interval into equal intervals. Let us consider, the set $V_{a_j} = \{v_{j,1}, \ldots, v_{j,L_j}\}$ is the domain of the attribute a_j, and L_j denotes the number of intervals for the j-th attribute, $j = 1, \ldots, K$. One can construct interval boundaries, i.e. cut points, in the following way:

$$\begin{aligned}
p_0 &= \min\{V_{a_1}, V_{a_2}, \ldots V_{a_{10}}\} = 0 \\
p_i &= p_0 + i \cdot 100, \quad i = 1, \ldots, 9 \\
p_P &= \max\{V_{a_1}, V_{a_2}, \ldots V_{a_{10}}\} = 1000.
\end{aligned} \tag{6}$$

So, the range of all attributes from 0 to 1000 is divided into ten equal subranges. Consecutive subranges are labeled by first ten letters of the alphabet, respectively, as it is shown in Fig. 39. Such labeling is done for each attribute and the new time series representation will be denoted as follows by the nominal attributes $\{a_j(n)\}_{j=1}^{j=K}$, $n = 1, 2, \ldots, 150$.

Below we will describe in details two cases of changing the real value attributes $\{c_j(n)\}_{j=1}^{j=5}$ and $\{c_j(n)\}_{j=1}^{j=10}$, $n = 1, 2, \ldots, 150$ into the nominal value attributes.

Unchanged essential attributes $\{c_j(n)\}_{j=1}^{j=5}$, $n = 1, 2, \ldots, 150$

After currying out assignment of real value attributes $\{c_j(n)\}_{j=1}^{j=5} := \{b_j(n)\}_{j=1}^{j=5}$, $n = 1, 2, \ldots, 150$ to corresponding subranges we obtained the new data series representation expressed by attributes $\{a_j(n)\}_{j=1}^{j=5}$, $n = 1, 2, \ldots, 150$, with nominal values $\{a, b, c, d, e, f, g, h, i, j\}$, see Fig. 40.

The exemplary values of the attributes after the nominalization for the aggregated 4-step upper envelopes are shown in Table 6.
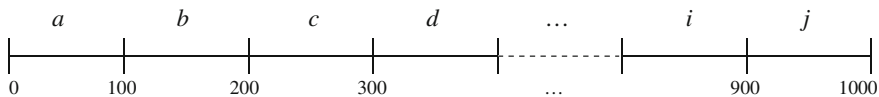
Fig. 39 The nominalization of the attributes
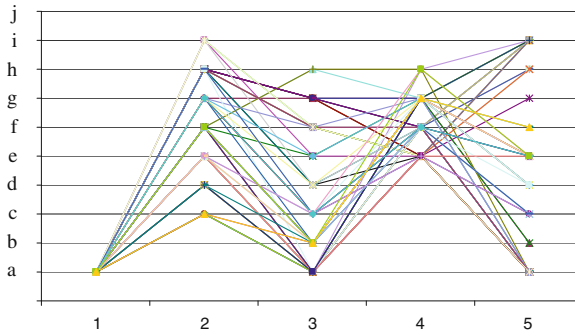
Fig. 40 The attributes $\{a_j(n)\}_{j=1}^{j=5}$, $n = 1, 2, \ldots, 75$, for the aggregated 4-step upper envelopes

Table 6 The attributes for the upper envelopes

n	$a_1(n)$	$a_2(n)$	$a_3(n)$	$a_4(n)$	$a_5(n)$	Class
1	a	d	a	e	i	1
15	a	d	a	h	i	1
40	a	h	g	e	a	2
48	a	g	f	g	a	2
55	a	e	b	g	e	3
75	a	c	b	g	f	3

Table 7 The attributes for the upper envelopes

n	$a_1(n)$	$a_2(n)$	$a_3(n)$	$a_4(n)$	$a_5(n)$	Class
1	a	d	a	e	i	1
3	a	d	a	e	i	1
20	a	d	a	e	i	1
23	a	d	a	e	i	1
27	a	h	g	f	a	2
42	a	h	g	f	a	2
44	a	h	g	f	a	2
52	a	f	b	g	d	3
58	a	f	b	g	d	3

We can notice that in the space of these five attributes there are several examples overlapping, it means that some different examples are described by exactly the same values of nominal attributes, e.g. some examples are not distinguishable, as exemplary shown in Table 7.

The exemplary values of the attributes after the nominalization for the aggregated 4-step lower envelopes are shown in Table 8 and Fig. 41.

New attributes $\{c_j(n)\}_{j=1}^{j=10}$, $n = 1, 2, \ldots, 150$

Table 8 The attributes for the lower envelopes

n	$a_1(n)$	$a_2(n)$	$a_3(n)$	$a_4(n)$	$a_5(n)$	Class
1	d	e	f	c	j	1
15	c	d	g	b	j	1
40	e	e	e	j	b	2
48	c	h	h	j	c	2
55	e	e	e	g	i	3
75	h	d	h	g	i	3
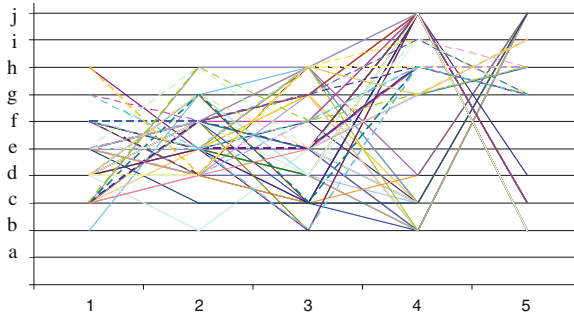
Fig. 41 The attributes $\{b_j(n)\}_{j=1}^{j=5}$, $n = 1, 2, \ldots, 75$, for the aggregated 4-step lower envelopes

Table 9 The new attributes for the upper envelopes

n	$a_1(n)$	$a_2(n)$	$a_3(n)$	$a_4(n)$	$\ldots$	$a_8(n)$	$a_9(n)$	$a_{10}(n)$	Class
1	g	d	g	g	…	g	h	9	1
15	h	c	h	g	…	h	g	i	1
40	i	e	e	d	…	g	b	f	2
48	i	e	f	c	…	i	b	f	2
55	h	d	h	d	…	i	e	h	3
75	g	e	h	e	…	i	g	h	3

The nominalization of a new set of the real values of the attributes $\{c_j(n)\}_{j=1}^{j=10}$, $n = 1, 2, \ldots, 150$ was arranged in the similar way described by (6). In results we obtained the nominal representation of the data series $\{a_j(n)\}_{j=1}^{j=10}\}$ $n = 1, 2, \ldots, 150$, and values of the attributes take one of the nominal values: $a, b, c, d, e, f, g, h, i, j$. Thus after nominalization each data series is represented by nominal values of ten attributes. Exemplary data series representations for the aggregated 4-step upper envelopes are shown in Table 9 and Fig. 42.

Exemplary data series representations for the aggregated 4-step lower envelopes are shown in Table 10 and Fig. 43.
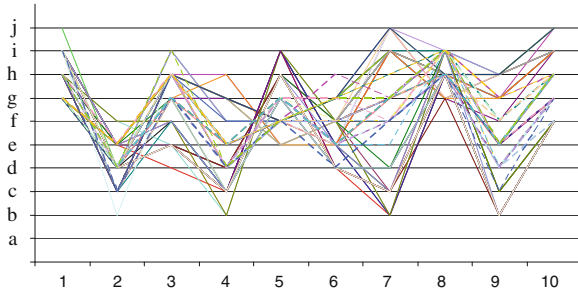
Fig. 42 The nominal attributes $\{a_j(n)\}_{j=1}^{j=10}\}$, $n = 1, 2, \ldots, 75$, for the *4*-step upper envelopes

Table 10 The new attributes for the lower envelopes

n	$a_1(n)$	$a_2(n)$	$a_3(n)$	$a_4(n)$	...	$a_8(n)$	$a_9(n)$	$a_{10}(n)$	Class
1	f	f	d	i	...	e	h	h	1
15	f	g	c	i	...	e	h	i	1
40	e	e	h	b	...	h	d	d	2
48	h	f	f	b	...	i	c	e	2
55	f	e	g	f	...	g	g	g	3
75	d	g	e	g	...	e	h	f	3
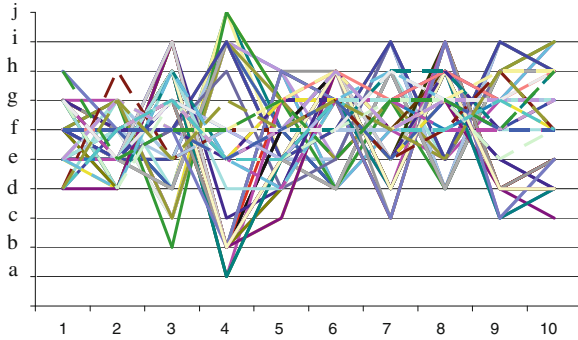
Fig. 43 The nominal attributes $\{a_j(n)\}_{j=1}^{j=10}\}$, $n = 1, 2, \ldots, 75$, for the *4*-step lower envelopes

Results of the new representation of the considered time series were used to the following time series mining problems:

- For classification problem with adopted nominal attributes $\{a_j(n)\}_{j=1}^{j=5}\}$, $n = 1, 2, \ldots, 150$, [17–20],
- For clustering problem with adopted new nominal attributes $\{a_j(n)\}_{j=1}^{j=10}\}$, $n = 1, 2, \ldots, 75$, (paper in preparation),

demonstrating suitability of the developed and described here methodology.

4 Conclusions

In this paper we introduced a new complex approach for reduction of dimension of data series. The concept is first based on the so called 'upper and lower envelopes' and 'aggregation of the envelopes', and then on essential attributes of the envelopes. Both representations provide the reduction of dimensionality of the original data series.

Performed calculations verified that the proposed methodology of reducing the dimensionality retains important features of the original data series. The classification problem gave the following results, Table 11:

The results contained in the above table show that even after a reduction of dimensionality (as well as reduction of information), the new representations preserves information, almost perfectly, about the data series characteristics of patterns, for both learning as well as testing data. The elements of the method used can be found in [7–11], [28–30].

In the case of clustering time series mining problem the obtained results are contained in Table 12: The algorithm belongs to a family of hierarchical clustering algorithms [6].

Solving this problem the affiliation of the data series was not used at all during the computational process, only for testing. Comparing the clustering results to known data series affiliation to classes it must be emphasized that all 75 objects have been separated into three groups according to their affiliation, so the clustering efficiency of the nominal attributes data series representation (as well as the clustering method) is completely perfect.

Additionally it was experimentally proved that there is not any remarkable difference in applying upper or lower envelopes, the obtained results are very similar and they are imperceptible.

The new results containing the full analysis as well as suitability of the described time series dimension reduction will be described in the succeeding authors' papers.

Table 11 The results of classification

Classification problem	Classification accuracy for learning data	Classification accuracy for testing data
For 4-step upper envelopes	100 %	97.3 %
For 4-step lower envelopes	100 %	98.7 %

Table 12 The results of clustering

Clustering problem	Accuracy for the set of data
For 4-step upper envelopes	100 %
For 4-step lower envelopes	100 %

References

1. Chan, K., Fu, A.W.: Efficient time series matching by wavelets. In: Proceedings 15th IEEE International Conference on Data Engineering. Sydney, Australia, pp. 126–133 (2005)
2. Choy, E., Krawczak, M., Shannon, A., Szmidt, E. (eds.): A Survey of Generalized Nets. KvB Institute of Technology, Sydney (2007)
3. Faloutsos, C., Ranganathan, M., Manolopulos, Y.: Fast subsequence matching in time-series databases. SIGMOD Rec. **23**, 519–529 (1994)
4. Fu, T.C.: A review on time series data mining. Eng. Appl. Artif. Intell. **24**, 164–181 (2011)
5. Jolliffe, I.T.: Principal Component Analysis. Springer, New York (2002)
6. Johnson, S.C.: Hierarchical clustering schemes. Psychometrika **2**, 241–254 (1967)
7. Kacprzyk, J., Szkatuła, G.: An inductive learning algorithm with a preanalysis data. Int. J. Knowl. Based Intel. Eng. Syst. **3**, 135–146 (1999)
8. Kacprzyk, J., Szkatuła, G.: An integer programming approach to inductive learning using genetic and greedy algorithms. In: Jain, L.C., Kacprzyk, J. (eds.) New Learning Paradigms in Soft Computing, pp. 323–367. Studies in Fuzziness and Soft Computing, Physica-Verlag Heidelberg (2002)
9. Kacprzyk, J., Szkatuła, G.: A softened formulation of inductive learning and its use for coronary disease data. Lect. Notes Artif. Intel. **3488**, 200–209 (2005a)
10. Kacprzyk, J., Szkatuła, G.: An inductive learning algorithm with a partial completeness and consistence via a modified set covering problem. Lect. Notes Comput. Sci. **3697**, 661–666 (2005b)
11. Kacprzyk, J., Szkatuła, G.: Inductive Learning: A Combinatorial Optimization. In: Koronacki J., Ras Z.W., Wierzchoń S.T., Kacprzyk J. (eds.) Advances in Machine Learning. Studies in, Computational Intelligence, vol. 262, Springer (2010)
12. Keogh, E., Chakrabarti K., Pazzani M.: Locally adaptive dimensionality reduction for indexing large time series databases. In: Proceedings of ACM SIGMOD Conference on Management of Data. Santa Barbara, pp. 151–162, May 21–24 2001
13. Krawczak, M.: Multilayer Neural Systems and Generalized Net Models. Ac. Publ House EXIT, Warsaw (2003a)
14. Krawczak, M.: Heuristic dynamic programming—learning as control problem. In: Rutkowski, L., Kacprzyk, J. (eds.) Neural Networks and Soft Computing, pp. 218–223. Physica Verlag, Heidelberg (2003b)
15. Krawczak, M.: A novel modelling methodology: generalized nets. In: Cader A., Rutkowski L., Tadeusiewicz R., Żurada J. (eds.) Artificial Intelligence and Soft Computing. Ac. Publ. House EXIT, Warsaw (2006)
16. Krawczak, M., Szkatuła, G., et al.: On decision rules application to time series classification. In: Atanassov, K.T. (ed.) Advances in Fuzzy Sets, Intuitionistic Fuzzy Sets, Generalized Nets and Related Topics. Ac. Publ. House EXIT, Warsaw (2008)
17. Krawczak, M., Szkatuła G. (2010a) Time series envelopes for classification. In: IEEE Intelligent Systems Conference, London, July 7–9 2010
18. Krawczak, M., Szkatuła, G.: On time series envelopes for classification problems. In: Atanassov K.T. et al. (eds.) Developments in Fuzzy Sets, Intuitionistic Fuzzy Sets, Generalized Nets and Related Topics, vol II, SRI PAS, Warsaw (2010b)
19. Krawczak, M., Szkatuła, G.: Dimentionality reduction for time series. Case Stud. Pol. Assoc. Knowl. **31**, 32–45 (2010c)
20. Krawczak, M., Szkatuła, G.: A hybrid approach for dimension reduction in classification. Control Cybern. **40**(2), 527–552 (2011)
21. Lin, J., Keogh, E., Patel, P., Lonardi, S.: Finding motifs in time series. In: The 2nd Workshop on Temporal Data Mining, the 8th ACM International Conference on Knowledge Discovery and Data Mining. Edmonton, Canada, pp. 53–68 (2002)
22. Lin, J., Keogh, E., Wei, L., Lonardi, S.: Experiencing SAX: a novel symbolic representation of time series. Data Min. Knowl. Disc. **2**(15), 107–144 (2007)

23. Matheus, C., Rendell, L.: Constructive induction on decision trees.In: Proceedings of the Eleventh International Joint Conference on Artifcial Intelligence, Mateo, CA, Morgan Kaufmann (1989)
24. Nanopoulos, A., Alcock, R., Manolopoulos, Y.: Feature-based classification of time-series data. Int. J. Comput. Res. **10**, 49–61 (2001)
25. Oja, E.: Principal components, minor components and linear neural networks. Neural Netw. **5**, 927–935 (1992)
26. Rodríguez, J. J., Alonso, C.J.: Interval and dynamic time warping-based decision trees. In: Proceedings of the 2004 ACM symposium on applied computing (SAC), pp. 548–552 (2004)
27. Shahabi, C., Tian, X., Zhao, W.: TSA-tree: A wavelet-based approach to improve the efficiency of multi-level surprise and trend queries. In: Proceedings of the 12th International Conference on Scientific and Statistical Database Management. Berlin, pp. 55–68 (2000)
28. Szkatuła, G.: Machine learning from examples under errors in data, Ph.D. Thesis, SRI PAS Warsaw, Poland (1995)
29. Szkatuła, G.: Application of modified covering problem in machine learning. In: Gutenbaum, J. (ed.) Automatics Control Manage., pp. 431–445. SRI PAS, Warsaw (2002)
30. Szkatuła, G., Kacprzyk, J.: An inductive learning algorithm with a partial completeness and consistency. In: Dramiński, M., Grzegorzewski, P., Trojanowski, T., Zadrożny, S. (eds.) Issues in Intelligent Systems. Models and Techniques, pp. 229–246. EXIT, Warszawa (2005)
31. Wang, B.: A new clustering algorithm on nominal data sets. In: Proceedings of International MultiConference of Engineers and Computer Scientists 2010 (IMECS 2010), Hong Kong, March 17–19 2010
32. Wu, Y., Chang, E.Y.: Distance-function design and fusion for sequence data. CIKM **04**, 324–333 (2004)
33. Yang, Q., Wu, X.: 10 Challenging problems in data mining research. Int. J. Inf. Technol. Decis. Making **5**(4), 597–604 (2006)

Bayesian Classification of Interval-Type Information

Piotr Kulczycki and Piotr A. Kowalski

Abstract The subject of Bayes classification of imprecise multidimensional information of interval type by means of patterns defined through precise data (i.e. deterministic or sharp) is investigated here. To this aim the statistical kernel estimators methodology was applied, which avoids the pattern shape for the resulting algorithm. In addition, elements of pattern sets which have insignificant or negative influence on correctness of classification are eliminated. The concept for realizing the procedure is based on the sensitivity method, used in the domain of artificial neural networks. As a result of this procedure the number of correct classifications and—above all—calculation speed increased significantly. A further growth in quality of classification was achieved with an algorithm for the correction of classifier parameter values.

P. Kulczycki (✉) · P. A. Kowalski
Centre of Information Technology for Data Analysis Methods,
Systems Research Institute, Polish Academy of Sciences, Warsaw, Poland
e-mail: Piotr.Kulczycki@ibspan.waw.pl

P. A. Kowalski
e-mail: Piotr.A.Kowalski@ibspan.waw.pl

P. Kulczycki · P. A. Kowalski
Department of Automatic Control and Information Technology,
Cracow University of Technology, Krakow, Poland

1 Introduction

The current dynamic development in computer technology offers a continuous increase in both capability and speed of contemporary calculational systems, thus allowing ever more frequent use of methods which up to now had only been applied to a relatively limited extent. One of these methods is the analysis of information which is imprecise in various—depending on a problem's conditioning—forms, for example uncertain (statistical methods [8]) or fuzzy (fuzzy logic [10]).

Lately many applications have noted an increase in the use of interval analysis. The basis for this concept is the assumption that the only available information on an investigated quantity is the fact that it fulfils the dependence $\underline{x} \leq x \leq \bar{x}$, and in consequence this quantity can be associated with the interval

$$[\underline{x}, \bar{x}]. \tag{1}$$

Interval analysis is a separate mathematical domain, with its own formal apparatus based on an axiom of the sets theory [20].

A fundamental application of interval analysis was to ensure the required precision of numerical calculations, through monitoring errors arising from rounding numbers [1], however as a result of its continuous development, this field is finding ever wider uses in engineering, econometrics and other related areas [9]. Its main advantage is the fact that by definition it models imprecision of a researched quantity, using the simplest possible formula. In many applications interval analysis shows to be absolutely sufficient, yet does not require many calculations (thus enabling its application in highly complex tasks) and is easy to identify and interpret, while also maintaining a formalism stemming from a convenient mathematical tool. Moreover, it can be noted that its concept is related to statistical interval estimation, and analysis of fuzzy numbers with rectangular membership functions.

Dynamic development is also currently taking place in information technologies in the area of data analysis and exploration [16]. This is due not only to an increase in the possibilities of the methodology used here, but above all to an increase in accessibility of its algorithms, up to now a domain only available to a relatively small group of specialists. Among the fundamental tasks of data analysis and exploration lies that of classification [7]. It consists of assigning a tested element to one of several previously selected groups. They are most often given by patterns, which are sets of elements representative for particular classes. This means that in many problems—including those where data containing imprecision is investigated—elements defining patterns are defined precisely (e.g. deterministic in probability approach, sharp for the case of fuzzy logic, or in relation to notation (1) fulfilling equality $\underline{x} = \bar{x}$).

This chapter offers a complete procedure for classification of imprecise information, defined as the interval vector

$$\begin{bmatrix} [\underline{x_1}, \overline{x_1}] \\ [\underline{x_2}, \overline{x_2}] \\ \vdots \\ [\underline{x_n}, \overline{x_n}] \end{bmatrix}, \tag{2}$$

where $\underline{x_k} \leq \overline{x_k}$ for $k = 1, 2, \ldots, n$, when the patterns of particular classes are given as sets of precise data (i.e. deterministic or sharp) elements, i.e. with $\underline{x_k} = \overline{x_k}$ ($k = 1, 2, \ldots, n$). The classification concept is based on the Bayes approach, ensuring a minimum of potential losses occurring through classification errors. For a such formulated task the statistical kernel estimators methodology was employed, thereby freeing the above procedure from arbitrary assumptions regarding pattern forms—their identification becomes an integral part of the presented algorithm. A procedure was also developed for reducing the size of pattern sets by elements having negligible or negative influence on correctness of classification. Its concept is founded on the sensitivity method, used in the domain of artificial neural networks, although the intention is to increase the number of accurate classifications and—above all—calculation speed. Furthermore a method was designed to ensure additional improvements in classification results, obtained by correcting the values of classifier parameters. Basic investigations are presented in the chapter [17]. First research in this subject was described in the work [13].

2 Preliminaries

2.1 Statistical Kernel Estimators

Kernel estimators belong to the group of nonparametric statistical methods. They allow calculation and clear illustration of characteristics of a random variable distribution, without knowledge of its membership of a given class.

Let (Ω, Σ, P) denote a probability space. Let also an n-dimensional random variable $X : \Omega \rightarrow \mathbb{R}^n$, with distribution density f, be given. Its kernel estimator $\hat{f} : \mathbb{R}^n \rightarrow [0, \infty)$ is calculated on the basis of an m-elements random sample $\{x_i\}_{i=1,2,\ldots,m}$ and defined—in the basic form—by the formula

$$\hat{f}(x) = \frac{1}{mh^n} \sum_{i=1}^{m} K\left(\frac{x - x_i}{h}\right), \tag{3}$$

where the positive coefficient h is known as a smoothing parameter, while the measurable function $K : \mathbb{R}^n \rightarrow [0, \infty)$ symmetrical with respect to zero, having at this point weak global maximum and fulfilling the condition $\int_{\mathbb{R}^n} K(x)dx = 1$ is termed a kernel. The choices of form for the kernel K and value for the smoothing parameter

h are most often made based on the criterion of minimization of integrated square error [15, 21, 23].

Thus, the form of the kernel K has practically no influence on the statistical quality of estimation. This chapter applies the generalized (one-dimensional) Cauchy kernel

$$K(x) = \frac{2}{\pi(x^2 + 1)^2},$$ (4)

in the multidimensional case defined using the product kernel concept

$$K(x) = K\left(\begin{bmatrix} x_1 \\ x_2 \\ \vdots \\ x_n \end{bmatrix}\right) = \mathscr{K}(x_1) \cdot \mathscr{K}(x_2) \cdot \; ... \; \cdot \mathscr{K}(x_n),$$ (5)

where $\mathscr{K}$ denotes here the one-dimensional kernel given by formula (4).

The value of the smoothing parameter h can be calculated in practice with confirmed algorithms available in literature. The effective and convenient plug-in method [15, Sect. 3.1.5]; [23, Sect. 3.6.1] is recommended here. In the multidimensional case, regarding application of the product kernel in this chapter, the smoothing parameter will be naturally denoted as $h_1, h_2, \ldots, h_n$ respectively for subsequent coordinates, and can be obtained separately for each of them by the above suggested method.

In practice one employs additional procedures to generally increase the quality of the kernel estimator and fit its features to those of the considered reality. In this chapter the modification of the smoothing parameter [15, Sect. 3.1.6]; [21, Sect. 5.3.1] will be applied, thereby significantly improving the properties of the kernel estimator, particularly in areas where it assumes small values. In classification tasks this takes place especially near boundaries of specific classes, which makes this procedure particularly useful here.

Consider therefore nonnegative modifying coefficients

$$s_i = \left(\frac{\hat{f}_*(x_i)}{\bar{s}}\right)^{-c} \text{ for } i = 1, 2, \ldots, m,$$ (6)

where the constant $c \geq 0$ is called a modification intensity, $\hat{f}_*$ denotes the kernel estimator in its basic form (3), and $\bar{s}$—the geometrical mean of the quantities $\hat{f}_*(x_i)$ with $i = 1, 2, \ldots, m$. The final definition of estimator (3) with product kernel (5) then takes the form:

$$\hat{f}(x) = \frac{1}{mh_1h_2...\,h_n} \sum_{i=1}^{m} \frac{1}{s_i^n} \mathscr{K}\left(\frac{x_1 - x_{i,1}}{h_1 s_i}\right) \mathscr{K}\left(\frac{x_2 - x_{i,2}}{h_2 s_i}\right) \; ... \; \mathscr{K}\left(\frac{x_n - x_{i,n}}{h_n s_i}\right),$$ (7)

where the natural notations

$$x = \begin{bmatrix} x_1 \\ x_2 \\ \vdots \\ x_n \end{bmatrix}, \quad x_i = \begin{bmatrix} x_{i,1} \\ x_{i,2} \\ \vdots \\ x_{i,n} \end{bmatrix} \text{ for } i = 1, 2, \ldots, m \quad (8)$$

are used, and together with formula (4) will be employed later in this chapter. The case $c = 0$ determines the lack of smoothing parameter modification, while together with an increase in the value c its intensity grows. Corollaries resulting from the mean-square criterion primarily point to the value

$$c = 0.5 \, . \quad (9)$$

Statistical kernel estimators are dealt with in the monographs [15, 21, 23]. Information on the subject of their applications in standard classification tasks can be found in the books [2, 3, 18, 19].

2.2 Sensitivity Analysis of Neural Networks

When modeling multidimensional problems using artificial neural networks [22], particular components of an input vector most often are characterized by diverse significance of information, and in consequence influence variously the result of the data processing. In order to eliminate redundant—from the point of view of the investigated task—input vector components, a sensitivity analysis of the network with respect to particular learning data is often used. A basic factor for network reduction is sensitivity of the output function with regards to particular input data.

The essence of the sensitivity method [24] consists in defining—after the network learning phase—the influence of the particular inputs u_i for $i = 1, 2, \ldots, m$ on the output value y, which is characterized by the real coefficients

$$S_i = \frac{\partial y(u_1, u_2, \ldots, u_m)}{\partial u_i} \quad \text{for} \quad i = 1, 2, \ldots, m. \quad (10)$$

Next, one aggregates the particular coefficients $S_i^{(p)}$ originating from successive iterations of the previous phase and corresponding to the sensitivity of subsequent learning data, with $p = 1, 2, \ldots, P$. The result is the final coefficient $\bar{S}_i$ given by the formula

$$\bar{S}_i = \sqrt{\frac{\sum_{p=1}^{P} (S_i^{(p)})^2}{P}} \quad \text{for} \quad i = 1, 2, \ldots, m. \quad (11)$$

After the sorting operation for the vector $\bar{S}_i$ according to decreasing values, an analysis of the relevance of particular components to the result of network operation is performed, and then the least important inputs are eliminated.

In the general case the above algorithm can be used repeatedly to achieve further reduction. However, during empirical testing of the classification method developed here, such action did not bring positive results and so was forsaken.

The application of the above method led to an increase in speed, as well as reduction of errors of learning and generalization, while at the same time reducing the input dimension of the artificial neural network by removing information of little significance or even elimination of data (input vector components) having unfavorable influence on the obtained result's correctness. Detailed considerations concerning the above procedure are found in the publications [4, 24].

3 An Algorithm for Interval Classification

3.1 One-Dimensional Case

This section considers the one-dimensional case, i.e. when $n = 1$. Let therefore be given the quantity having undergone the classification procedure, for the case currently being considered, represented by the (one-dimensional) interval

$$[\underline{x}, \overline{x}] \,, \tag{12}$$

while $\underline{x} \leq \bar{x}$; if $\underline{x} = \bar{x}$ then the classic case is obtained where the quantity is precise (e.g. deterministic or sharp). Assume also that the real number sets (patterns):

$$x_1^1, \, x_2^1, \ldots, x_{m_1}^1 \tag{13}$$

$$x_1^2, \, x_2^2, \ldots, x_{m_2}^2 \tag{14}$$

$$\vdots$$

$$x_1^J, \, x_2^J, \ldots, x_{m_J}^J \tag{15}$$

represent subsequent J marked classes. The upper index, introduced in the above notation, characterizes membership of an element to a given class. As stated before, the task of classification consists of deciding to which of these groups tested element (12) should be assigned.

Let now $\hat{f}_1, \hat{f}_2, \ldots, \hat{f}_J$ denote kernel estimators of probability distribution density, calculated successively based on sets (13)–(15) treated as random samples—a description of the methodology used for their construction is contained in Sect. 2.1.

In accordance with the classic Bayes approach [3], the classified element $\tilde{x} \in \mathbb{R}$ should then be given to the class for which the value

$$m_1 \hat{f}_1(\tilde{x}), m_2 \hat{f}_2(\tilde{x}), \ldots, m_J \hat{f}_J(\tilde{x}) \tag{16}$$

is the biggest. In the case of information of interval type, represented by element (12), one can infer that this element belongs to the class for which the expression

$$\frac{m_1}{\overline{x} - \underline{x}} \int_{\underline{x}}^{\overline{x}} \hat{f}_1(x)\mathrm{d}x, \frac{m_2}{\overline{x} - \underline{x}} \int_{\underline{x}}^{\overline{x}} \hat{f}_2(x)\mathrm{d}x, \ldots, \frac{m_J}{\overline{x} - \underline{x}} \int_{\underline{x}}^{\overline{x}} \hat{f}_J(x)\mathrm{d}x \tag{17}$$

is the greatest.

Considering the limit transitions $\overline{x} \to \tilde{x}$ and $\underline{x} \to \tilde{x}$ for the fixed $\tilde{x} \in \mathbb{R}$, then due to the continuity of the function K used here, given by formula (4), consequently implying the continuity of the kernel estimator $\hat{f}_j$, one obtains

$$\lim_{\substack{\underline{x} \to \tilde{x} \\ \overline{x} \to \tilde{x}}} \frac{1}{\overline{x} - \underline{x}} \int_{\underline{x}}^{\overline{x}} \hat{f}_j(x)\mathrm{d}x = \hat{f}_j(\tilde{x}) \quad \text{for } j = 1, 2, \ldots, J. \tag{18}$$

The expressions specified in formula (17) reduce therefore to the classic type (16).

In formula (17), the positive expression $1/(\overline{x} - \underline{x})$ can be omitted as irrelevant in an optimization problem, and so it is equivalent to

$$m_1 \int_{\underline{x}}^{\overline{x}} \hat{f}_1(x)\mathrm{d}x, m_2 \int_{\underline{x}}^{\overline{x}} \hat{f}_2(x)\mathrm{d}x, \ldots, m_J \int_{\underline{x}}^{\overline{x}} \hat{f}_J(x)\mathrm{d}x . \tag{19}$$

What is more, for any $j = 1, 2, \ldots, J$ one can note

$$\int_{\underline{x}}^{\overline{x}} \hat{f}(x)\mathrm{d}x = \hat{F}(\overline{x}) - \hat{F}(\underline{x}) , \tag{20}$$

where

$$\hat{F}(x) = \int_{-\infty}^{x} \hat{f}(y)\mathrm{d}y . \tag{21}$$

Taking into consideration dependence (21) substituting equalities defining kernel estimator (7) (for $n = 1$) and kernel (4) used, one can analytically calculate that

$$\hat{F}(x) = \sum_{i=1}^{m} \left[\frac{(x^2 - 2xx_i + x_i^2 + h^2 s_i^2)\, \mathrm{arctg}\left(\frac{x-x_i}{s_i h}\right) + h s_i (x - x_i)}{x^2 - 2xx_i + x_i^2 + h^2 s_i^2} + \frac{\pi}{2} \right],$$

(22)

where again the positive constant $1/m\pi$ has been omitted. Finally it should be acknowledged that the considered element belongs to the class for which the corresponding expression in formula (19) is the greatest, whereby the integral appearing there for any $j = 1, 2, \ldots, J$ can be effectively calculated using dependences (20) and (22). The above completes the classification algorithm for the one-dimensional case.

3.2 The Multidimensional Case

The concept presented in the previous subsection can be naturally generalized for the multidimensional case, i.e. when $n > 1$. Thus, if information of interval type is represented by the interval vector

$$\begin{bmatrix} [\underline{x_1}, \overline{x_1}] \\ [\underline{x_2}, \overline{x_2}] \\ \vdots \\ [\underline{x_n}, \overline{x_n}] \end{bmatrix},$$

(23)

and sets (13)–(15) contain the elements of the space $\mathbb{R}^n$, then one can infer that the considered element is assigned to the class with the greatest value for the expression

$$m_1 \int_E \hat{f}_1(x)\mathrm{d}x, \; m_2 \int_E \hat{f}_2(x)\mathrm{d}x, \ldots, m_J \int_E \hat{f}_J(x)\mathrm{d}x \;,$$

(24)

where $E = [\underline{x_1}, \overline{x_1}] \times [\underline{x_2}, \overline{x_2}] \times \cdots \times [\underline{x_n}, \overline{x_n}]$. It is slightly different, though, for the algorithm for calculating the integrals appearing above. However, thanks to the properties of the product kernel used here, for any fixed $j = 1, 2, \ldots, J$ and the kernel K, the following dependence is true:

$$\int_E K(x)\mathrm{d}x = [\mathscr{F}(\overline{x_1}) - \mathscr{F}(\underline{x_1})][\mathscr{F}(\overline{x_2}) - \mathscr{F}(\underline{x_2})] \ldots [\mathscr{F}(\overline{x_n}) - \mathscr{F}(\underline{x_n})] \;,$$

(25)

where $\mathscr{F}$ denotes the primitive of the function $\mathscr{K}$ introduced by definition (5). Taking into account the definition of the kernel estimator with product kernel (7) as well as the analytical form of the primitive function contained in formula (22), the above completes the procedure for classification of interval type information, for the multidimensional case also.

3.3 Calculational Complexity of the Algorithm

From the point of view of calculational complexity, it is worth underlining the two-phased nature of the method presented in this chapter. The first stage contains the complex procedures for constructing the classifier, which are executed once at the beginning. The most time-consuming is the algorithm for calculating the smoothing parameter using the plug-in method of complexity $O(nm^2)$. This same complexity characterizes the calculations for the smoothing parameter modification procedure.

On the contrary, the procedure for calculating the values of the kernel estimator has the complexity $O(nm)$. Taking into account that the number of the operations above is equal to the number of assumed classes J, then the calculational complexity of the second phase is linear with respect to all three parameters: n, m and J, where m characterizes here the size of particular patterns. It implies a relatively short calculation time, which after earlier execution of the first phase, in most practical problems allows for the application of the investigated algorithm in real time, in an on-line regime.

4 Procedures for Increasing Classification Quality

4.1 Reducing Pattern Size

In practice, some elements of sets (13)–(15), constituting patterns of particular classes, may have insignificant or even negative—in the sense of classification correctness—influence on quality of obtained results. Their elimination should therefore imply a reduction in the number of erroneous assignations, as well as decreasing calculation time. To this aim the sensitivity method for learning data, used in artificial neural networks, described in Sect. 2.2, will be applied.

To meet requirements of this procedure, the definition of the kernel estimator will be generalized below with the introduction of nonnegative coefficients $w_1, w_2, \ldots, w_m$, adjusted by the condition

$$\sum_{i=1}^{m} w_i = m \,, \tag{26}$$

and mapped to particular elements of the random sample. The basic form of kernel estimator (3) then takes the form

$$\hat{f}(x) = \frac{1}{mh^n} \sum_{i=1}^{m} w_i K\left(\frac{x - x_i}{h}\right). \tag{27}$$

Formula (7) undergoes analogous generalization. The coefficient w_i value may be interpreted as indicating the significance of the i-th element of the pattern to classification correctness. Note that if $w_i \equiv 1$, then dependence (27) is regressed to initial form (3).

In the method designed here, for the purpose of reduction of sets (13)–(15), separate neural networks are built for each investigated class. In order to ensure coherence of the notation below, let now the index $j = 1, 2, \ldots, J$ characterizing particular classes, be arbitrarily fixed.

The constructed network has three layers and is unidirectional, with m inputs (corresponding to particular elements of a pattern), a hidden layer whose size is equal to the integral part of the number $\sqrt{m}$, and also one output neuron. This network is submitted to a learning process using a data set comprising of the values of particular kernels for subsequent pattern elements, while the given output constitutes the value of the kernel estimator calculated for the pattern element under consideration. Apart from the above topology, as a result of empirical research, the maximum number of epochs was assumed as 100, the maximum learning error 0.01, the learning speed 0.3, and the momentum coefficient as 0.1. On finishing the learning process, the thus obtained network undergoes sensitivity analysis on learning data, in accordance with the method presented in Sect. 2.2. The resulting coefficients $\bar{S}_i$ describing sensitivity, obtained on the basis of formula (11), constitute the fundament for calculating preliminary values

$$\tilde{w}_i = \left(1 - \frac{\bar{S}_i}{\sum_{j=1}^{m} \bar{S}_j}\right), \tag{28}$$

after which they are adjusted to the form

$$w_i = m \frac{\tilde{w}_i}{\sum_{i=1}^{m} \tilde{w}_i} \tag{29}$$

to guarantee condition (26). It is worth noting that the form of formulas (10)–(11) accounting in practice for all coefficients $\bar{S}_i$ can not be equal to zero, which guarantees feasibility of the above operation. The formula for dependence (28) results from the fact that the network created here is the most sensitive to atypical and redundant elements, which—taking into account the form of kernel estimator (27)—implies a necessity to map the appropriately smaller values $\tilde{w}_i$, and in consequence w_i, to them. The coefficients (29) characterize—according to the idea presented during formulation of generalized form (27)—the significance of particular elements of the pattern, for classification procedure correctness.

Empirical research confirmed the natural assumption that the pattern set should be relieved of those elements for which $w_i < 1$. (Note that, thanks to adjustments made by formula (29), the mean value of coefficients w_i equals 1.) Decreasing of a such assumed threshold value resulted in a significant drop in the degree of a pattern size reduction, while in vicinity of the value 1 the influence on classification quality was practically unnoticeable, however considerable diminishing implied a sizable

rise in number of errors. On the other hand, an increase in this value caused a sharp fall in classification quality, due to a loss of valuable and non-redundant information included in the pattern.

4.2 Correcting the Smoothing Parameter and Modification Intensity Values

Subject literature often presents the opinion that the classic universal methods of calculating the smoothing parameter value— most often based on a quadratic criterion— are not satisfying for the classification task. For example, in the article [6] experimental research conducted on two classes was presented showing the significant difference between the value of this parameter when calculated by minimizing integrated square error, and when obtained by minimizing the number of misclassifications. However the latter method is difficult in practical use for the multidimensional case, due to an extraordinarily long calculation time—a problem which becomes more important the greater the number of classes. Available literature does not propose a definitive solution for such a task.

This chapter suggest introducing $n + 1$ multiplicative correcting coefficients for the values of the parameter defining the intensity of modification procedure c and smoothing parameters for particular coordinates $h_1, h_2, \ldots, h_n$, with respect to optimal ones calculated using the integrated square error criterion. Denote them as $b_0 \geq 0, b_1, b_2, \ldots, b_n > 0$, respectively. It is worth noticing that $b_0 = b_1 = \cdots = b_n = 1$ means in practice no correction. Next through a comprehensive search using a grid with a relatively large discretization value, one finds the most advantageous points regarding minimal incorrect classification sense. The final phase is a static optimization procedure in the $(n+1)$-dimensional space, where the initial conditions are the points chosen above, while the performance index is given as

$$J(b_0, b_1, \ldots, b_n) = \#\{incorrect \quad classifications\}, \qquad (30)$$

when # denotes the power (size) of a set. The value of the above functional for a fixed argument is calculated with the help of the classic leave-one-out method. This is an integer—to find the minimum a modified Hook-Jeeves algorithm [11] was applied.

Following experimental research it was assumed that the grid used for primary searches has intersections at the points $0.25, 0.5, \ldots, 1.75$ for every coordinate. For such intersections the value of functional (30) is calculated, after which the obtained results are sorted, and the 5 best become subsequent initial conditions for the Hook-Jeeves method, where the value of the initial step is taken as 0.2. After finishing every one of the above 5 "runs" of this method, the functional (30) value for the end point is calculated, and finally among them is shown the one with the smallest value.

5 Final Remarks and Conclusions

This chapter presents the complete Bayes algorithm—thereby ensuring minimum potential losses—for the classification of multidimensional imprecise information of interval type, where patterns of particular classes are given on the basis of sets of precisely defined elements, with no limits to the number of classes. In addition two optional procedures are provided, which improve and enhance the quality of classification: a reduction in pattern size and a correction of the classifier parameter values.

Numerical testing wholly confirmed the positive features of the method worked out. It was carried out with the use of pseudorandom and benchmark data. In particular, the results show that the classifying algorithm can be used successfully for inseparable classes of complex multimodal patterns as well as for those consisting of incoherent subsets at alternate locations. This is thanks to the application of the statistical kernel estimators methodology, which makes the above procedure independent of the shapes of patterns—their identification is an integral part of the presented algorithm. As shown by numerical verification, the algorithm has beneficial features in the multidimensional case too. The results also compared positively to those obtained by applying support vectors machines as well as by the two natural methods.

In particular, during numerical testing it was established that, after applying the procedure for reducing pattern sets, presented in Sect. 4.1, the number of wrong classifications was lowered by approximately 15 %, while the size of patterns was reduced by approximately 40 %. The conjunction of these results is particularly worthy of attention: while appropriately reducing pattern sizes, which does imply a significant increase in calculation speed, the classification quality is also importantly improved. In addition, the procedure of correcting the smoothing parameter and intensity of its modification, presented in Sect. 4.2, conducted after the reduction of patterns caused a further decrease in the number of classification errors to approximately 14 %.

The task of classifying interval information based on precise data can be interpreted illustratively with the example where the patterns present actual, precisely measured quantities, while intervals being classified represent uncertainties and imprecision in plans, estimations or difficult measurements to make. In particular, pattern sets may consists of very accurate measurements, in which errors are practically ignored, while the classified interval constitutes a measurement taken from another, much less accurate apparatus or carried out in much worse conditions. Another example of the application of this kind of classification is the possibility of treating precise data as actual information from the past, e.g. temperature or currency exchange rates, while the classified element represents a prognosis which by nature is limited in precision.

In particular, the method investigated here can be applied for purposes of the diagnosis process [5, 12, 14]. Namely, let interval (12) or interval vector (23) represent a quantity or n quantities, respectively, whose values attest to the current or—in the case of fault prognosis—predicted technical state of a supervised device. Because of measurement errors and natural fluctuations, the interval form can be

justified in many practical tasks. Let also sets (13)–(15) constitute patterns of particular types of possible faults. The classification procedure presented in this chapter allows for precise diagnostic readings to be obtained, with regard to interval character of investigated quantities.

References

1. Alefeld, G., Hercberger, J.: Introduction to Interval Computations. Academic Press, New York (1986)
2. Devroye, L., Gyorfi, L., Lugosi, G.: A Probabilistic Theory of Pattern Recognition. Springer, New York (1996)
3. Duda, R.O., Hart, P.E., Stork, D.G.: Pattern Classification. Wiley, New York (2001)
4. Engelbrecht, A.P., Cloete, I., Zurada, J.: Determining the significance of input parameters using sensitivity analysis. In: International Workshop on Artificial Neural Networks, Torremolinos (Spain), 7–9 June 1995. LNCS 930, pp. 382–388
5. Gertler, J.: Fault Detection and Diagnosis in Engineering Systems. Dekker, New York (1998)
6. Ghosh, A.K., Chaudhuri, P., Sengupta, D.: Classification Using Kernel Density Estimation: Multiscale Analysis and Visualization. Technometrics, **48**, 120–132 (2006)
7. Hand, D.J.: Construction and Assessment of Classification Rules. Wiley, Chichester (1997)
8. Hryniewicz, O.: Reliability Sampling; in Encyclopedia of Statistics in Quality and Reliability. Wiley, Chichester (2008)
9. Jaulin, L., Kieffer, M., Didrit, O., Walter, E.: Applied Interval Analysis. Springer, Berlin (2001)
10. Kacprzyk, J.: Multistage Fuzzy Control: A Model-Based Approach to Control and Decision-Making. Wiley, Chichester (1997)
11. Kelley, C.T.: Iterative Methods for Optimization. SIAM, Philadelphia (1999)
12. Korbicz, J., Koscielny, J.M., Kowalczuk, Z., Cholewa, W., (eds.): Fault Diagnosis. Models, Artificial Intelligence Applications. Springer, Berlin (2004)
13. Kowalski, P.A.: Klasyfikacja bayesowska informacji niedokladnej typu przedzialowego. Ph.D. thesis, Systems Research Institute, Polish Academy of Sciences (2009)
14. Kulczycki, P.: Wykrywanie uszkodzen w systemach zautomatyzowanych metodami statystycznymi. Alfa, Warsaw (1998)
15. Kulczycki, P.: Estymatory jadrowe w analizie systemowej. WNT, Warsaw (2005)
16. Kulczycki, P., Hryniewicz, O., Kacprzyk, J. (eds.): Techniki informacyjne w badaniach systemowych. WNT, Warsaw (2007)
17. Kulczycki, P., Kowalski, P.A.: Bayes classification of imprecise information of interval type. Control Cybern. **40**, 101–123 (2011)
18. Ledl, T.: Kernel density estimation, theory and application in discriminant analysis. Austrian J. Stat. **33**, 267–279 (2004)
19. McLachlan, G.J.: Discriminant Analysis and Statistical Pattern Recognition. Wiley, Hoboken (2004)
20. Moore, R.E.: Interval Analysis. Prentice-Hall, Englewood Cliffs (1966)
21. Silverman, B.W.: Density Estimation for Statistics and Data Analysis. Chapman and Hall, London (1986)
22. Tadeusiewicz, R., Ogiela, M.R.: Medical Image Understanding Technology. Springer, Berlin (2004)
23. Wand, M.P., Jones, M.C.: Kernel Smoothing. Chapman and Hall, London (1995)
24. Zurada, J.: Introduction to Artificial Neural Systems. West Publishing, St. Paul (1992)

Reduction of Dimension and Size of Data Set by Parallel Fast Simulated Annealing

Piotr Kulczycki and Szymon Łukasik

Abstract A universal method of dimension and sample size reduction, designed for exploratory data analysis procedures, constitutes the subject of this paper. The dimension is reduced by applying linear transformation, with the requirement that it has the least possible influence on the respective locations of sample elements. For this purpose an original version of the heuristic Parallel Fast Simulated Annealing method was used. In addition, those elements which change the location significantly as a result of the transformation, may be eliminated or assigned smaller weights for further analysis. As well as reducing the sample size, this also improves the quality of the applied methodology of knowledge extraction. Experimental research confirmed the usefulness of the procedure worked out in a broad range of problems of exploratory data analysis such as clustering, classification, identification of outliers and others.

P. Kulczycki (✉) · S. Łukasik
Systems Research Institute, Centre of Information Technology for Data Analysis Methods,
Polish Academy of Sciences, Warsaw, Poland
e-mail: Piotr.Kulczycki@ibspan.waw.pl

S. Łukasik
e-mail: Szymon.Lukasik@ibspan.waw.pl

P. Kulczycki · S. Łukasik
Department of Automatic Control and Information Technology,
Cracow University of Technology, Cracow, Poland

1 Introduction

Contemporary data analysis avails of a broad and varied methodology, based on both traditional and modern—often specialized—statistical procedures, currently ever more supported by the significant possibilities of computational intelligence. Apart from the classical methods—fuzzy logic and neural networks, metaheuristics such as genetic algorithms, simulated annealing, particle swarm optimization, and ants algorithms [1] are also being applied here more widely. The proper combination and exploitation of the advantages of these techniques allows in practice for the effective solution to fundamental problems in knowledge engineering, particularly those connected with exploratory data analysis.

More and more frequently the process of knowledge acquisition is realized using multidimensional data sets of large size. This stems from the dynamic growth in the amount of information collected in database systems requiring permanent processing. The extraction of knowledge from extensive data sets is a highly complex task. Here difficulties are mainly related to limits in efficiency of computer systems—for large-sized samples—and problems exclusively connected with the analysis of multidimensional data. The latter arise mostly from a number of phenomena occurring in data sets of this type, known in literature as "the curse of multidimensionality". Above all, this includes the exponential growth in sample size necessary to achieve appropriate effectiveness of data analysis methods with increasing dimension (the empty space phenomenon), as well as the vanishing difference between near and far points (norm concentration) using standard Minkowski distances [2].

As previously mentioned, the data set size can be reduced mainly to speed up or make at all possible calculations. In the classical approach, this is realized mostly with sampling methods or advanced data condensation techniques. Useful algorithms have also been worked out allowing the problem to be simplified by decreasing its dimensionality. Therefore, let X denote a data matrix of dimension $m \times n$:

$$X = [x_1\,|x_2|\cdots|x_m\,]^{\mathrm{T}} \tag{1}$$

with particular m rows representing the realizations of an n-dimensional random variable.[1] The aim of reducing a dimension is to transform the data matrix in order to obtain its new representation of the dimension $m \times N$, where N is considerably—from the point of view of conditioning of a problem in question—smaller than n. This reduction can be achieved in two ways, either by choosing N most significant coordinates/features (feature selection) or through the construction of a reduced set, based on initial features (feature extraction) [3]. The latter can be treated as more general—the selection is a particularly simplecase of extraction. Noteworthy among

---

[1] Particular coordinates of a random variable of course constitute one-dimensional random variables and if the probabilistic aspects are not the subject of research, then in data analysis these variables are given the terms "feature" or "attribute".

extraction procedures are linear methods, where the resulting data set Y is obtained through the linear transformation of initial data set (1), therefore using the formula

$$Y = X \cdot A, \tag{2}$$

where A is a matrix of dimension $n \times N$, as well as nonlinear methods for which the transformation can be described by the nonlinear function $g : \mathbb{R}^n \to \mathbb{R}^N$. This group also contains the methods for which such a functional dependence, expressed explicitly, does not exist. Comparisons of effectiveness of extraction procedures carried out in subject literature show that nonlinear methods, despite having more general mathematical apparatus and higher efficiency in the case of artificially generated specific sets of data, for real samples frequently achieve significantly worse results [4].

The goal of this paper is to develop a universal method of reducing dimension and size of a sample designed for use in data exploration procedures. The reduction of the dimension will be implemented using a linear transformation on the condition that it affects as little as possible the mutual positions of original and resulting samples' elements. For this aim a novel version of the heuristic method of parallel fast simulated annealing will be researched. Moreover, those elements of a random sample which significantly change their position following transformation will be eliminated or assigned less weight for the purposes of further analysis. This concept achieves an improvement in quality of knowledge discovery and—possibly—a reduction in sample size. The effectiveness of the presented method will be verified for fundamental procedures in exploratory data analysis: clustering, classification and detection of atypical elements (outliers).

2 Preliminaries

2.1 Reduction in Dimension and Sample Size

The dimension can be reduced in many ways. Correctly sorting the procedures applied here requires, therefore, a wide range of criteria to be taken into account. Firstly the aforementioned systematic for linear and nonlinear methods is associated with character of dependence between initial and reduced data sets. Most important of these, a reference linear procedure for dimension reduction even, is the Principal Component Analysis (PCA). Among nonlinear methods the most often mentioned is Multidimensional Scaling (MDS). Reduction procedures are often considered with respect to facility of description of mapping between initial and reduced data sets. This can be defined as *explicite* (which allows to generalize the reduction procedure on points not belonging to initial data set), as well as given only *implicite*, i.e. through reduced representation of elements of an initial data set. The type of method chosen has particular significance in the cases of data analysis tasks, where a continuous influx of new information is present—in this form of problem, the reduction methods belonging to the first of the above groups are preferred. The third division of transformation procedures is related to their level of relationship with the data

analysis algorithms used in the next step. It is worth noting here universal techniques which, through analogy to machine learning methods, can be termed as unsupervised. These work autonomously, without using results of exploration procedures [5]. The second category concerns algorithms dedicated to particular techniques in data analysis, in particular considering class labels. Here are often used statistical methods [6] as well as heuristic procedures of optimization, e.g. evolutionary algorithms [7].

A reduction in data set size can be realized with a wide range of sampling or grouping methods. The former most often uses random procedures or stratified sampling [8]. The latter applies either classical clustering techniques or special procedures for data condensation problems. There exists also a significant number of methods for reducing size which take into account additional knowledge, for example concerning whether elements belong to particular classes [9, 10]. Moreover methods dedicated to particular analytical techniques, for example kernel estimators [11, 12], have been developed (see e.g. [13]).

The method presented in this paper is based on a concept of dimension reduction which is linear, *explicite* defined and of universal purpose. Its closest equivalents can be seen to be the Principal Component Analysis method (due to its linear and unsupervised nature), feature selection using evolutionary algorithms [14] and the projection method with preserved distances [15–17], with respect to the similar quality criterion.

A natural priority for the dimension reduction procedure is maintaining distances between particular data sets elements—a wide range of methods treat this as a quality indicator. Typical for this group of algorithms is the classic multidimensional scaling, also known as principal coordinates analysis. It is a linear method, which creates the analytical form of the transformation matrix A, minimizing the index

$$S(A) = \sum_{i=1}^{m-1} \sum_{j=i+1}^{m} \left(d_{ij}^2 - \delta_{ij}(A)^2 \right), \tag{3}$$

where d_{ij} denotes the distance between the elements x_i and x_j of the initial data set, while $\delta_{ij}(A)$ are respective distances in the reduced data set. A different strategy is required when searching for a solution with different structural characteristics or performance indicator, or else a nonlinear relation between initial and reduced data sets. This type of procedure is termed multidimensional scaling (MDS), mentioned before. A model example of this is nonlinear Sammon mapping, which—thanks to the application of a simple gradient algorithm—allows to find a reduced representation of the investigated data set, ensuring minimization of the so-called Sammon stress:

$$S_S(A) = \frac{1}{\sum_{i=1}^{m-1} \sum_{j=i+1}^{m} d_{ij}} \sum_{i=1}^{m-1} \sum_{j=i+1}^{m} \frac{(d_{ij} - \delta_{ij}(A))^2}{d_{ij}}. \tag{4}$$

Such a defined criterion enables more homogenous treatment of small and large distances [18], while the value $S_S(A)$ is further normalized to the interval [0,1].

An alternative index, also considered in the context of MDS is so-called raw stress, defined by

$$S_R(A) = \sum_{i=1}^{m-1} \sum_{j=i+1}^{m} \left(d_{ij} - \delta_{ij}(A) \right)^2. \tag{5}$$

The multidimensional scaling methods are mostly nonlinear procedures. However, the task was undertaken to formulate the problem of minimization of indexes (4) and (5) with assumed linear form of transformation. The first example of this technique is the algorithm for finding linear projection described in the paper [17]. Here an iterative method of greatest descent is applied, which gives in consequence better results than PCA in the sense of index (4). A similar procedure was investigated for function (5), with the additional possibility to successively supplement a data set [16]. In both cases the applied approach did not account for the multimodality of the stress function. To avoid becoming trapped in a local minimum one can use the appropriate heuristic optimization strategy. In particular, for minimization of index (4), the paper [14] uses the evolutionary algorithm. The solution for this investigation is, however, only to choose the reduced features set. A more effective approach seems to be the concept of their extraction—being more general, it will be the subject of investigation in this paper.

In the construction of the algorithm presented here, an auxiliary role is played by an unsupervised technique of feature selection using to this aim an appropriate measure of similarity—index of maximal compression of information [19]. It is based on the concept of dividing features into clusters, with the similarity criterion of features defined by the aforementioned index. This division is based on the algorithm of k-nearest neighbors, where it is recommended that $k \cong n - N$. The number of clusters achieved then approaches N, although it is not strictly fixed, but in a more natural manner is adapted to a real data structure.

Another aspect of the procedure presented here is a reduction in size of sample (1). Conceptually, the closest technique is the condensation method [20]. It is unsupervised and to establish the importance of elements takes into account their respective distances. In this case the algorithm of k-nearest neighbors is also applied, where the similarity measure between sample elements is Euclidean distance. Within this algorithm, in the data set are iteratively found prototype points, or points for which the distance r to the kth nearest neighbor is the smallest. With every iteration, elements closer than $2r$ from the nearest prototype point, are eliminated.

2.2 Simulated Annealing Algorithm

Simulated annealing (SA) is a heuristic optimization algorithm, based on the iterative technique of local search with appropriate criterion for accepting solutions. This allows to establish a valid solution for every iteration, mostly using the quality index value for the previous and current iteration, and variable parameter called the

annealing temperature, which decreases in time. In this way it becomes possible to
accept a valid solution worse than the previous, thereby reducing the danger of the
algorithm getting stuck at local minimums. In addition it is assumed that the proba-
bility of accepting a worse solution should decrease over time. All of the above traits
contain the so-called Metropolis rule, which is most often applied as acceptance
criterion in simulated annealing algorithms.

Let therefore $Z \subset \mathbb{R}^t$ denote the set of admissible solutions to a certain opti-
mization problem, while the function $h : Z \to \mathbb{R}$ is its quality index, hereinafter
referred to as cost. Furthermore, let $k = 0, 1, \ldots$ mean the number of iteration,
whereas $T(k) \in \mathbb{R}$, $z(k) \in Z$, $c(k) = h(z(k))$, $z_0(k) \in Z$, $c_0(k) = h(z_0(k))$—
respectively—temperature and solution valid for the iteration k and its cost, and also
the best solution found to date and its cost. Under the above assumptions the basic
variant of the SA algorithm can be described thus:

```
procedure Simulated_annealing
  begin
    Generate(T(1),z(0))
    c(0)= Evaluate_quality(z(0))
    z₀(0)= z(0)
    c₀(0)= c(0)
    k = 1
    repeat
      z(k)= Generate_neighbor(z(k-1))
      c(k)= Evaluate _quality(z(k))
      Δc = c(k) – c(k-1)
      z(k)= Metropolis_rule(Δc,z(k),z(k-1),T(k))
      if c(k)  < c₀(k-1)
            z₀(k)= z(k)
            c₀(k)= c(k)
        else
            z₀(k)= z₀(k-1)
            c₀(k)= c₀(k-1)
        Calculate(T(k+1))
      stop_condition = Check_stop_condition()
      k=k+1
    until stop_condition == FALSE
  return kstop=k-1, z₀(kstop), c₀(kstop)
  end
```

where the procedure for the Metropolis rule is realized by

```
procedure Metropolis_rule(Δc,z(k),z(k-1),T(k))
  if Δc < 0
    return z(k)
  else
    if Random_number_from_(0,1) < exp(-Δc/T(k))
```

```
            return z(k)
        else
            return z(k-1)
    end
```

The SA algorithm requires in the general case the assumption of the appropriate initial temperature value, formula of its changes associated with an accepted method of generating a neighboring solution, as well as a condition for ending the procedure. However in particular applications one should also define other functional elements, such as method of generating the initial solution and form of the quality index. The first group of tasks will now be discussed, while the second—as specific for the application of the SA algorithm investigated here—will be the subject of detailed analysis in Sect. 3.

Numerous fundamental and applicational works have resulted in creation of many variants of the algorithm described here. Their main difference is the scheme for temperature changes and method for obtaining a neighboring solution. The standard approach is the classical simulated annealing algorithm, also known as the Boltzmann annealing algorithm (BA). This assumes an iterative change in temperature according to a logarithmic schedule and generation of a subsequent solution by adding to the current one the value of step $\Delta Z \in \mathbb{R}^t$, which is the realization of t-dimensional pseudorandom vector with normal distribution. The BA algorithm—although effective in the general case—has a large probability of acceptance of worse solutions, even in the final phase of the search process. This allows for the effective escape from local minimums of a cost function and guarantees asymptotic convergence to a global one [21], while also ensuring the procedure represents—in some sense—a random search of the space of admissible solutions. For the SA algorithm to be more deterministic in character, and at the same time keeping convergence to the optimal solution, the following scheme for temperature change can be applied:

$$T(k+1) = \frac{T(1)}{k+1}, \tag{6}$$

together with the generation of neighboring solution using a Cauchy distribution

$$g(\Delta z) = \frac{T(k)}{\left(\Delta z^2 + T(k)^2\right)^{(t+1)/2}}. \tag{7}$$

The procedure defined by the above elements is called Fast Simulated Annealing (FSA) [22]. It will be a base—in the framework of this paper—for the dimension reduction algorithm.

The problem of practical implementation of FSA is the effective generation of random numbers with multidimensional Cauchy distribution. The simplest solution is the application for each dimension of the vector, of a one-dimensional number generator with the same distribution. This strategy was used in the Very Fast Simulated Annealing algorithm (VFSA), expanded later within the framework of a complex procedure of Adaptive Simulated Annealing [23]. Such a concept has, however, a

fundamental flaw: the step vectors generated here concentrate near the axes of the coordinate system. An alternative could be to use a multidimensional generator based on the transformation of the Cartesian coordinate system to a spherical one. It is suggested here that the step vector $\Delta z = [\Delta z_1, \Delta z_2, \ldots, \Delta z_t]$ be obtained by generating first the radius r of the hypersphere, using the method of inverting the Cauchy distribution function described with the spherical coordinates, and then selecting the appropriate point on the t-dimensional hypersphere. The second phase is realized by randomly generating the vector $u = [u_1, u_2, \ldots, u_t]^T$ with coordinates originating from the one-dimensional normal distribution $u_i \sim N(0, 1)$, and then the step vector Δz:

$$\Delta z_i = r \frac{u_i}{|\mathbf{u}|}, \quad i = 1, 2, \ldots, t. \tag{8}$$

The presented procedure ensure a symmetric and multidirectional generation scheme, with heavy tails of distribution, which in consequence causes effective exploration of a solution space [24]. Taking the above into account, it has been applied in the algorithm investigated in this paper.

Establishing an initial temperature is vital for the correct functioning of the simulated annealing algorithm. It implies the probability of acceptance of a worse solution at subsequent stages of the search in the solutions space. Subject literature tends to suggest choosing the initial temperature so that the probability of acceptance of a worse solution at the first iteration, denoted hereinafter as $P(1)$, is relatively large. These recommendations are not absolute, however, and different proposals can be found in literature, for example close to 1.0 [25], around 0.8 [26] or even only 0.5 [27]. Often in practical applications of SA algorithms, the temperature value is fixed during numerical experiments [28]. An alternative is to choose a temperature according to a calculational criterion which has the goal of obtaining $T(1)$ the value on the basis of a set of pilot iterations, consisting of generating the neighbor solution $z(1)$ so that the assumed $P(1)$ value is ensured. For this purpose one can—analyzing the mean difference in cost between the solutions $z(1)$ and $z(0)$, denoted as $\overline{\Delta c}$ in the following—calculate the temperature $T(1)$ value by substituting $\overline{\Delta c}$ to the right-side of the inequality in the Metropolis rule defining the probability of the worse solutions acceptance:

$$P(1) = e^{-\frac{\overline{\Delta c}}{T(1)}}, \tag{9}$$

thus in consequence

$$T(1) = -\frac{\overline{\Delta c}}{\ln P(1)}. \tag{10}$$

The mean difference in cost can be replaced with e.g. the standard deviation of the cost function value, marked as $\overline{\sigma}_c$, also estimated on the basis of the set of pilot iterations [29]. A problem which appears in the case of SA algorithms dedicated to minimizing functions with real arguments (including the aforementioned BA, FSA, VFSA and ASA), is the dependence of the strategy for generating a neighbor solution on temperature. Therefore, both the standard deviation $\overline{\sigma}_c$ and the mean $\overline{\Delta c}$

are directly dependent on it. The application of formula (10) is not possible here and in the case of these algorithms, the initial temperature value is usually arbitrary. This paper proposes a different strategy based on the generation of a set of pilot iterations, allowing the value $T(1)$ to be obtained on the assumption of any value of initial probability of worse solutions acceptance.

As equally important as the choice of initial temperature is the determination of the iteration at which the algorithm should be terminated. The simplest—although not flexible and often requiring too detailed knowledge of the investigated task—stop criterion is reaching a previously assumed number of iterations or a satisfactory cost function value. An alternative could be to finish the algorithm when following a certain number of iterations, the best obtained solution is not improved, or the use of an appropriate statistical method based on the analysis of cost function values as they are obtained. The last concept is universal and—desirable among heuristic algorithms stop criterions—related to the expected result of their works. This usually consists of calculating the estimator of expected value of the global minimum $\hat{c}_{min}$ and finishing the algorithm in the iteration k, when the difference between it and the discovered smallest value $c_0(k)$ is not greater than the assumed positive ε, so if

$$|c_0(k) - \hat{c}_{min}| \le \varepsilon. \tag{11}$$

One the most recent techniques using this type of strategy is the algorithm proposed in the work [30]. In order to calculate the value c_{min} an estimator is applied here based on order statistics [31]. This algorithm constitutes a universal and effective tool for a wide range of stochastic optimization techniques. Such a method, used as part of the FSA procedure, will now be described.

Let therefore $\{c_0(k), c_1(k), c_2(k), \ldots, c_r(k)\}$ denote the ordered non-decreasing set of r lowest cost function values, obtained during k iterations of the algorithm. In the case of an algorithm convergent on a global minimum, the condition $\lim_{k \to \infty} c_j(k) = c_{min}$ is fulfilled for every $j \in \mathbb{N}$, while the sequences $c_j(k)$ can be applied to construct the aforementioned estimator value c_{min}. This estimator makes use of the assumption of asymptotic convergence of order statistic distribution to the Weibull distribution, and in the iteration k takes the general form:

$$\hat{c}_{min}(k) = c_0(k) - \frac{2^{\frac{t}{\beta}} - 1}{r} (c_r(k) - c_0(k)). \tag{12}$$

The parameter β occurring above is termed a homogenous coefficient of the cost function h around its minimum. On additional assumptions, in calculational practice one can take $\beta = 2$ [32]. The confidence interval for the cost function minimum, at the assumed significance level $\delta \in (0, 1)$, is of the form

$$\left[c_0(k) - \frac{\left(1 - (1 - \delta)^{1/r}\right)^{\beta/t}}{1 - \left(1 - (1 - \delta)^{1/r}\right)^{\beta/t}} (c_r(k) - c_0(k)), c_0(k) \right]. \tag{13}$$

The paper [30] suggests that point estimator (12) can be replaced by confidence interval (13) with the algorithm being stopped when the confidence interval width is less than the aforementioned, assumed value ε. Such an idea, modified for the specific problem under investigation, will be applied here.

The simulated annealing procedure can be easily parallelized, whether for required calculations, or in the scheme of establishing subsequent solutions. While parallelizing the SA algorithm is not a new idea, and was already investigated a few years after its creation [33], it needs to be adapted for particular applicational tasks [34]. At present the suitability of the Parallel Simulated Annealing (PSA) algorithm continuously increases with the common availability of multicore systems. In the algorithm worked out in this paper, a variant will be taken with parallel generation of neighbor solutions, assuming that the number of SA threads equals the number of available processing units.

3 Procedure for Reducing Dimension and Sample Size

The algorithm investigated in this paper consists of two functional components: a procedure for reducing the dimension and a way of allowing sample size to be decreased. They are implemented sequentially, with the second dependent on the results of the first. The reduction of sample size is optional here.

3.1 Procedure for Dimension Reduction

The aim of the algorithm under investigation is a decrease in the dimensionality of the data set elements, represented by the matrix X with the form specified by formula (1), so of the dimension $m \times n$, where m means the data set size, and n—the dimension of its elements. In consequence the reduced form of this data set is represented by the matrix Y of the dimension $m \times n$, while N denotes the assumed reduced dimension of elements, appropriately less than n. The procedure for reducing the dimension is based on linear transformation (2), with the matrix A given in form

$$A = \begin{bmatrix} a_{11} & a_{12} & \cdots & a_{1N} \\ a_{21} & a_{22} & \cdots & a_{2N} \\ \vdots & \vdots & & \vdots \\ a_{n1} & a_{n2} & \cdots & a_{nN} \end{bmatrix}, \tag{14}$$

although for the purposes of notation used in the simulated annealing algorithm, its elements are denoted as the row vector

$$[a_{11}, \ a_{12}, \ \ldots, \ a_{1N}, \ a_{21}, \ a_{22}, \ \ldots, \ a_{2N}, \ \ldots, a_{n1}, \ a_{n2}, \ \ldots, \ a_{nN}], \tag{15}$$

which represents the current solution $z(k) \in \mathbb{R}^{n \cdot N}$ in any iteration k. In order to generate neighbor solutions, a strategy was used based on the multidimensional generator of the Cauchy distribution (formulas (7) and (8)). The quality of the obtained solution can be evaluated with the application of the cost function h, which is the function of the raw stress S_R given by dependence (5), where the matrix Y elements are defined on the basis of Eq. (2). The alternative possibility of using Sammon stress (4) for this purpose was also examined.

The developed procedure requires firstly that the basic parameters are specified: the dimension of the reduced space N, a coefficient defining directly the maximum allowed width of the confidence interval ε_w for the stop criterion based on the order statistics, the number of processing threads of the FSA procedure p_{thread}, initial scaling coefficient (length of step) for the multidimensional Cauchy generator T_{scale}, as well as the probability of acceptance of a worse solution $P(1)$ in the first iteration of the FSA algorithm.

Starting the algorithm requires moreover the generation of the initial solution $z(0)$. To this aim the feature selection procedure of [19], described in the previous section, was realized. Here $k = n - N$ should be assumed, which in consequence usually results in obtaining approximately N clusters. The aforementioned procedure described leads to getting the auxiliary vector $b \in \mathbb{R}^n$, the particular coordinates of which characterize the number of cluster, to which the coordinate from the original space was mapped, as well as the vector $b_r \in \mathbb{R}^n$ of binary values $b_r(i) \in \{0, 1\}$ for $i = 1, 2, \ldots, n$, defining whether a given feature was chosen as a representative of the cluster to which it belongs, in which case $b_r(i) = 1$, or not—then $b_r(i) = 0$. The auxiliary vectors b and b_r can be used in the considered algorithm for generating the initial solution in two ways:

1. Each of N features of the initial solution is a linear combination of features mapped to one of N clusters—to define the form of the matrix A one can use

$$\begin{cases} a_{ij} = 1, & \text{if } b(i) = j \\ a_{ij} = 0, & \text{if } b(i) \neq j \end{cases} \quad \text{for} \quad i = 1, 2, \ldots, n \quad \text{and} \quad j = 1, 2, \ldots, N . \quad (16)$$

2. Each of N features of the initial solution is given as representative for one of N clusters—the form of the matrix A is then defined as

$$\begin{cases} a_{ij} = 1, & \text{if } b_r(i) = 1 \quad \text{and} \quad b(i) = j \\ a_{ij} = 0, & \text{if } b_r(i) = 0 \end{cases} \quad \text{for} \quad i = 1, 2, \ldots, n \quad \text{and} \quad j = 1, 2, \ldots, N .$$

$$(17)$$

The possibility of applying both the above ways of generating an initial solution—the first called a linear combination of features and the second, referred to as features selection—is a subject of detailed experimental analysis concerning dimensional reduction, described in Sect. 4.

After generating the initial solution, in order to carry out the simulated annealing algorithm, the temperature $T(1)$ should be fixed in the first iteration. To this aim the technique presented in the previous section can be followed, allowing at the start to

obtain the assumed initial value of the probability of worse solution acceptance $P(1)$. In the case of the algorithm for generating neighbor solutions, it is not recommended to use the relation resulting from equality (9). As mentioned in the previous section, this is implied by the dependence of a formula for generating a neighbor solution on the annealing temperature. In order to avoid this inconvenience, an additional coefficient T_{scale} was introduced, being the parameter of the Cauchy distribution in the first iteration of the FSA algorithm (also known as an initial step length), and furthermore the temperature occurring in the generating distribution was scaled. The coefficient T_{scale} is thus used as a parameter of the random numbers generator, with the aim of calculating a set of pilot iterations (the size of this set is assumed to be 100). These iterations consist of the generation of an appropriate number of transitions from $z(0)$ worse in the sense of cost function used, to the neighbor solution $z(1)$, and the establishment of the mean value of the cost difference $\overline{\Delta c}$ between $z(1)$ and $z(0)$. This value is inserted to formula (10), through which the initial temperature can be obtained. Moreover, in order to find the assumed shape of the generated distribution, in the first iteration of the FSA algorithm, the additional scaling coefficient is calculated:

$$c_{temp} = -\frac{\overline{\Delta c}}{\ln P(1)T_{scale}}. \tag{18}$$

In consequence, in the first iteration of the actual algorithm, in order to generate a neighbor solution, the scaled temperature $T(1)/c_{temp}$ (therefore T_{scale}) is used, and for the Metropolis rule—just the value $T(1)$. Similar scaling takes place during the generation of neighbor solutions in each consecutive iteration of the FSA algorithm. Thanks to this kind of operation it becomes possible to fix the initial probability of acceptance of a worse solution, which determined by the coefficient $P(1)$, while retaining the additional possibility of establishing—by assuming the value T_{scale}— the parameter of initial spread of values obtained from a pseudorandom numbers generator.

All iterations of the FSA algorithm have been parallelized using a strategy with parallel generation of neighbor solutions. So each of p_{thread} threads creates a solution neighboring the one established in the previous iteration $z(k-1)$. This occurs with the application of a random generator with multidimensional Cauchy distribution. For all threads, the annealing temperature is identical and equals $T(k)/c_{temp}$. Furthermore, every thread realizes the procedure for the Metropolis rule, accepting or rejecting its own obtained neighbor solutions.

The next two steps of the algorithm are performed in sequence. So, first the current solution is fixed for the SA algorithm. The procedure for this is to choose as a current solution either the best from those better than that found in the previous iteration obtained by different threads, or—if such a solution does not exist—random selection of one of the worse solutions. Calculated thus, the current solution, together with the temperature updated according to formula (6), is also used in the next iteration of the FSA algorithm as the current solution. This kind of strategy can be classified as a method of parallel processing based on speculative decomposition.

The last step performed as part of single iteration is verifying the criterion for stopping the SA procedure. To this aim the confidence interval for the minimum value of the cost function, given by formula (13), is calculated. The order statistics used for interval estimation have the order r assumed as 20, in accordance with the proposals of the paper [30]. As a significance level δ for the confidence interval defined by formula (13), a typical value 0.99 [35] is assumed. The width of the confidence interval is compared with the threshold value ε calculated at every iteration with

$$\varepsilon = 10^{-\varepsilon_w} c_0\left(k\right). \tag{19}$$

Finally, the simulated annealing procedure is terminated if

$$\frac{\left(1 - \left(1 - \delta^{1/r}\right)^{\beta/t}\right)}{1 - \left(1 - \left(1 - \delta^{1/r}\right)^{\beta/t}\right)} \left(c_r\left(k\right) - c_0\left(k\right)\right) > \varepsilon, \tag{20}$$

with notations introduced at the end of Sect. 2. Finding the threshold value ε based on formula (20) allows the adaptation of a such defined criterion to a structure of a specific data set under investigation. The sensitivity of the above procedure can be set by assuming the value of the exponent $\varepsilon_w \in \mathbb{N}$, one of the arbitrarily fixed parameters of the procedure worked out in this paper.

It is worth noting that the nature of the method presented here for dimension reduction enables establishment of the "contribution" which particular elements of the data set Y make to the final value $c_0\left(k_{stop}\right)$. This fact will be used in the procedure for reducing the sample size, which will be presented in Sect. 3.2.

3.2 Procedure for Sample Size Reduction

In the case of the dimension reduction method presented above, some sample elements may be subject to an undesired shift with respect to the others and, as a result, may noticeably worsen the results of an exploratory data analysis procedure in the reduced space $\mathbb{R}^N$. A measure of the location deformation of the single sample element x_i compared to the others, resulting from transformation (2), is the corresponding stress value $c_0(k_{stop})$ calculated for this point (called stress per point) [36]. In the case of raw stress it is given by

$$c_0(k_{stop})_i = S_R(A)_i = \sum_{\substack{j=1 \\ j \neq i}}^{m} (d_{ij} - \delta_{ij}(A))^2, \tag{21}$$

whereas for the Sammon stress it takes the form

$$c_0(k_{stop})_i = S_s(A)_i = \frac{1}{\sum_{i=1}^{m-1} \sum_{j=i+1}^{m} d_{ij}} \sum_{\substack{j=i \\ j \neq i}}^{m} \frac{d_{ij} - \delta_{ij}(A))^2}{d_{ij}}. \qquad (22)$$

It is worth noticing that in both cases these values are nonzero, except for the case—unattainable in practice—of "perfect" matching of respective distances of elements in original and reduced spaces. The values $c_0(k_{stop})_i$ for particular elements can be used to construct a set of weights, defining the adequacy of their location in a reduced space.

Let therefore w_i represent nonnegative weight mapped with the element x_i. Taking the above into account, it is calculated according to the following formula:

$$w_i = \frac{m \frac{1}{c_0(k_{stop})_i}}{\sum_{i=1}^{m} \frac{1}{c_0(k_{stop})_i}}. \qquad (23)$$

The normalization which occurs in the above dependence guarantees the condition

$$m = \sum_{i=1}^{m} w_i. \qquad (24)$$

The weights in this form contain information as to the degree to which a given sample element changed its relative location compared to the rest, where the larger the weight, the more relatively adequate its location, and its significance should be greater for procedures of exploratory data analysis carried out in a space of reduced dimension.

The weights' values which are calculated on the basis of the above formulas can be used for further procedures of data analysis. They also allow the following method of reducing sample size. Thus, from the reduced data set Y one can remove those m_{el} elements, for which their respective weights fulfill the condition $w_i < W$ with assumed $W > 0$. Intuitively $W = 1$ is justified—taking into account formula (24), this results in the elimination of elements corresponding to the values w_i less than the mean.

In conclusion, conjoining the methods from Sects. 3.1 and 3.2 enables a data set with reduced dimension as well as size to be obtained, with the degree of compression implied by the parameters N and W values.

3.3 Comments and Suggestions

In the case of the procedure for reducing dimension and sample size presented here, efforts were made to limit the number of parameters, the arbitrary selection of which is always a significant practical problem for heuristic algorithms. At the same time,

conditioning of data analysis tasks, in which the procedure investigated here will be applied, means that—from a practical point of view—it is useful to propose specific values of those parameters with an analysis of the influence of their potential changes.

One of the most important arbitrarily assumed parameters is the reduced space dimension N. It can be fixed initially using one of the methods for estimating a hidden dimension [37], or by taking a value resulting from other requirements, for example $N = 2$ or 3 to enable a suitable visualization of the investigated data set. It is worth remembering that the procedure applied earlier for generating an initial solution with the fixed parameter $k = n - N$, creates a solution which does not always have a dimensionality identical to the assumed (as mentioned in Sect. 3.2). If a strictly defined dimension of the reduced data set is required, one should adjust the parameter k by repeating the feature selection algorithm with its correctly modified value, or use the initial solution, generated randomly, of assumed dimension of reduced space.

It is also worth mentioning the problem of computational complexity of the procedure worked out here, in particular regarding calculation of the cost function value. In practice, the calculational time for the PSA algorithm increases exponentially with an increase in sample size. So, despite the heuristic algorithm being the only method available in practice to minimize the stress function S_S or S_R for data sets of large dimensionality and size, its application must, however, be limited to those cases which are in fact feasible. Therefore, although the number of simulated annealing treads can be fixed at will, it should take the available number of processing units into account. This allows efficient parallel calculation of a cost function value by particular threads.

It should also be noted that the subject algorithm, due to its universal character, can be applied to a broad range of problems in statistics and data analysis. An example, from the case of statistical kernel estimators [11, 12], is the introduction of generalization of the basic definition of the estimator of probability distribution density to the following form:

$$\hat{f}(y) = \frac{1}{h^n \sum_{i=1}^m w_i} \sum_{i=1}^m w_i K\left(\frac{y - y_i}{h}\right). \tag{25}$$

Such a concept allows not only a reduction of sample size (for removed elements $w_i = 0$ is assumed), but also alternatively—an improvement in quality of estimation in the reduced space without eliminating any elements from the initial data set. In the former case care should also be given to normalize the weights after eliminating parts of elements, to fulfill condition (24).

Weights w_i calculated in the above manner can also be introduced to modified classical methods of data analysis, such as a weighted k-means algorithm [39], or a weighted technique of k-nearest neighbors [40]. In the first case, the weights are activated in the procedure for determining centers of clusters. The location of the center of the cluster C_i, denoted by $s_i = [s_{i1}, s_{i2}, \ldots, s_{iN}]^T$, is updated in every iteration if $\sum_{y_l \in C_i} w_l \neq 0$, according to formula

$$s_{ij} = \frac{1}{\sum_{y_l \in C_i} w_l} \sum_{y_l \in C_i} w_l y_{lj} \quad \text{for} \quad j = 1, 2, ..., N. \tag{26}$$

In the k-nearest neighbors procedure however, each distance from neighbors of any element from the learning set is scaled using the appropriate weight.

4 Summary and Final Remarks

The subject of this paper was a complete algorithm for reducing dimension and sample size, ready to use in a wide range of exploratory data analysis problems. It constitutes a universal, unsupervised linear transformation of a features space, with the aim of best maintaining distances between sample elements, additionally supplemented by a reduction in significance of those elements whose locations in relation to the rest have changed considerably. The foundation for this algorithm is an innovative version of the parallel fast simulated annealing procedure, with stop criterion based on order statistics, automatic generation of initial temperature and a multidimensional generator of pseudorandom numbers with Cauchy distribution. The sample size was reduced as a result of calculating weights for particular elements, with the possibility of continuous adjustment of this procedure's intensity, through establishing an appropriate—for an investigated problem—value for the compression coefficient.

The presented methodology underwent detailed numerical testing. The basic research was carried out on the functionality of the method worked out, in particular the sensitivity to its assumed version and parameters. In general one can note that the proposed algorithm is not particularly sensitive to the choice of these parameters, which may be said to be, in practice, its valuable property. Further testing compared results with selected reference methods, especially the classic PCA procedure and the aforementioned selection of features by evolutionary algorithms, in the range of reduction of sample size, joined with an algorithm for data compression as presented in the paper [20]. In general, the results achieved with the application of the procedures investigated in this paper were frequently better, often significantly, than the reference methods mentioned before.

It should be also noted that the particular functional components of the procedure presented here can be applied in other tasks of information processing. Thus, the parallel fast simulated annealing algorithm may be used successfully in a wide range of optimization problems, thanks to its universal structure and relatively intuitive selection of arbitrarily assumed parameters. What is more, the proposed procedure for reducing the sample size can equally be applied together with other, also nonlinear, strategies for dimension reduction.

Finally, it is worth stressing that, despite the calculational complexity of the proposed algorithm, its execution—thanks to the possibility of creating highly efficient parallel implementation—is not very time-consuming. Even for the most complex of the tested data sets, it took only a few minutes while, thanks to the application of

an adaptive stop criterion, this time is fitted to the difficulty of the problem under analysis, thus eliminating the need to introduce arbitrary assumptions. And lastly, due to the use of linear transformation, which is easy to generalize, and the simple idea of a set of weights, it is possible to use the investigated method effectively in a wide range of contemporary data analysis problems, from the areas of engineering, medicine, economics and social sciences, to name a few.

A detailed description of the methodology presented here can be found in the work [40] as well as in the paper [41] which will appear soon.

References

1. Gendreau, M., Potvin, J.-Y.: Handbook of Metaheuristics. Springer, New York (2010)
2. Francois, D., Wertz, V., Verleysen, M.: The concentration of fractional distances. IEEE Trans. Knowl. Data Eng. **19**, 873–886 (2007)
3. Xu, R., Wunsch, D.C.: Clustering. Wiley, New Jersey (2009)
4. van der Maaten, L.J.P.: Feature extraction from visual data. Ph.D. thesis, Tilburg University (2009)
5. Bartenhagen, C., Klein, H.-U., Ruckert, C., Jiang, X., Dugas, M.: Comparative study of unsupervised dimension reduction techniques for the visualization of microarray gene expression data. BMC Bioinformatics, 11, paper no 567 (2010)
6. Yan, S., Xu, D., Zhang, B., Zhang, H.-J., Yang, Q., Lin, S.: Graph embedding and extensions: a general framework for dimensionality reduction. IEEE Trans. Pattern Anal. Mach. Intell. **29**, 40–51 (2007)
7. Rodriguez-Martinez, E., Goulermas, J.Y., Tingting, M., Ralph, J.F.: Automatic induction of projection pursuit indices. IEEE Trans. Neural Netw. **21**, 1281–1295 (2010)
8. Han, J., Kamber, M.: Data Mining: Concepts and Techniques. Morgan Kaufmann, San Francisco (2006)
9. Kulczycki, P., Kowalski, P.A.: Bayes classification of imprecise information of interval type. Control Cybern. **40**, 101–123 (2011)
10. Wilson, D.R., Martinez, T.R.: Reduction techniques for instance-based learning algorithms. Mach. Learn. **38**, 257–286 (2000)
11. Kulczycki, P.: Estymatory jadrowe w analizie systemowej. WNT, Warsaw (2005)
12. Wand, M.P., Jones, M.C.: Kernel Smoothing. Chapman and Hall, London (1995)
13. Deng, Z., Chung, F.-L., Wang, S.: FRSDE: fast reduced set density estimator using minimal enclosing ball approximation. Pattern Recogn. **41**, 1363–1372 (2008)
14. Saxena, A., Pal, N.R., Vora, M.: Evolutionary methods for unsupervised feature selection using Sammon's stress function. Fuzzy Inform. Eng. **2**, 229–247 (2010)
15. Sammon, J.W.: A nonlinear mapping for data structure analysis. IEEE Trans. Comput. **18**, 401–409 (1969)
16. Strickert, M., Teichmann, S., Sreenivasulu, N., Seiffert, U.: 'DIPP' online self-improving linear map for distance-preserving data analysis. 5th Workshop on Self-Organizing Maps (WSOM), Paris, 5–8 September 2005, pp. 661–668 (2005)
17. Vanstrum, M.D., Starks, S.A.: An algorithm for optimal linear maps. Southeastcon Conference, Huntsville, 5–8 April 1981, pp. 106–110 (1981)
18. Cox, T.F., Cox, M.A.A.: Multidimensional Scaling. Chapman and Hall, Boca Raton (2000)
19. Pal, S.K., Mitra, P.: Pattern Recognition Algorithms for Data Mining. Chapman and Hall, Boca Raton (2004)
20. Mitra, P., Murthy, C.A., Pal, S.K.: Density-based multiscale data condensation. IEEE Trans. Pattern Anal. Mach. Intell. **24**, 734–747 (2002)

21. Geman, S., Geman, D.: Stochastic relaxation, Gibbs distribution and the Bayesian restoration in images. IEEE Trans. Pattern Anal. Mach. Intell. **6**, 721–741 (1984)
22. Szu, H., Hartley, R.: Fast simulated annealing. Phys. Lett. A **122**, 157–162 (1987)
23. Ingber, L.: Adaptive simulated annealing (ASA): lessons learned. Control Cybern. **25**, 33–54 (1996)
24. Nam, D., Lee, J.-S., Park, C.H.: N-dimensional Cauchy neighbor generation for the fast simulated annealing. IEICE Trans. Inf. Syst. **E87–D**, 2499–2502 (2004)
25. Aarts, E.H.L., Korst, J.H.M., van Laarhoven, P.J.M.: Simulated annealing. In: Aarts, E.H.L., Lenstra, J.K. (eds.) Local Search in Combinatorial Optimization. Wiley, Chichester (1997)
26. Ben-Ameur, W.: Computing the initial temperature of simulated annealing. Comput. Optim. Appl. **29**, 367–383 (2004)
27. Kuo, Y.: Using simulated annealing to minimize fuel consumption for the time-dependent vehicle routing problem. Comput. Ind. Eng. **59**, 157–165 (2010)
28. Mesgarpour, M., Kirkavak, N., Ozaktas, H.: Bicriteria scheduling problem on the two-machine flowshop using simulated annealing. Lect. Notes Comput. Sci. **6022**, 166–177 (2010)
29. Sait, S.M., Youssef, H.: Iterative Computer Algorithms with Applications in Engineering: Solving Combinatorial Optimization Problems. IEEE Computer Society Press, Los Alamitos (2000)
30. Bartkute, V., Sakalauskas, L.: Statistical inferences for termination of Markov type random search algorithms. J. Optim. Theory Appl. **141**, 475–493 (2009)
31. David, H.A., Nagaraja, H.N.: Order Statistics. Wiley, New York (2003)
32. Zhigljavsky, A., Zilinskas, A.: Stochastic Global Optimization. Springer-Verlag, Berlin (2008)
33. Azencott, R.: Simulated Annealing: Parallelization Techniques. Wiley, New York (1992)
34. Alba, E.: Parallel Metaheuristics: A New Class of Algorithms. Wiley, New York (2005)
35. Kendall, M.G., Stuart, A.: The Advanced Theory of Statistics; Vol. 2: Inference and Relationship. Griffin, London (1973)
36. Borg, I., Groenen, P.J.F.: Modern Multidimensional Scaling. Theory and Applications. Springer-Verlag, Berlin (2005)
37. Camastra, F.: Data dimensionality estimation methods: a survey. Pattern Recogn. **36**, 2945–2954 (2003)
38. Kerdprasop, K., Kerdprasop, N., Sattayatham, P.: Weighted k-means for density-biased clustering. Lect. Notes Comput. Sci. **3589**, 488–497 (2005)
39. Parvin, H., Alizadeh, H., Minati, B.: A modification on k-nearest neighbor classifier. Glob. J. Comput. Sci. Technol. **10**, 37–41 (2010)
40. Łukasik, S.: Algorytm redukcji wymiaru i licznosci proby dla celow procedur eksploracyjnej analizy danych. Ph.D. thesis, Systems Research Institute, Polish Academy of Sciences (2012)
41. Kulczycki, P., Łukasik, S.: An algorithm for reducing dimension and size of sample for data exploration procedures. In press (2014)

Part VII
Control

Intelligent Computations in an Agent-Based Prosumer-Type Electric Microgrid Control System

Weronika Radziszewska, Zbigniew Nahorski, Mirosław Parol and Piotr Pałka

Abstract The growing number of small prosumers, progress in construction of the renewable energy sources and opening of the energy markets lead to development of the concept of a microgrid. To increase efficiency of electricity consumption, production, and trading, energy managing systems (EMS) are being developed. In this paper we present a project of a complex EMS that will combine load scheduling, power balancing and smart trading methods to optimize electric energy costs of running a simulated research and education center. We present a concept of a distributed Agent-based Power Balancing System that controls the power flow in a microgrid by decentralized and distributed decision making. The program optimizes the operating (exploitation) cost of the devices in the microgrid by internally balancing, as much as possible, the produced and consumed power and by trading the remaining energy excesses or deficits on the external market. Agents associated with the devices cooperate using communication protocols. Their aim is to use the energy from renewable energy sources whenever it is only available, and at the same time limit use of the energy from the sources that are more expensive and less environment friendly.

W. Radziszewska (✉) · Z. Nahorski
Polish Academy of Sciences, Systems Research Institute, Warsaw, Poland
e-mail: Weronika.Radziszewska@ibspan.waw.pl

Z. Nahorski
e-mail: Zbigniew.Nahorski@ibspan.waw.pl

M. Parol
Faculty of Electrical Engineering, Institute of Electrical Power Engineering,
Warsaw University of Technology, Warsaw, Poland
e-mail: miroslaw.parol@ien.pw.edu.pl

P. Pałka
Institute of Control and Computation Engineering, Warsaw University of Technology,
Warsaw, Poland
e-mail: P.Palka@ia.pw.edu.pl

1 Introduction

Renewable energy sources emit much less greenhouse gases and are getting cheap enough to be considered cost-effective. Increasing popularity of green technologies causes constant decrease in purchasing, installation, and maintenance costs of the renewable energy sources, so soon they can be available for average family and small companies. The price of energy comes out of the lack of competition on the markets and of the high costs of transmitting energy on large distances. It is possible to reduce the cost of the energy used in the microgrid by a careful planning of the energy that is bought from the external network and using own sources of the energy as much as possible. This leads to an idea of separating parts of (often low voltage) grids, which can individually manage its own energy. Participation of small energy customer or producer in the energy market is not yet available in Poland. But discussions about the necessity to modify the legal regulations to allow participation of small entities in the energy market are in progress. Particularly, an idea is to introduce virtual power plants or virtual consumers that will represent aggregated small facilities.

Renewable technologies are still rather expensive when installed, but cheap in operational stage. However, when discussing scenarios for popularization of new technologies in the future, Lovins et al. [14] find that in every considered case the ecological microsources play an important role, and their prevalence would cause decrease of prices of micro power plants, electrical energy and would lead to clearer environment.

Important devices in the microgrids are energy storage units, like e.g. batteries. In [26] a detailed analysis of the consequences of installing micro energy storage in a community is presented. It is assumed that agents behave rationally, i.e. they react only to the price/cost signal. The whole system maximizes the social welfare by optimizing charging the battery when the price of electricity is low and discharging it when it is high, in 48 equal periods of a day. The study concludes that there is a threshold of 38 % of users with energy storage units, above which it is not profitable to install them anymore. If the energy storage capacity is unlimited, the price on the market will become completely flat, which makes use of such storage units superfluous.

In real grids with renewable energy sources, this way of exact balancing of power may be practically too costly, as it would require installing big energy storages. It may be more profitable to make long term, fixed deals for electric energy with the external grid operator. But to realize it, an intelligent management system is needed that can make an overview of production abilities, daily load profiles, and analyzes market prices.

There has been many papers dealing with this problem, see for example [13]. However, as pointed out in [25], due to a dynamic generation and demand of the

electric power, and need to obtain the power balance, the grids with renewable energy sources require application of even more complex control systems. They are usually called the energy management systems (EMS). These systems often include such modules as a control module oriented to optimization of the grid operating costs, a module cooperating with the distribution grid operator, and a module ensuring reliable supply of energy. Another goal of these systems can be management of demand, like load reduction in the peak periods and shifting loads to the off-peak periods, but also acquiring additional supply of the energy in the peak times [1, 18, 24, 28].

In [8] mathematical analysis of demand side management of energy is presented, with heterogeneous customers having a standard or a smart meter. Authors show that the optimal tariffs for both groups of customers differ. The paper [22] compares the load balancing problem with fixed or dynamic demand. In particular, of interest is whether the communication between a subset (neighbors) of agents improves the overall system performance.

For the content of this paper the most interesting are EMS for distributed energy management, and those in which the auctions are used [13]. In them, often consumers and producers are represented by programmable agents. An idea of using multiagent approach has been discussed in many papers [1, 10, 11, 15, 16, 21, 22, 25] but they either consider general matters or simple networks. Moreover, as definition of a multi-agent system does not specify the agent tasks, the setup of the agent system is different in them than in this paper.

Auctions are also discussed as a way to establish the contracts for exchanged energy and its price. Paper [5] deals with an auction among microgrids. The paper [21] describes the multi-agent system application for a public facility, powered from the distribution grid, with installed distributed sources. The paper [11] comprises more details of the multi-agent system structure. The agents apply fuzzy logic algorithms to regulate the sources, storages and loads. A management system for microgrids, which is based on the multi-agent paradigm, is presented in [9]. However, it is actually not a decentralized system, but a hierarchical one.

The system described in the present paper is designed for a microgrid with microsources (e.g. wind turbines, photovoltaic panels, gas microturbines). Its aim is to reduce exchange of the spot electric energy between a microgrid and an external grid. The tested simulated microgrid is a research and conference center that can be compared in size and energy consumption to a complex of buildings or a facility such as a hospital or a school campus.

In Sect. 2 the concept of a prosumer and a microgrid is introduced. The next section describes a general concept of EMS. Section 4 presents the simulated center that is considered in this project. Section 5 gives a description of the microgrid devices. In Sect. 6 the architecture of the designed EMS is presented. Section 7 describes the basic part of the system, which is the Agent-based Power Balancing System. In Sect. 8 some testing results of the agent system operation are presented. The last section summarizes and concludes the paper.

2 Microgrids and Prosumers

Prosumer is a concept that was originally defined in economy as a junction between words professional and consumer. It was adapted by the energy sector as a junction of the words producer and consumer. A prosumer is a unit that internally produces and consumes energy. As the production and consumption of the power within the prosumer grid do not always balance, a prosumer can be seen by the external grid as a source that delivers energy to the grid or as a load that consumes it, depending on a current power flow. Usually prosumers are small energy units and individually they do not impact a lot on an overall balance of the grid. In a big mass they can impact, but due to the internal management of energy they may create fewer problems to control systems of the big power plants than completely uncontrolled small individual users, like e.g. residential homes.

It is more and more noticeable that the power systems actually evolve in the direction of microgrids, see [3] for discussion of advantages and details of solutions. However, there are still a lot of issues that have to be solved before reliable, safe and trustful microgrids appear.

A microgrid is a separated part of a grid which produces and consumes energy, and only occasionally exchanges it with the rest of the grid. A microgrid is a group of consumers, producers, prosumers or energy storage devices located on small area that can operate autonomously. The range of a microgrid is usually within low (400/230V) or medium (1–60kV) voltage network. Prosumers have usually small power production units, up to a dozen or so kW, like for example photovoltaic panels, hydroturbines, wind turbines and gas turbines. A characteristic feature of a microgrid is that it can be treated as one entity from the point of view of the larger network. For discussion of advantages of using microgrids see [3].

To manage the energy, it is important to understand specifity of the microgrids. There are many features that discern microgrids from big power systems. The issue has been discussed in detail in [12]. The essential features for functioning microgrids as semiautonomous power systems include use of power electronic converters, specific control systems, and ability to communicate within the microgrid. Another fundamental feature of microgrids is installation of many renewable energy sources, which is of great importance from the point of view of environment protection. Most of the microsources are being connected to microgrids via power electronic converters, which also provide them with required control abilities. These abilities are also necessary from the point of view of ensuring security and proper level of reliability of supply.

The key issue is also control of the microgrid operation and requirements for protection of the microgrid functioning. Particularly it concerns such tasks as voltage regulation, frequency regulation, power flow control, and voltage stability. These issues are especially significant during island operation. It is also important for a microgrid to have an ability to change smoothly the state from the synchronous operation mode to the island operation mode or vice versa.

Protection systems applied in microgrids have to be specific with regard to connecting microsources via power electronic converters, low level of short-circuit power in island operation states and bi-directional power flows in microgrid branches. Protection systems installed in microgrids have to work properly in the case of faults appearing both in the microgrid and in the external distribution network.

In the microgrid island operation mode, control systems have to take into account the inertia of the different types of the microsources. Some microsources have long respond times and low inertia. In contrast to this, a big power system is highly inertial, which is ensured by big generators installed in the system. It is especially significant during frequency regulation in the island operation mode of a microgrid. One of the most important feature is also the Demand Side Management (DSM) function when controllable loads exist in the microgrid. Loads supply reliability is a strict requirement for a microgrid to work in the island operation mode. For methods developed to control the load see e.g. [4, 7, 17].

The concept of a microgrid is based on the fact that there is a cooperation or at least non-hostility among the participants in the microgrid. This problem is simpler when all sources and loads in the microgrid belong to the same owner. Then there are no conflicting views, no problems with distributing the profits from producing the energy or sharing the costs of buying additional energy. This is actually the case considered in this paper, where it is assumed that the whole infrastructure belongs to a single owner. However, the described approach of treating devices as independent agents can be also applied in a many-owner microgrid, providing that economic result of the whole grid operation is the common goal.

3 Energy Management Systems

Microgrids consist of a number of small, independent consumers, producers, prosumers and energy storage units. In this situation the normal mechanisms for energy distribution may be not sufficient and not optimal. Energy Management Systems (EMS) are being implemented to manage sources, loads and energy storage devices to balance the power and minimize operational costs of the grid. Thus, EMS ([6]) have much bigger responsibility than Energy Information Systems (EIS) that are oriented only toward monitoring the state of the network, gathering data about devices and storing them for later analysis.

The current approaches to energy management involve shifting loads in time to increase consumption of energy during off-peak hours, and fitting generation to the load. Shifting and scheduling load tasks were described by many researchers, for example in [2, 4, 17, 23]. The idea is to counteract the periodic change of the consumed energy by shifting load as much as possible toward the off-peak periods of the day and night. For example, a computer system can inform about the best time of switching on a washing machine or an air conditioning device, limited by user needs and preferences. When energy storage units are present, an EMS task is also

to use the stored energy when the price of the energy is high and charge the units when it is low.

Controllable energy sources, like gas microturbines, are extremely helpful in optimization of the generation side. Controllable generators can be not only switched on or off when necessary, but also make it possible to control the generation in a continuous way.

An architecture of an EMS system may assume centralized planning and managing of the power. This allows in principle for exact optimization of the costs, but participants have to agree to conform to the decisions of the system and also send to the system information about electricity consumption plan and details of the installed facilities. It raises trust problems. Problems may be also caused when grid structure changes quite often and/or when frequent rapid changes of the production and consumption of energy occur in the microgrid.

Decentralized EMS (DEMS) reach, perhaps suboptimal, solutions by negotiating the production consumption plans of each device in the grid. This type of agreements can be reached by using a market based schemes and multilateral negotiations. Very often an auction algorithm is used for negotiations, as an often used mechanism of distributed decision making.

4 Simulated Research and Education Center

The aim of the paper is to present a DEMS based on the multi-agent paradigm and to test operation of this DEMS in a simulated research and education center. The objective of the system is to optimize the operating costs of electric energy consumed, taking into consideration also its ecological impact. Energy management system is expected to assure constant supply for all devices and maximize the utilization of its own green energy sources as wind turbines and photovoltaic panels. The system performs it by planning and forecasting production and consumption levels, trading energy on the energy market and balancing on-line small variations of the power in the grid. It also considers physical limitations of the microgrid and maintains good power quality factors (voltage deviations) in the process.

The considered research and education center (REC) is designed to develop technologies and techniques in the renewable energy area. It consists of five buildings [20, 27]:

- Laboratory of Solar Techniques,
- Laboratory of MicroCHP and Ecological Boilers + Laboratory of Wind Power Engineering,
- Laboratory of Energy Consumption Rationalization,
- Laboratory of Power Industry Safety Engineering (located in two buildings).

The size of the whole complex exceeds 9000 sqm. It is connected to the external 15 kV distribution network by a 15/0.4 kV power transformer. The buildings contain conference rooms, laboratories, offices, hotel rooms, social facilities, a restaurant, a

coffee corner, etc. It carries out specialized experiments in the area of producing and consuming energy, but also holds conferences, trainings, etc.

Due to its research, educational, conference, and hotel functions the center has a number of facilities that have different profiles of power demand. The complex is equipped with its own power sources, but they cannot fully cover all power needs of the center, particularly during its intensive activity. Thus, the EMS looks for decreasing energy that have to be bought by possible best management of produced energy.

Some of the events can be planned or can be foreseen, for example the dates of the conference, the number of people inhabiting the hotel rooms, etc. An average value of needed energy for these events can be estimated. Knowing an average, typical load profile for a given day of the year and the energy used in the planned events provides us with a better estimation of the expected load. On the other hand, other activities, like using electric kettles or coffee machines, microwaves, charging car batteries or laptops, are hardly predictable. Some of these non-planned events take considerable power, though for a rather short time. But if a number of such cases happen at once, they may create a noticeable change in the power used, as compared to the assumed profile. This requires an energy management system to act and control accordingly the devices in the grid. Actions of the system should be possibly unnoticeable for users and should not limit their activities.

5 Center Microgrid Devices

The models of the devices in the simulated REC are devided into three groups: energy sources, energy storage units, energy consumption units (loads). The energy sources comprise [20, 27]:

- Wind turbines—they produce electricity by converting the power of the wind that moves the blades of a windmill. The wind turbine operates within a defined range of wind speeds. The amount of the produced energy depends on the wind speed, the size of the blades and the efficiency of the windmill.
- Photovoltaic panels—they produce electricity by converting the power of the solar radiation to electricity. The power produced depends on the size of the panel (its area), efficiency of the process and intensity of the solar radiation. An important element is also the temperature, as the efficiency of the panel decreases with increase of the temperature. Thus, the same panel usually produces more electricity in early spring than during hot summer days.
- A reciprocating engine—this category includes a combustion engine (a Diesel, a spark-ignition engine) or a gas engine. Although it is not a really ecological friendly power source, in an island mode it is very reliable and may play a role of a balancing node.
- A gas microturbine—the natural gas is considered the most "green" power source acquired out of all fossil fuels. It is also fairly cheap. This solution is even more

interesting when the biogas is used. It is assumed here that the gas or the biogas is bought on the market and the accessibility of the fuel is unlimited.

- A hydropower plant—the center is placed near a small river with a small hydropower plant constructed on it. Its production abilities depend on accumulation of water in the water reservoir. In wet seasons the hydropower plant can work with its maximal power, but in situation of a drought the water supply has to be carefully controlled.

To make the power balancing easier, energy storage units are considered, as follows [20, 27]:

- Flywheels—their efficiency is very high, reaching 93.5 %. The electric energy is transformed to the kinetic energy of the flywheel that can turn with the speed up to 60, 000 rpm. This is a very fast reacting storage that can even survive short-time overload (up to 150 % for 1 min).
- Batteries—gel accumulators have efficiency of about 88 %, but the charging and discharging power is limited. Batteries are suitable for keeping power for a long time, can be charged and discharged frequently and the density of the stored energy is high.

Along with the sources and storage units of energy, the third group of the active elements in the center are consumers of electricity, such as refrigerators, computers, lights, air conditioner, special devices for experiments, etc. Considering every single device or socket in the building as a separate power consuming device would be unpractical, because it would require equipping each device with an energy meter or even a power electronic converter. Such technology is available, but it would be exceptionally expensive to install it in all small devices. In this simulation, it is assumed that the power is measured in nodes of the electric installation which gather several consuming units, for example sockets in few rooms, or the chain of corridor lights.

All receiving points have day load profiles assigned. In the project 26 of such load profiles were defined, for example external lighting, air conditioning, heat pomp power supply, preparation of the food. With addition of some randomness in the switching on/off the devices, this allows for defining different stochastic demand patterns of electricity.

All of the loads are divided into two groups: the ones that have to be powered in any conditions and the ones that can be switched off under power deficit. If the connection to the external grid is cut, the center switches to the island mode. Then the reciprocating engine is switched on and less important circuits are disabled, to keep the core of the electrical system in operation. When the connection to the external grid is restored, the system automatically returns to the normal (synchronous) operation mode.

6 Simulated System Structure

The structure of the simulated system consists of two layers: the physical and the logic ones, consisting of multiple modules, as presented in Fig. 1. The modules contain device models, such as a model of the electric grid, models of the physical devices, a short time balancing system, a scheduler for the planned task and a module for trading energy on the external grid market. The whole system is monitored and managed from a single interface.

The basic part of the physical layer is the simulated model of the electric grid, which is responsible for electric energy flow calculation. It can be defined how many load nodes are considered, and what types of the devices are connected to the grid. Also parameters of the devices and their way of working are recorded there. The model computes the power flow in the network and reports any violation of the grid physical constraints. For the simulation purpose, the data to this layer are fed from the Planner module and from the short-time power balancing multi-agent system, which are parts of EMS.

Description of the program which calculates the load flow in the considered REC microgrid has been presented in [20]. The program is an integral part of the simulated system. It includes the electric part and the heat part. It allows for load flow calculations either for the currently considered configuration of the whole internal electric power network or for the electric installations in particular buildings of the REC. It has been implemented in the Java programming language.

The electric part of the model includes the data of internal electric network and installation elements; the data on the structure of the electric networks and installations; the data on the considered electric energy sources (the gas microturbine, the reciprocating engine, the photovoltaic panels, the water micro power plant, the wind microturbines); the data on the analyzed electrical energy storages (the battery energy storage, the set of the flywheels); the electric power loads data; the sun and
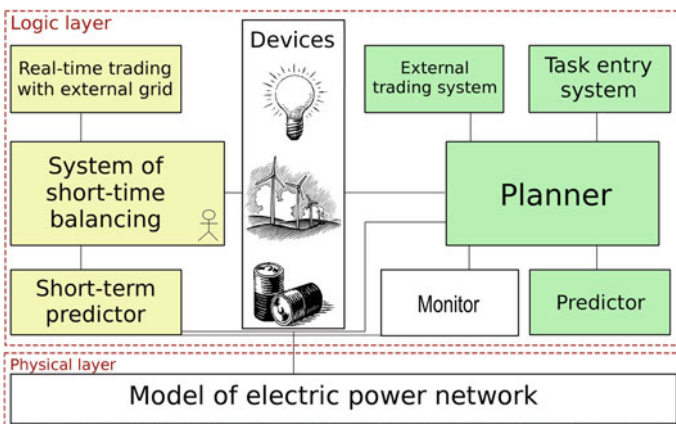

Fig. 1 Diagram of main components of the system

wind generation data, which include the insolation (irradiance) and the wind velocity. Twenty six different types of electric power loads are currently distinguished in the computer model.

Two different types of sources are specified in the program (model), [20]. Some of the sources can not be controlled (the wind microturbine, the photovoltaic panels). Thus, when carrying out load flow calculations, the program provides appropriate values of the generated active power for them using simulated models of their activities. All other sources are treated as the controlled ones. Then, the user is responsible to define (set) the proper values of the generated active power for them. In our case the powers are set by EMS. Electric energy storages can operate in either the charging (taking energy from the network) or the discharging (turning back energy to the network) mode. Before starting the load flow calculations, it is necessary to define the voltage in the balance (slack) node, the operation points of the electric energy distributed sources and also the operation modes and points of electric energy storages.

The program allows for computations both in the synchronous and the island modes. In the island mode the REC network is supplied only by its own sources and does not take energy from the external network of the electricity utility. In this mode, the role of the balancing (slack) node is played by the reciprocating engine. The input data include the branches data, the nodes data, the sources (generators) data. The results of the load flow calculations include data about the nodes, the branches, and the power balancing. The electric current and voltage violated constraints are written down into a disk file. Some results of a simulated load flow calculations in the synchronous and the island mode of the considered REC microgrid have been presented in [20, 27].

Events that are planned to happen are characterized by the amount of electric power consumed or produced. These events might be of different types, as for example performing a research laboratory experiment, switching off a device for maintenance, organizing a conference or any other meeting, etc. Also average day load profiles, aggregating all loads that are too small to be inserted separately, are treated as tasks. Examples may be a total power of using kettles, microwaves, lights, charging laptops, etc. The hotel reception system reports the number of hotel guests, which is also used to plan the schedule of giving meals (cooking facilities consume a significant amount of energy, especially during some periods in the day). The event description includes information about its shiftability, and particularly if it is possible to postpone the task for some time and for how long. An important information for the scheduler is also if operation of some devices can be interrupted and restarted during their work.

The EMS (logic) layer consists of few complementary parts. The Planner module analizes the list of submitted tasks and suggests better time for realizing them taking into account limitations defined by the user. Some tasks require negotiations before the execution time has been fixed. For example, when a conference is planned, the system checks if the suggested dates do not collide with other events, in terms of resources used, or with some energy-consuming experiment, and may suggest postponing it for few days. The Planner takes into account the expected load provided

by the Predictor on the basis of historical data, the profiles of usual power production and consumption, the prices and availability of electric energy, and evaluates the cost to realize the task at the proposed time. The Planner constructs a schedule using heuristic algorithms, which allow for a compromise to be made. The schedule is only suboptimal but it guarantees to provide a result within a specified time. The schedules are repeated in half an hour time. The schedule includes not only the list of tasks that are executed at certain time point, but also the operating level of all controllable devices in the system. Having such information, it is possible to compute the total surplus or deficit of power in every time period by comparing the planned consumption of power to the expected amount of production.

The total inner production of energy cannot be known exactly because of, to some extend random production by renewable energy sources, as wind turbines and photovoltaic panels. To balance the power in the center, the energy bought from the external network is used. It is assumed that the external network can send unlimited power.[1] Trading with external network is realized by the user, supported by the External Trading module, that knows the load profiles and the schedule. The module prepares required amounts and times of delivery of electric energy and suggests deals. Better energy prices are possible to be negotiated on the electric energy market, if the amount and time of buying the deficit energy is known in advance. Advanced planning of the lacking energy helps in diminishing the cost of its buying. If the connection to the external system is deactivated, the center system switches to the island mode, and all plans are invalidated.

The managing of the energy is devided between two modules. The Planner operates in a long time scale, usually few days ahead of the planned events, although it updates the plans every half an hour, if necessary. It considers historical data from a number of previous years and daily consumed and produced energy, gathers information about the events that may last from a part of an hour to days (such as conferences or experiments).

Because of uncertainties of energy consumption and production, the schedule can differ from the actual values. Short time power imbalances may be caused by unpredictable activity of some sources, non-exact realization of planned events and by unregistered energy consumption. The Short-time Power Balancing module takes care of this. The scheme of this module is presented in Fig. 2. This is a multi-agent system, in which each device and nodes are represented by autonomic agents. Agents monitor the physical devices (in our simulated case the models of physical devices) and when the change in the state is sensed, the agents look for covering it by other devices. A negotiation process allows the agent for choosing a possibly cheapest complementary producer or consumer of the energy. Agents set changes of the operating point of the devices (the amount of power the device can produce or consume), if the units allow for that. More details about this module will be presented in Sect. 7. This module is supported by its own predictor that, unlike the Planners predictor, forecasts power demand and generated power just few minutes ahead. There is also

---

[1] The power is actually limited by the transmission ability of the transformer. It is, however, assumed that this limit is never achieved.
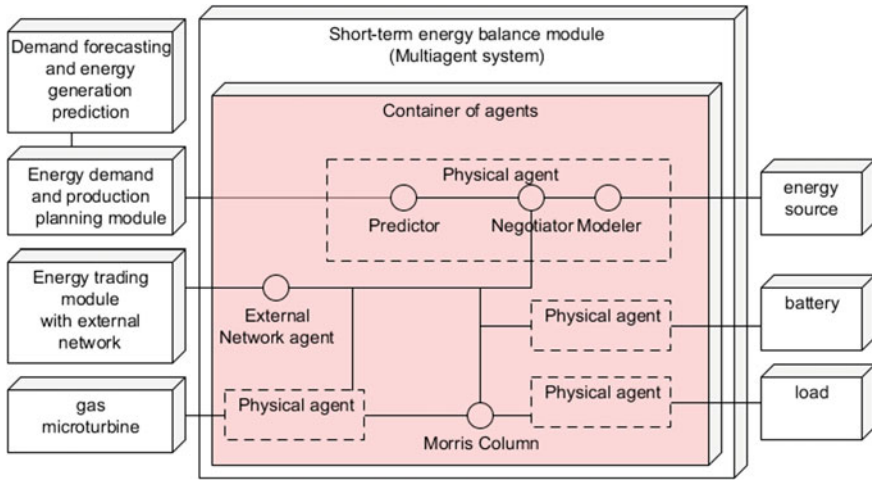
Fig. 2 An outline of multi-agent system for short-time power balancing

a module that is planned to trade the amount of energy that has to be purchased or sold on a real-time market. This module is not ready yet, and the needed energy is just drawn on the spot prices.

The Agent-based Power Balancing module is directly connected to the devices interfaces and can change the operating points of the controllable devices. A model of a device includes a simulator of its work, in which the operation profile and information about the date and time are used. The inputs to the model that depends on meteorological conditions are simulated as some random processes imitating real atmospheric conditions. Simulation of the wind strength uses a wavelet model with a random component. The operating abilities of the water turbine depend on the amount of water in a reservoir. A simplified model of the water inflow is used, which patterns the flow of a real small river in a vicinity of Warsaw, taking into account its seasonality. In simulation of the sunshine, the amount of irradiation that reaches the photovoltaic panels has to be considered. The irradiation for the clear air is acquired from the geophisical models. Because the exact simulation of clouds is a complicated task, a simplified mathematical model of cloudiness is used.

7 Agent-Based Power Balancing System

7.1 Organization of the System

Agent is an abstraction of a unit that has certain amount of independence and distinguishes itself from the environment. As was mentioned before, multi-agent technology is very suitable for modeling electricity-connected issues, as was widely described in [15] and [16].

A concept of an agent is used in this project to describe the participant in the microgrid, that is the energy producer or the energy consumer. It is also applied to programmable agents, that are autonomously working programs.

The planning system can schedule certain tasks and predict the average load level, but it is impossible and not welcome to schedule small human activities as making coffee or using microwaves. Renewable energy sources like wind turbines and photovoltaic panels depend not only on general weather conditions but also on local meteorological situation of the wind gusts and on cloudiness of the sky in the area.

These small variabilities are impossible to avoid and the EMS has to cope with them. This is the task of the Agent-based Power Balancing System that reacts within a second to unexpected changes in power demand or power generation. The events in the system are not synchronized, so the power demand and generation fluctuate. However, it is necessary to wait with measuring the values of these changes until the established state has been reached. The minimal frequency of measuring the power for some of the devices (as for example the wind turbine) is one minute.

As mentioned earlier, all devices were divided to three groups: controllable, uncontrollable and energy storages. Controllable devices are the ones that can adjust their operating points to produce a determined power at the time, or consume certain power at the time. Such devices are, for example, a reciprocating engine, a gas microturbine, an intelligent fridge, an air conditioner, a battery energy storage, a flywheel, etc. Devices like wind turbines, computers, light bulbs are impossible to control, so, from the point of view of the system, they are uncontrollable devices. Battery energy storages can be set either to the charge or the discharge mode, so they are controllable devices, but they have been also designed with a mechanism, that at some point changes their operating mode to charging, to avoid the deep discharge state.

An outline of the power balancing system is presented in Fig. 2. The agent associated with a device (the physical agent) consists of up to three blocks that have different functions in the system. The Predictor anticipates the operating point of the device. For this, it needs sometimes forecasts of weather conditions, like in the renewable energy sources case. For other devices, the Predictor is much more simplified, or not needed at all. The Modeler analyses the situation of the device; detects changes of the operating point, checks its regulatory capabilities, determines the cost of producing the energy, sends the appropriate data to the Negotiator for starting the trading process, and orders a controllable device to change the operating point as a result of the trading. The Negotiator deals with other agents to compensate a detected change in the produced or consumed power in order to secure the balance of the power in the grid. The blocks of the physical agents were designed to simplify the computing within an agent and make it simpler to program for parallel computations. Their implementation differs depending on whether an agent represents controllable (a 'passive' one) or uncontrollable (an 'active' one) device. Passive devices are the ones that represent controllable sources. Other devices are active, with exception of the battery energy storage that is represented by two agents: the passive one

(that responds to the balancing request) and the active one (that is actively trying to maintain the state of charge on the safe level).

An important feature of the system is that the need for balancing is recognized by the device itself. It is the device that sends information about change in consumed or produced power. The Modeler agent decides if the consumed or produced by the device power is constant. If it is not, the modeler detects the imbalance and takes an appropriate action. It sends a request to the Negotiator to arrange a deal. The Negotiator checks with whom he can communicate to find the compensating power, then it starts conversations by asking for available regulation capabilities. When the deal is set, the controllable sources adjust their operating point to reach the state of balance. There is no central planning and agents are unaware of the whole amount of energy in the system or the value of the total imbalance. Buying the energy from the external grid has the same mechanism as balancing with any other agent, the difference is in the price of energy. The price is set on the external market and may depend on the already made deals.

The communication protocols between the agents has been presented in [19].

7.2 Types of Agents

Six main agent roles are designed and implemented in the Agent-based Power Balancing module:

- Active and passive **predictors** that anticipate the device power demand or power production, taking into account the meteorological condition forecast, if necessary;
- **Modelers** that communicate with the device to receive its current state and with the predictor to learn its anticipated value to prepare a decision of trading/no trading, which is sent to the negotiator; it also updates the operating point of the device when appropriate;
- Active and passive **negotiators** that negotiate the delivery or dispatch of the energy;
- **Morris Column** agents, whose goal is to provide public repository, where agents are able to report information about their regulation abilities, as well as seek for it;
- The **external trading agent** which trades with the external grid; it actually consists of two agents, one that is responsible for drawing energy from the external grid in case of deficit and another one that is responsible for transmitting energy to the network in case of its overproduction in the research center; two agents are used to reflect the difference in prices for 1 kWh of power between sending and receiving the energy;
- The **monitor** agent, whose goal is to monitor the state of the network and particular agents, detect unexpected imbalance conditions, unnoticed by other agents, and start actions in order to have them corrected;

The Agent-based Power Balancing System is implemented using JADE 4.0 framework, and the Java 1.6 language.

7.3 Auction Algorithm for Energy Balancing

The deals are made by sending balancing offers from the active to the passive agents of the devices. This is done to limit the number of messages sent in the system. When taking decisions on the choice of the compensating device, the agents consider the cost of balancing provided by the active agents. The negotiation method is a one-side, sealed bid auction. Traded commodity is a change in the amount of electric power, that device generates or consumes, expressed in kW.

The procedure of balancing the power is as follows. An active agent receives the current operating point of its device and checks if an imbalance occurs, i.e. if the power that device receives or transmits to the network has changed or is going to change. If imbalance state is discovered, the active agent informs his (active) negotiator to interrogate the Morris Column agent (it can be implemented as a set of agents that are backups of each other) about the devices that have regulation capabilities to compensate the change. Having got the list of passive agents, the active negotiator sends a "call for proposal" message to devices from the list and then waits for offers (waiting is done simultaneously for all responses, in a non-blocking way). Having all responses collected or a defined amount of time waited (in this case 300 ms was assumed), the negotiator accepts the best offers. Each passive device which sends a balancing offer specifies in it the (generalized) cost of balancing. The decision is made by the interrogating agent taking into account the specified costs. The costs may depend on the fuel used or depend on the external market prices, but for some devices the proportions have been predefined to prefer the renewable energy sources over the fuel powered ones or the external network. Offers are sorted according to these costs, but the order of browsing the sorted list depends on the direction of the power sent. If a device needs energy, its active agent prefers the cheapest offer. It makes rather a deal with the wind turbine than with the gas microturbine. Thus, the sorting is browsed in the ascending order. On the other hand, if the device is releasing power (or producing it) then its agent prefers to provide it to the agent, whose offer is the most expensive, as this means lowering the amount of energy produced by this device. Consequently, the sorting is browsed in the descending order.

Some devices may cover only a part of the imbalanced power. The active negotiator chooses offers from the most preferred ones and with available power to cover as big part of the imbalance as it can. If the power is not sufficient, it takes the next offer in the queue, until the device is totally balanced. The remaining offers are rejected and the offerers get the appropriate message. The accepted offers are sent to the proper passive devices and the Modelers there finally send the order to their units to change the operating point.

Two kinds of costs are defined, one for 'balancing up' and another for 'balancing down'. The cost of 'balancing up' is used when the device has to compensate

increased consumption of the energy. The balancing down is used in situation when the device reacts to decrease in the energy consumed or to increase of the energy produced in the system. For some devices these costs are equal, while for another differ.

Some of the devices, like reciprocating engine, have fixed costs. The costs of others depend on the operating point of the device, as for example on the state of charge of the battery energy storage or the amount of water in the reservoir.

The cost of the water turbine actually does not depend on the amount of water used. However, it is modeled artificially as depending on the state of filling the reservoir, to avoid an excessive decrease of the water in the reservoir.

The costs of the battery energy storage unit and the flywheels depend on the state of their charge. The preferred state of the battery is the state of half charge. It gives the equal possibility of charging and discharging. The battery energy storage unit does not allow the total discharge or overcharge. In this case the device stops offering services in one direction. This happens when the state of charge is below 10 % or over 90 %.

The flywheel is a device that is more resistant to overload (it can be even overcharged to 150 % of its power, but for very short time). Its cost changes according to the state of (over) charge in the way to make the time of overcharging short.

8 An Example of the Algorithm Performance

The algorithm for balancing the power was tested on simulated data. There were 19 devices considered in the grid. Simulation of each device and its agent were run on a separate machine. The database and the Morris Column agent were placed on an additional twentieth machine. Each computer was an Intel(R) Core(TM) i5-3450 CPU@3.10 GHz 8 GB RAM machine, with 64-bit Windows 7. The computers were connected by the 1 Gb Ethernet network. The test revealed that the balancing takes less than 60 ms, except for the initial slightly longer time (up to 800 ms). This longer initial time is due to the necessary registration of the agents to the Morris Column during the first few seconds and their interrogation of the devices about their operating points. Agents in the system are not centrally synchronized and the delays between agent initial actions caused initial delays in balancing the power.

To show how the system balances the power, a simple example has been planned. Only 3 devices are considered, a gas microturbine, a wind turbine, and a single consumer that has a total power demand of up to 100 kW in the peak time. Additionally, to make the power balancing possible, the external power grid is introduced that has unlimited power consumption and production abilities. The negotiating device agents try to avoid buying/selling the energy from/to the external grid agent, but instead strive to balance the power by negotiations between producers and consumers within the grid, and keep the exchange on the zero level.

The power produced or consumed by devices during the test are presented in Fig. 3. The gas microturbine operating point is bounded by 12,5 kW from below and
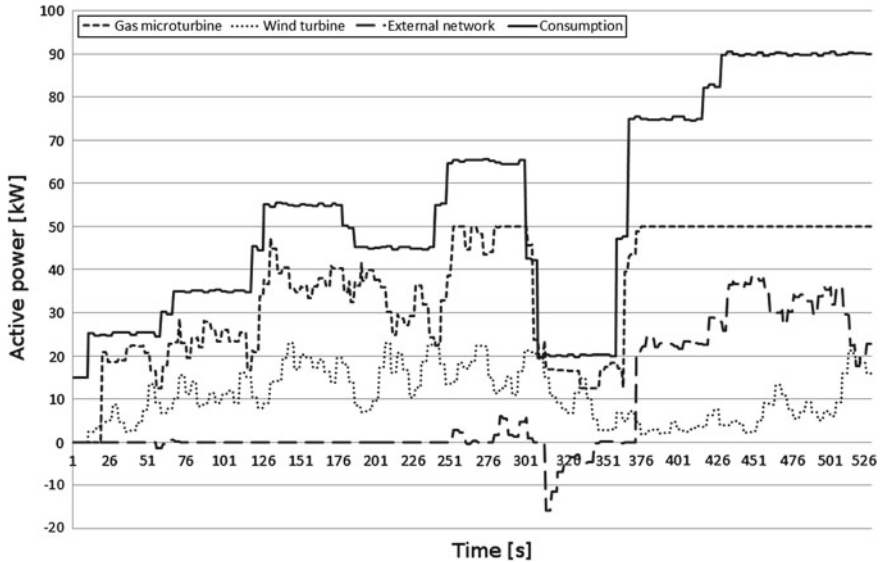
Fig. 3 The amount of power produced by the controllable source, the uncontrollable source, the amount of power consumed by consumer and the amount exchanged with external power grid

50 kW from above. When the total demand power from the microturbine is out of these ranges, the trade with the external grid has to be used to balance the energy. In Fig. 3 the negative value of the power for the external power grid means that the microgrid sells power. It happens when the power consumed in the microgrid is lower than produced by the wind turbines and the microturbine operating on the minimal level. On the other hand, when the power demand is greater than production by the wind turbine and the microturbine operating on the maximum level, the external grid compensates the lacking power, which is depicted by the positive values for the external grid.

To show more clearly the power balancing process, the sum of production and consumption are presented in Fig. 4. It can be seen that there are small imbalances in short periods that are due to lack of synchronization in the system, but also to the time aggregation on the graph (the data in Fig. 4 are averaged within one second period).

Balancing can be done faster than the time assigned for the devices to report their state. This shows that the power balancing system can be an efficient method for matching the produced power and the consumption. There may be some small imbalances, but the time of their existence is so short that they do not influence the operation of the system as a whole.
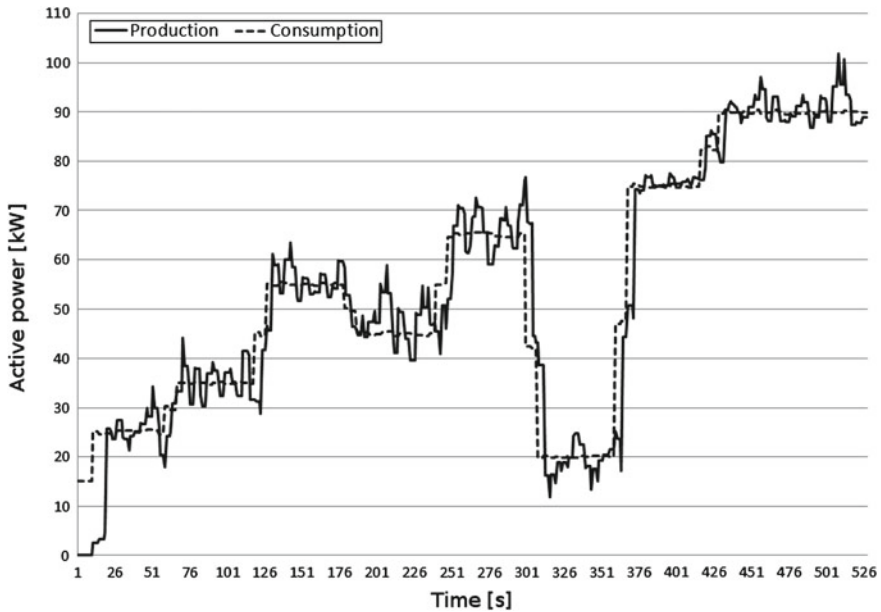
Fig. 4 Aggregated powers of production by the microgrid devices and consumption

9 Conclusions

Impressive changes in electricity grid structures have been initiated by the emergence of new technologies, the new regulations to fight against the global warming, increasing demand for the secure supply of energy and rising prices of electricity. These changes gravitate toward renewable energy sources, prosumers and microgrids. Recent research results indicate that it is possible to create an energy self-sufficient community, that can be even selling surpluses of energy. The energy produced by renewable sources is, however, volatile, as it depends on changing meteorological conditions. Also the consumption of the energy in microgrids is proportionally much more volatile than in bigger grids. The problems caused by uncertain production and consumption can be overcome by using the computer based Energy Management Systems.

In this paper, a modular distributed EMS is presented. The novelty of the solution presented is first of all in the complex treatment of the problem. It includes two modules dealing with balancing the power produced and consumed in the microgrid. One module solves in advance the task scheduling problem, in order to find a suboptimal way of shifting the loads to be possibly covered by the energy produced within the microgrid. The second module balances the power in the real time by activating both the generation and the load side of the microgrid. For this, it uses the multi-agent technology. Thus, both production and consumption of the energy in the grid self-

adapt to the changing energy needs and supply. The reaction of the real-time system is accelerated by using short time forecasts of generation and demand of energy.

The main aim of the system is to optimize (generalized) costs of exploiting the electric energy in a Research and Education Center, which is simulated with a considerable high accuracy to allow for testing the EMS operation. As compared to the simple reduction of the energy bought, caused by straight exploitation of the renewable energy sources, application of the EMS provides savings due to making long-term deals with external power grid, which is cheaper in comparison to trading on the balancing (spot) market, and then possibly precisely following the contracted power trajectory, in spite of disturbances resulted from randomness in generation and demand of energy. In all decision making stages soft suboptimal algorithms are applied, as metaheuristic or multi-agent ones.

Although a Research and Educational Center is considered in the paper, the elaborated system and methodology is of a general character. Many solutions are opened and can be easily redefined. So, it can be applied as well for other grids.

References

1. Abbey, C., Joos, G.: Energy management strategies for optimization of energy storage in wind power hybrid system. In: The 36th IEEE Power Electronics Specialists Conference, PESC'05, pp. 2066–2072 (2005)
2. Agnetis, A., Dellino, G., Detti, P., Innocenti, G., de Pascale, G., Vicino, A.: Appliance operation scheduling for electricity consumption optimization. In: IEEE CDC-ECE, pp. 5899–5904 (2011)
3. Borbely-Bartis, A.-M., Awerbuch, S.: Small is profitable: the hidden economic benefits of making electrical resources the right size. Energy Policy **31**(15), 1705–1708 (2003)
4. Derin, O., Ferrante, A.: Scheduling energy consumption with local renewable micro-generation and dynamic electricity prices. In: CPSWEEK/GREEMBED 2010: Proceedings of the First Workshop on Green and Smart Embedded System Technology: Infrastructures. Methods and Tools, Stockholm (2010)
5. Dimeas, A.L., Hatziargyriou, N.D.: Operation of a multiagent system for microgrid control. IEEE Trans. Power Syst. **20**(3), 1447–1455 (2005)
6. Granderson, J., Piette, M., Ghatikar, G.: Building energy information systems: user case studies. Energy Efficiency **4**, 17–30 (2011)
7. Iwayemi, A., Yi, P., Dong, X., Zhou, C.: Knowing when to act: an optimal stopping method for smart grid demand response. IEEE Netw. **25**(5), 44–49 (2011)
8. Joskow, P., Tirole, J.: Retail electricity competition. RAND J. Econ. **37**(4), 799–815 (2006)
9. Kouluri, M.K., Pandey, R.K.: Intelligent agent based micro grid control. In: 2011 2nd International Conference on Intelligent Agent and Multi-Agent Systems (IAMA), pp. 62–66 (2011)
10. Kwak, J., Varantham, P., Mahesvaran, R., Tambe, M., Jazizadeh, F., Kavulya, G., Klein, L., Becerik-Gerber, B., Hayes, T., Wood, W.: Saves: A sustainable multiagent application to conserve building energy considering occupants. In: Conitzer, V., Winikoff, M., Padgham, L.,

van der Hoek, W. (eds.) Proceedings of the 11th International Conference on Autonomous Agents and Multiagent Systems–Innovative Applications Track (AAMAS 2012), (2012)

11. Lagorse, J., Simões, M.G., Miraoui, A.: A multiagent fuzzy-logic-based energy management of hybrid systems. IEEE Trans. Indus. Appl. **45**(6), 2123–2129 (2009)

12. Lasseter, R., Akhil, A., Marnay, Ch., Stephens, J., Dagle, J., Guttromson, R., Meliopoulous, A.S., Yinger, R., Eto, J.: White paper on integration of distributed energy resources: The CERTS microgrid concept. Technical report, CERTS, April 2002

13. Linnenberg, T., Wior, I., Schreiber, S., Fay, A.: A market-based multi-agent-system for decentralized power and grid control. In: Mammeri, Z. (ed.) Proceedings of 2011 IEEE 16th Conference on Emerging Technologies and Factory Automation ETFA 2011, 8 pp. Paul Sabatier University, Toulouse (2011)

14. Lovins, A., Odum, M., Rowe, J.W.: Reinventing Fire: Bold Business Solutions for the New Energy Era. Chelsea Green Publishing, Vermont (2011)

15. McArthur, S.D.J., Davidson, E.M., Catterson, V.M., Dimeas, A.L., Hatziargyriou, N.D., Ponci, F., Funabashi, T.: Multi-agent systems for power engineering applications part i: concepts, approaches, and technical challenges. IEEE Trans. Power Syst. **22**(4), 1743–1752 (2007)

16. McArthur, S.D.J., Davidson, E.M., Catterson, V.M., Dimeas, A.L., Hatziargyriou, N.D., Ponci, F., Funabashi, T.: Multi-agent systems for power engineering applications part ii: technologies, standards, and tools for building multi-agent systems. IEEE Trans. Power Syst. **22**(4), 1753–1759 (2007)

17. Nistor, S., Wu, J., Sooriyabandara, M., Ekanayake J.: Cost optimization of smart appliances. In: Innovative Smart Grid Technologies (ISGT Europe), 2011 2nd IEEE PES International Conference and Exhibition on, 5 pp. (2011)

18. Palma-Behnke, R., Benavides, C., Aranda, E., Llanos, J., Saez, D.: Energy management system for a renewable based microgrid with a demand side management mechanism. In: 2011 IEEE Symposium on Computational Intelligence Applications in Smart Grid (CIASG), 8 pp. (2011)

19. Pałka, P., Radziszewska, W., Nahorski, Z.: Balancing electric power in a microgrid via programmable agents auctions. Control Cybern. **41**(4), (in print) (2012)

20. Parol, M., Wasilewski, J., Wójtowicz, T., Nahorski, Z.: Low voltage microgrid in a research and educational center. In: Proceedings of the Conference "Elektroenergetika ELEN 2012", 15 pp. (2012)

21. Ricalde, L.J., Ordonez, E., Gamez, M., Sanchez, E.N.: Design of a smart grid management system with renewable energy generation. In: IEEE Symposium on Computational Intelligence Applications in Smart Grid (CIASG), pp. 147–150 (2011)

22. Schaerf, A., Shoham, Y., Tennenholtz, M.: Adaptive load balancing: a study in multi-agent learning. J. Artif. Intell. Res. **2**, 475–500 (1995)

23. Srikantha, P., Rosenberg, C., Keshav, S.: An analysis of peak demand reductions due to elasticity of domestic appliances. In: Proceedings of the 3rd International Conference on Future Energy Systems: Where Energy, Computing and Communication Meet, e-Energy '12, vol. 28, pp. 1–28:10. ACM, New York (2012)

24. Tsikalakis, A.G., Hatziargyriou, N.D.: Centralized control for optimizing microgrids operation. In: IEEE Power and Energy Society General Meeting, pp. 241–248 (2011)

25. Vogt, H., Weiss, H., Spiess, P., Karduck, A.P.: Market-based prosumer participation in the smart grid. In: 4th IEEE International Conference on Digital Ecosystems and Technologies (DEST), pp. 592–597 (2010)

26. Vytelingum, P., Voice, T.D., Ramchurn, S.D., Rogers, A., Jennings, N.R.: Agent-based micro-storage management for the smart grid. In: Proceedings of the 9th International Conference on Autonomous Agents and Multiagent Systems: volume 1–Volume 1 AAMAS '10, pp. 39–46 Richland (2010)

27. Wasilewski, J., Parol, M., Wójtowicz, T., Nahorski, Z.: A microgrid structure supplying a research and education centre–Polish case. In: Proceedings of the 3rd IEEE PES Innovative Smart Grid Technologies (ISGT 2012) Europe Conference, 8 pp. (2012)

28. Westermann, D., John, A.: Demand matching wind power generation with wide-area measurement and demand-side management. IEEE Trans. Energy Convers. **22**(1), 145–149 (2007)

Test Generation for Short-Circuit Faults in Digital Circuits

József Sziray

Abstract   In the first part, the paper presents a test calculation principle which serves for producing tests of logic faults in digital circuits. The name of the principle is composite justification. The considered fault model includes stuck-at-0/1 logic faults. Both single and multiple faults are included. In this paper only combinational logic is taken into consideration. The computations are performed at the gate level. The calculation principle is comparatively simple. It is based only on successive line-value justification, and it yields an opportunity to be realized by an efficient computer program. The first part serves for presenting the basic principle which is used in the second part of the paper. The second part deals with another fault class, namely, short-circuit or bridging faults. A short circuit is an erroneous galvanic connection between two circuit lines. Here, a new algorithm is presented for generating tests, where the composite justification is extended to handle this type of faults, as well.

Keywords Test-pattern generation · Logic faults · Short-circuit faults · Multi-valued logic · Digital circuits

1 Introduction

Due to the ever increasing complexity of digital integrated circuits, associated with the rapid development in their manufacturing processes, the importance of testing for correct functioning is steadily increasing. All this implies new fault models which require new methods in test design [1]. The fulfillment of this requirement is especially important in the field of VLSI CMOS circuits which are widely used in the modern hardware construction.

J. Sziray (✉)
Department of Informatics, Széchenyi University, Győr, Hungary
e-mail: sziray@sze.hu

At first, the paper gives an overview of a general test-calculation principle that is suitable for producing tests for digital circuits which are modeled at the gate level. The name of the algorithm is **composite justification** [2]. It is assumed that the circuits are of combinational type. The principle is comparatively simple, and it yields an opportunity to be realized by an efficient computer program. It should also be added that the calculation process can be extended to sequential circuits in a straightforward way [3].

The considered fault model includes stuck-at-0/1 logic faults on the primary inputs and the gate outputs. Both single and multiple faults are included.

The second part of the paper deals with an other fault class, namely, short-circuit or bridging faults. A short circuit is an erroneous galvanic connection between two circuit lines. Here the composite justification will be extended to handle this type of faults, as well. The extension has resulted in a new algorithm.

2 The Basic Principle

First the test calculation principle in general is presented below.

Let the vector of primary input and output variables for a general logic network be $\bar{x} = (x_1, x_2, \ldots, x_n)$ and $\bar{z} = (z_1, z_2, \ldots, z_m)$, respectively. Let the set of possible logic values in the network be $V = \{v_1, v_2, \ldots, v_s\}$. In addition to the elements of V, the indifferent or don't care value d will be applied.

The principle of test calculation is based on the formerly elaborated composite justification algorithm that has originally been intended for various permanent logic faults, such as stuck-at, timing and functional faults [2, 3]. At first, the overall concept of composite justification will be summarized.

Suppose that a sequence of primary input vectors $X(t) = \bar{x}_1, \bar{x}_2, \ldots, \bar{x}_t$ detects $q \geq 1$ simultaneous logic faults at a primary output z_j. Now the task of calculating $X(t)$ can be stated in the following way. Find a sequence of input patterns which implies $z_j = \alpha$ in the fault-free network, and $z_j = \beta$ in the faulty network, where

$$\alpha \in V, \ \beta \in V, \ \text{and} \ \alpha \neq \beta.$$

To reach this goal, we associate the logic values α and β with z_j, and attempt to find a sequence of input patterns which equally justifies

(1) the normal value of z_j for the normal (fault-free) network, and
(2) the faulty value of z_j for the faulty network.

In the first case, $X(t)$ justifies $z_j = \alpha$ through the values of all the necessary network lines in the usual manner. In the second case, however, since the faulty values are self-dependent, they need not be justified by $X(t)$. Thus, in the faulty network, $X(t)$ and the faulty values justify $z_j = \beta$ jointly.

The test sequence can be derived by applying the **line-value justification concept**. As known, line-value justification is a procedure with the aim of successively

assigning input values to the logic elements in such a way that they are consistent with each previously assigned value. (This concept is an auxiliary calculation process for justifying an initial set of logic values in a network, first applied in the D-algorithm for two-valued logic [1, 4]).

In our approach, the computations are carried out simultaneously in the normal and faulty network, i.e., in the normal and the faulty domain. Logic values simultaneously representing signal values in both the normal and the faulty networks are called **composite values**. Line justification performed in terms of composite values is referred to as **composite justification** [2, 3]. The two components of a composite value will be separated by a slash, with the normal component preceding the faulty one. The actual logic value of the *i*-th line in the network will be denoted by *v(i)*. Then, for example, a composite value of line *i* is

$$v(i) = v_a/v_b$$

In the composite justification the computational costs can be greatly reduced by the following consideration [2]. The signal values in the normal and faulty networks cannot differ at the lines that do not carry any signals propagating from the sites of the faults. These are called **inactive lines**, for which $v_a \neq v_b$ would represent inconsistency if they had the composite value of v_a/v_b. It should be realized that for our purposes it is sufficient to determine which lines (called **potentially active lines** or **PAL's**) carry signals from the faulty lines to z_j. This holds true, since all the other lines in the network are either inactive or are not involved in the justification process. The set of potentially active lines can be generated by intersecting the set of the lines that are reached from the faulty lines with the set of the lines from which z_j can be reached. The two sets are very easy to obtain by topologically tracing out the signal connections. This is done by starting from the faulty lines and proceeding forward, then starting from z_j, and proceeding backward. If a line is encountered in both the forward and backward tracing then it is potentially active. At the end of the calculations, those lines which actually carry the fault signal to z_j will be the real **active lines**. These lines have the so-called **active composite values** which are equivalent with the **fault signals**.

The other consideration relates to the initial values associated with line z_j. It is not known in advance which normal and faulty values are to be assumed. Therefore we make an arbitrary choice. However, in the case of single faults, there is no need to repeat the justification process with interchanged values for z_j, even if the initial choice has failed. Whenever the last in a series of active values along a path between the fault site *i* and z_j encounters contradiction at *i*, we have to interchange the components of each composite value, then proceed with the calculations in the same way as before.

The implementation of the above principle for a synchronous sequential network may require the justification process to be performed through different storage states of the network, which results in a test sequence X(t) of length *t*. The detailed principle of doing it for stuck-at-0/1 faults is described in [3].

3 Extension to Short-Circuit Faults

In the following we are going to deal with an other fault class, and show how the composite justification can be extended in a straightforward way to calculating tests for this class. Here **galvanic coupling** between circuit lines, i.e., **short-circuit faults** or **bridging faults** will be considered.

A short-circuit fault is defined for two signals. This type of fault occurs when a signal erroneously takes up the normal logic value of another signal. In this case the two signals are said to be bridged (coupled). Only **single occurrence** is stipulated here for the faults. The other assumption is that **no feedback coupling** occurs between any two lines, which would cause a combinational network to become a sequential one.

Let the **dominant logic value** of two bridged lines be ω: It means that the value ω will appear on both lines, instead of the normal differing values. If the bridged lines are b_1 and b_2 then the initial values for the composite justification will be as follows:

$$z_j = \alpha / \beta \text{ for a selected primary output, where}$$

$$\alpha \in V, \ \beta \in V, \text{ and } \alpha \neq \beta,$$

and on the other hand,

$$v(b_1) = v(b_2) = d / \omega.$$

In the justification process, the following measures have to be taken for the two bridged lines:

(1) If either of them is reached by a determined logic value (i.e., a value other than d) in the normal domain, then the value of the other bridged line must be set to ω / ω. (Note that a completely determined composite value first appearing at a bridged line has necessarily different values, i.e., it is a possible fault signal.)

(2) If in a backtrack process, b_1 or b_2 is reached, then the initial value d/ω has to be assigned to both lines again, as the solution when canceling the former decisions, i.e., when canceling the former calculated logic values.

As an example, we take the network shown in Fig. 1. Here, the coupled pair of lines are $b_1 = 9$ and $b_2 = 10$. Now let the dominant logic value be $\omega = 1$.

It is easy to see that a short circuit between two lines b_1 and b_2 manifests itself in a multiple-fault situation, involving two fault sites, namely b_1 and b_2. From the viewpoint of fault propagation, b_1 and b_2 are the starting elements of the potentially active lines. In our example, the united set of PAL's is the following:

$$\text{PAL}(9 - 12) \bigcup \text{PAL}(10 - 12) = \{9, 10, 11, 12\}.$$

These line are marked heavy in the schematic.

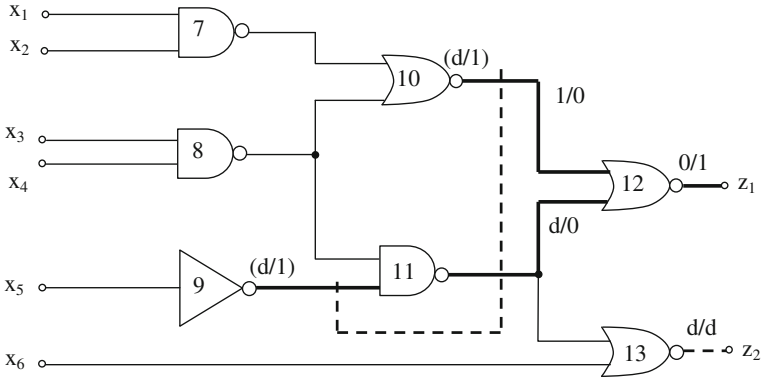The initial values are $v(9) = v(10) = d/1$, and $z_1 = v(12) = 0/1$.

Fig. 1 Test generation for a short-circuit fault: initial phase

The process of test calculation is as follows:

Step 1: $v(10) = 1/0$, $v(11) = d/0$ represent a contradiction.
$v(10) = d/0$, $v(11) = 1/0$ are also a contradiction

So, next we select the opposite composite value, i.e., $z_1 = v(12) = 1/0$. From this point on, the calculations are demonstrated in Fig. 2.

Step 2: $v(10) = 0/1$, $v(11) = 0/d$.
Due to the determined normal component of $v(10)$,

$$v(9) = \omega / \omega. = 1/1.$$

Step 3: $v(7) = 1$, $v(8) = d$.
Step 4: $v(8) = 1$. (Justification for gate 11.)
Step 5: $x_1 = 0$, $x_2 = d$.
Step 6: $x_3 = 0$, $x_4 = d$.
Step 7: $x_5 = 0$.
Step 8: $x_6 = d$.

Now, the found test vector is:

$$\bar{x}_t = (0, d, 0, d, 0, d).$$

The test can easily be verified. In the fault-free network, $z_1 = 1$, while in the presence of the short circuit between lines 9 and 10, $z_1 = 0$ will occur, which is the criterion of fault detection.
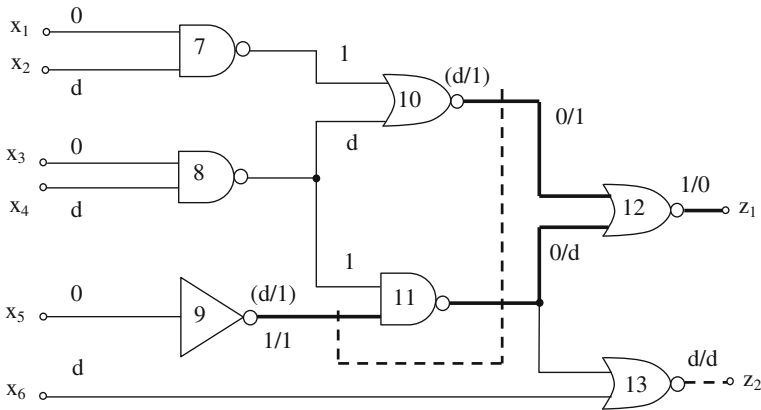
Fig. 2 Test generation for a short-circuit fault: final result

4 Conclusions

This paper has been meant for showing how the test calculation algorithm presented in [2] can be generalized for treating short-circuit (bridging) faults in digital circuit models. The efficiency of the composite justification is based on the fact that it establishes **the minimal necessary and sufficient set of logic values** which yield the test conditions for the faults. As seen, the tests are obtained by justifying the initial logic conditions. The salient advantage of composite justification is **the total absence of the fault propagation** phase. This feature makes the approach extremely flexible in terms of circuit modeling and fault classes. The same applies to the use of an HDL. As known, the fault propagation phase, i.e., D-propagation is an inherent part of the wide-spread D-algorithm, where this phase implies serious difficulties for functional level models and multiple faults. Functional algorithms for constructing computational tools of complex logic modules have been presented in [5]. This paper clearly illustrates the problems encountered in this topic.

When multiple faults are considered, the complete procedure of the D-algorithm has to be repeated $2^q - 1$ times in worst case, for one primary output, where q is the multiplicity of faults. In this case, attempts are made to propagate different combinations of the individual faults. On the other hand, composite justification requires only 2 iterations in worst case, also for one primary output, independent of the number of simultaneous faults. As seen, the difference in the computational complexity, i.e., $3^q - 1$ and 2, is an absolute advantage. At this point, it should be mentioned that in case of sequential circuits, multiple faults are always to be handled, even if a single fault is under consideration. The cause is the occurrence of virtual faults during the propagation [1, 3].

Another promising approach is the use of Boolean proof engines, where the so-called Satisfiability (SAT) problem [6] is converted to the problem of test generation [7]. Here, a Boolean proof engine serves for solving Boolean equations, thus

yielding tests for digital circuits. However, this approach requires having the Boolean descriptions, and is used only for **single faults**. It should also be added that the generation of Boolean functions is a necessary task of this approach, which has to be performed with knowledge of the gate-level description related to an actual circuit. This task is to be performed with knowledge of the circuit schematic, and it requires an extremely time consuming procedure.

As far as the computer implementation is concerned, only line justification is to be accomplished in the presented principle, which is also an advantage. In order to perform the line-value justification, the **inverse models** of the building elements in the network are required. An inverse model defines the set of possible input patterns which result in a specific state or an output pattern [5, 8]. For this purpose, high level hardware-description languages, such as VHDL can also be applied [9, 10].

The computerized implementation of the proposed principle will handle multi-valued logic, where the number of logic values corresponds to the number of the possible signal values in the HDL applied for modeling.

As far as the calculation of tests for short-circuit faults is concerned, all the advantages of composite justification apply also to solving that different computation task. It is all the more so, because this problem always requires handling multiple-faults.

Finally, the principle presented in this paper can also be extended to handling bridging faults in logic networks that are modeled at the functional level.

References

1. Abramovici, M., Breuer, M.A., Friedman, A.D.: Digital Systems Testing and Testable Design. Computer Science Press, Piscataway (1990)
2. Sziray, J.: Test calculation for logic and delay faults in digital circuits. In: Proceedings of the IEEE Microprocessor Test and Verification Workshop, (MTV-06), pp. 20–29, Austin (2006)
3. Sziray, J.: Test Design of Digital Systems. Széchenyi University Press, Győr (2012)
4. Roth, J.P.: Diagnosis of automata failures: a calculation and a method. IBM J. Res. Dev. **10**, 278–291 (1966)
5. Breuer, M.A., Friedman, A.D.: Functional level primitives in test generation. IEEE Trans. Comput. **C-29**, 223–235 (1980)
6. Lewis, H.R., Papadimitriou, C.H.: Elements of the Theory of Computation. Prentice-Hall, Upper Saddle River (1998)
7. Drechsler, R., Eggersglüss, S., Fey, G., Tille, D.: Test Pattern Generation Using Boolean Proof Engines. Springer, Heidelberg (2009)
8. Sziray, J., Nagy, Zs.: OPART: a hardware-description language for test generation. In: Nunez, P. (ed.) Microprocessing and Microprogramming, pp. 525–530. North-Holland, Amsterdam (1991)
9. Sallay, B., Petri, A., Tilly, K., Pataricza, A., Benyó, B., Sziray, J.: High level test pattern generation for VHDL circuits. In: Proceedings of the IEEE European Test Workshop'96, pp. 201–205, Montpellier, June 1996
10. Benyó, B., Sziray, J.: The use of VHDL models for design verification. In: Proceedings of the IEEE European Test Workshop, pp. 289–290, Cascais, 23–26 May 2000